รายงานวิจัยฉบับสมบูรณ์

การประยุกต์ใช้อินทราบอดีส์ในการลดจำนวนโมเลกุล CD147 บนผิวเซลล์เม็ดเลือดขาวชนิดทีเซลล์ โดยใช้ระบบการนำส่งยีนด้วยอะดิโนไวรัสรูปแบบใหม่ เพื่อใช้ในการศึกษาหน้าที่ของโมเลกุล

ชัชชัย ตะยาภิวัฒนา

สิงหาคม 2553

สัญญาเลขที่ RMU5080022

รายงานวิจัยฉบับสมบูรณ์

การประยุกต์ใช้อินทราบอดีส์ในการลดจำนวนโมเลกุล CD147 บนผิวเซลล์เม็ดเลือดขาวชนิดทีเซลล์ โดยใช้ระบบการนำส่งยีนด้วยอะดิโนไวรัสรูปแบบใหม่ เพื่อใช้ในการศึกษาหน้าที่ของโมเลกุล

ชัชชัย ตะยาภิวัฒนา
แขนงวิชาภูมิคุ้มกันวิทยาคลินิก
ภาควิชาเทคนิคการแพทย์
คณะเทคนิคการแพทย์
มหาวิทยาลัยเชียงใหม่

สนับสนุนโดยสำนักงานกองทุนสนับสนุนการวิจัย

(ความเห็นในรายงานนี้เป็นของผู้วิจัย สกว.ไม่จำเป็นต้องเห็นด้วยเสมอไป)

กิตติกรรมประกาศ

งานวิจัยนี้ได้รับทุนสนับสนุนประเภท ทุนพัฒนานักวิจัย ประจำปี 2553 จากสำนักงานกองทุนสนับสนุนการวิจัย ผู้วิจัยขอขอบพระคุณมา ณ ที่นี้ด้วย

ผู้วิจัยขอขอบคุณ คณาจารย์, บุคลากร และนักศึกษา ภาควิชาภูมิคุ้มกันวิทยาคลินิก ที่มีส่วนร่วมอำนวยความสะดวก และสนับสนุนในเชิงวิชาการ โดยเฉพาะ รศ.ดร.วัชระ กสิณฤกษ์ ที่ให้แนวคิดและสนับสนุนงบประมานส่วนหนึ่งสำหรับการวิจัยในครั้งนี้ นอกจากนี้ผู้วิจัยขอขอบคุณเจ้าหน้าที่ของสำนักงานกองทุนสนับสนุนการวิจัยที่ช่วยประสานงานทุกด้าน

ท้ายนี้ขอขอบพระคุณ ศ.ดร.สถิตย์ สิริสิงห และ รศ.ดร.กำจัด มงคลกุล ซึ่งเป็นทั้งผู้ให้โอกาสและเป็นต้นแบบในการทำงานทางวิทยาศาสตร์ของผู้วิจัย

บทคัดย่อ

รหัสโครงการ : RMU5080022

ชื่อโครงการ : การประยุกต์ใช้อินทราบอดีส์ในการลดจำนวนโมเลกุล CD147 บนผิวเซลล์เม็ดเลือดขาวชนิดทีเซลล์ โดยใช้ระบบการนำส่งยีนด้วยอะดิโนไวรัสรูปแบบใหม่ เพื่อใช้ในการศึกษาหน้าที่ของโมเลกุล

ชื่อนักวิจัย : นายชัชชัย ตะยาภิวัฒนา

แขนงวิชาภูมิคุ้มกันวิทยาคลินิก คณะเทคนิคการแพทย์ ม.เชียงใหม่

E-mail Address : asimi002@chiangmai.ac.th

ระยะเวลาโครงการ : 3 ปี

CD147 มีบทบาทเกี่ยวข้องกับกระบวนการเปลี่ยนแปลงทางด้านสรีรและพยาธิสภาพของเซลล์ กระบวนการส่งสัญญาณเข้าสู่เซลล์ และยังมีบทบาทที่สำคัญเกี่ยวข้องกับการลุกลามและแพร่กระจายของเซลล์มะเร็ง ดังนั้นการลดการแสดงออกของโมเลกุล CD147 อาจมีประโยชน์ต่อการยับยั้งความก้าวหน้าในการเจริญของเซลล์มะเร็ง ในการศึกษาครั้งนี้มีวัตถุประสงค์เพื่อสร้างและศึกษาคุณสมบัติของ scFv-M6-1B9 แอนติบอดีต่อ CD147 โดยใช้เฟจดิสเพลย์เทคโนโลยีมาประยุกต์ใช้ในการสร้างแอนติบอดีต่อ CD147 จากนั้นได้ทำการสร้าง scFv-M6-1B9 แอนติบอดีต่อ CD147 ให้มีการแสดงออกและยังคงทำหน้าที่อยู่ภายในระบบของเอนโดพลาสมิกเรติคูลั่มโดยใช้ระบบการนำส่งยีน ด้วยอะดิโนไวรัส และได้ประเมินคุณสมบัติทางชีวภาพ หน้าที่ และผลของ scFv-M6-1B9 ต่อการแสดงออกของ CD147 จากการศึกษาพบว่ารีคอมบิแนนท์ Fab- และ scFv- M6-1B9 แอนติบอดีต่อCD147 สามารถจับได้อย่างจำเพาะกับรีคอมบิแนนท์ CD147-BCCP ด้วยวิธี indirect ELISA และเมื่อทำการศึกษาหน้าที่ของ scFv M6-1B9 แอนติบอดีที่อยู่ในรูปสารละลายที่ผลิตจากแบคทีเรีย E. coli HB2151 พบว่ามีความสามารถในการจับกับ CD147 ที่แสดงออกบนผิวเซลล์ U937 และยับยั้งการแบ่งตัวของเม็ดเลือดขาวชนิดทีเซลล์เมื่อถูกกระตุ้นร่วมกับ OKT3 แอนติบอดี นอกจากนั้นแล้ว scFv M6-1B9 แอนติบอดีที่ได้จากการแตกเซลล์ 293A ที่ถูก transduced ด้วยอะดิโนไวรัสที่กำหนดการสร้าง scFv M6-1B9 แอนติบอดีสามารถจับกับ CD147 ได้ทั้งในรูปแบบที่พบตามธรรมชาติและรูปแบบรีคอมบิแนนท์ที่สร้างขึ้น ซึ่งบ่งชี้ถึงความมีประสิทธิภาพและความจำเพาะอย่างสูงในการจับกับแอนติเจน ที่สำคัญอย่างยิ่งคือ scFv M6-1B9 อินทราบอดีได้แสดงให้เห็นถึงความมีคุณสมบัติทางชีวภาพที่ดี โดยสามารถลดการแสดงออกของ CD147 ที่ผิวของเซลล์ 293A, Jurkat และ HeLa ได้ จากการศึกษาในครั้งนี้แสดงให้เห็นว่า scFv M6-1B9 มีศักยภาพที่ดีในการจับกับ CD147 ทั้งภายในและภายนอกเซลล์ ซึ่งจะช่วยทำให้เข้าใจบทบาทและหน้าที่ของ CD147 มากขึ้นและอาจใช้ในการพัฒนาวิธีการรักษามะเร็งชนิดแพร่กระจายรูปแบบใหม่ได้ในอนาคต

Keywords : phage display technique, CD147, intrabody

Abstract

Project Code : RMU5080022

Project Title : Intrabody application on decreasing of CD147 molecule on T-cell surface using a novel Adenovirus gene transfer system for functional studies

Investigator : Mr. Chatchai Tayapiwatana

Div. of Clinical Immunology, Fac. of Associated Medical Sciences

Chiang Mai University

E-mail Address : asimi002@chiangmai.ac.th

Project Period : 3 year

CD147 involves in signal transduction pathways and also plays a crucial role in the invasive and metastatic activity of malignant tumor cells. Diminished expression of this molecule has been shown to be beneficial in suppression of tumor progression. In this study, we aimed to generate and characterize a recombinant antibody fragment, scFv, which reacted specifically to CD147. Phage display technology was introduced to generate the functional antibody fragment to CD147, and we subsequently constructed a CD147-specific scFv that was expressed intracellularly and retained in the endoplasmic reticulum by adenoviral gene transfer. The biological properties, function and the effect of generated scFv on CD147 expression were investigated. The result showed that recombinant antibody fragments, Fab and scFv, of the murine monoclonal antibody (clone M6-1B9) reacted specifically to CD147 by indirect ELISA using a recombinant CD147-BCCP as a target. We further studied the function of soluble scFv-M6-1B9 produced from E. coli HB2151. The results demonstrated that it was able to bind with CD147 surface molecule of U937 and inhibited OKT3-induced T cell proliferation. Furthermore, soluble lysate of scFv-M6-1B9 from 293A cells, transduced with a scFv-M6-1B9 expressing adenovirus vector, recognized both recombinant and native CD147. These results indicate that scFv-M6-1B9 binds with high efficiency and specificity. Importantly, scFv-M6-1B9 intrabody reduced the expression of CD147 on the cell surface of 293A, Jurkat and HeLa cells, suggesting that scFv-M6-1B9 is biologically active intrabody. In conclusion, our present study demonstrated that scFv-M6-1B9 has a great potential to target both the intracellular and the extracellular CD147. This study represents a step toward understanding the role of the CD147 cell surface protein and may aid in efforts to develop a novel treatment for a variety of metastatic tumors in the near future.

Keywords : phage display technique, CD147, intrabody

สารบัญ

INTRODUCTION

1.1 Statement and significance of the problem

CD147 is a cell surface glycoprotein that belongs to the immunoglobulin superfamily. This surface molecule is expressed on all leukocytes, erythrocytes, thrombocytes and endothelial cells (Stockinger H, 1997). It plays an important role in mediating signal transduction induced by the binding of specific ligands and regulating central cellular processes such as cell proliferation (Wang et al., 2006), apoptosis (Intasai et al., 2006), or cell adhesion (Kasinrerk et al., 1999; Khunkeawla et al., 2001). In addition, CD147 also is involved in the invasion and metastasis processes of tumor cells in many types of cancers (Reimers et al., 2004; Tang et al., 2005; Nabeshima et al., 2006a). An increase in expression of CD147 in cancer cells has not only been linked to deregulation of epidermal growth factor receptor (EGFR) signaling (Menashi et al., 2003) but may also be a response to transforming growth factor-β stimulation (Gabison et al., 2005). CD147, also named extracellular matrix metalloproteinase inducer (EMMPRIN), has been identified as a cell surface inducer of matrix metalloproteinases (MMPs) both in tumor and stromal cells (Sun and Hemler, 2001; Gabison et al., 2005; Yan et al., 2005). Furthermore, CD147 is also defined as a lymphocyte activation-associated molecule (Kasinrerk et al., 1992; Stockinger, 1997; Koch et al., 1999). In T cells a negative regulatory signal arises from cross-linking of CD147 molecules and T cell regulation has been demonstrated (Igakura et al., 1996; Koch et al., 1999; Staffler et al., 2003;

Chiampanichayakul et al., 2006). Recently, two anti-CD147 mAbs, M6-1E9 and M6-1B9, which react with the membrane-distal Ig domain, inhibited OKT3-induced T cell proliferation (Chiampanichayakul et al., 2006). These mAbs inhibited cell proliferation by delivery of a negative signal through CD147 to suppress CD25 and IL-2 expression (Chiampanichayakul et al., 2006). Therefore, developing a tool for studying the function of CD147 would be valuable.

Advances in antibody engineering have allowed the manipulation of the antibody segments containing the antigen-binding regions and generation of small fragments that can be expressed in cells. These recombinant proteins are called intracellular antibodies or intrabodies. They have being successfully applied, mainly in the single chain Fv antibodies (scFv) format, to inhibit the function of intracellular target proteins in specific cellular compartments (Marasco et al., 1993; Lobato and Rabbitts, 2004). scFvs are the smallest fragment of an IgG molecule capable of maintaining the antigen-binding specificity of the parental antibody. They have the capacity to inhibit the translocation of cell surface molecules from the ER to the cell surface as ER-intrabodies (Richardson and Marasco, 1995; Steinberger et al., 2000b; Jendreyko et al., 2003). Intrabodies offer an effective alternative to gene-based knockout technologies to study the protein functions (Stocks, 2004). This technique has more advantages than RNA interference (RNAi) technology since intrabodies possess a much longer active half-life compared to RNA, and are also much more specific to their target molecules (Cao and Heng, 2005; Heng et al., 2005) and generally do not disrupt target gene transcription. Moreover, these gene knock-out and silencing techniques cannot be used for domain structure and function analysis,

including analysis of post-translationally modified protein functions. A recent study demonstrated that intrabody-mediated down-regulation of major histocompatibility complex (MHC) class I reduces the immunogenicity of rat aortic EC (RAEC) which may provide a suitable alternative supply for the lining of vascular prostheses (Doebis et al., 2006). In particular, intracellular use of antibody fragments can offer an effective alternative to gene-based knockout technologies. Therefore, intrabodies can be used as the most powerful tools to study the function of human leukocyte surface molecule especially CD147.

Normally, intrabodies are often introduced into cells by transfection of expression vectors encoding the intrabodies (Lobato and Rabbitts, 2004). Viral and nonviral gene transfer systems are available. Retroviral vectors as well as nonviral gene delivery methods such as calcium phosphate coprecipitation, electroporation and liposomal transfection target only a small fraction of cell population after extended selection periods, many of which, however, are not appropriate for transduction of human lymphocytes. Furthermore, expression levels are often low and insertion site-dependent silencing of the transgene expression is a frequent predicament (Doerfler et al., 1997; Baum et al., 2003; Hacein-Bey-Abina et al., 2003). In addition, the genome of retroviruses and lentiviruses is small, limiting the size of exogenous genes that can be packaged and transferred to target cells by the derivative vectors. Conversely, adenoviral vectors are an attractive alternative since they can efficiently transduce both dividing and non-dividing cells, and achieve transgene expression within hours (Nevins et al., 1997). Moreover, adenoviruses do not integrate into the host genome, thus leaving the genetic package of targeted cells unmodified. This results in

reproducible gene expression levels and also eliminates any undesirable effects related to the site of integration, allowing the specific analysis of the transgene effects (Kay et al., 2001). This characteristic, together with their relative ease of preparation and purification, has led to their extensive use as gene vectors.

From these data, we purposed to generate the recombinant scFv-M6-1B9 against CD147 as soluble form and as intrabody and study the biological activity of these recombinants. The suppression of CD147 expression on cancer cell surface may offer a novel approach for treatment of metastatic tumors in the near future.

1.2 Literature review

1.2.1 The human CD147

1.2.1.1 CD147 structure

The human cell surface molecule CD147 was designated at the Sixth International Workshop and Conference of Human Leukocyte Differentiation Antigens (Stockinger, 1997). It is a glycoprotein of 50–60 kDa having typical features of a type I integral membrane protein of the immunoglobulin superfamily as shown in **Figure 1.1**. CD147 is also known as M6 antigen (Kasinrerk et al., 1992), extracellular matrix metalloproteinase inducer (EMMPRIN) (Biswas et al., 1995) or human basigin (BSG) (Miyauchi et al., 1991). In various species glycoproteins homologous to CD147 have been identified, i.e. the rat protein OX-47/CE9 (Fossum et al., 1991; Nehme et al., 1993), the chicken blood–brain barrier-related molecule HT7/neurothelin/5A11 (Schlosshauer and Herzog, 1990; Seulberger et al., 1990; Fadool and Linser, 1993), the mouse protein gp42/basigin (Altruda et al., 1989;

Miyauchi et al., 1990) and the rabbit homologue (Schuster et al., 1996). The CD147 gene, designated BSG for basigin, is located on chromosome 19p13.3 (Muramatsu and Miyauchi, 2003) and encodes a 29 kDa protein, though migration on SDS-PAGE usually occurs between 35 and 65 kDa, depending on the degree of glycosylation (Kasinrerk et al., 1992; Kirsch et al., 1997; Kasinrerk et al., 1999). Treatment of the protein with endoglycosidase F demonstrated that almost half of CD147 molecular weight was due to the addition of N-linked carbohydrates (Kasinrerk et al., 1992). The structure of CD147 is composed of the extracellular region with two immunoglobulin domains, a single transmembrane domain and a short cytoplasmic domain (Miyauchi et al., 1991; Biswas et al., 1995; Muramatsu and Miyauchi, 2003). The protein is composed of an extracellular domain of 185 amino acid (aa.), a 24 aa residue transmembrane domain and a 39 aa cytoplasmic region as shown in Figure 1 (Kasinrerk et al., 1992; Biswas et al., 1995; Nabeshima et al., 2006b). The extracellular region contains three N-linked glycosylation sites, associated with 5–35 kDa glycosylation (glycan) content (Biswas et al., 1995; Tang et al., 2004a). The first extracellular Ig domain (EC I) is involved in matrix metalloproteinase (MMP) induction, binding to counter-receptors for itself (Sun and Hemler, 2001), carrying high-mannose-type L3 epitope (Heller et al., 2003) and association with integrins (Berditchevski et al., 1997). The second extracellular Ig domain (EC II) is required for association with caveolin-1 which leads to decreased self-association on the cell surface (Muramatsu and Miyauchi, 2003). The single transmembrane domain (TD) sequence is completely conserved among human, mouse and chicken species. It may serve critical biological functions (Miyauchi et al., 1991). The presence of Pro211 and

Glu218, in the middle of this domain are involved in association with cyclophilin 60 (Cyp60) and membrane targeting of CD147, respectively (Pushkarsky et al., 2005; Yurchenko et al., 2005). Similar to the leucine zipper motif, 3 leucines are repeated every seventh amino acid residue in the CD147 transmembrane domain (Seulberger et al., 1990; Fossum et al., 1991). This motif may be involved in the association between membrane proteins. By using fluorescence resonance energy transfer (FRET), Wilson *et al*. revealed that a cytoplasmic domain (CD) of CD147 binds to two molecules of monocarboxylate transporter 1 (MCT1) (Wilson et al., 2002).

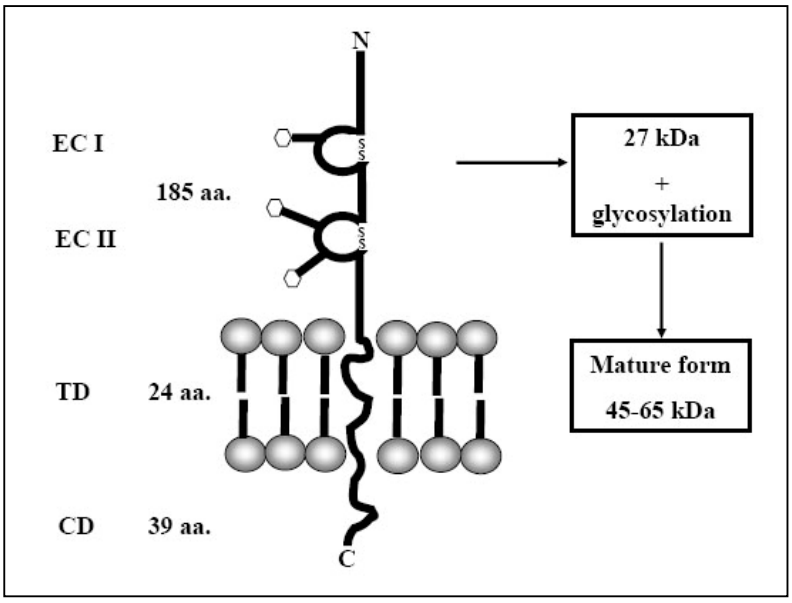

Figure 1.1 Schematic representation of the CD147 structure. EC I, first extracellular Ig domain; EC II, second extracellular Ig domain; TD, transmembrane domain; CD, cytoplasmic domain. Three N-linked oligosaccharides are shown by hexagons.

1.2.1.2 CD147 expression and their functions

The CD147 molecule is broadly expressed on human peripheral blood cells, endothelial cells, hemopoietic and non-hemopoietic cell lines (Stockinger, 1997). In T cells, its expression level is dependent on the differentiation state. Thymocytes are more strongly positive than mature T cells (Kirsch et al., 1997) and CD147 is up-regulated upon activation (Kasinrerk et al., 1992). Significant expression of CD147 has also been reported in malignant cells (Toole, 2003; Yan et al., 2005). The molecular function of neither CD147 nor any of its species homologues is fully understood. However, it has been suggested that CD147 is involved in signal transduction and cell adhesion functioning either directly as a signal transmitting adhesion molecule or as a regulator of adhesion.

A function of CD147 is also defined as a lymphocyte activation-associated molecule (Kasinrerk et al., 1992; Stockinger, 1997; Koch et al., 1999). In T cells a negative regulatory signal arises from cross-linking of CD147 molecules and T cell regulation has been demonstrated (Igakura et al., 1996; Koch et al., 1999; Staffler et al., 2003; Chiampanichayakul et al., 2006). Recently, anti-CD147 monoclonal antibodies (mAbs) *i.e.* M6-1B9 (IgG3), M6-2B1 (IgM), M6-1D4 (IgM), M6-1E9 (IgG2a), M6-1F3 (IgM) and M6-2F9 (IgM) have been generated (Kasinrerk et al., 1999). Some CD147 mAbs (M6-1D4, M6-1F3 and M6-2F9) induced homotypic aggregation of U937 cell line (Kasinrerk et al., 1999). Cell aggregation induced by the engagement of CD147 using mAbs to CD147 was described as a LFA-1/ICAM-1-dependent pathway (Kasinrerk et al., 1999). Furthermore, CD147 mAbs induced cell aggregation depends upon the activation of protein kinases and a functional

cytoskeleton (Khunkeawla et al., 2001). Two anti-CD147 mAbs, M6-1E9 and M6-1B9, which react with the membrane-distal Ig domain inhibited OKT3-induced T cell proliferation but did not induce cell aggregation (Chiampanichayakul et al., 2006). These mAbs inhibited cell proliferation by delivery of a negative signal through CD147 to suppress CD25 and IL-2 expression (Chiampanichayakul et al., 2006). In addition, CD147 was also demonstrated to induce apoptosis in U937 cells and that at least a portion of this cell death program involves a caspase-dependent pathway (Intasai et al., 2006). CD147 mAbs inhibited homotypic aggregation of the estrogen-dependent breast cancer cell line MCF-7, as well as MCF-7 cell adhesion to type IV collagen, fibronectin and laminin has been reported (Staffler and Stockinger, 2000) .

CD147 was also found to co-precipitate with $\alpha 3\beta 1$ and $\alpha 6\beta 1$ integrins and to co-localize with these integrins in areas of cell-cell contact (Berditchevski et al., 1997). Moreover, Tang *et al.* reported that using anti-integrin $\alpha 3\beta 1$ antibody can decrease the enhancing effect of CD147 on adhesion, invasion capacities and secretion of matrix metalloproteinases (MMPs) in human 7721 hepatoma cells (Tang et al., 2008).

CD147 is enriched on the surface of tumor cells and stimulates adjacent stromal cells to produce several matrix metalloproteinases (MMPs), including interstitial collagenase (MMP-1), gelatinase A (MMP-2) and stromelysin-1 (MMP-3) (Majmudar et al., 1994; Biswas et al., 1995; Heppner et al., 1996; Guo et al., 1997; Lim et al., 1998). CD147 was termed as extracellular matrix metalloproteinase inducer (EMMPRIN) (Sun and Hemler, 2001; Gabison et al., 2005;

Yan et al., 2005) and is involved in the invasion and metastasis processes of tumor cells in many types of cancers (Reimers et al., 2004; Tang et al., 2005; Nabeshima et al., 2006a). An increase in expression of CD147 in cancer cells has not only been linked to deregulation of epidermal growth factor receptor (EGFR) signaling but may also be a response to transforming growth factor-β stimulation (Gabison et al., 2005). In addition, CD147 and P-glycoprotein (P-gp) is also overexpressed in multi-drug resistance (MDR) cancer cell lines (Yang et al., 2003; Yang et al., 2007; Jia et al., 2008). Increased production of MMP-2, MMP-9, and MMP-11 was observed only in MDR cancer cells (Li et al., 2007; Wang et al., 2008). Thus, CD147 and P-gp may play a crucial role in MDR cancer cells with the invasiveness and metastasis of tumor cells.

CD147 is reported to exist in both soluble and membrane bound forms (Sidhu et al., 2004; Tang et al., 2004b). Interestingly, several studies have provided evidence that microvesicular release of CD147 from tumor cells could play a role in tumor-stromal interactions through upregulation of MMP production (Sidhu et al., 2004). Shedding of membrane vesicles is observed in eukaryotic cells and suggested to be involved in several pathophysiological processes (Taraboletti et al., 2002). These shed vesicles are unstable and rapidly degraded over time, giving rise to increasing levels of CD147 in non-vesicle fractions (*i.e.* supernatant) of cell-conditioned medium. Recently, Millimaggi *et al.* demonstrated that tumor vesicle-associated CD147 cells could modulate the angiogenic capability of human umbilical vein endothelial cells (HUVECs) (Millimaggi et al., 2007).

Despite the interaction of mAbs and their targets mimicked the native ligand-receptor signaling. However, substrates or ligands for CD147 are still not identified. It is not clear whether CD147 is directly involved in signal transduction and cell adhesion as a signal transmitting adhesion molecule or as a regulator of adhesion in the interactions between epithelial cells and the extracellular matrix.

1.2.2 Recombinant protein expression in *Escherichia coli*

E. coli is one of the most widely used hosts for the heterologous protein production. This is due to its ability to grow rapidly and at high density on inexpensive substrates, its well-characterized genetics and the availability of an increasingly large number of cloning vectors and mutant host strains. The genetics of *E. coli* are far better characterized than those of any other microorganism. Recent progress in the fundamental understanding of transcription, translation, and protein folding in *E.* coli, together with serendipitous discoveries and the availability of improved genetic tools are making this bacterium more valuable than ever for the expression of complex eukaryotic proteins. Although there is no guarantee that a recombinant gene product will accumulate in *E. coli* at high levels in a full-length and biologically active form, a considerable amount of effort has been directed at improving the performance and versatility of this workhorse microorganism (Makrides, 1996; Baneyx and Mujacic, 2004).

1.2.2.1 Protein translocation across bacterial cytoplasmic membrane

The targeting and transport of proteins across biological membranes into the periplasm is one of the fundamental features of cellular life. Proteins located within the periplasmic space perform many crucial roles. For example, the detoxifying enzymes play a role in the inhibition of the activity of molecules which are toxic to cell. Nucleases, peptidases and other scavenging enzymes metabolize large complex molecules into simpler ones that can be utilized by the cell. Proteins that are exported to the bacterial periplasm are usually synthesized with cleavable N-terminal signal sequences, termed signal peptides, which direct the protein to a specific transporter complex in the cytoplasmic membrane. The signal sequences in general have a tripartite structure where a short, basic N-region precedes a longer hydrophobic stretch of amino acid (h-region), followed by the c-region, which normally contains a recognition sequence for the enzyme signal peptidase. In bacteria, three major routes are used to achieve protein translocation across the cytoplasmic membrane *e.g.* the secretory (Sec), signal recognition particle (SRP) and the twin-arginine translocation (Tat) pathway as shown in **Figure 1.2**.

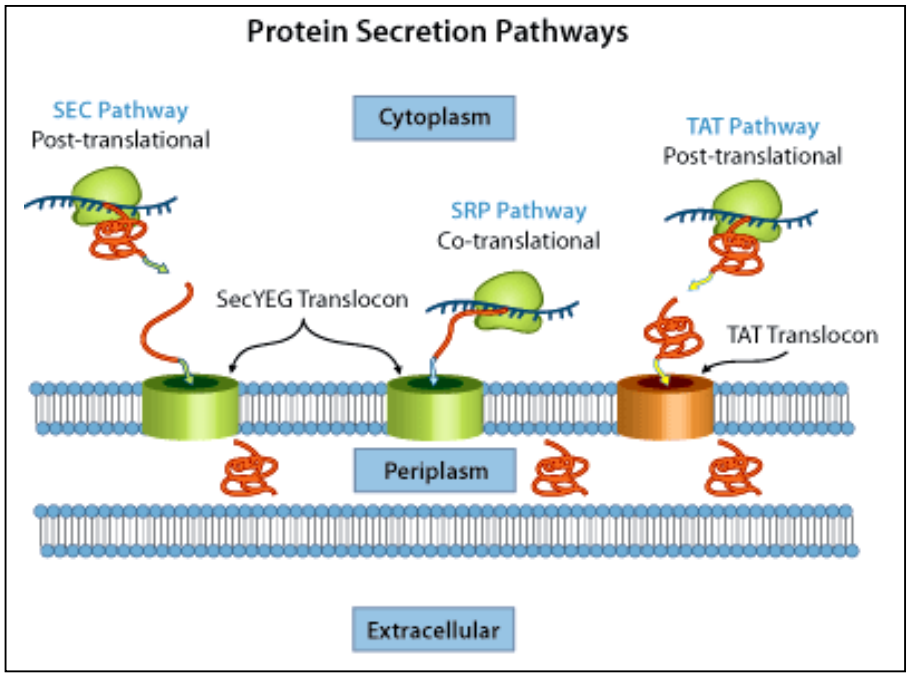

Figure 1.2 Diagram of the secretion pathways of *E. coli*.

(http://www.athenaes.com/tech_brief_ACESyebf.php)

.

1.2.2.1.1 The general secretory (Sec) pathway

The major route of protein translocation in bacteria is the so-called general secretion pathway (Sec pathway) (Choi and Lee, 2004). This transporter complex is build by multimeric proteins which are spanning through the inner membrane of *E. coli*. Secretion *via* this pathway involves 9 different components: Trigger factor (TF), SecA, SecB, SecY, SecE, SecG, SecD, SecF and YajC. The core of the translocase consists of a proteinaceous channel formed by the protein complex of SecYEG and the peripheral adenosine triphosphatase (ATPase) SecA as molecular motor. Ribosome-associated nascent chains of secreted proteins bind TF (**Figure 1.3**), which is bound to the ribosomes (Maier et al., 2003). This association is maintained until the preprotein leaves the ribosome, thus preventing cotranslational binding of the nascent chain to SRP components (Mergulhao et al., 2005).

Secreted proteins targeted to the SecB-dependent pathway contain an amino-terminal signal peptide that functions as a targeting and recognition signal. These signal peptides are usually 18–30 amino acid residues long and are composed of a positively charged amino terminus (n-region), a central hydrophobic core (h-region), and a polar cleavage region (c-region) (Fekkes and Driessen, 1999; Choi and Lee, 2004). The n-region is believed to be involved in targeting the preprotein to the translocase and binding to the negatively charged surface of the membrane lipid bilayer. Increasing the positive charge in this region has been shown to enhance translocation rates, probably by increasing the interaction of the preprotein with SecA (Fekkes and Driessen, 1999). The h-region varies in length from 7 to 15 amino acids.

Translocation efficiency increases with the length and hydrophobicity of the h-region, and a minimum hydrophobicity is required for function (Wang et al., 2000).

Secreted proteins are kept in a translocation-competent state by the chaperone SecB (de Gier and Luirink, 2001), which interacts with the mature region of the preprotein to prevent premature folding (Khokhlova and Nesmeianova, 2003) and targets it to SecA (Figure 3). In the presence of preprotein, SecB binds SecA (Fekkes et al., 1998; Woodbury et al., 2000), thus releasing the precursor protein that is transferred to SecA (Fekkes and Driessen, 1999). SecA binding to the preprotein is facilitated by the signal peptide, which it recognizes specifically. At this point SecA is bound to the SecY subunit of the SecYEG complex. SecYEG constitutes a pathway (‘channel’) for polypeptide movement. Binding of ATP at one of the two ATP-binding sites on SecA causes the release of SecB from the membrane (Mergulhao et al., 2005). There is no consensus on how the Sec components form a functional translocon, and monomeric, dimeric and oligomeric translocons have been proposed (Mergulhao et al., 2005). Binding of the preprotein to membrane-bound SecA results in the translocation of approximately 20 amino acids, and subsequent binding of ATP to SecA promotes SecA membrane insertion and translocation of additional 15-20 amino acids. ATP hydrolysis releases the preprotein from SecA into the translocation channel (Driessen et al., 1998). ADP is then released and SecA deinserts from the membrane where it can be exchanged with cytosolic SecA. Multiple rounds of SecA insertion and deinsertion promote protein translocation through the channel (de Keyzer et al., 2003). Proton-motive force (PMF) can complete translocation when the preprotein is halfway through the translocase, even in the absence of SecA

(Nishiyama et al., 1999). The mechanism by which PMF drives translocation is unknown but it has been suggested that PMF assists in the initiation phase of protein translocation (Mori and Ito, 2003) and that it accelerates SecA membrane deinsertion (Nishiyama et al., 1999). Finally, the folded substrate protein was released into the periplasmic space. SecD, F and YajC are accessory proteins that aid in translocation into the periplasm, where proteins are folded into their final confirmation.

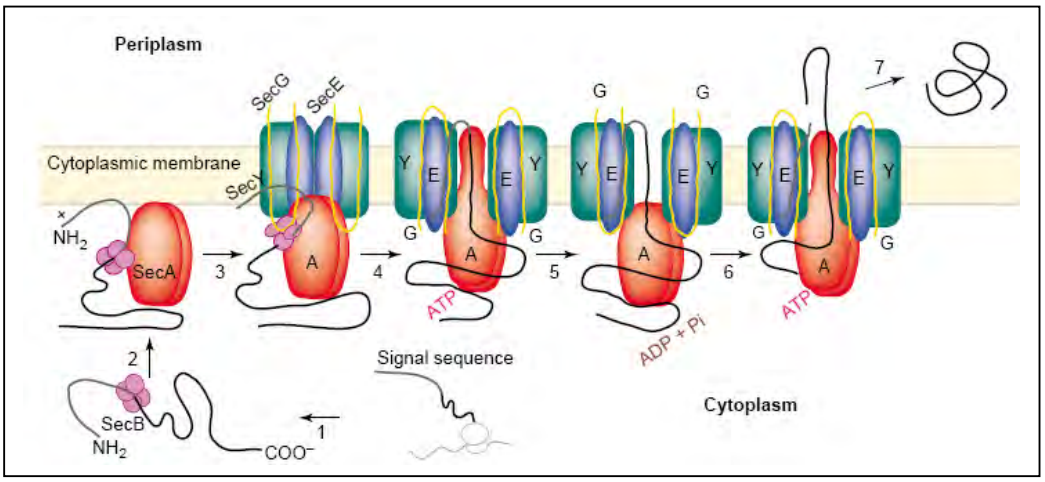

Figure 1.3 The general Sec pathway in bacteria (Mori and Ito, 2001).

1.2.2.2 Protein folding in *E. coli*

Newly synthesized polypeptide chains must fold and assemble into unique three-dimentional structures in order to attain their biological function. In general, small peptides or single domain host proteins efficiently reach a native conformation owing to their fast folding kinetic, whereas large multidomain and overproduced recombinant proteins often require the assistance of folding modulators which include molecular chaperones and folding catalysts. Molecular chaperones are an ubiquitous class of proteins that play an essential role in protein folding by helping other polypeptides reach a proper conformation without becoming part of the final structure. The chaperone protein acts in preventing off-pathway by shielding the hydrophobic amino acid residues and stabilizing nonnative polypeptides, whereas the folding catalysts accelerate specific rate-limiting steps in folding, such as isomerization of peptide bonds and rearrangement of disulfide bonds. Molecular chaperones can be divided into three functional subclasses based on their mechanism of action (**Figure 1.4**). Folding chaperones (e.g. DnaK and GroEL) are the core of the chaperone network which uses conformational changes fueled by ATP hydrolysis to promote the folding of bound substrates. Holding chaperones (e.g. IbpA, IbpB, Hsp31 and Hsp33) stabilize partially folded proteins on their surface to await availability of folding chaperones upon stress abatement. Finally, the disaggregating chaperone ClpB promotes the solubilization of proteins that have become aggregated as a result of stress and transfer them to the folding chaperones for subsequent refolding (Baneyx and Mujacic, 2004). Clear evidence that molecular chaperones are needed to prevent misfolding and its consequences come from the fact that the concentrations of many

of these species are substantially increased during cellular stress; indeed, the designation of many as heat shock proteins (Hsps) reflects this fact. It is also clear that some molecular chaperones are able not only to protect proteins as they fold but also to rescue misfolded and even aggregated proteins and enable them to have a second chance to fold correctly (Bukau and Horwich, 1998; Hartl and Hayer-Hartl, 2002). Active intervention in the folding process requires energy, and ATP is required for most of the molecular chaperones to function with full efficiency.

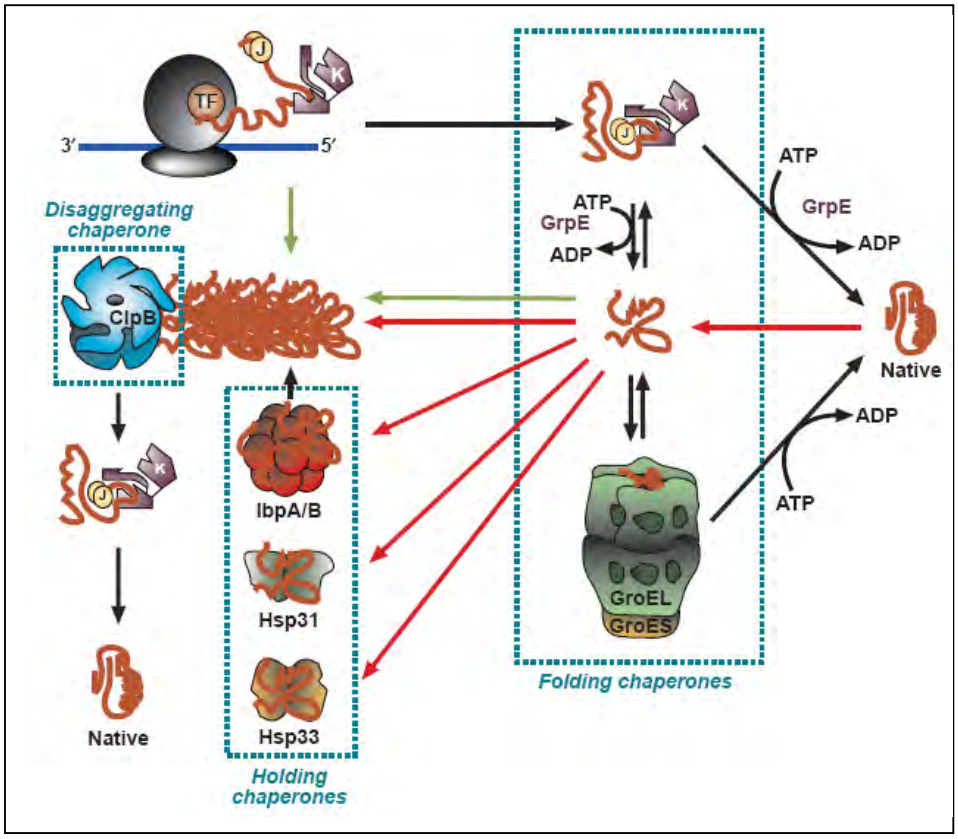

Figure 1.4 Chaperone-assisted protein folding in the cytoplasm of *E. coli*. Nascent polypeptides requiring the assistance of molecular chaperones first encounter trigger factor (TF) or DnaK-DnaJ. In times of stress (red arrows), thermobile proteins unfold and aggregate. IbpB is required to serve partially folded proteins on its surface to serve as a reservoir of unfolded intermediates until folding chaperone available. Recombinant proteins that miss an early interaction with TF or DnaK-DnaJ, that undergo multiple cycles of abortive interactions with folding chaperones, or titrate them out, accumulate in inclusion bodies (green arrows) (Baneyx and Mujacic, 2004).

1.2.2.2.1 Periplasmic protein folding

The proteins that translocate across the inner membrane exert their biological functions in the periplasmic or destine for insertion into outer membrane. These proteins must transverse the periplasm and the peptidoglycan layer to reach their destination. During their transit as nascent or partially folded polypeptide they require protection from misfolding and aggregation. The periplasm contains a lower group of molecular chaperones than does the cytoplasmic compartment and all of them are ATP-independent chaperones. The periplasmic chaperones have been proposed to assist the folding and membrane insertion of outer membrane proteins. Skp is a 17 kDa protein that binds several outer membrane proteins including OmpA, OmpC, OmpF, PhoE and LamB (Tamm et al., 2004). The Skp central cavity can accommodate the substrates up to 20 kDa (Walton and Sousa, 2004). Skp chaperone activity is likely a holdase. It binds to unfolded substrate immediately after they are translocated across the inner membrane that keeps them in an unfolded form and prevents them from aggregation in the periplasm (Harms et al., 2001).

The *E. coli* periplasm contains a series of enzymes such as disulfide-binding proteins (DsbA, DsbB, DsbC, and DsbD) and petidyl-prolyl isomerases (SurA, RotA, FklB, and FkpA) that promote the appropriate folding of thiol-containing proteins (Shokri et al., 2003). FkpA is the peptidyl-prolyl-*cis*/*trans* isomerase (PPIase), which catalyses the interconversion between *cis* and *trans* form of the peptide bond X-Pro, where X is any amino acid. FkpA is an important periplasmic chaperone with the generic folding activity (Missiakas et al., 1996). It is believed to cradle partially folded substrates within the hydrophobic cleft formed at the

dimerization interface, allowing the flexible C-terminal domains easy access to prolyl bonds requiring isomerization (Saul et al., 2004). The other well characterized periplasmic protein folding modulator is SurA. SurA is a periplasmic PPIase that has been shown to assist the folding of several outer membrane proteins, including OmpA, OmpF and LamB. SurA is classified as specialized chaperone since it preferentially recognizes an Ar-X-Ar motif (where Ar is an aromatic and X is any amino acid residue) that is common in outer membrane proteins but infrequent in other polypeptides (Bitto and McKay, 2003). It contains a 50 Å deep cleft within its core module that may be responsible for substrate binding (Bitto and McKay, 2002).

1.2.2.3 Disulfide bond formation

In addition to chaperones, which facilitate protein folding by binding to and stabilizing partially folded intermediates, cells contain enzymes that catalyze protein folding by breaking and reforming covalent bonds. Many proteins secreted into the periplasm form specific disulfide bonds that help in both the folding and stabilization of the mature protein. Disulfide bonds are generally restricted to secreted proteins and some membrane protein because the cytosol has a reducing environment that maintains cysteine residues in their reduced form. In contrast, the periplasm has an oxidizing condition that allows the formation of structural disulfide bonds. This difference appears to be the result of the particular enzymatic systems present in these compartments, which are responsible for oxidation, reduction and isomerization of disulfide bonds in proteins. The cytoplasm has two systems that catalyzed the NADP-dependent reduction of disulfide bridges in target proteins, the thioredoxin/

thioredoxin reductase system and glutaredoxinn/glutathione system (Holmgren, 1989). The proper formation of disulfide bonds in the periplasm is catalyzed by specific thiol-disulfide oxidoreductase. In both the periplasmic and cytoplasmic systems, the proteins responsible for catalizing oxidation or reduction have a common thioredoxin active site motif, Cys-X-X-Cys (Martin et al., 1993). Oxidation and reduction of disulfide bonds is mediated by thiol-disulfide exchange between the active site cysteines of the enzyme and cysteines in the target protein (Darby and Creighton, 1995; Frech et al., 1996).

There are a number of membrane and soluble thiol-disulfide oxidoreductases that contribute to proper oxidation of structural disulfide bonds in periplasmic proteins (**Figure 1.5**). The first of these is DsbA, which is responsible for the formation of disulfide bonds in newly translocated proteins (Bardwell et al., 1991). DsbA oxidizes its substrate by transferring the disulfide bond from its active site to the target protein, leaving its active site in the reduced state. The reduced DsbA is reoxidized in order for DsbA to catalyze another round of disulfide bond formation. Reoxidation of DsbA is performed by the integral membrane protein DsbB (Missiakas et al., 1993). The genetic study suggests that DsbB is itself oxidized by passing electrons to respiratory chain (Kobayashi et al., 1997). Although DsbA can catalyze the formation of disulfide bonds, they are insufficient in catalyzing the rearrangement or isomerization of incorrectly formed disulfide bonds in substrate proteins with multiple cysteines. The isomerization of disulfide bonds is a function of DsbC, a periplasmic disulfide bond oxidoreductase (Rietsch et al., 1996) .The Cys-X-X-Cys active site of DsbC is usually found in the reduced state, making it competent for

disulfide rearrangement. Maintaining DsbC in reduced form is the function of the cytoplasmic membrane protein, DsbD (Rietsch et al., 1996). DsbD supports DsbC in the reduced state *via* an interaction with its own reduced active site motif. Evidence suggests that the reducing power of DsbD is acquired by electron transfer from cytoplasmic thioredoxin (Hiniker and Bardwell, 2003).

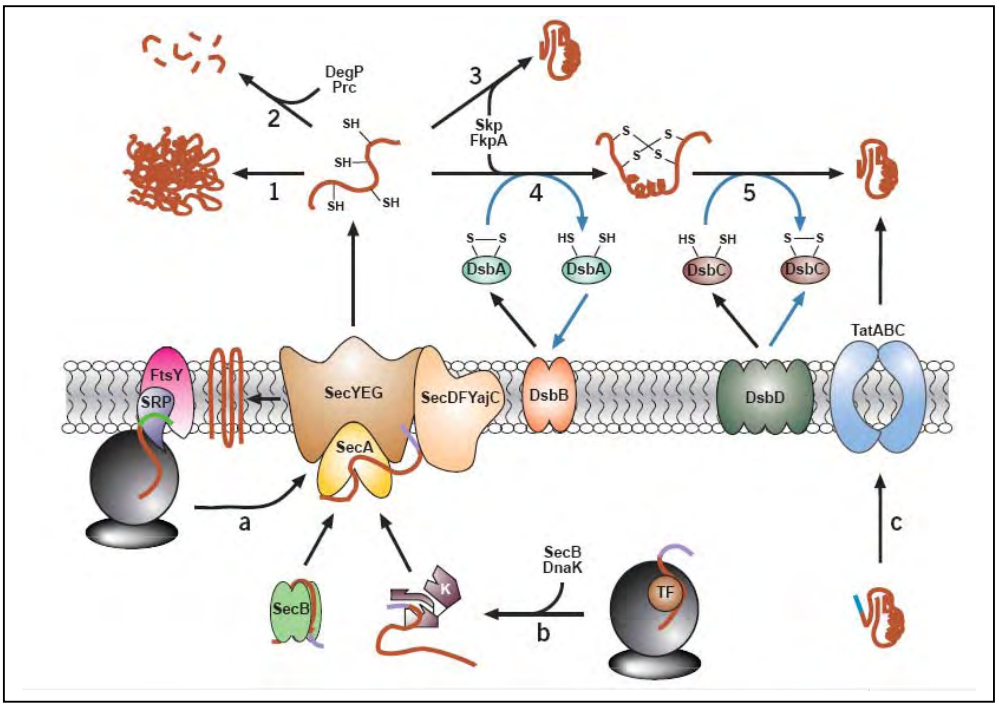

Figure 1.5 Disulfide bond formations in bacterial periplasm. Cysteine pairs in proteins containing disulfide bonds are oxidized by DsbA whereas incorrect disulfides are isomerized by DsbC. These oxidoreductases are reactivated by DsbB and DsbD, respectively (Baneyx and Mujacic, 2004).

1.2.2.4 Protein misfolding and inclusion body formation

Protein activity demands its folding into precise three-dimentional structure. The proteins which fail to reach a native conformation or to interact with folding modulator have two possible consequences: form inclusion body and degradation. Stress situations including heat shock, starvation, exposure to toxic compounds, recombinant protein overexpression, and oxidative stress, impair protein folding and cause the formation of folding intermediates and protein misfolding. In recombinant bacteria, the overexpression of plasmid-encoded genes triggers transcription of heat-shock genes and other stress responses and often results in the aggregation of the encoded protein as inclusion bodies. The aggregation is formed by non-native intermolecular hydrophobic interactions between protein folding intermediates, which have not yet buried their hydrophobic amino acid residues (Kiefhaber et al., 1991). Factors contributing to the formation of inclusion body are the use of high inducer concentration, strong promoter and the inability of bacteria to support all post-translational steps that a protein requires in folding (Baneyx and Mujacic, 2004).

The degradation by host protease is the fate of misfolded proteins to ensure that the abnormal polypeptides do not accumulate within the cell and to allow amino acid recycling. In the cytoplasm, proteolytic degradation is initiated by five ATP-dependent heat shock proteases (Lon, ClpYQ/HslUV, ClpAP, ClpXP and FtsH) and completed by peptidases that hydrolyze sequences 2-5 residues in length. These proteases consist of a remodeling component that binds substrate proteins and couples ATP hydrolysis to unfolding and transfer of the polypeptide to an associated protease

domain or proteolytic component. Since the periplasmic compartment has no ATP, the misfolded proteins are degraded by ATP-independent proteases. The generic periplasmic proteases are DegP, Tsp, protease III and OmpT and the most active of which are DegP and Tsp. DegP is a serine endopeptidase in which the proteolytic site is located within an inner cavity bounded by mobile side walls formed by PDZ domain. Tsp degrades nonpolar carboxy-terminal regions of protein with broad primary sequence specificity (Keiler et al., 1995).

1.2.2.5 The stress response systems in *E. coli*

All cells appear to have systems that respond to stress situation. In *E. coli,* the stress response is compartmentalized into cytoplasmic and extracytoplasmic responses. The cytoplasmic response is operated by σ^{32}, the *rho*H gene product, which responds to the accumulation of misfolded protein by directing the transcription of a well-characterized set of genes, including those encoding the GroEL/ES and DnaK/DnaJ chaperone and Lon protease (Bukau, 1993). These chaperones, in turn, are thought to down-regulate σ^{32} activity upon relief of cytoplasmic stress (Liberek et al., 1992; Gamer et al., 1996). In contrast, the extracytoplasmic is believed to be controlled by at least two signal transduction system, the σ^{E} mediated system and the Cpx two-component system. The σ^{E} transcription factor protein appears to control the synthesis of several proteins, some of which are involved in protein folding or degradation in the periplasm. The σ^{E} regulates the synthesis of DegP protease and FkpA, as well as its own synthesis (Erickson and Gross, 1989; Raina et al., 1995). The σ^{E} pathway is induced by the conditions that lead to misfolding of periplasmic

protein. RseA and RseB appear to be negative regulator of σ^E (De Las Penas et al., 1997). It has been proposed that when the periplasmic protein folding or degradation is impaired, misfolded proteins bind RseB, lowering the binding affinity of RseA for σ^E in the cytoplasm. This results in the release of σ^E to activate transcription of its own gene and of the gene for DegP protease and FkpA (Missiakas and Raina, 1997).

The second periplasmic stress response system is the two component Cpx pathway, which is composed of a sensory histidine kinase encoded by *cpxA* and a response regulator encoded by *cpxR* (Danese et al., 1995; Snyder et al., 1995). This pathway appears to regulate the expression of genes encoding the DsbA thiol-disulfide oxidoreductase, CpxA periplasmic protein, DegP proteinase and PpiD peptidyl-prolyl-*cis*/*trans* isomerases (Danese and Silhavy, 1997; Pogliano et al., 1997). The periplasmic misfolding and misfolded subunits of pili serve as potent activators of the Cpx signal transduction cascade (Jones et al., 1997). In the absence of protein misfolding, CpxA is maintained in an inactive state by the CpxP periplasmic inhibitor. Envelope protein misfolding or pilus assembly is predicted to lead to relief of CpxP inhibition and activation of phosphotransfer between CpxA and cpxR. Phosphorylated CpxR upregulates expression of genes whose products involved in envelope protein folding and degradation by binding to their promoter. There is another operon that appears to be induced under stress conditions but the role of its product is not clearly proposed. Phage shock protein A (PspA), is a peripheral cytoplasmic membrane protein which is encoded by the first gene in the pspA-E operon. PspA expression can be induced by filamentous phage infection, heat shock and membrane-associated stress condition. Although the precise function of PspA is

not clearly proposed, the studies demonstrated that the presence of PspA allows *E. coli* to survive in stationary phase at alkaline pH (Weiner and Model, 1994) as well as maintain the proton motive force under stress conditions (Kleerebezem et al., 1996).

1.2.3 Protein transporting in Eukaryotes

In contrast to most prokaryotic cells, eukaryotic cells contain, in addition to the plasma membrane, internal membranes. These internal membranes are structural components of organelles and vesicles. Most proteins are synthesized by cytosolic ribosomes and must pass a membrane to reach their final destination. Plasma membrane proteins and extracellular proteins are synthesized and processed at the rough endoplasmic reticulum. Therefore the initial step in secretion of most eukaryotic proteins is their transport into the lumen of the endoplasmic reticulum (ER) as shown in **Figure 1.6**. Transport of presecretory proteins into the ER involves cleavable signal peptides at the amino terminus of the precursor proteins and a transport machinery which operates co- or post-translationally. Typically this transport occurs as a sequence of three consecutive steps: i) specific membrane association of the precursor protein, ii) membrane insertion, and/or iii) completion of translocation (**Figure 1.7**).

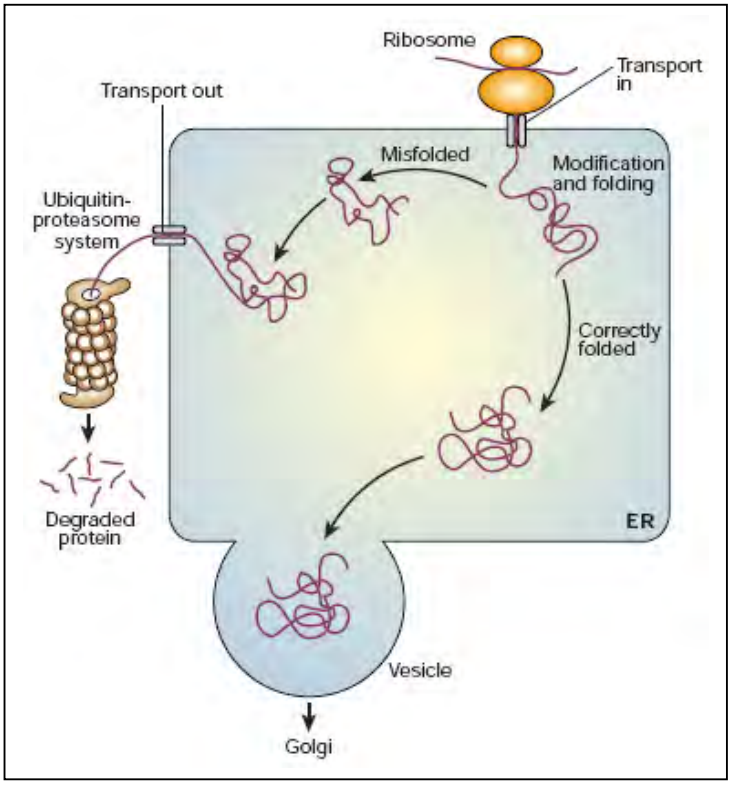

Figure 1.6 Regulation of protein folding in the ER (Dobson, 2003).

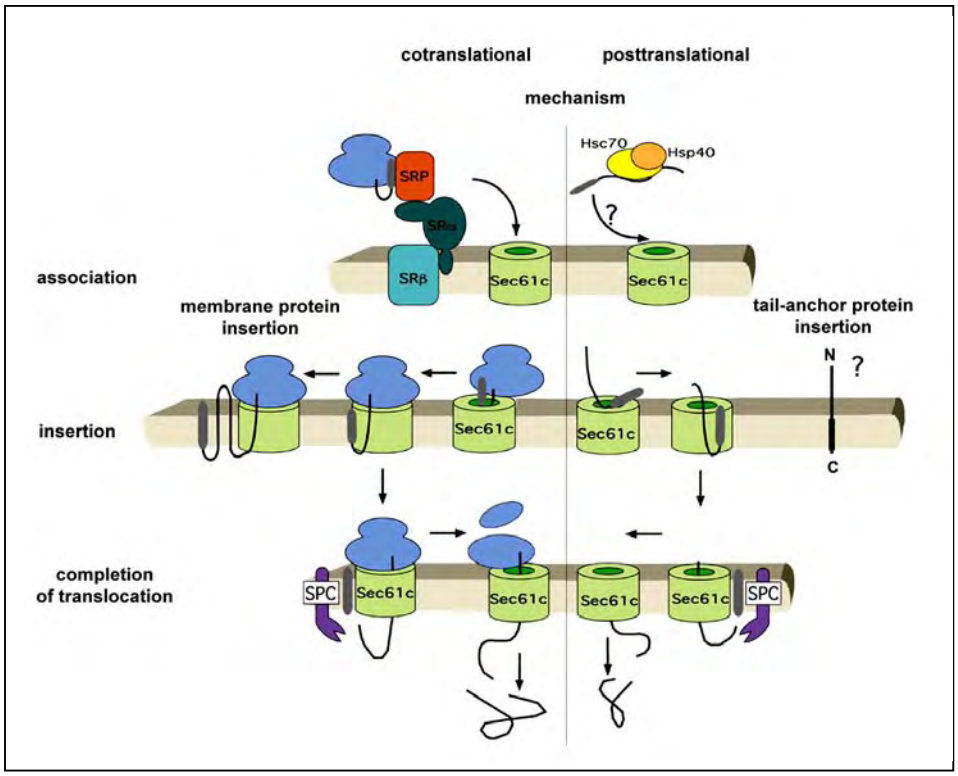

Figure 1.7 Protein transport- and insertion-pathways at the ER-membrane.

(http://wwwalt.med-rz.uni-sb.de/med_fak/biochemie/MartinJ/Eninformation.html)

It is well established that proteins destined for the secretory pathway begin their nascent polypeptide chains on the ribosomes and that SRP (signal recognition particle) is required to bring these chain bearing ribosomes to the ER membrane for translocation. There are several proteineaous factors located at the ribosomal polypeptide exit site which interact or bind directly to the emerging polypeptide chain, for example the nascent polypeptide associated complex (NAC) and cytosolic molecular chaperones (Hsc70, Hsp40). Therefore SRP-dependent cotranslational transport needs a specific signal sequence in the nascent polypeptide chain for successful targeting to the ER-membrane. The ER signal peptides have features similar to those of their bacterial counterparts. The eukaryotic signal sequences typically contain three regions: a short and positively charged hydrophilic amino-terminal segment, a central hydrophobic part (7-15 residues) and a more polar carboxy-terminal region. This signal sequence is recognized by SRP, a ribonucleoprotein complex consisting of a 7S RNA and six different polypeptide subunits. SRP interacts through its 54 kDa subunit with the signal sequence of nascent polypeptide chains and directs the entire complex, consisting of the ribosome, the nascent chain and the SRP to the ER membrane. Elongation of the polypeptide chain is delayed or even arrested until SRP is bound to the SRP receptor, an integral protein complex of the ER membrane. Once bound, SRP is released from the signal sequence in a GTP-dependent manner, and the ribosome together with the nascent chain is then passed onto the protein translocase. The continuing translation inserts the polypeptide into the lumen of the ER. Cleavable signal sequences are cotranslationally processed by the signal peptidase complex (SPC) at the lumenal side of the ER membrane

(Paetzel et al., 2002). Co- or post-translational proteins are translocated to the Sec61p complexes (**Figure 1.8**). The Sec61p complex seems to be the main structural component of the protein conducting channel. In mammals, the Sec61p complex contains a Sec61α-subunit with ten membrane-spanning domains, and the Sec61β- and Sec61γ-subunit, which belong to the class of tail-anchored proteins. In addition to these heterotrimeric Sec61p complexes, ATP-binding proteins of the mammalian ER lumen are part of protein translocase which facilitates insertion of presecretory proteins into the Sec61p complex as well as completion of translocation. The ATP-binding proteins (BiP, Grp170) were identified as ER resident members of the Hsp70 protein family. These Hsp70 protein family members of the mammalian ER may be recruited to the Sec61p complex by either one or both of the two membrane integrated Hsp40 protein family members, Sec63p and Mtj1p.

The ER contains a wide range of molecular chaperones and folding catalysts, and in addition the proteins that fold here must satisfy a quality-control check before being exported (Hammond and Helenius, 1995; Kaufman, 2002). Such a process is particularly important because there seem to be few molecular chaperones outside the cell, although one (clusterin), at least, has recently been discovered (Wilson and Easterbrook-Smith, 2000). This quality-control mechanism involves a remarkable series of glycosylation and deglycosylation reactions that enables correctly folded proteins to be distinguished from misfolded ones (Hammond and Helenius, 1995). Correctly folded proteins with the help of a series of molecular chaperones and folding catalysts are then transported to the Golgi complex and

proceed to their final destinations *via* the secretory pathway (Lewin et al., 2007). However, incorrectly folded proteins are detected by a quality-control mechanism and sent along another pathway (the unfolded protein response) in which they are ubiquitinated and then degraded in the cytoplasm by proteasomes (Schubert et al., 2000).

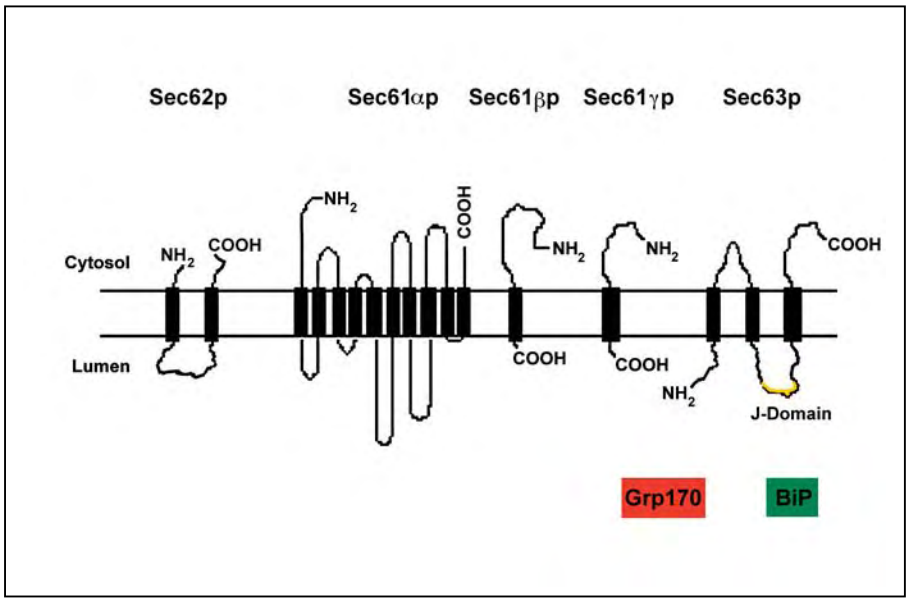

Figure 1.8 Components of the protein translocase of the ER-membrane.

(http://wwwalt.med-rz.uni-sb.de/med_fak/biochemie/MartinJ/Eninformation.html)

1.2.4 Phage display technology

1.2.4.1 Introduction

Phage display was first developed with the *E. coli* specific bacteriophage M13 (Smith, 1985), and the success of M13 phage display has prompted the development of numerous alternative display systems (Ren and Black, 1998; Santini et al., 1998). Phage display is a powerful method for selecting and engineering polypeptides with desired binding specificities. This technology can be applied in the field of immunology, cell biology and pharmaceutical biotechnology (Sidhu, 2000). Displaying of peptides and gene fragments enables the analysis of protein-protein interactions such as structural mapping of epitopes (Tayapiwatana et al., 2003; Abbasova et al., 2007), characterization of receptor and ligand interaction (Jager et al., 2007; Mohrluder et al., 2007; Casey et al., 2008), functional analysis (Intasai et al., 2006; Yang et al., 2006) and immunodiagnosis (Robles et al., 2005; Hell et al., 2009). This method is accomplished by inserting the gene fragments encoding the protein of interested into a phagemid genome as a fusion with M13 coat protein genes. These fusion genes can be incorporated in bacteriophage particles that also display the heterologous proteins on their surfaces. In this way, a physical linkage is established between phenotype and genotype of the expressed protein.

1.2.4.2 Biology and structure of M13 filamentous bacteriophage

(Smith and Petrenko, 1997; Barbas CF. III, 2001; Barbas, 2001; Sidhu, 2001)

The filamentous phage constitutes a large family of bacterial viruses that infect a variety of Gram-negative bacteria, using pili as receptors. The best characterized are the very similar phages M13, fd and f1, that infect *E. coli via* F pili. The filamentous bacteriophages are a group of viruses that contain a circular single-stranded DNA genome encased in a long protein capsid cylinder. The Ff phage particles are flexible rods about 1 μm long and less than 10 nm in diameter. The mass of particle is approximately 16.3 MD, of which 87% is contributed by protein. The particle consists of a single-stranded DNA core surrounded by a proteinaceous coat. The length of the cylinder consists of approximately 2,700 molecules of 50 amino acid major coat protein, called gene VIII protein (gpVIII). The four minor coat proteins are present at about 5 copies per particle; protein-VII and protein-IX (gpVII and gpIX) cap one end of the particle while protein-III and protein-VI (gpIII and gpVI) cap the other end (**Figure 1.9** and **Table 1.1**). Each of the five different coat proteins has been successfully used as a platform for the functional display of heterologous polypeptides as either N- or C-terminal fusions. Protein VI and gpIII are crucial for host recognition and phage infectivity, whereas gpVII and gpIX are required for phage assembly (Gailus et al., 1994). The gpIII is the most commonly used coat protein for display. This protein is made up of three domains separated by glycine-rich regions. These three domains have been designated N1 or D1, N2 or D2 and CT or D3 by different groups. The first domain, N1, is required during infection

for the translocation of the DNA into the cytoplasm and insertion of the coat proteins into membrane. N2 is responsible for binding to F pilus (Deng et al., 1999). The carboxy-terminal end makes up the CT domain and is essential for forming a stable phage particle. The DNA is oriented within the virion such that a 78 nucleotide hairpin region called the packaging signal (PS) is always located at the end of the particle containing the gpVII and gpIX proteins.

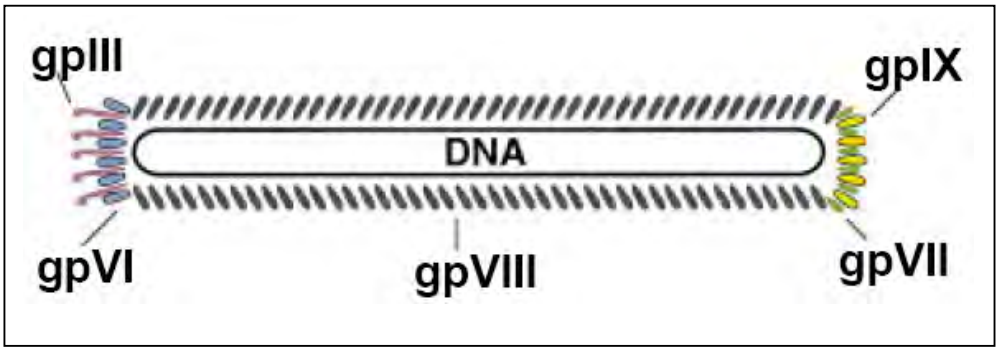

Figure 1.9 Structure of a filamentous bacteriophage. A diagram of the bacteriophage particle represents the single-stranded DNA core surrounded by a proteinaceous coat (Sidhu, 2001).

Table 1.1 Phage coat proteins.

Protein	Number of amino acids	Molecular weight	Copies per phage	Function
gpIII	406	42,500	~5	Minor capsid protein
gpVI	112	12,300	~5	Minor capsid protein
gpVII	33	3,600	~5	Minor capsid protein
gpVIII	50	5,200	~2,700	Major capsid protein
gpIX	32	3,600	~5	Minor capsid protein

1.2.4.3 M13 filamentous bacteriophage life cycle

Infection of *E. coli* by a filamentous phage is a multistep process requiring interactions of the phage gpIII protein with the F conjugative pilus and the bacterial TolQ, R and A cytoplasmic membrane proteins. These three Tol proteins are bacterial proteins that appear necessary for maintaining the integrity of the bacterial outer membrane, to avoid a leak of periplasmic proteins into the culture medium (Lazzaroni et al., 1999). The TolQRA proteins are required during phage infection for translocation of the Ff phage DNA into the cytoplasm and translocation of the phage coat proteins into the cytoplasmic membrane (Russel et al., 1988; Russel et al., 1997). Infection is initiated by attachment of the N2 domain of gpIII to the tip of the pilus; this is the end of the particle that enters the cell first (Holliger and Riechmann, 1997; Witty et al., 2002; Karlsson et al., 2003). This binding releases N1 from N2, and allows N1 to interact with TolA. As the process continues, the coat proteins dissolve into the periplasm. The major coat protein, gpVIII, gpVII and gpIX minor capsid proteins, and the uncoated ssDNA concomitantly enters the cytoplasm (**Figure 1.10**). Once the viral (+) strand DNA enters the cytoplasm, the complementary DNA (-) strand is synthesized by bacterial enzymes, resulting in a covalently closed, supercoiled and double-stranded replicative form (RF). The (-) strand of this RF is a template for transcription and consequencing mRNAs are translated into all of phage proteins. Of the 11 phage-coated proteins, three (gpII, gpX, gpV) are required to generate ssDNA, three (gpI, gpXI, gpIV) are required for phage assembly and five (gpIII, gpVI, gpVII, gpVIII, gpIX) are components of the phage particle. After one round, gpII circularizes the displace viral (+) strand DNA, which then is converted to

a covalently closed, supercoiled and double-stranded RF molecule by bacterial enzyme. The gpV dimers bind cooperatively to newly generated (+) strand RF and prevent its conversion to RF DNA. The RF DNA synthesis continues until the amount of gpV reaches a critical concentration. The gpX is crucial for the proper replication of the phage DNA and functions as an inhibitor of gpII (Fulford and Model, 1984). The RF replicates to make progeny RFs and is also the template for transcription of phage genes and synthesis of progeny ssDNAs. Assembly occurs at specific sites in the bacterial envelope where the cytoplasmic and outer membranes are in close contact by the interaction of gpI, gpVI and gpXI and form a gated pore complex that spans the inner and outer membranes. Phage assembly is initiated by the incorporation of gpVII and gpIX at one end of the particle. This process continues until the end of the DNA is reached and the assembly is terminated by the incorporation of gpVI and gpIII (**Figure 1.11**). Progeny virions are secreted continuously without lysis of the *E.coli* host; chronically infected cells continue to divide, though at a slower rate than uninfected cells.

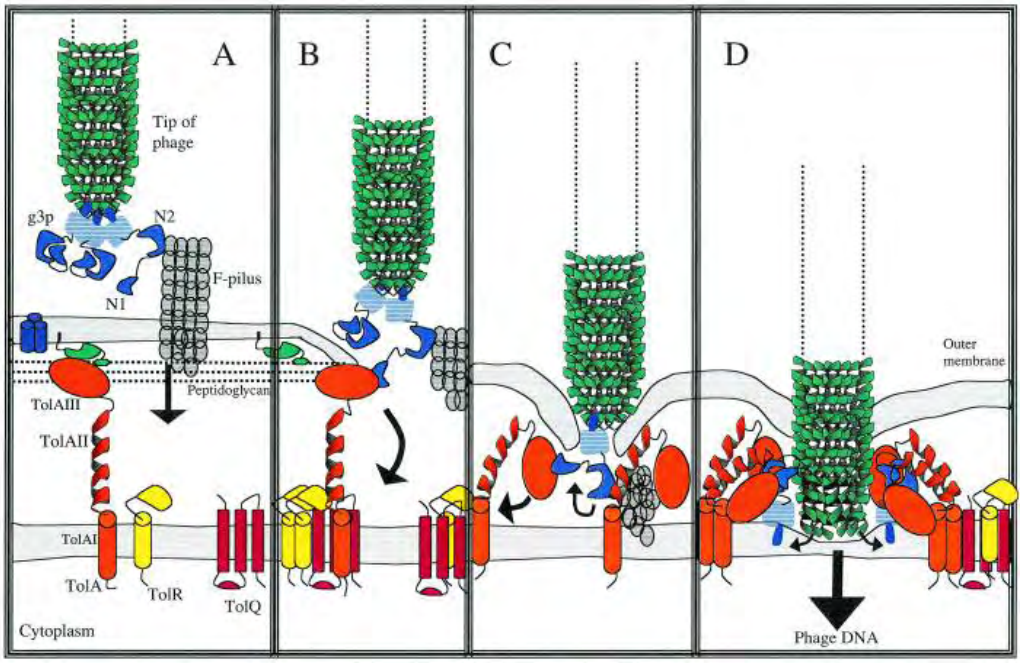

Figure 1.10 Model of filamentous phage infection. A) The phage N2 domain of pIII protein interacts with the F-pilus on the outside of the bacteria. The outer membrane proteins OmpF (blue cylinders) and Pal lipoprotein (greenish) are also included, as there have been reports of TolA interacting with these proteins prior to infection (Lazdunski et al., 1998; Cascales et al., 2000). **B)** After F-pilus retraction, N1 domain of gpIII binds to the C-terminal domain of bacterial TolA domain III (TolAIII). **C)** The retracting pilus brings phage gpIII domains in closer contact with TolA domains. As a consequence, TolA can assume a more compact state of assembly, thus bringing the outer and inner membranes of the bacteria closer together. At this stage, the central domain of TolA (TolAII) has the possibility to interact with the N2 domain of gpIII. **D)** The phage gpIII is inserted into the inner membrane, and the cap of the phage head is opened to allow phage DNA to enter the bacteria (Karlsson et al., 2003).

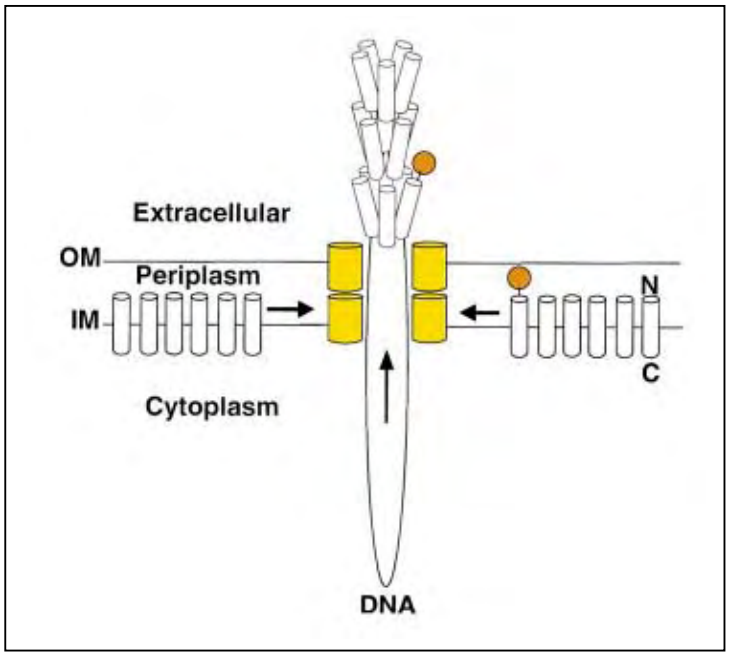

Figure 1.11 M13 bacteriophage assembly. Newly-synthesized coat proteins (white cylinders) are embedded into the inner membrane (IM) with their N termini in the periplasm and their C termini in the cytoplasm. Single-stranded viral DNA is extruded through a pore complex (yellow cylinders) that spans the inner membrane and the outer membrane (OM). Coat proteins also interact with the pore complex, where they surround the DNA and are thus transferred from the bacterial membrane into the assembling phage coat. The assembled phage particle is extruded to the extracellular environment. A heterologous protein (red circle) will be displayed on the phage surface if it is fused to a coat protein that can successfully incorporate into the phage coat (Sidhu, 2001).

1.2.4.4 Phagemid vector

Protein can be displayed using vectors based on the natural filamentous phage sequence (phage vector) or using plasmids that contain only the fusion phage gene and no other phage genes (phagemid vectors) (Lowman, 1997). Phagemids, a more popular vector for display, are designed to contain the origins of replications for both the M13 phage and *E. coli*, appropriate multiple cloning sites for insertion the gene of interest, and an antibiotic-resistance gene for selection and propagation as with typical phagemids (Barbas, 2001). Phagemids can be grown as plasmids or alternatively packaged as recombinant M13 phage with the aid of a helper phage that contains a slightly defective origin of replication (such as M13KO7 or VCSM13) and supplies, *in trans*, all the structural proteins and enzymes required for generating a complete phage. They also carry a kanamycin resistance gene to allow antibiotic selection of helper-infected cells. Thus almost the phage particles may incorporate either gpIII derived from the helper phage or the polypeptide-gpIII fusion protein, encoded by the phagemid. A major advantage of phagemid vectors is their small size and ease of cloning, compared with the difficulties of cloning in phage vector without disruption of the structure of gene and promoter. In addition, the large DNA inserts are more readily maintained by phagemid genomes than phage genomes. Two-gene display systems (Type 3+3 and 8+8 phagemid and Type 33 and 88 phage systems) allow modulation of the valency (i.e., the number of copies per phage particle, Table 2) of the displayed fusion protein. However, the ratios of polypeptide-gpIII fusion protein: wild type gpIII may range between 1:9 and 1:1000 depending on the type of

phagemid, growth conditions, the nature of the polypeptide fused to gpIII, and proteolytic cleavage of antibody-gpIII fusions (Azzazy and Highsmith, 2002).

Table 1.2 Classification of phage-display vectors.

Vector type	Coat protein used for display	Display on all or some copies of coat protein	Number of coat protein genes	Fusion encoded on genome of
3	pIII	All	1	phage
8	pVIII	All	1	phage
33	pIII	Some	2	phage
88	pVIII	Some	2	phage
3+3	pIII	Some	2	phagemid
8+8	pVIII	Some	2	phagemid

1.2.4.5 Applications of phage display

Since the phage display reported in 1985 (Smith, 1985), this technology has rapidly evolved into an efficient tool used by structural biologists for the discovery and characterization of diverse ligand-receptor-binding interactions. By this technique, the gene of interest is inserted between the C-terminal of the signal peptide and N-terminal coding region of phage coat protein. The recombinant proteins are synthesized in *E. coli* host together with other coat and accessory proteins of filamentous phage, and they will be incorporated into phage in the assembly process. The released phage particles expose the recombinant protein as a fusion product to one of the phage coat protein. By inserting different DNA fragments, a library of phage particles bearing different recombinant coat protein can be generated. Each phage particle contains only one type of recombinant coat proteins encoded by the corresponding gene fusion present inside the same phage particle. Individual phages can be rescued from libraries by an interaction of the displayed protein with the cognate ligand by a panning step, which allows to select of the hundreds of millions of clones, those few phages that display a peptide that binds the target molecule. These phages can be amplified by infection of bacteria. The recombinant polypeptides or proteins displayed on the phage surface can be used for identifying and characterizing the interaction with their binding targets (Cesareni, 1992).

Phage display of a functional protein has now become a standard first step of proof of principle prior to the application of combinatorial strategies using the cloned DNA template to evaluate or remold functional activity (Bass et al., 1990; Roberts et al., 1992). Even though a natural functional domain can represent the end

product of a highly directed evolutionary process, phage-display approaches can create variations of the domain with altered binding affinity or fine specificity, or with structural refinements that greatly enhance stability (Lowman et al., 1991; Lowman and Wells, 1993; Hao et al., 2008; Hoyer et al., 2008; Kwong et al., 2008; Berntzen et al., 2009; Hertveldt et al., 2009).

Advances in phage display and antibody engineering have led to the development of phage-displayed antibody technology (McCafferty et al., 1990; Sidhu, 2000). This technology allows one to isolate antibodies directly from diverse repertoires of antibody genes, generating high affinity binding sites and unique specificity (McCafferty et al., 1990; Winter et al., 1994; Neri et al., 1995; Hoogenboom et al., 1998). Phage antibody genes can be easily sequenced, mutated, and screened to improve antigen binding. The advantage of this technology can also be amplified immunoglobulin variable (V) genes from hybridomas or B lymphocytes using polymerase chain reaction (PCR) technology, cloned into phagemid vectors and rescued the monoclonal antibodies from genetically unstable hybridomas. Finally, soluble recombinant antibodies (not displayed on phage) can be produced rapidly and economically and can be used as *in vitro* diagnostic reagents. Various formats of antigen binding fragments, including Fab and scFv have been cloned and displayed on the surface of M13 viral particles with no apparent loss of the antibody's specificity and affinity as shown in **Figure 1.12** (Nissim et al., 1994; Azzazy and Highsmith, 2002). These antibodies have become important tools in several fields, including molecular biology (Kwong et al., 2008; Kato-Takagaki et al., 2009), pharmaceutical

and medical research (Sidhu, 2000), as well as in the treatment of diseases such as cancer (Schrama et al., 2006) and infectious diseases (Mullen et al., 2006).

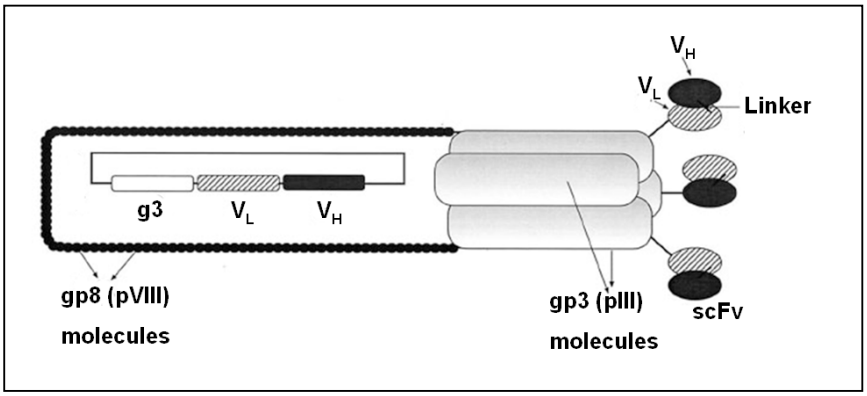

Figure 1.12 Schematic diagram of a filamentous phage displaying single chain variable fragment (scFv) molecules. The phage consists of circular ssDNA surrounded by a coat protein. The genes encoding the variable domains of the scFv and a linker are fused to gene III (g3) in the genome of the filamentous phage. Consequently, the scFv is displayed as a fusion to gp3 (gpIII) protein at the tip of the phage (Azzazy and Highsmith, 2002).

1.2.5 Intracellular antibody (Intrabody)

1.2.5.1 Introduction

Intrabodies are defined as antibody molecules which are expressed intracellularly and directed to defined subcellular compartments. Although mammalian cells are the most commonly used target cells (Williams and Zhu, 2006), expression of intrabodies is not restricted to these cells and a variety of other cell types, including plant cells (Tavladoraki et al., 1993; Tavladoraki et al., 1999), fungal cells (Carlson, 1988; Reinman et al., 2003), and even bacteria (Tavladoraki et al., 1999), have been used. The therapeutic concept of using intrabodies is based on the induction of a phenotypic knockout of a relevant target molecule either by directly inhibiting the function of the antigen or by diverting it from its normal intracellular location. In some cases, intrabodies have also been used to restore the function of a target antigen and thus rescuing a phenotype. Thus, intrabody therapy combines the specificity of antibodies with a gene-therapeutic strategy to selectively affect an intracellular target protein. In contrast to the direct administration of a therapeutic drug, this approach engages the cellular machinery to produce the therapeutic agent. As the intrabodies are produced only inside the cells, this strategy has advantages regarding safety and efficacy (Kontermann, 2004).

1.2.5.2 Antibody structure and format

The basic structure of antibodies (also called immunoglobulins; Igs) consists of two identical heavy and two identical light polypeptide chains. The chains are held together by disulfide bonds leading to a 'Y' shaped protein molecule (**Figure 1.13**). The most common immunoglobulin class is IgG. The amino-terminal protein

domains contain regions of highest sequence variability which mostly contribute to the antigen binding site. These regions, called complementary-determining regions (CDRs) enable the antibody to be specific for a particular target. The rest of the IgG is composed of constant domains that only vary between Ig classes.

Recombinant antibodies are finding an ever increasing number of applications in biotechnology and medicine. A variety of antibody formats have been employed, which reflect differences in the production method, the need for mono- or multivalency as well as the intended use (Worn and Pluckthun, 2001). Antibody formats smaller than the full IgG can be created by genetic engineering as shown in Figure 13. In particular, intrabodies are in the form of single-chain Fv (scFv) antibody fragment contains only the heavy variable domain (V_H) and the light variable domain (V_L) of a full immunoglobulin are fused *via* a peptide linker, generally (Gly4Ser)3, to create a single polypeptide (Williams and Zhu, 2006). This is the smallest antibody fragment which retains the binding specificity of the parental molecule as shown in **Figure 1.14**.

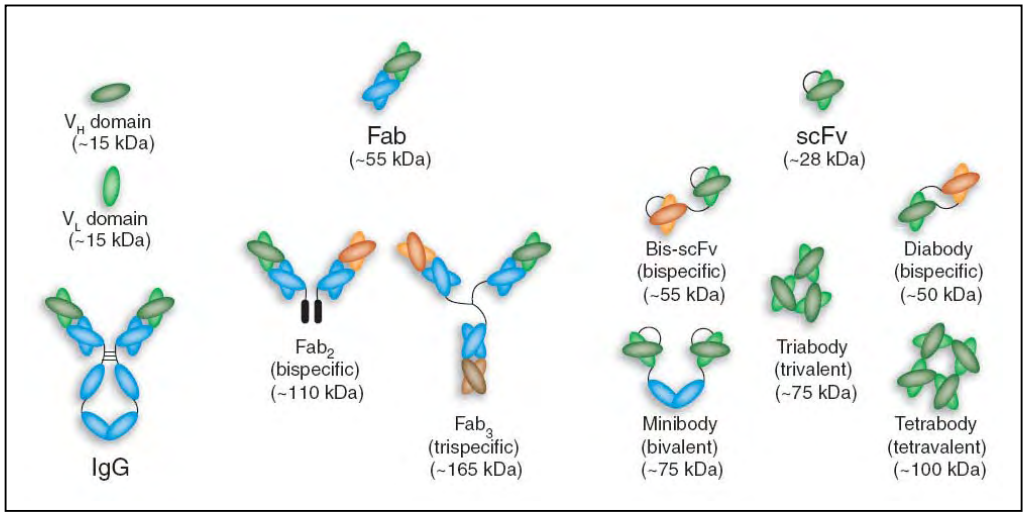

Figure 1.13 Schematic representation of different antibody formats, showing intact immunoglobulin G (IgG). A variety of antibody fragments are depicted, including Fab, scFv, single-domin V_H and multimeric formats, such as minibodies, bis-scFv, diabodies, triabodies, tetrabodies and chemically conjugated Fab' multimers. Sizes are approximately given in kilodaltons (kDa) (Holliger and Hudson, 2005).

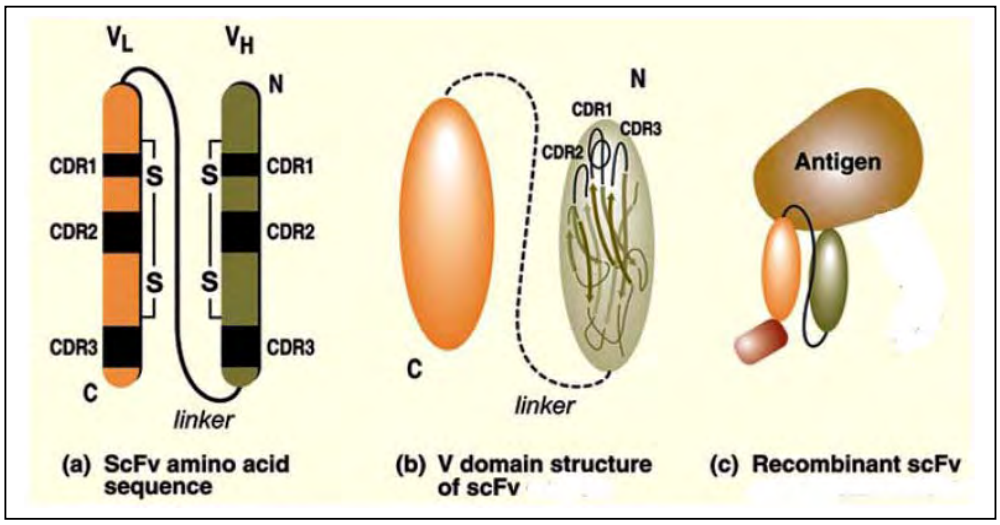

Figure 1.14 scFv fragment format. a) There are three hypervariable regions, the complementary determining regions (CDR), which change in size and sequence among different antibodies, determining the specificity of the antigen-antibody interactions. To facilitate expression of both V_H and V_L domains as single antibody fragments, a short linker peptide (Gly4Ser)3 is added between the carboxy-terminal (C) ends of V_H domain and the amino-terminal (N) of V_L domain. The locations of the cysteines implicated on the formation of the intra-domain disulfide bridge (-S-S-) are also indicated. **b)** The V domain structure of scFv. The structure of a scFv (with linker as dotted line) shows the outline structural representation of a single domain (in this case VH) indicating the three CDRs that determine the antigen specificity occurring in the loop regions**. c**) Schematic recombinant scFv intrabodies binding their antigen. The lighter ends of the V segments represent antigen-binding sites, and the various tags at the carboxy-terminal end, indicate additional protein domains or targeting signals which may add cellular localization signals (nuclear, cytoplasmic, endoplasmic reticulum) (Lobato and Rabbitts, 2004).

1.2.5.3 Mechanisms of action

Intrabodies, in their various forms, function by utilizing the antibody binding site coupled with a molecular tag to direct the antibody-antigen interaction to a specific cellular compartment, or by directly interfering with or neutralizing the function of a target as shown in **Figure 1.15**. Compartmental targeting is achieved through the use of N- or C-terminal tags that encode specific signal sequences used (Williams and Zhu, 2006). These signals allow the intrabody to enter cellular compartments it would not normally enter. As a result, the mechanisms through which intrabodies can achieve their therapeutic effect are expanded.

The most commonly used intrabodies can be targeted to the ER through the use of a leader sequence and an ER retention signal, such as the KDEL peptide, ensuring that they are retained within the ER–Golgi complex (Munro and Pelham, 1987). The purpose of these antibodies is usually to prevent secretion of target proteins, or the maturation of target proteins that would normally be expressed on the cell surface. Under most circumstances, protein secretion occurs *via* a forward pathway. Proteins are synthesized in the ER, transported to the cis-Golgi network (CGN) apparatus and secreted from the secretory vesicles that bud from the trans-Golgi network (TGN). However, there is also a retrograde pathway from the Golgi to the ER. Proteins that have the ER trapping signals can bind to ERD2.1 or ERD2.2 (ERD) and return to the ER. ERD exists in a nonbinding state in the forward pathway, but undergoes a conformational change to allow ligation of the KDEL sequence in the retrograde pathway. Retained proteins are degraded either within the ER by the non-lysosomal degradative pathway or by the cytoplasmic proteasome. The intrabody can

be targeted to the nucleus with a nuclear localization sequence (NLS) or to the mitochondria with appropriate signal sequences or to the cytosol by deleting the signal leader sequence. The intrabody may neutralize protein function, such as that of enzymes, or function primarily by trapping, rerouting, or enhancing the degradation of the target protein (Wheeler et al., 2003a; Boldicke, 2007).

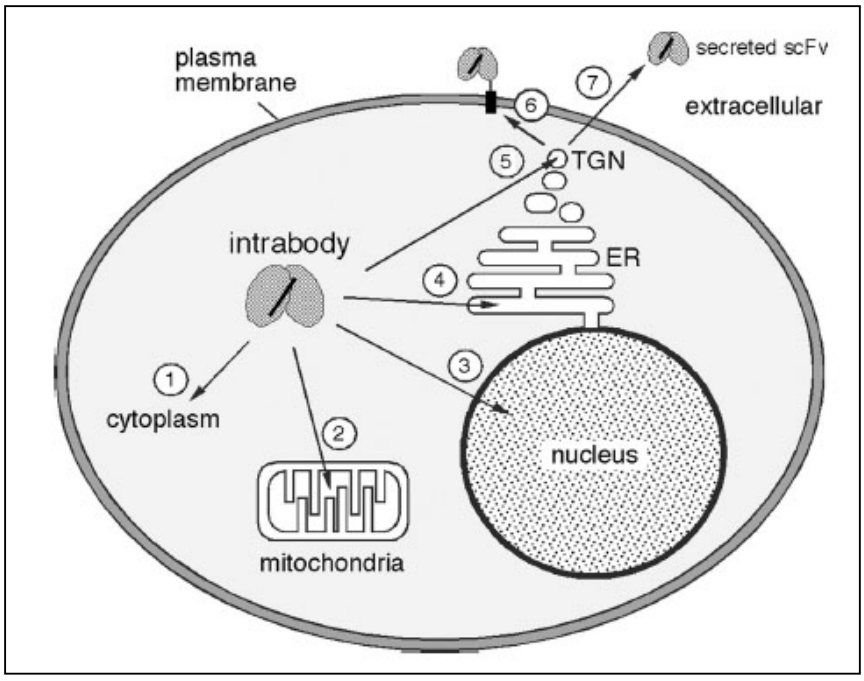

Figure 1.15 Subcellular location of intrabodies. Intrabodies have been expressed intracellularly and directed to the cytoplasm (1), mitochondria (2), the nucleus (3), the endoplasmic reticulum (4), the *trans*-Golgi network (TGN) (5), the plasma membrane (6), or secreted into the extracellular space (7) (Kontermann, 2004).

1.2.5.4 Intrabodies and their application

The use of an intrabody against an intracellular target was first described in 1988. Neutralization of yeast alcohol dehydrogenase I (ADH I) enzyme activity *in vivo* was observed using heavy and light-chain cDNAs expressed in *Saccharomyces cerevisiae* (Carlson, 1988). Recent studies have demonstrated that an intrabody strategy can successfully produce both phenotypic and functional knockouts of target molecules (Alvarez et al., 2000; Steinberger et al., 2000a; Wheeler et al., 2003b; Liu et al., 2005; Peng et al., 2007). This approach depends on a receptor-mediated system for retention of certain proteins within the endoplasmic reticulum. Intrabodies could be a useful tool not only for clinical applications such as neurologic disorders (Messer and McLear, 2006; Emadi et al., 2007; Lynch et al., 2008) and cancer therapy (Popkov et al., 2005; Griffin et al., 2006; Tanaka et al., 2007) but also for functional analysis of proteins inside the cells (Wheeler et al., 2003b; Boldicke et al., 2005; Doebis et al., 2006; Goenaga et al., 2007).

Intrabodies against several different HIV-1 proteins have been tested in cultured and primary human cell lines. These intrabodies have targeted the HIV-1 envelope protein gp120 by localizing the intrabody to the endoplasmic reticulum, the transcriptional regulatory proteins tat and rev by localizing the intrabodies to the cytoplasm or the nucleus, and the structural protein gp17. Notably, scFvs have been shown to reduce HIV viral production and the infectivity of released particles (Marasco et al., 1993; Mhashilkar et al., 1995; Marasco et al., 1998). Similarly, intrabodies have also been used to down-regulate the expression of CCR5 which is known as a co-receptor for HIV infection into macrophages. This CCR5-intrabody

efficiently blocked surface expression of human and rhesus CCR5 and thus prevented cellular interactions with CCR5-dependent HIV-1 and simian immunodeficiency virus envelope glycoprotein. Intrabody-expressing cells were shown to be highly refractory to challenge with R5 HIV-1 viruses or infected cells. These results suggest that deletion of the functional receptor or reduced expression of CCR5 should be beneficial in the treatment of HIV-1 disease (Steinberger et al., 2000a; Steinberger et al., 2000b).

Intrabodies are being developed to bind to, neutralize, or modify the function or localization of cancer-related targets and thereby affect the malignant phenotype. This has resulted in a promising new tool for the study and treatment of cancer. Their small size facilitates expression and assembly of functional molecules (Hudson, 1998). Growth factor receptors like erbB-2, transferrin receptor (TfR), vascular endothelial growth factor receptor 2 (VEGFR2) or epidermal growth factor receptor (EGFR) are the molecular targets thus far studied with the use of scFv (Lobato and Rabbitts, 2004). An anti-erbB-2 scFv construct containing an ER-directed leader sequence was transiently expressed in the human ovarian carcinoma cell line SKOV3 using the adenovirus-polylysine vector. This strategy can knock-out erbB-2 expression and induce a significant anti-neoplastic effect in ovarian cancer cells overexpressing this growth factor receptor. In addition, the ability to accomplish selective abrogation of erbB-2 expression in animal models and to transfect and eradicate primary ovarian cancer cells justifies further investigation of this novel strategy in ovarian cancer patients (Deshane et al., 1995a; Deshane et al., 1995b; Alvarez et al., 2000). Intrabodies have been also generated to a number of growth

factor receptors, such as VEGFR2 (Afanasieva et al., 2003; Boldicke et al., 2005; Jendreyko et al., 2005) and EGFR (Beerli et al., 1994; Jannot et al., 1996). They have been shown to markedly decrease the cell surface expression of the targeted receptor, leading to cell growth inhibition both *in vitro* and *in vivo* (Beerli et al., 1994; Jannot et al., 1996; Afanasieva et al., 2003; Boldicke et al., 2005). Likewise, intrabodies have been used to inhibit the proliferation of tumor cells. Peng et al. have been developed an anti-TfR scFv-intrabody (scFv-HAK) as a growth inhibitor of TfR overexpressing tumors. This intrabody was able to block surface expression of TfR in tumor cells MCF-7. Furthermore, expression of scFv-HAK can dramatically induce cell cycle G1 phase arrest and apoptosis of tumor cells, and consequently significantly suppress proliferation of tumor cells MCF-7 (Peng et al., 2007).

The application of intrabodies has more advantages than RNA interference (RNAi) since they possess a much longer active half-life compared to RNAi, and are also much more specific and affinity to their target molecules as shown in **Table 1.3** (Cao and Heng, 2005; Heng et al., 2005; Williams and Zhu, 2006). Furthermore it is possible to analyze the function of specific domains of a protein in its native environment without destroying the structure of the target protein. Binding of the antibody to an intracellular molecule directly has a potential to block, suppress, alter or even enhance the process mediated by that molecule. In particular, intracellular use of antibody fragments can offer an effective alternative to gene-based knockout technologies (Stocks, 2004). Therefore expression of intrabodies becomes a broadly applicable technology for probing the biological function of interested

protein. Therefore, this technique will be applied, in this study, for functional study of CD147 surface molecule.

Table 1.3 The properties of intrabodies and RNAi (Boldicke, 2007).

Intrabodies	**RNAi**
Prerequisite is a specific antibody	Prerequisite is the sequence of the mRNA or promoter of the target
Time consuming technology	Much less technical challenge
Very high specificity to the target	Non-specific effects
Long active half-life	Relatively short active half-life
Targeting of specific protein domains	Loss of multiple functions of the target
Inhibition of post-translational modifications	Not possible

1.2.5.5 Intrabody and gene delivery

A major goal is the development of vectors to selectively deliver the genetic material encoding the intrabody to a specific target cell type. There are two methods to transfer the intrabody genes into living cells *e.g.* non-viral or viral transfer systems. Non-viral vectors are often composed of cationic peptides, polymers, and lipids that interact with the negatively charged backbone of DNA to form nanometer sized particles that spontaneously transfect cells in culture (Bloomfield, 1996). At present, the main disadvantage is the low transduction efficiency and transient transgene expression, no specific cell targeting and difficult *in vivo* applications (Boldicke, 2007). Since, the intracellular dissociation and subsequent metabolism of a cationic peptide polymer leads to the release and premature metabolism of plasmid DNA by DNase leading to a low level and short duration of expression (Liu and Knapp, 2001). The enzymes responsible for the metabolism of peptide-mediated non-viral delivery systems are believed to be in the lysosomes (Wiethoff and Middaugh, 2003). However, recent evidence has implicated the involvement of the proteasome (Kim et al., 2005).

Traditionally, gene therapy approaches utilize viral infection to deliver the genetic material to the target cells. An advantage of this method can yield continuous expression of an intrabody to knock-out protein functions inside a target cell. Recombinant adenoviruses are attractive vectors for gene delivery. This DNA virus can infect a wide variety of cell types including dividing and quiescent cells and can be easily produced at high titer. The expression of the transgene is transient and the viral genome does not normally integrate into the host genome with no risk for

insertional mutagenesis (Robbins et al., 1998; Boldicke, 2007). Recombinant adenovirus have been successfully employed for *in vitro* transduction of ER intrabodies into cell lines (Wright et al., 1997; Mhashilkar et al., 2002) and primary cells (Wheeler et al., 2003b; Beyer et al., 2004). Conversely, retroviral vectors are not able to transduce non-dividing cells. Further disadvantages are low vector titer and low transfection efficiency and particle instability. Retroviral vectors are suitable for *ex vivo* gene therapy, and despite the disadvantages, retroviral gene delivery systems have been used already in a number of clinical trials (Rainov and Ren, 2003).

1.2.6 Adenovirus (Ad)

1.2.6.1 Biology of adenovirus

Adenovirus is an infectious agent that had been derived from human adenoids in 1953 by Rowe. Adenoviruses are widespread in many species and can be isolated from both sick and healthy individuals. Adenoviruses infections are mostly asymptomatic but may be associated with diseases of the respiratory, ocular and gastrointestinal systems. In 1962, Trentin reported that human adenovirus type 12 can cause tumors in newborn hamsters. However, later studies could not demonstrate any association with malignant disease in humans (Berk, 2007).

Adenoviruses are classified in two genera based on the basis of the presence of a genus-specific antigen: the mastadenoviruses that infect mammals and the aviadenoviruses with infecting birds. There are 51 immunologically distinct human adenovirus serotypes, further classified into 6 subgroups (A-F) (**Table 1.4**)

that can cause human infections ranging from respiratory disease, conjunctivitis, pharyngoconjunctival fever and gastroenteritis, but do not show oncogenic potential in humans. Adenoviruses are primarily spread *via* respiratory droplets, however they can also be spread by fecal routes (Russell, 2000; Majhen and Ambriovic-Ristov, 2006).

Table 1.4 Subgrouping of human adenoviruses: association with diseases

Subgroup	Serotypes	Syndrome
A	12, 18, 31	Gastroenteritis
B	3, 7, 11, 14, 16, 21, 34, 35, 50	Upper respiratory illness, conjunctivitis, cystitis
C	1, 2, 5, 6	Pharyngoconjunctival fever
D	8, 9, 10, 13, 15, 17, 19, 20, 22-30, 32, 33, 36-39, 42-49, 51	Epidemic keratoconjunctivitis, Immunocompromised host disease
E	4	Respiratory disease
F	40, 41	Gastroenteritis

The serotypic origin of the E1A gene determines the oncogenic phenotype of adenovirus-transformed cells. Viruses belonging to subgroup A (such as adenovirus 12, Ad12) induce tumors with high frequency and short latency, while viruses from subgroup B (such as Ad3 and Ad7) are weakly oncogenic. In harmless Adenoviruses from subgroup C (which includes the well studied serotypes Ad2 and Ad5), D, E and F are non-oncogenic (Russell, 2000).

1.2.6.2 Morphology and structure of adenovirus

The human adenoviruses are non-enveloped icosahedral particles approximately 90 nm in diameter, with fibers projecting from the vertrices of the icosahedron. Virions consist of a protein shell (capsid) surrounding a DNA-containing core. There are three major capsid proteins that make up the viral particle. Hexon is the most abundant structural component and constitutes the bulk of the mature virion. Five subunits of the penton base are found at each of the twelve vertices of the capsid and form the platform for the twelve fiber homo-trimers that protrude from the virion. At the distal tip of each linear fiber is a globular knob domain (**Figure 1.16A**) (Glasgow et al., 2004). The fiber is composed of three domains, an N-terminal domain that binds to the penton base (**Figure 1.16D**), central shaft with slight flexibility important for infection and a globular C-terminal knob that binds the primary receptor on host cells. The length of shaft varies among serotypes from six repeating units in Ad3 to 22 in Ad2 and Ad5. Adenoviral particles have no membranes or lipids and are therefore stable in chemical or physical agents and

adverse pH condition, allowing for prolonged survival outside of the body and water (Berk, 2007).

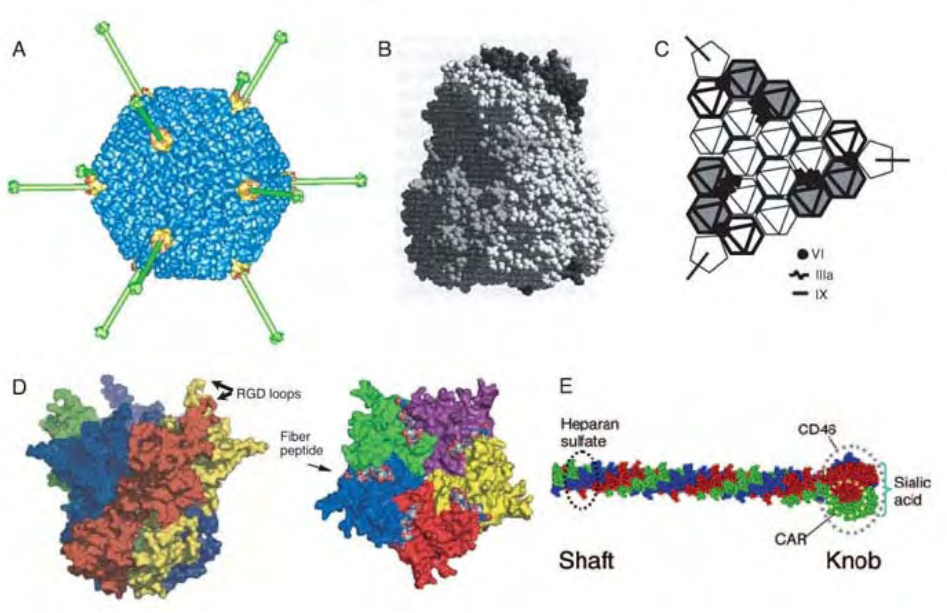

.**Figure 1.16 Adenovirus structure. A)** Model of the Ad2 virion from computer reconstruction of cryo-electron microscopic images. Each of the 20 triangular faces of the capsid is composed of 12 copies of the hexon trimer (blue). At each fivefold vertex, a fiber (green) emerges from the pentameric penton base (yellow). **B)** Space-filling model of the Ad5 hexon trimer. Each subunit is shown in a different shade. **C)** Schematic of the current model for the locations of polypeptides in one facet of the icosahedron. Hexons belonging to adjacent facets are shaded gray. Pentagon and bars represent penton bases and fibers. The minor coat proteins are depicted as shown in the key. **D)** Penton base viewed from the side (left) and top (right) and showing flexible RGD loops projecting from the surface. The insertion sites for fiber are also shown. **E)** Fiber structure and receptor binding sites. The fiber is a trimer whose monomers are indicated in red, blue, and green; the shaft is a tightly wound triple spiral; the knob is a more bulbous trefoil (Zhang and Bergelson, 2005).

1.2.6.3 Adenovirus genome

Adenoviruses are nonenveloped viruses possessing a double-stranded DNA genome. A virus-coded terminal protein is covalently linked to the 5'end of each DNA strand. The genome of the most commonly used human adenovirus (serotype 5) has 36-kb, and contains inverted terminal repetitions (ITRs) of 103 bp. In general, Ad composed of multiple copies of 11 different structural proteins, 7 of which form the icosahedral capsid (II, III, IIIa, IV, VI, VIII, IX) and 4 of which are packaged with the linear double-stranded DNA in the core of the particle (V, VII, μ and terminal protein) as shown in **Table 1.5**.

Table 1.5 Type of proteins in adenovirus capsid.

Name	Location	Known Functions
II	Hexon monomer	Structural
III	Penton base	Penetration
IIIa	Associated with penton base	Penetration
IV	Fiber	Receptor binding haemagglutination
V	Core associated with DNA and penton base	Histone-like; packaging?
VI	Hexon minor polypeptide	Stabilization/assembly of particle?
VII	Core	Histone-like
VIII	Hexon minor polypeptide	Stabilization/assembly of particle?
IX	Hexon minor polypeptide	Stabilization/assembly of particle?
TP	Terminal protein	Genome replication

As shown in **Figure 1.17**, Hexon bases are packed together to form a protein shell with 12 pentons at the apices of the icosahedral capsid. The positions of hexons (II), penton bases (III), fibers (IV) and protein (IX) are well established; 12 copies of polypeptides IX are found between 9 hexons in the center of each facet. The positions of proteins IIIa, VI and VIII are tentatively assigned. Two monomers of IIa appear to penetrate the hexon capsid at the edge of each facet. Multiple copies of VI form a ring underneath the peripentonal hexons. The 12 penton bases are formed by the interaction of 5 polypeptides (III) and are less tightly associated with the neighboring (peripentonal) hexons. Each of the vertex pentons carries 1 or 2 fibers, each consisting of 3 polypeptides (IV) that interact to form a shaft of characteristic length and a distal knob. Polypeptide VIII has been assigned to the inner surface of the capsid. Other polypeptides (monomers of IIIa, trimers of IX and multimers of VI) seem to interact with hexons to stabilize the capsid. The core consists of the DNA genome complexed with 4 polypeptides (V, VII, μ, TP).

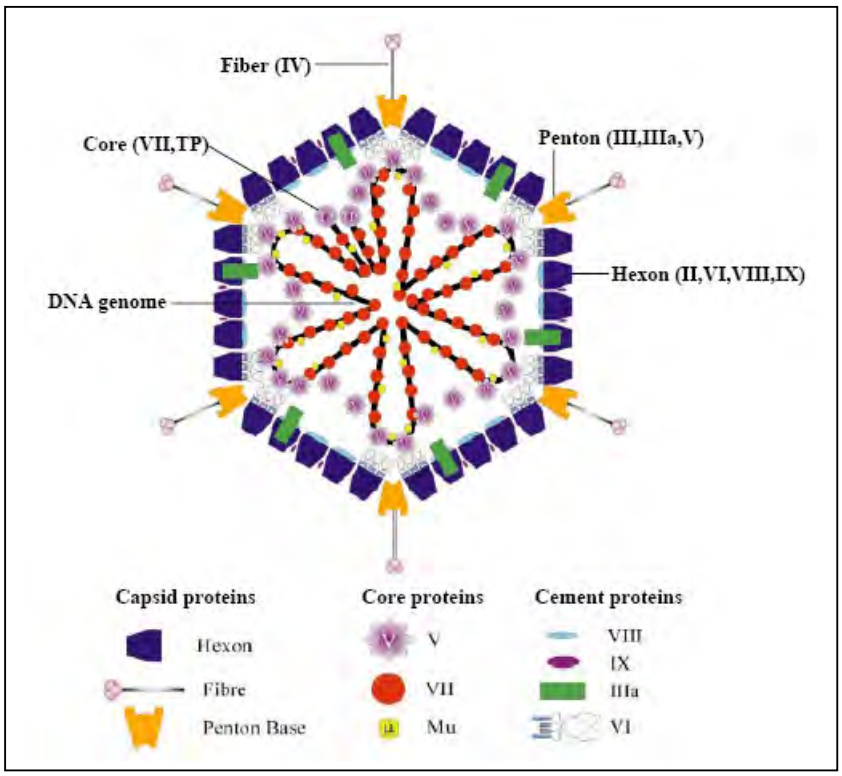

Figure 1.17 Schematic of adenovirus virion summarizing the current model for locations of polypeptides in the capsid and core of the particle.

1.2.6.4 Adenovirus entry

Adenovirus entry into cells, as defined by experiments with cultured cells, generally involves attachment to a primary receptor, followed by interaction with a secondary receptor responsible for internalization. The route of intracellular trafficking is influenced by the fiber knob and, thus, by interaction with a specific primary receptor. Many experiments demonstrate that the 46-kDa coxsackievirus B and adenovirus receptor (CAR), a member of the immunoglobulin superfamily, is the receptor for most Ads from subgroups A, D, E, and F, but not for subgroup B or the short fiber of subgroup F (Bergelson et al., 1997). Both human and mouse CARs have been identified. CAR is expressed on the surface of many cell types and is present within the tight junctions between polarized epithelial cells (Cohen et al., 2001). In addition, other receptors have been described such as α2 domain of the class I major histocompatibility complex (MHC-I) (Hong et al., 1997), heparan sulfate glycosaminoglycans (HS-GAGs) (Dechecchi et al., 2001), vascular cell adhesion molecule 1 (VCAM-1) (Li et al., 1993). In some cases, virus attachment may depend on direct interaction between the penton base and a cell surface integrin, without the need for a primary fiber receptor. Fiber-deficient Ad2 virions can infect CAR-negative monocytic cells by a mechanism that involves a primary attachment to integrins αMβ2 and αLβ2, followed by an interaction with αv integrins that is needed for internalization (Huang et al., 1996). After knob-CAR binding, receptor mediated endocytosis of the virion is affected by interaction of penton base Arg-Gly-Asp (RGD) motifs with cellular integrins $\alpha_V\beta_3$, $\alpha_V\beta_5$ or other integrins as shown in **Figure**

1.18 (Wickham et al., 1993; Wickham, 2000; Li et al., 2001). Once endocytosed, acidification of the endosome triggers a conformational change in the viral capsid, the virion is then released into the cytoplasm and translocated to the nucleus. The viral genome then enters the nucleus and from its episomal location undergoes transcription and then replication. Viral gene products are then produced in the cytoplasm following translation and capsid proteins localize to the nucleus where virus assembly occurs. Virus can then be released from the cell following lysis.

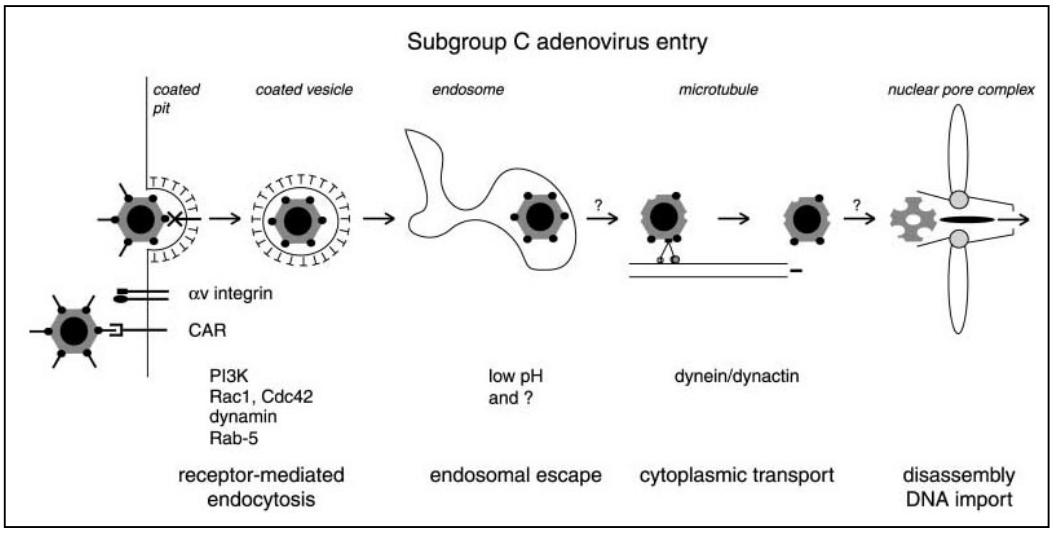

Figure 1.18 Illustration of subgroup C adenovirus entry. Ad-2 or Ad-5 bind to the coxsackievirus-adenovirus receptor (CAR) and the secondary receptor αv integrin and enter cells by receptor-mediated endocytosis *via* coated pits and coated vesicles. Early entry steps require PI3K, Rac1 and Cdc42, and also dynamin. Virus then escapes from endosomes by an unknown mechanism, somehow assisted by low pH. Cytosolic virus particles are transported by the dynein/dynactin motor complex along microtubules in the minus-end direction towards the nucleus. Nuclear pore complex-docked virus particles are dismantled, and the DNA genome is released into the nucleus (Greber, 2002).

1.2.6.5 Transcription and replication of adenovirus

Adenovirus transcription can be defined largely as a two-phase event, early and late, respectively occurring before and after virus DNA replication. Transcription is accompanied by a complex series of splicing events, with four early cassettes of gene transcription termed E1, E2, E3 and E4. The different transcripton units for the wild-type Ad5 are indicated by arrows (**Figure 1.19**). Inverted-terminal-repeat (ITR) sequences function as replication origins, and the ψ sequence is required for packaging of the viral genome. The viral genome is transcribed from both DNA strands by host cell enzymes (Russell, 2000).

The E1 gene products can be subdivided further into E1A and E1B. E1A itself has two major components sharing substantial stretches of sequence that are termed 289R (or 13S) and 243R (or 12S), based on the number of amino acid residues. These E1A proteins are primarily concerned with modulating cellular metabolism to make the cell more susceptible to virus replication. E1A proteins interfere with the processes of cell division and with the regulation of NF-κB and p53, and do this by a great variety of strategies involving both direct and indirect interaction with cellular proteins. They can also modulate transcription patterns in favour of virus transcription. Moreover, other virus gene products can modulate these cellular interactions significantly. For instance, the E4 gene products can co-operate with E1A to promote cell cycle-independent adenovirus growth (Goodrum and Ornelles, 1999). The E1B gene product 19K also seems to function cooperatively with E1A and p53 in promoting oncogenesis and transformation (Kannabiran et al., 1999),

mainly by ensuring that the downstream consequences of cell cycle release do not induce apoptosis.

The E1B 19K gene product is analogous to that from the cellular Bcl-2 gene. This gene product is concerned with prolonging cell survival by interacting and ablating members of the Bax family (whose transcription can be promoted by p53), which induce apoptosis and necrosis (Han et al., 1996).

The E2 gene products are subdivided into E2A (DBP) and E2B (pTP and Pol). These provide the machinery for replication of virus DNA (Hay et al., 1995) and the ensuing transcription of late genes, and this is mediated by interaction with a number of cellular factors. The E3 genes, which are dispensable for the replication of virus in tissue culture, provide the essential of proteins that subverts the host defense mechanisms. One of these E3 gene products has been termed the adenovirus death protein (ADP), since it facilitates late cytolysis of the infected cell and thereby releases progeny virus more efficiently (Tollefson et al., 1996). The gene products derived from the E4 cassette (termed orfs 1-6/7) mainly facilitate virus messenger RNA metabolism (sometimes in association with E1B gene products) (Goodrum and Ornelles, 1999) and provide functions to promote virus DNA replication and shut-off of host protein synthesis (Halbert et al., 1985). They are also associated with resistance to lysis by CTLs (Kaplan et al., 1999).

Adenoviruses also transcribe a set of RNAs that are not translated, termed the VA RNAs, and these play a role in combating cellular defense mechanisms. DNA replication begins from both DNA termini and requires sequences within the ITRs as origins of replication (Hay et al., 1995). Thereafter, late

transcription ensues, with five cassettes of transcripts (termed L1 to L5) resulting from a complex series of splicing events. These lead to the production of the virus structural components and the encapsidation and maturation of virus particles in the nucleus. A key player in the control of transcription is the major late promoter (MLP), which is attenuated during transcription of the early genes. However, it should be noted that there is a low basal level of late transcription occurring early in infection, even before the MLP comes into play. After the onset of virus DNA replication, the IVa2 and IX genes are expressed at high levels and transcription *via* the MLP is fully functional by specific activation. This is accomplished *via* the IX and IVa2 gene products (Lutz et al., 1997) and is also influenced by effective competition for the limiting transcription factors (Fessler and Young, 1998). The encapsidation process is governed by the presence in the virus DNA of a packaging signal at the conventional left end, which consists of a series of AT-rich sequences (Hearing et al., 1987). These events are accompanied by major changes in the nuclear infrastructure and the permeabilization of the nuclear membrane (Rao et al., 1996). At the very late stages of infection, when the cellular nucleus is packed full of virions, adenovirus synthesizes an ADP, which promotes cell lysis and thereby allows adenovirus to be released from cells and infect other cells.

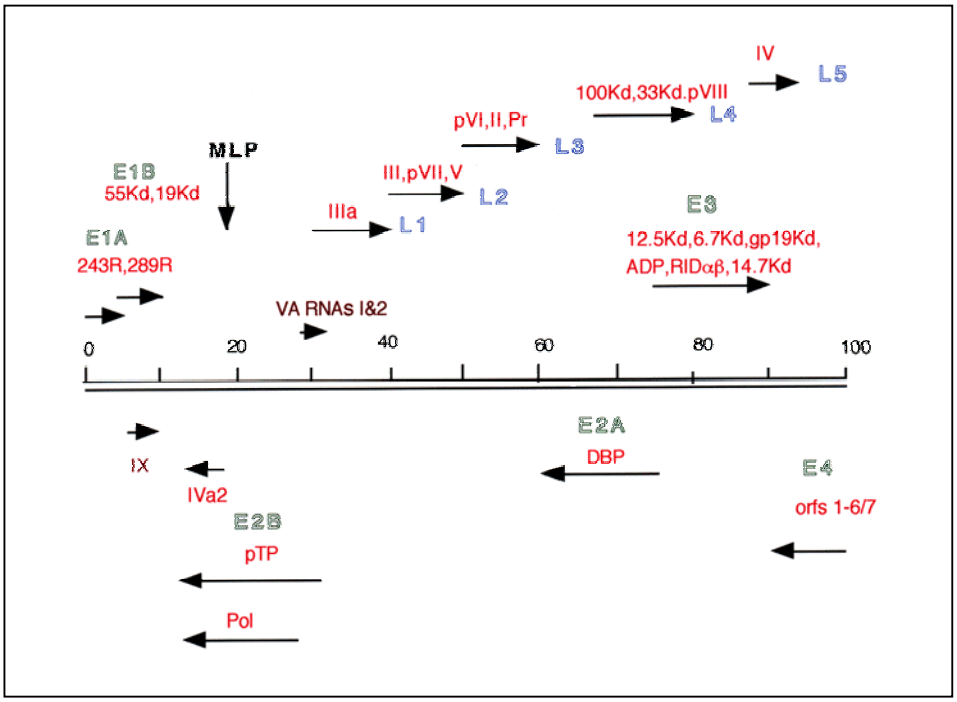

Figure 1.19 Transcription of the adenovirus genome. The early transcripts are outlined in green, the late in blue. Arrows indicate the direction of transcription. The gene locations of the VA RNAs are denoted in brown. MLP, Major late promoter (Russell, 2000).

1.2.6.6 Adenoviral vector for gene delivery

Gene delivery consists in introducing DNA and RNA into cells, tissues, or organisms, in order to study regulation and function of genes and proteins. The biggest hurdle that gene delivery technologies have to overcome is the cell membrane, which is impermeable to negatively charged macromolecules such as DNA and RNA. Several gene delivery systems are available. Retroviral vectors as well as nonviral gene transfer methods such as calcium phosphate coprecipitation, electroporation and liposomal transfection, target only a small fraction of cell population after extended selection periods, many of which, however, are not appropriate for transduction of human lymphocytes. Furthermore, expression levels are often low and insertion site-dependent silencing of the transgene expression is a frequent predicament (Doerfler et al., 1997; Baum et al., 2003; Hacein-Bey-Abina et al., 2003). In addition, the genome of retroviruses and lentiviruses is small, limiting the size of exogenous genes that can be packaged and transferred to target cells by the derivative vectors. Conversely, adenoviral vectors are an attractive alternative since they can efficiently transduce both dividing and non-dividing cells, and achieve transgene expression within hours (Nevins et al., 1997). Moreover, adenoviruses do not integrate into the host genome, thus leaving the genetic package of targeted cells unmodified. This results in reproducible gene expression levels and also eliminates any undesirable effects related to the site of integration, allowing the specific analysis of the transgene effects (Kay et al., 2001). This characteristic, together with their relative ease of preparation and purification, has led to their extensive use as gene transfer vectors.

The adenovirus group C (Ad2 and Ad5) is most commonly used as gene transfer vectors by deleting the E1 and/or E3 gene cassettes, allowing the introduction of up to 6.5 kb of foreign DNA, often under the control of a heterologous promoter. In the case of the E1 deletions, care was taken to ensure the retention of the ITR and the packaging sequences (ψ). The E1 deletion renders the viruses defective for replication and incapable of producing infectious viral particles in target cells. The El-, replication-defective virus can be propagated in a cell line that provides the El polypeptides *in trans*, such as the human embryonic kidney cell line, 293. A gene of interest (GOI) can be inserted by recombination in place of the El gene; expression is driven from either the El promoter or a heterologous promoter. In the case of the E3-deleted vectors, there were similar sequelae as a result of the elimination of the E3 gene-mediated defenses against host responses (Poller et al., 1996).

1.2.6.7 Adenoviral vector and their application

Recombinant adenovirus technology is largely used in gene therapy which aims at treating both genetic diseases such as cancer (Korn et al., 2004; Mizuguchi and Hayakawa, 2004; Tuve et al., 2007), cystic fibrosis (Driskell and Engelhardt, 2003; Griesenbach et al., 2006) and infectious diseases e.g. AIDS (Wu and Nemerow, 2004; Barouch and Nabel, 2005; Ura et al., 2008) by introducing new genetic material into selected cells. This technology is used to overexpress proteins of interest and to subsequently study their functions. In contrast to prokaryotic or insect cell-based systems, the use of human cells permits the complex post-translational

protein modifications required to ensure the proper folding and post-translational modifications of the protein.

Adenovirus type 2 and 5 (Ad2 and Ad5) are most commonly used as gene transfer vectors. The primary receptor responsible for attachment of all Ad serotypes except those from group B is the CAR and following knob-CAR binding, receptor mediated endocytosis of the virion is affected by interaction of penton base Arg-Gly-Asp (RGD) motifs with cellular integrins $\alpha_V\beta_3$, $\alpha_V\beta_5$ and/or other integrins. Unfortunately, Ad5 has been ineffective at infecting hematopoietic progenitor cells (HPC). Human hematopoietic cells including lymphocytes express low levels of CAR and $\alpha_V\beta_3$ integrins, which results in poor adenoviral transduction efficiencies (Neering et al., 1996; Rebel et al., 2000). In order to overcome the refractoriness of CAR-negative cells to conventional Ad vectors, several groups have developed several types of fiber-mutant Ad vectors (Mizuguchi et al., 2001; Mizuguchi and Hayakawa, 2002) and Ad vectors derived from other serotypes (Sakurai et al., 2003) which are able to transduce cells *via* CAR-independent pathways, leading to high transduction efficiencies even in CAR-negative cells.

Recently, it has been demonstrated that CD46 also acts as a receptor for the majority of subgroup B adenoviruses (Ads), including Ad serotypes 11 (Ad11) and 35 (Ad35) (Gaggar et al., 2003; Segerman et al., 2003). The fiber knob domain of Ad11 or Ad35 binds to short consensus repeats (SCRs) 1 and/or 2 in CD46 for infection (Fleischli et al., 2005; Gaggar et al., 2005; Sakurai et al., 2006). CD46 is a membrane glycoprotein that protects cells from complement damage. CD46 is also a

receptor for measles virus laboratory strains, for human herpes virus 6, and for certain pathogenic bacteria (Cattaneo, 2004). In humans, CD46 is expressed on all nucleated cells at a low level. Adenovirus serotype 5 (Ad5)-based vectors can be retargeted with fiber receptor specificity of serotype 35 adenovirus (Ad5/F35) and thereby bypass the insufficiency of the CAR on hematopoietic cells by utilizing CD46 as cellular receptor (Gaggar et al., 2003; Nilsson et al., 2004). This chimeric Ad5/F35 vector efficiently transduced human hematopoietic progenitor cells (Shayakhmetov et al., 2000), dendritic cells (Rea et al., 2001), primary human T lymphocytes and NK (Schroers et al., 2004), normal human B lymphocytes (Jung et al., 2005), primary chronic myeloid leukemia cells, chronic lymphocytic leukemia B cells (Nilsson et al., 2004), and B cell acute lymphoblastic leukemia cells (Yotnda et al., 2001).

1.3 Objectives

The ultimate goal of this study is to down-regulate the cell surface CD147 expression using intrabody technology. The studies provide insight into a better understanding of CD147 molecule. The specific aims of this study were as follows:

1. To generate the soluble form of scFv-M6-1B9 against CD147
2. To generate recombinant adenoviruses expressing scFv-M61B9
3. To assess the biological activity of scFv-M6-1B9 against CD147 as soluble form and intrabody

MATERIALS AND METHODS

2.1 Chemicals and equipments

Chemicals and equipments used in this study were shown in Appendix A and Appendix B.

2.2 *E. coli* strains and vectors

E. coli strains, TG-1 and HB2151 were kindly provided by Dr. A.D. Griffiths, MRC, Cambridge, UK. *E. coli* strains, Origami B and XL-1 Blue were purchased from Novagen (Madison, WI) and Stratagene (La Jolla, CA), respectively. The pComb3HSS, pComb3X, modified pAdTrack and pAdEasy vectors were generous gifts from Dr. Carlos F Barbas, The Scripps Research Institute, La Jolla, California, USA (Steinberger et al., 2000; Jendreyko et al., 2003). The pAK400cb vector was a kind gift from Dr. V. Santala (University of Turku, Finland). The modified pAdEasy-1/35 vector was generous gift from Prof. Xiaolong Fan (Nilsson et al., 2004), Department of Molecular Medicine and Gene Therapy, Lund University, Lund, Sweden.

2.3 Extraction and qualification of total RNA from M6-1B9 hybridoma cells

Hybridoma cells producing anti-CD147 mAb, M6-1B9 (isotype IgG3) was kindly provided from Prof. Dr. Watchara Kasinrerk, Division of Clinical Immunology, Department of Medical Technology, Faculty of Associated Medical Sciences, Chiang Mai University, Chiang Mai, Thailand (Kasinrerk et al., 1999).

Cells were cultured in Iscove's Modified Dulbecco's medium (Gibco, Grand Island, NY) supplemented with 10% fetal bovine serum (FBS) (Gibco), 40 μg/ml gentamicin and 2.5 μg/ml amphotericin B. Total RNA was extracted from 5×10^6 M6-1B9-producing hybridoma cells using TRIzol® (Invitrogen) according to the manufacturer's instructions. Initially, M6-1B9 hybridoma cells were washed and lysed by adding 1 ml TRIzol® reagent. Following homogenization, insoluble material was removed from the homogenate by centrifugation at 12,000 rpm for 10 min at 4 °C. The resulting pellet contains extracellular membranes, polysaccharides, and high molecular weight DNA, while the supernatant contains RNA. The supernatant was transferred to a new microcentrifuge tube and incubated the homogenized samples for 5 min at room temperature (RT) to permit the complete dissociation of nucleoprotein complexes. Two-hundred microliter of chloroform per 1 ml of TRIzol® reagent was added and tubes were shaken vigorously by hand for 15 sec and incubated them at RT for 2-3 min. Then, the sample was centrifuged at 12,000 rpm for 15 min at 4 °C. The aqueous phase (clear) was collected to a fresh microcentrifuge tube and 500 μl of isopropanol was added to precipitate the total RNA from the aqueous phase. The solution was mixed by inversion and incubated for 10 min at RT. Centrifugation was performed at 12,000 rpm for 10 min at 4 °C. The supernatant was discarded and the RNA pellet was washed once with 1 ml of 75% ethanol. Then the sample was mixed by vortexing and centrifuged at 7,500 rpm for 5 min at 4 °C. The RNA pellet was dried at RT for 5-10 min and finally dissolved in 20-30 μl of DEPC-treated water. The amount of the total RNA was determined by UV spectrophotometer (1 OD at 260 nm is equal to 40 μg/ml).

2.4 RT-PCR amplification of Fd heavy chain and κ light chain cDNA fragments

First stranded cDNA was generated from 1 μg total RNA using random primers for Fab fragment construction. The set of oligonucleotides were synthesized according to the genes coding the κ light chain and the Fd region of the IgG3 heavy chain as shown in **Table 2.1** *Xho*I and *Sac*I restriction sites were added to the sense primers of the heavy and light chains, respectively. The antisense primers were introduced the *Spe*I site for heavy chains and the *Xba*I site for light chains.

The PCR amplification was performed in 50 μl reactions. Both sense and antisense primers were used at a concentration of 10 μM. Fourty cycles of the PCR were done as follows: denaturation at 94 °C for 15 sec, annealing at 52 °C for 50 sec, and extension at 68 °C for 1 min. An initial cDNA synthesis of 30 min at 55 °C and follow with denaturation step of 2 min at 94 °C and a final extension step of 5 min at 68 °C were also included. The PCR products were electrophoresed on a 1.5% agarose gel, stained with ethidium bromide and photographed under UV illumination.

Table 2.1 A list of primers use for constructing the Fab anti-CD147 (M6-1B9) cDNA.

Primers	Sequences

Heavy-chain Fd 3’ primer	5’- GGG GGT act agt CTT GGG TAT TCT AGG CTC-3’
Heavy-chain variable 5’ primer	
Hc1	5’- AGG TCC AGC TGc tcg agT CTG G-3’
Hc2	5’- AGG TCC AGC TGc tcg agT CAG G-3’
Hc3	5’- AGG TCC AGC TTc tcg agT CTG G-3’
Hc4	5’- AGG TCC AGC TTc tcg agT CAG G-3’
Hc5	5’- AGG TCC AAC TGc tcg agT CTG G-3’
Hc6	5’- AGG TCC AAC TGc tcg agT CAG G-3’
Hc7	5’- AGG TCC AAC TTc tcg agT CTG G-3’
Hc8	5’- AGG TCC AAC TTc tcg agT CAG G-3’
Hc9	5’- AGG TII AIC TIc tcg agT CAG G-3’
Hc10	5’- AGG TII AIC TIc tcg agT CTG G-3’
Murine κ light-chain 3’ primers	5’- GCG CCG tct aga ATT AAC ACT CAT TCC TGT TGA A-3’
Murine κ light-chain 5’ primers	
Lc1	5’- CCA GTT CCg agc tcG TTG TGA CTC AGG AAT CT-3’
Lc2	5’- CCA GTT CCg agc tcG TGT TGA CGC AGC CGC CC-3’
Lc3	5’- CCA GTT CCg agc tcG TGC TCA CCC AGT CTC CA-3’
Lc4	5’- CCA GTT CCg agc tcC AGA TGA CCC AGT CTC CA-3’
Lc5	5’- CCA GAT GTg agc tcG TGA TGA CCC AGA CTC CA-3’
Lc6	5’- CCA GAT GTg agc tcG TCA TGA CCC AGT CTC CA-3’
Lc7	5’- CCA GTT CCg agc tcG TGA TGA CAC AGT CTC CA-3’

Footnote: Restriction enzyme recognition sites are designated in small letters, with actagt for *Spe*I, ctcgag for *Xho*I, tctaga for *Xba*I and gagctc for *Sac*I. I in primer sequences is stand for inosine.

2.5 PCR product purification by QIAquick Extraction kit

The DNA fragment was excised from the agarose gel with a clean-sharp scalpel. The gel slice was later weighted in a colorless tube and calculated the volume by 100 mg estimated 100 μl. Three volume of the QG buffer to 1 volume of gel was added to dissolute the gel. The mixture was further incubated at 50 °C for 10 min or until the gel was completely dissolved. After dissolution, the mixture was transferred to QIAquick spin column, which was placed on a 2 ml collection tube. To bind the DNA, the spin column was subsequently centrifuged at 13,000 rpm for 1 min. The flow through was discarded. The QIAquick spin column was washed using 750 μl of PE buffer and centrifuged another 2 times at 13,000 rpm for 1 min in order to eliminate the flow through solution. Finally, the DNA binding column was eluted using 30 μl of distilled water and spun at 13,000 rpm for 1 min. The size of DNA was checked by 1% agarose gel electrophoresis.

2.6 Construction of phagemid expressing Fab-M6-1B9

2.6.1 Construction of pComb3H-SS possessing heavy chain gene

The Fd heavy chain DNA fragments of PCR products were digested with *Spe*I and *Xho*I (Fermentas), and 100 ng of digested PCR products was ligated with 210 ng of *Spe*I/*Xho*I sites of the linearized phagemid expression vector pComb3HSS in a total volume of 20 μl with 5 units of T4 DNA ligase enzyme (Fermentas). The reaction mixture was incubated at 4 °C for 16 h. The ligated product was transformed into the competent *E. coli* XL-1 Blue (Stratagene, La Jolla, CA). The ligated DNA was co-incubated with 200 μl of cold-thawed $CaCl_2$ competent cells on

ice for 1 h. The mixture was transferred into cooled screw cap tube and subsequently shocked at 42 °C for 1.5 min, then abruptly chilled on ice for 1 min. Three milliliter Luria-Bertani (LB) broth without antibiotic was added and bacteria was further cultured with shaking at 120 rpm, 37 °C for 3 h. The transformed bacteria were centrifuged at 2,500 rpm, RT for 10 min and plated on LB agar containing 100 μg/ml of ampicillin. The plates were incubated at 37 °C for 14-16 h.

2.6.2 Phagemid purification by using alkaline lysis method

An ampicillin resistant colony was picked and grown in 3 ml of LB broth containing 100 μg/ml of ampicillin with vigorous shaking (180 rpm) at 37 °C for 8 h. Half of culture volume was centrifuged at 10,000 rpm, 4 °C for 5 min. The supernatant was discarded and the bacterial cell pellet was lysed by adding 100 μl of 1× glucomix-lysozyme and vortexed vigorously. Two hundred microliters of freshly prepared NaOH/SDS was added and mixed by inverting. Then, 150 μl of potassium acetate was added and gently mixed by vortexing. The solution was centrifuged at 10,000 rpm, 4 °C for 5 min for collecting the clear supernatant. Nine hundred microliters of absolute ethanol was added and kept on ice for 2 min. The DNA was spun down at 10,000 rpm, 4 °C for 5 min and discarded the supernatant. The DNA pellet was reconstituted by 100 μl of steriled DW and followed by adding 50 μl of 7.5 M ammonium acetate and incubated at -70 °C for 10 min. The supernatant was collected by centrifugation at 10,000 rpm at 4 °C for 5 min. Three hundred microliters of absolute ethanol was added to the solution and incubated at -70 °C for 10 min. The solution was spun down to harvest the pellet. The pellet was cleaned up with 1 ml 70% ethanol by centrifugation at 10,000 rpm, 4 °C for 10 min. The DNA pellet was

dried at 37 °C for 30 min, reconstituted with 30 µl of steriled DW and stored at -20 °C.

2.6.3 Characterization of recombinant clones

The purified phagemids were firstly checked by fractionating on 1% agarose gel electrophoresis. In order to verify the corrected *E. coli* clones, the purified phagemid from individual clone was characterized by digesting with *Spe*I and *Xho*I to identify the corrected band of insertion fragment. The PCR was used to confirm the corrected size of Fd heavy chain fragment. The newly constructed phagemid was named pComb3H-Fd.

2.6.4 Construction of pComb3H-Fd harboring light chain fragment

Phagemids containing the Fd heavy chain were prepared from overnight culture by QIAGEN Miniprep kit (Qiagen, Hilden, Germany) and digested with *Sac*I and *Xba*I restriction enzymes. The κ light chain fragments were also treated with the same restriction enzymes. After digestion, 1,200 bp light chain stuffer was removed by agarose gel extraction kit (Qiagen) and 4,000 bp linearized pComb3H-Fd was collected to further insert κ light chain. The ligation, transformation, phagemid purification of recombinant *E. coli* was performed as described above. Resriction fragment analysis of the purified plasmid was checked by *Sac*I and *Xba*I digestion. The PCR amplified product was checked for an insertion gene in the purified plasmid as described above. Finally, the DNA sequencing were prepared with specific reverse primers Hc1 (5'- AGG TCC AGC TGc tcg agT CTG G-3') and Heavy-chain Fd 3' primer (5'- GGG GGT act agt CTT GGG TAT TCT AGG CTC-3') for V_H and Lc7 primer (5'- CCA GTT CCg agc tcG TGA TGA CAC AGT CTC CA-3') and κ light-

chain primer (5'- GCG CCG tct aga ATT AAC ACT CAT TCC TGT TGA A-3') for V_L genes, using the ABI automatic sequencer (Perkins Elmer), following manufacturers' instructions. The newly constructed phagemid harboring κ light chain fragment was named pCom3H-Fab-M6-1B9.

2.6.5 Plasmid Mini Prep (Qiagen)

An amplicillin resistant colony was picked and grown in 3 ml LB broth with 100 ug/ml of ampicillin with vigorous shaking (200 rpm) at 37 °C for 8 h. Cell suspension was spun at 10,000 rpm, 4 °C for 5 min. The supernatant was discarded and the pelleted bacterial cells were resuspended in 250 μl Buffer P1. Two hundred and fifty microliters of Buffer P2 were added and gently inverted the tube 4-6 times until the solution becomes viscous and slightly clear. Then, 350 μl Buffer N3 was added and mixed the solution gently but thoroughly, immediately for 4-6 times. The solution was centrifuged at 13,000 rpm for 10 min. The supernatant was collected, applied to the QIAprep spin column and centrifuged for 1 min at 13,000 rpm. QIAprep spin column was washed by adding 750 μl Buffer PE and centrifuging for 1 min. The flow-through was discarded, and centrifuged for an additional 1 min to remove residual wash buffer. Finally the QIAprep column was placed in a new microcentrifuge tube. DNA was eluted by adding 50 μl steriled DW to the center of each QIAprep spin column. The column was standed for 1 min and centrifuged at 13,000 rpm for 1 min. The DNA was stored at -20 °C.

2.7 Conversion of a M6-1B9 specific Fab into a single chain antibody fragment (scFv)

IgG-specific variable heavy (V_H) and light (V_L) chain gene fragments from purified pCom3H-Fab-M6-1B9 were amplified using PCR system (Eppendorf, England) for 30 cycles in first round (at 94 °C for 15 sec, at 56 °C for 30 sec, at 72 °C for 90 sec and 10 min at 72 °C for final extension), with each sense and anti-sense oligonucleotide primers set in **Table 2.2**. The fragments were isolated from a 1.5% agarose gel with the QIAGEN PCR purification kit (Qiagen). Then fragments were used as templates for the second round of PCR amplification to extend a linker, V_H fragments used MSCVH14 and MSCG3_B primers, V_L fragments used OmpSeq and MSCJK5-BL primers, respectively (Barbas, 2001). The amplified V_H-linker and V_L-linker PCR products were combined in a PCR reaction mixture. Twenty cycles (at 94 °C for 15 sec, at 56 °C for 30 sec, at 72 °C for 2 min and final extension for 10 min at the same temperature) were performed. These were gel-purified, digested with *Sfi*I, cloned into phagemid vector pComb3X and transformed into electro-competent *E. coli* TG1. The electroporated cells were then grown and plated onto LB agar with ampicillin. Colonies bearing the pComb3X-scFv-M6-1B9 construct were confirmed by *Sfi*I restriction enzyme digestion and PCR. Finally, the inserted gene fragment was sequenced using an ABI 3100 automatic sequencer.

Table 2.2 A list of primer used for constructing the scFv-M6-1B9.

Primers	Sequences
Heavy-chain variable (V_H) primer sets :	
Sense primer: MSCVH14	5'- GGT GGT TCC TCT AGA TCT TCC CTC GAG GTR AAG CTT CTC GAG TC -3'
Antisense primer: MSCG3_B	5'- CCT GGC CGG CCT GGC CAC TAG TGA CAG ATG GGG CTG TTG TTG T -3'
Light-chain variable (V_L) primer sets **:**	
Sense primer: OmpSeq	5'- AAG ACA GCT ATC GCG ATT GCA G -3'
Antisense primer: MSCJK5-BL	5'- GGA AGA TCT AGA GGA ACC ACC CCC ACC ACC GCC CGA GCC ACC GCC ACC AGA GGA TTT CAG CTC CAG CTT GGT CCC -3'

2.8 Phage displaying scFv-M6-1B9 (or Fab-M6-1B9) *via* gpIII

2.8.1 Preparation of phage-displayed scFv-M6-1B9

A single colony of *E. coli* TG1 harboring pComb3X-scFv-M6-1B9 was chosen from an LB agar plate containing ampicillin for phage-displayed scFv-M6-1B9 preparation as previously described (Intasai et al., 2003). The transformed bacteria were grown in 10 ml of 2×TY broth containing ampicillin (100 μg/ml) at 37°C with shaking at 200 rpm. The precultured bacteria were subsequently transferred to the same medium containing 1% (w/v) glucose, 1 mM Isopropyl-β-D-thiogalactopyranoside (IPTG) and cultivated at 25 °C until the optical density at 600 nm (OD_{600}) reach 0.5. After induction, the bacterial culture was further infected with 10^{12} t.u./ml of VCSM13 helper phages and left at 37 °C for 30 min without shaking. Phage infected TG-1 was spun down at 3,000 rpm for 10 min at 4 °C. The pellet was resuspended in 30 ml 2×TY broth containing ampicillin (100 μg/ml) and kanamycin (70 μg/ml) and then transferred to 220 ml of the same broth and shaken at 180 rpm, 25 °C for 16 h.

2.8.2 Harvesting phage by polyethylene glycol (PEG) precipitation

Bacteriophage harboring scFv-M6-1B9 *via* gpIII was pelleted at 3,000 rpm, 4 °C for 30 min. The culture supernatant was further collected. The recombinant phages were harvested by 4% w/v of PEG 8,000 and 3% w/v of NaCl precipitation with shaking at 180 rpm, RT for 15 min or until PEG/NaCl completely dissolved. The supernatant was kept on ice for 30 min and centrifuged 10,800 rpm at 4 °C for 30 min. The pellet was air dried for 30 min and reconstituted with 2.5 ml of PBS pH 7.2.

The suspension was subsequently centrifuged at 12,000 rpm for 10 min at 4 °C. The supernatant was preserved in 30% glycerol and stored at -70 °C.

2.8.3 Phage displaying scFv-M6-1B9 titration by *E. coli* infection

A single colony of *E. coli* TG1 was inoculated into 10 ml 2×TY broth and grown at 37 °C until the OD_{600} reach 0.6. One microliter of phage-displayed scFv-M6-1B9 was added into 999 ml of PBS pH 7.2 (dilution $1:10^3$) and then 1 μl of mixture was added into 1 ml of cultured bacteria (dilution $1:10^6$) and incubated for 15 min. The infected *E. coli* TG1 was further diluted into 10^8 and 10^{10} in PBS pH 7.2. Fifty microliters of each dilution was plated onto LB agar containing 100 μg/ml ampicillin and incubated at 37 °C overnight. The ampicillin resistant colonies were counted and calculated for the phage concentration using the formula at below.

$$A = B \times C \times (1000/V)$$

A = The original amount of phage obtained from preparation process (CFU/ml)

B = The number of ampicillin resistant colonies

C = Titer of viral infected bacteria

V = Volume (μl) of viral infected bacteria

In addition, *E. coli* TG1 harboring pCom3H-Fab-M6-1B9 which used for phage-displayed Fab-M6-1B9 *via* gpIII preparation was performed with the same method as described in section 2.8.1 - 2.8.3.

2.9 Immunoassay for detection of phage expressing recombinant M6-1B9

2.9.1 Determination the reactivity of phage expressing M6-1B9 by ELISA

Fifty microliters of 10 μg/ml avidin in carbonate/bicarbonate buffer pH 8.6 were coated in microtiter plates (NUNC, Roskilde, Denmark) at 4 °C overnight. The plate was then blocked with 200 μl of 2% skimmed milk in PBS pH 7.2 and incubated for 1 h at room temperature (RT). The wells were washed five times with 0.05% Tween-20 in PBS pH 7.2. After washing, 50 μl of 100 μg/ml BCCP fusion proteins, *i.e.* CD147-BCCP or SVV-BCCP (Tayapiwatana et al., 2006) in 2% skimmed milk, was added and the mixture was incubated for 1 h at RT. Unbound antigen was washed out and 50 μl of phage-displayed scFv-M6-1B9 (or phage-displayed Fab-M6-1B9 and VCSM13 phage) were added and incubated in a moist chamber for 1 h at RT. The plate was washed thoroughly with 0.05% Tween 20 in PBS pH 7.2 for 5 times, and peroxidase-conjugated anti-M13 phage mAb (Amersham Pharmacia Biotech, Buckinghamshire, UK) was added to each well. Wells were then washed again prior to adding 100 μl 3, 3', 5, 5'-tetramethyl-benzidine (TMB) substrate. The OD at 450 nm was measured by an ELISA plate reader (TECAN, Austria) after adding 1 N HCl to stop the reaction. Monoclonal antibody M6-1B9 specific for CD147 was kindly provided by Prof. Dr. Watchara Kasinrerk, Division of Clinical Immunology, Department of Medical Technology, Facullty of Associated Medical Sciences, Chiang Mai University, Chiang Mai, Thailand (Kasinrerk et al., 1999) and used as an antibody control in the ELISA system.

2.9.2 Determination of phage expressing M6-1B9 by SDS-PAGE and Western immunoblotting

10^{13} t.u/ml of recombinant phage-displayed scFv-M6-1B9 (or phage-displayed Fab-M6-1B9 and VCSM13 phage) were separated by SDS-PAGE under reducing conditions on a 12% polyacrylamide gel. The sample were boiled for 5 min and loaded onto the well of SDS-PAGE. Electrophoresis was carried out by applying constant voltage at 100 Volts using 0.025 M Tris/glycine, pH 8.5 containing 0.1% SDS as an electrophoretic buffer. After electrophoresis, the separated proteins were blotted onto a polyvinylidene fluoride (PVDF) membrane. Blocking was performed for 2 h at room temperature with 5% skimmed milk in PBS pH 7.2 and further incubated with mouse anti-gpIII mAb (Exalpha Biologicals, Water town, MD) (dilution 1:2500) for 1 h. The membrane was washed five times with 0.05% Tween 20 in PBS pH 7.2 and then incubated with peroxidase-labeled goat anti-mouse immunoglobulins (KPL, Gaithersburg, MD) 1:8000 diluted in 5% skimmed milk in PBS pH 7.2 for 1 h. Unbound conjugate was washed out five times with 0.05% Tween 20 in PBS pH 7.2; the specific bands were visualized using an ECL chemiluminescent substrate detection system (Amersham Pharmacia) according to the manufacturer's protocol.

2.10 Preparation of soluble scFv-M6-1B9

E. coli TG1 harboring pComb3X-scFv-M6-1B9 was cultured in LB broth containing ampicillin and used for phagemid preparation by QIAGEN Miniprep Kit (Qiagen) (See in section 2.6.5). The phagemid, pComb3X-scFv-M6-1B9 was

transformed into the competent the non-suppressor *E. coli* strain HB2151 and incubated on ice for 1 h. The mixture was transferred into cooled screw cap tube and subsequently shocked at 42 °C for 1.5 min, then abruptly chilled on ice for 1 min. Three milliliters LB broth without antibiotic was added and bacteria was further cultured with shaking at 120 rpm, 37 °C for 3 h. the transformed bacteria was centrifuged at 2,500 rpm, RT for 10 min and plated on LB agar containing 100 μg/ml of ampicillin. The plates were incubated at 37 °C for 14-16 h. A single colony of transformed bacteria were grown in 10 ml of SB broth containing ampicillin (100 μg/ml) at 37 °C for 18 h. Ten microliters of precultured bacteria were subsequently transferred to 10 ml of the same medium containing 1% (w/v) glucose and ampicillin (100 μg/ml), then cultivated at 37 °C until the absorption at 600 nm reached 0.5. The precultured bacteria were then transferred to 90 ml of the same medium and cultivated at the same temperature until the OD_{600} reached 1.5. Then, IPTG was added to the culture at a final concentration of 1 mM. After induction, the bacteria were grown at 25 °C for 20 h. Cells were centrifuged at 15,000 g for 30 min at 4 °C to collect the supernatant (containing extracellular soluble scFv). Protein was precipitated with saturated $(NH_4)_2SO_4$ in an ice bath and concentrated with Amicon Ultra centrifugal filter units (Millipore, Cork, Ireland). Finally, the concentrated protein was reconstituted with 500 μl of 0.15 M PBS, pH 7.2.

2.11 Immunoassay for detection of the antigen- binding affinity of soluble scFv-M6-1B9

2.11.1 Binding assay of soluble scFv-M6-1B9 by ELISA

Fifty microliters of 10 μg/ml avidin in carbonate/bicarbonate buffer pH 8.6 were coated microtiter plates and incubated at 4°C overnight. The plates were then blocked with 200 μl of 2% bovine serum albumin (BSA) in PBS pH 7.2 for 1 h at RT. The wells were washed five times with 0.05% Tween-20 in PBS pH 7.2 and 50 μl of 100 μg/ml BCCP fusion proteins (Tayapiwatana et al., 2006) in 2% BSA were added and incubated for 1 h at RT. The unbound antigen was washed out. Fifty microliters of scFv-M6-1B9 at various dilutions were added and incubated in a moist chamber for 1 h at RT. The plates were washed thoroughly with 0.05% Tween 20 in PBS pH 7.2 for 5 times. Peroxidase-conjugated mAb anti-HA (Roche, Indianapolis, IN) was diluted to 1:100 and added to each well. The wells were then washed again prior to adding 100 μl TMB substrate and the OD at 450 nm measured after adding 1 N HCl to stop the reaction. mAb M6-1B9 was used as an antibody control in the ELISA system.

2.11.2 Competitive binding analysis of soluble scFv-M6-1B9 and mAb M6-1B9

Fifty microliters of 10 μg/ml avidin in carbonate/bicarbonate buffer pH 8.6 were coated microtiter plates and left overnight at 4 °C. The plate was then blocked with 200 μl of 2% BSA in PBS pH 7.2 for 1 h at RT. The wells were washed 5 times with 0.05% Tween-20 in PBS pH 7.2. Fifty microliters of 100 μg/ml BCCP fusion proteins in 2% BSA were added and incubated for 1 h at RT. The unbound

antigen was washed out. Fifty microliters of the mixture containing soluble scFv-M6-1B9 at dilution 1:250 and 20 μg/ml mAb M6-1B9 or mAb against survivin (MT-SVV3) at ratio 1:1 were added. After incubation in a moist chamber for 1 h at RT, the plate was washed thoroughly with 0.05% Tween 20 in PBS pH 7.2 for 5 times. Peroxidase-conjugated mAb anti-HA was diluted to 1:100 and added to each well. The wells were then washed again prior to adding 100 μl TMB substrate. The OD at 450 nm was measured after adding 1 N HCl to stop the reaction.

2.11.3 Culture of the human monocytic cell line (U937)

The human monocytic cell line (U937) was kindly provided from Prof. Dr. Watchara Kasinrerk, Division of Clinical Immunology, Department of Medical Technology, Faculty of Associated Medical Sciences, Chiang Mai University, Chiang Mai, Thailand. U937 cells were cultured in RPMI 1640 medium (Gibco), 10% FBS, penicillin (100 Units/ml), and streptomycin (100 μg/ml) and maintained in a humidified atmosphere of 5% CO_2 at 37°C.

2.11.4 Immunofluorescence analysis of the reactivity of soluble scFv-M6-1B9

U937 cells were adjusted to 1×10^7 cells/ml with 1% BSA-PBS-NaN_3 and blocked on ice with human AB serum at the ratio of 1:10 for 30 min. Fifty microliters of 1:10 dilution in 1% BSA-PBS-NaN_3 of soluble scFv-M6-1B9 were added to 50 μl of blocked cells and incubated on ice for 30 min. Cells were washed twice with 1% BSA-PBS-NaN_3. Subsequently, fifty microliters of 20 μg/ml mouse anti-HA-biotin (Sigma, St Louis, MO) were added and the cells were incubated on ice for 30 min. After washing, cells were resuspended with 20 μl 1% BSA-PBS-NaN_3.

FITC-conjugated sheep anti-mouse immunoglobulins antibody (Chemicon International, Melbourne, Australia) was then added. Cells were incubated on ice for another 30 min. Finally, cells were washed 3 times with 1% BSA-PBS-NaN_3 and fixed with 350 µl of 1% paraformaldehyde-PBS. Fluorescence reactivity of soluble scFv-M6-1B9 with CD147 on U937 cells was analyzed by flow cytometry.

2.11.5 Immunoblot analysis

To determine the binding activity of soluble scFv-M6-1B9, BCCP fusion proteins were separated in 12% polyacrylamide gel under reducing condition. The separated proteins were electroblotted onto polyvinylidene fluoride (PVDF) membrane for Western immunobloting. Blotted membrane was blocked at 4 °C overnight in 5% skimmed milk in PBS pH 7.2 and then incubated with the HRP-conjugated anti-HA antibody diluted in 5% skimmed milk in PBS pH 7.2 for 1 h at room temperature on a shaking platform. After washing step, the immunoreactive bands were then visualized by chemiluminescent substrate detection system.

2.11.6 Peripheral blood mononuclear cells isolation

For separation of peripheral blood mononuclear cells (PBMCs) from whole blood the density gradient centrifugation is performed. PBMCs were prepared by density centrifugation over IsoPrep solution (Robbins Scientific Corporation, Sunnyvale, CA). Twenty milliliters of heparinized blood were diluted with PBS pH 7.2 to 20 ml total volume. Two 50 ml tubes were filled with 10 ml IsoPrep each. Twenty milliliters of diluted cell suspension were over-layered on top of each 10 ml of IsoPrep. The tubes were spun at 1,500 rpm for 30 min without breaking. The white blood cell ring fractions from each tube were transferred to a new 50 ml tube using

steriled Pasteur's pipette. Cells were washed with 20 ml of PBS pH 7.2 for three times at 1,500 rpm for 10 min. The pellet was resuspended in 1 ml RPMI 1640 medium (Gibco), 10% FBS, penicillin (100 Units/ml), and streptomycin (100 μg/ml and counted the cell viability. The PBMCs were maintained in a humidified atmosphere of 5% CO_2 at 37°C.

2.11.7 Cell proliferation assay

Cell proliferation was assessed using 5-carboxyfluorescein diacetate succinimidyl ester (CFSE) labeling. PBMCs were washed with PBS for 3 times and adjusted into 1×10^7 PBMCs/ml with PBS. CSFE (Molecular Probes, Eugene, OR) in the form of 5 mM stock solution in DMSO was added at final concentration of 0.5 μM for 10 min at 37 °C. To determine the effect of soluble scFv M6-1B9 on T-cell proliferation, triplicate aliquots of 1×10^5 PBMCs were cultured with immobilized CD3 mAb OKT3 (20 ng/ml) in the presence or absence of CD147 mAb clone M6-1B9 or soluble scFv M6-1B9. The culture was incubated for 5 days in a 5% CO_2 incubator at 37 °C. Cells from each treatment group were then washed twice with PBS, fixed with 1% formaldehyde in PBS and analyzed by a FACSCalibur flow cytometer (Becton Dickinson, Sunnyvale, CA).

2.12 Generation of recombinant adenoviruses expressing scFv-M61B9

2.12.1 Assembly of intrabody construct in pAdTrackCMV

The scFv coding regions were flanked by a human κ light chain leader sequence at the 5'-end, and a sequence encoding the HA tag (YPYDVPDYA) and the

ER retention signal (KDEL) at the 3'-end. The intrabody coding regions from pComb3X-scFv-M6-1B9 were then excised by digestion with *Sfi*I and cloned into modified pAdTrackCMV (Steinberger et al., 2000) and named pAdT-scFv-M6-1B9. This adapter fragment contains compatible *Sfi*I sites, which were used for cloning the scFv-M6-1B9 intrabody against CD147 into the adenovirus vector. The plasmid was transformed into the competent *E. coli* XL-1B and used for plasmid preparation by QIAGEN Miniprep Kit (Qiagen) as mentioned in section 2.6.5. Restriction enzyme analysis with *Sfi*I was verified the ligation.

2.12.2 ***Pme*I linearlization of the pAdT-scFv-M6-1B9** (He et al., 1998; Luo et al., 2007)

Four microgram of pAdT-scFv-M6-1B9 (a shuttle vector plasmid) was linearized with *Pme*I. The linearization was proceeded at 37 °C for 3 h. The linearized plasmid DNA was isolated and purified with QIAGEN Miniprep kit (See section 2.6.5).

2.12.3 Preparation of *E. coli* BJ5183 competent cells

The *E. coli* strain BJ5183 cells were prepared by using $CaCl_2$ method. An ampicillin resistant colony was selected from plate and further cultured at 37 °C for 8 h in 10 ml of LB broth containing 100 µg/ml ampicillin. The cultured bacteria were further pelleted at 2,500 rpm, 4 °C for 10 min and reconstituted by 10 ml of 0.1 M $CaCl_2$ at 4°C. Two rounds were repeatedly performed. Finally, the suspended bacteria were pelleted and further resuspended by 2 ml of 0.1 M $CaCl_2$. The BJ5183 competent cells were added by 0.4 ml of 85% glycerol and stored at -70°C.

2.12.4 Co-electroporation of pAdT-scFv-M6-1B9 and pAdEasy-1 vectors

The linearized and purified pAdT-scFv-M6-1B9 vector was co-electroporated with 100 ng of supercoiled pAdEasy-1 (Adenoviral backbone vector) in a total volume of 6.0 μl. Twenty microliters of electrocompetent *E. coli* BJ5183 cells were added, and electroporation was performed in 2.0 mm cuvettes at 2,500 V, 200 ohms, and 25 mF in a Bio-Rad Gene Pulser electroporator (**Figure 2.1**). The cells were immediately placed in 500 μl of SOC-medium and grown at 37 °C for 20 min with shaking at 200 rpm. One hundred twenty-five microliters of the cell suspension was plated on LB agar containing 50 μg/ml of kanamycin. After 16–20 h growth at 37 °C, 10-20 smallest colonies (which usually represented the recombinants) were picked and grown in 3 ml of LB broth containing 50 μg/ml of kanamycin. The plasmid DNA isolation and purification were performed with QIAGEN miniprep kit. Clones were first screened by analyzing their supercoiled sizes on agarose gels, comparing them to pAdEasy-1 control.

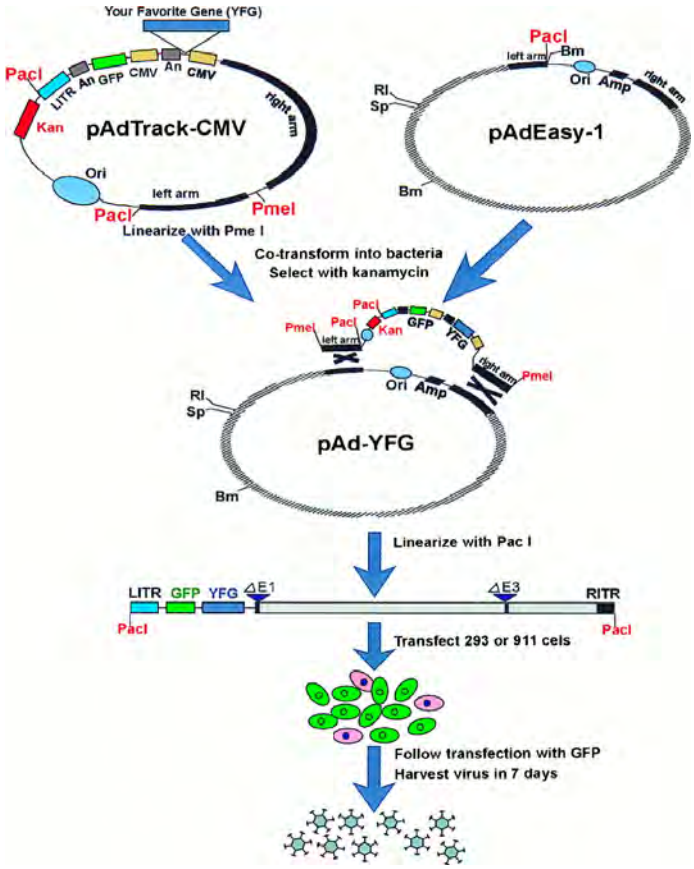

Figure 2.1 Schematic outline of the AdEasy system. The gene of interest is first cloned into a shuttle vector, *e.g.* pAdTrack-CMV. The resultant plasmid is linearized by digesting with restriction endonuclease *Pme*I, and subsequently cotransformed into *E. coli* BJ5183 cells with an adenoviral backbone plasmid, *e.g.* pAdEasy-1. Recombinants are selected for kanamycin resistance, and recombination confirmed by restriction endonuclease analyses. Finally, the linearized recombinant plasmid is transfected into adenovirus packaging cell lines, *e.g.* 293 cells. Recombinant adenoviruses are typically generated within 7 to 12 days. The left arm and right arm represent the regions mediating homologous recombination between the shuttle vector and the adenoviral backbone vector (He et al., 1998).

2.12.5 *Pac*I restriction analysis of pAdEasy-1 vector containing scFv-M61B9 gene

Three hundred nanograms of the purified vectors were digested with 5 U of *Pac*I at 37 °C for 3 h. The digested DNA fragments were checked by fractionating on 1% agarose gel electrophoresis to identify the band of corrected insert.

2.12.6 Electroporation of the recombinant pAdEasy-1 vector into *E. coli* DH10B

Those clones that had inserts were confirmed and electroporated into *E. coli* DH10B. One microliter of a 1:50 dilution of recombinant construct DNA was electroporated into 50 µl competent *E. coli* DH10B cells under conditions as described in section 2.12.4. One milliliter prewarmed SOC medium was added immediately and suspension was incubated at 37 °C for 1 h with shaking at 200 rpm. One hundred microliter cells were plated on LB agar containing 50 µg/ml of kanamycin and grown at 37 °C for overnight. At the following day two clones were picked, cultured in 10 ml SB medium containing 50 µg/ml of kanamycin and grown at 37 °C with shaking at 200 rpm for overnight. The plasmid DNA isolation and purification were performed with QIAGEN Midi prep kit. The DNA concentration was measured by spectrophotometry. The recombinant adenoviral vector DNA containing scFv-M61B9 gene was named pAdE-scFv-M6-1B9.

2.12.7 Purification of pAdE-scFv-M6-1B9 vector by using QIAGEN Plasmid Midi Kit

A single colony of transformant was picked and inoculated with a starter culture of 2-5 ml LB medium containing kanamycin (70 µg/ml). After incubation at 37 °C for 8 h with vigorous shaking, two hundred microliters of the starter culture was further grown in 100 ml of LB medium containing kanamycin (70 µg/ml) at 37 °C for 16 h with vigorous shaking. The bacterial cells were harvested by centrifugation at 6000 g at 4 °C for 15 min. The bacterial pellets were resuspended in 4 ml of P1 buffer. The bacteria were completely resuspended leaving no cell clump. The P2 buffer of 4 ml was added and the mixture was gently mixed but thoroughly by inverting for 4-6 times. The mixture was incubated at room temperature for 5 min. Four microliters of chilled P3 buffer were added to the lysate. The mixture was mixed immediately and gently by inverting for 4-6 times and poured into the barrel of the QIAfilter cartridge. The cartridge was incubated at RT for 10 min. A QIAGEN-tip 100 was equilibrated by applying 10 ml of QBT buffer. The column was allowed to empty by gravity flow. The cap from the QIAfilter nozzle was removed. The plunger was gently inserted into the QIAfilter. The cell lysate was filled into the previously equilibrated QIAGEN-tip until lysate passing through the QIAfilter cartridge. Approximately 10 ml of the lysate were generally recovered after filtration. The clear lysate was allowed to enter the resin by gravity flow. The QIAGEN-tip was washed twice with 10 ml of QC buffer. The QC buffer was allowed to move through the QIAGEN-tip by gravity flow. The DNA was eluted with 5 ml of QF buffer. The eluate was collected in a 10 ml tube. To precipitate DNA, 3.5 ml of isopropanol was

added to the eluted DNA at room temperature. After mixing and centrifuging immediately at 15,000 g for 10 min, the supernatant was carefully decanted without disturbing the pellet. The pellet was dried for 10 min and re-dissolved in suitable volume of DW.

2.12.8 Detection of pAdE-scFv-M6-1B9 by using polymerase chain reaction (PCR)

Twenty five nanograms of the pAdE-scFv-M6-1B9 vectors were amplified with 125 ng of each primer in a 20 µl of PCR mixture containing 2.5 U Taq polymerase (Eppendorf). The pAdE-scFv-M61B9 was proved with sense primer (ScFvM6cyt: 5'-GAG GAG GAG GTG TCG ACA TGG TGA TGA CCC AGA CTC C-3') and anti-sense primer (SVV3_Rcy: 5'-GAG GAG GAG CTG CGG CCG CTT AAG CGT AGT CCG GAA CGT C-3'). The amplification condition was initiated with jump start at 95 ℃ for 5 min followed by 35 rounds of 3 steps amplification: denaturation at 95 °C for 50 sec, annealing at 68 °C for 50 sec and extension at 72 °C for 1.5 min. Finally, the mixture was extended at 72 °C for 10 min. The amplified product was checked for the correct molecular size by 1% agarose gel electrophoresis (Pingmuang, 2008).

2.12.9 *Pac*I linearization of the pAdE-scFv-M6-1B9

One microgram of pAdE-scFv-M6-1B9 vector containing scFv-M61B9 gene was digested with 10 U of *Pac*I at 37 °C for 16 h. The *Pac*I digestion was heat inactivated at 70 °C for 10 min and stored at -20 °C.

2.12.10 Culture of an embryonic human kidney cell line (293A)

An embryonic human kidney transformed carrying sheared human adenovirus type 5 DNA cell line (293A)(Invitrogen, Carlsbad, CA) was cultured in Dulbecco's modified Eagle's medium (DMEM) supplemented with 10mM nonessential amino acids, 10% fetal bovine serum, penicillin (100 U/ml) and streptomycin (100 µg/ml). The cell line was maintained in a humidified atmosphere of 5% CO_2 at 37°C. Low passage 293 cells (less than passage 40) and high passage 293 cells were kindly obtained from Prof. Dr. Andre Lieber, University of Washington, Seattle, Washington, USA. Both cell lines cells were maintained in the same medium.

2.12.11 Transfection of 293A cells with *Pac*I linearized pAdE-scFv-M6-1B9

6×10^4 293A cells in 500 µl DMEM containing 10% FBS and antibiotics were plated on a polystyrene 24-well plate for 24 h before transfection, by which time they reached 60–70% confluence. Cells were washed once with 1 ml of DMEM (Gibco). Six micrograms of *Pac*I linearized pAdE-scFv-M6-1B9 were used for transfection. A transfection mixture was prepared by adding 1 µg of linearized pAdE-scFv-M6-1B9 DNA and 0.25 µl of Transfectin (Biorad) to 100 ul of DMEM (Gibco). After incubation at RT for 30 min, the transfection mixture was added to the cells. After 4–6 h in a humidified atmosphere of 5% CO_2 at 37 ^oC, the media containing the transfection mixture was removed and added 500 µl of prewarmed DMEM. The culture medium containing recombinant adenovirus was harvested after 7-10 days post transfection, when GFP plaques had appeared. After three cycles of

freezing in a methanol/dry ice bath (or liquid nitrogen) and rapid thawing at 37 °C, 1 ml of viral lysate was stored at -70 ^{o}C as virus stock.

2.12.12 Agar plaque purification of adenovirus

A method used for purification of virus stocks was the agar plaque purification method. Low passage 293 cells (less than passage 40) were plated in 10 cm diameter dish, by which the time they would achieve ~80 % confluence. One milliliter of virus serial dilution (in the range of $10^{-3} – 10^{-8}$) was added and incubated at 37 ^{o}C. Twenty-four hours after infection, cells were carefully overlaid with 15 ml overlay media to each dish and allowed to solidify at room temperature before incubating at 37^{o}C. Overlay media for 293 cells is made by mixing 37 ^{o}C 2 × Minimum Essential Medium (supplemented with 25% fetal bovine serum, 4mM L-glutamine, 200 units/ml penicillin G, and 200μg/ml streptomycin sulfate) with an equal volume of 62 ^{o}C 1% UltraPURE agarose (GIBCO, Grand Island, NY). After 3 more days, 10 ml overlay media was added, and if necessary, 5 ml more were added 6 days later. Between 6 and 14 days after infection individual plaques were presented.

2.12.13 Plaque analysis

For each virus, 12 plaques were generally chosen to analyze. Plaques were picked as agarose plugs, mixed with 1 ml media, subjected to 4 freeze/thaw cycles in order to lyse cells and release virus, and added to 3×10^{4} low passage 293 cells seeded the day before in a 24 well plate. After the development of cytopathic effect (CPE) (usually 2-4 days), the virus was amplified by collecting the cells plus media, freezing and thawing four times, and adding them to 3×10^{5} low passage 293 cells along with 500 μl fresh media. After the development of CPE (usually 48 h),

1/3 of the cells and media were frozen at -70 ^{o}C for later amplification and 2/3 were used for DNA analysis. For DNA analysis, the cells were pelleted by centrifugation at 14,000 rpm for 2 min, and all but 200 μl of the supernatant was discarded. The pellet was resuspended by pipetting and slowly added to 200 μl pronase stock diluted 1:5 in pronase buffer (final concentration of 0.5 mg/ml pronase). The samples mixed by pipetting and vortexing and incubated at 37 ^{o}C for 2-6 h. Next, the sample was extracted with an equal amount of phenol/chloroform/isoamyl alcohol (400 μl), collecting the aqueous phase. The aqueous phase was extracted again with 400 μl chloroform. DNA was precipitated from the aqueous phase with 1/10 volume 3M Sodium acetate (pH 5.3) plus 3 volumes ethanol and incubation of at least one hour at –70 ^{o}C. The DNA was pelleted by centrifuging 12 min at 14,000 rpm and 4 ^{o}C, and the supernatant is discarded. The pellet was washed with 500 μl 70% ethanol and repelleted at 14,000 rpm for 5 min. The pellet was then air dried and dissolved in 50 μl TE. Twenty microliters of the sample was digested with *Hind*III and run on an agarose gel. The corrected restriction pattern was further amplified and purified.

2.12.14 Adenovirus amplification and purification

For a large scale preparation, the correct frozen 1/3 viral stock from above was subjected to 4 freeze/thaw cycles to release virus and added to 4×10^5 high passage 293 cells in one well of a 12 well plate with a final volume of 1.5 ml media. After the development of CPE, cells and media were collected, frozen/thawed four times, and this time added to 2×10^6 high passage 293 cells in a 6 cm dish with a final media volume of 5 ml. The next amplification step was performed in an 80%

confluent 10 cm dish of high passage 293 cells in 10 ml media. Then, a 95% confluent 15 cm dish was infected with 25 ml media. From one 15 cm dish, four 15 cm dishes were infected. The last amplification step was thirty 15 cm dishes. After the development of CPE this time, the cells were pelleted by centrifuging at 2,000 rpm for 10 min, and the supernatant was discarded. The cells were then resuspended in 1 ml Dulbecco's phosphate buffered saline (GIBCO, Grand Island, NY) and 10 mM $MgCl_2$ per 15cm dish. The cells were lysed by four freeze/thaw cycles. The lysates were centrifuged at 2,000 rpm for 10 min to remove cellular debris, and the supernatants were stored at -70 ^{o}C.

2.12.15 Cesium chloride gradient purification of adenovirus

The lysates were run on Cesium chloride (CsCl) step gradients for purification. CsCl was dissolved in 5mM Tris-HCl, 1mM EDTA, pH 7.8 at density of 1.25 g/cm^3 and 1.35 g/cm^3. The gradients were formed by layering 3.5 ml 1.25 g/cm^3 CsCl on top of 3.5 ml 1.35 g/cm^3 CsCl in a 12 ml Beckman ultra-clear tube and adding 5 ml lysate on top. The tube was then balanced, placed in a SW40Ti swing bucket rotor and centrifuged in a Beckman ultracentrifuge for 2 h at 35,000 rpm. After centrifugation two bands were observed in the gradient as shown in **Figure 2.2**. The lower band containing parental full-length virus was carefully collected from each tube, combined, and subjected to ultracentrifugation in an equilibrium gradient derived from 1.35 g/cm^3 CsCl for 18 h at 14 ^{o}C and 35,000 rpm. The full-length band was collected again and dialyzed twice against 1 liter dialysis buffer at 4 ^{o}C in the dark for 6-8 h each. Dialysis was carried out to remove CsCl from the virus preparation whilst keeping virus at a pH of 7.5 since lower pH storage buffers reduce adenoviral

titers significantly. Virus was then aliquoted into steriled microcentrifuge tubes and stored at –70 ^{o}C. The viral DNA was checked again by restriction analysis as described above using 50 µl virus diluted with 150 µl serum-free media.

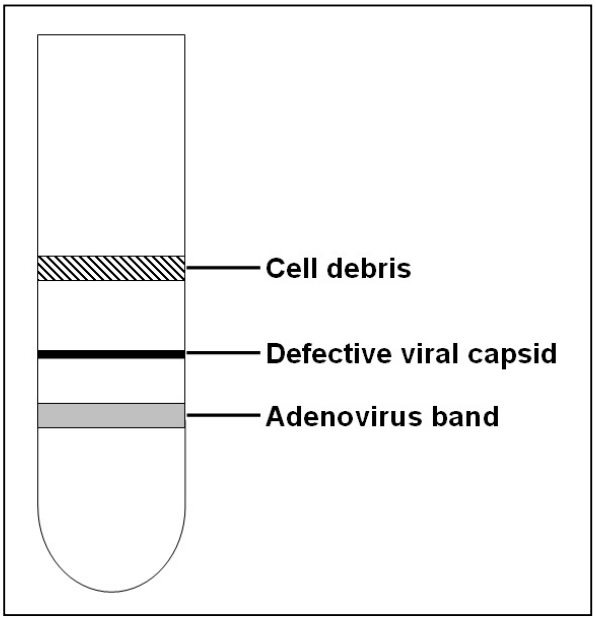

Figure 2.2 Cesium chloride separation of adenovirus from defective capsids and cell debris.

2.12.16 Calculation of Adenovirus titer

The titer can be determined by a spectrophotometer. Virus (dilution 1:20) was lysed by lysing solution (0.1% sodium dodecyl sulfate in TE) and measured their absorbance at 260 nm, where one optical density unit equals 10^{12} particles/ml.

2.12.17 Extraction of adenoviral DNA from CsCl purified virus

To an aliquot of CsCl purified adenovirus in a screw cap microcentrifuge, 200 µl of virion digestion buffer (solutions appendix) was added before incubating horizontally at 37 ^{o}C for 2 h. DNA was then extracted once with phenol:chloroform:isoamyl alcohol, ethanol precipitated (See section 2.12.13), washed with 70% ethanol, air dried and resuspended in 50 µl steriled DW.

2.12.18 Construction of recombinant pAdE/F35-scFv-M6-1B9

The modified pAdEasy-1/35 vector was generous gifts from Prof. Xiaolong Fan (Nilsson et al., 2004), Department of Molecular Medicine and Gene Therapy, Lund University, Lund, Sweden to Prof. Dr. Andre Lieber, Division of Medical Genetics, Department of Medicine, University of Washington, Seattle, Washington, USA. In the pAdEasy-1/F35, the Ad5 sequence from nt 30644 to 32781 (Genbank accession no. M73260/M29978) was replaced by the Ad35 fiber sequence from nt 129 to 972 (Genbank accession no. U10272) as shown in **Figure 2.3** (Shayakhmetov et al., 2000).

For generation of the pAdE/F35-scFv-M6-1B9 vector, the *Pme*I linearized and purified pAdT-scFv-M6-1B9 vector (See section 2.12.2) was co-electroporated with 100 ng of supercoiled pAdEasy-1/35. This shuttle plasmid was used to generate a recombinant adenoviral genome encoding Ad5F35-scFv-M6-1B9

by homologous recombination in *E. coli* BJ5183 with the fiber gene modified pAdEasy-1/F35 by using a standard method as described previously in section 2.12.4 (He et al., 1998). The genomic plasmid encoding Ad5F35-scFv-M6-1B9 was digested with *Pac*I (See section 2.12.9) and transfected into 293 cells by using the $CaPO_4$ precipitation method (He et al., 1998). The adenoviral vectors were expanded in 293 cells, purified, and titered in 293 cells by serial dilutions according to methods described previously in section 2.12.10-2.12.17.

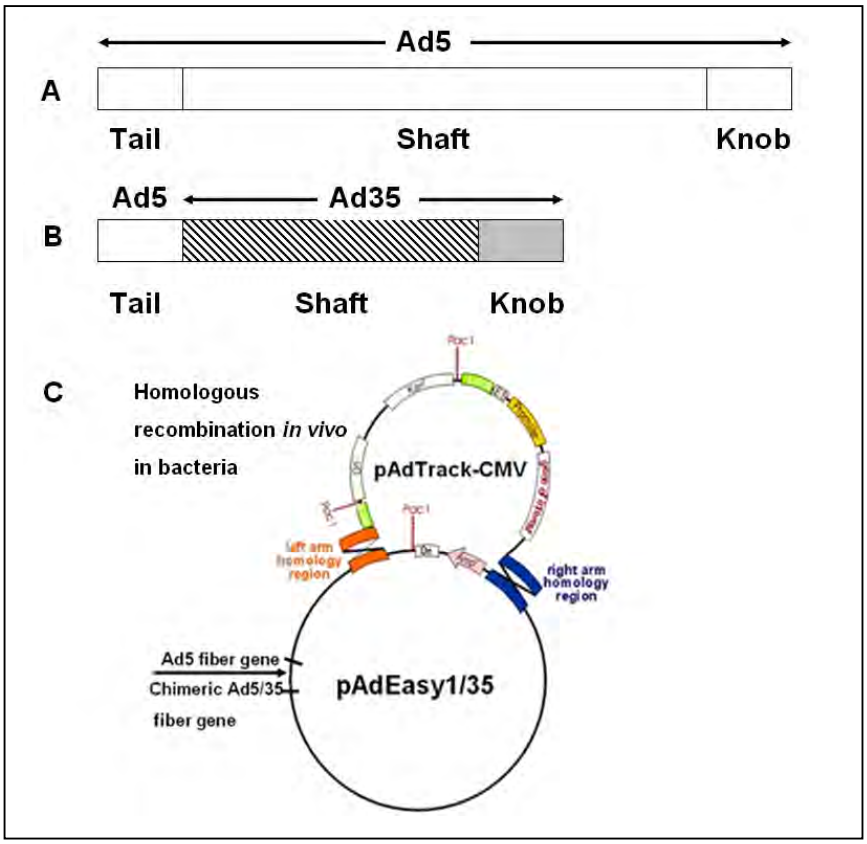

Figure 2.3 Construction of Ad5/F35 vectors. A) the Ad5 fiber gene. **B)** the chimeric fiber gene encoding the Ad5 fiber tail domain and Ad35 fiber shaft and knob domains. **C)** the fiber gene modified AdEasy system. The fiber gene in the pAdEasy-1 will be replaced with the indicated chimeric fiber gene. The fiber gene modified pAdEasy-1/F35 will be used to recombine with the shuttle plasmid encoding the *GFP* gene expression cassette in *E. coli* BJ5183 for generation of the recombinant adenoviral vector genome encoding the Ad5F35- scFv-M6-1B9-GFP vector (Nilsson et al., 2004).

2.12.19 Verification of Ad5-scFv-M6-1B9 and Ad5F35-scFv-M61B9 by using polymerase chain reaction (PCR)

One microliter of each purified Ad was amplified with 125 ng of each primer in a 50 µl of PCR mixture containing 2.5 U Taq polymerase (Fermentas). The specific primer sets for Ads knob amplification were used and listed in **Table 2.3**. The amplification condition was initiated with jump start at 95 °C for 5 min followed by 35 rounds of 3 steps amplification: denaturation at 95 °C for 50 sec, annealing at 57 °C for 50 sec for Ad5 knob (or 54.4°C for 50 sec for Ad35 knob) and extension at 72 °C for 1.5 min. Finally, the mixture was extended at 72 °C for 10 min. The amplified product was checked for the correct molecular size by 1% agarose gel electrophoresis.

Ad5-GFP and Ad35-GFP were used as control. These adenoviral vectors were kindly provided from Prof. Dr. Andre Lieber, University of Washington, Seattle, Washington, USA.

Table 2.3 A list of primer used for Ads knob and shaft amplification.

Primers	Sequences
Ad5 knob-For	5’-ACT GAA GGC ACA GCC TAT AC-3’
Ad5 knob-Rev	5’-AGT TGT GGC CAG ACC AGT CC-3’
Ad35 knob-For	5’-TCT TCT ACA GCG ACC AGT GA-3’
Ad35 knob-Rev	5’-ATG GCA TAG GCA ACA TTG GA-3’

2.12.20 Transduction of Ad5-scFv-M6-1B9 and Ad5F35-scFv-M61B9 in cell lines

Several cell lines (293A, HeLa, Jurkat, HepG2 and U937) were transduced with Ad5-scFv-M6-1B9 or Ad5F35-scFv-M6-1B9 at 100 and 1,000 MOI. After 48 h, the transduced cells were harvested, washed twice with 1% BSA-PBS-NaN_3 and resuspended with 350 µl 1% BSA-PBS-NaN_3. Percentage of GFP-positive cells was determined by flow cytometry.

2.12.21 CAR and αv-integrin staining

Cell lines (from section 2.12.19) were stained with mouse anti-CAR mAb (Clone RmcB) and mouse anti- αv-integrin mAb (Clone L230). These mAbs were generous gifts from Prof. Dr. Andre Lieber, University of Washington, Seattle, Washington, USA. PE-conjugated $F(ab')_2$ fragment of sheep anti-mouse immunoglobulins antibody were used as a secondary antibody. Finally, cells were washed 3 times with 1% BSA-PBS-NaN_3 and fixed with 1% paraformaldehyde-PBS. Fluorescence reactivity of the stained cells was investigated by flow cytometry (See section 2.11.4).

2.13 Immunological methods for functional analysis of intrabody against CD147 by adenoviral gene transfer

2.13.1 ScFv-M61B9 extraction by FractionPREP™ Cell Fractionation System

293A cells were transduced at a multiplicity of infection (MOI) of 10 pfu/cell of Ad-scFv-M6-1B9 and harvested after 48 h. Transduced cells were fractionated using FractionPREP™ Cell Fractionation System (BioVision, Mountain View, CA) according to the manufacturer's instructions. Briefly, the transduced cells were collected by centrifugation at 700 g for 5 min and washed with 5-10 ml of ice-cold PBS. After centrifugation at 700 g for 5 min, the pellet was resuspended in 1 ml of ice-cold PBS and transferred to a 1.5 ml microcentrifuge tube. The resuspended cells were spun for 5 min at 700 g and the supernatant was removed. The pellet was resuspended in 400 µl of Cytosol Extraction Buffer-Mix and incubated sample on ice for 20 min with gentle tapping 3-4 times every 5 min. After centrifugation at 700 g for 10 min, the supernatant (Cytosolic Fraction) was collected and kept on ice. The pellet was resuspended in 400 µl of ice-cold Membrane Extraction Buffer-A Mix and mixed well by vortex for 10-15 sec. Twenty two microliters of Membrane Extraction Buffer-B was added and then mixed by vertex for 5 sec. After incubation on ice for 1 min, the mixture was mixed by vertex for 5 sec again and centrifuged for 5 min at 1000 g. The supernatant (Membrane Fraction) was transferred immediately to a clean pre-chilled tube and kept on ice. The pellet was resuspended in 200 µl of ice-cold Nuclear Extraction Buffer Mix and mixed by vertex for 15 sec. The mixture was kept on ice

for 10 min with constant vortex for 15 sec every 10 min. After centrifugation at top speed in a microcentrifuge for 10 min, the sample was transferred to a clean pre-chilled tube (Nuclear Fraction). All Fractions were stored at -70 °C for future use.

2.13.2 Detection of scFv-M6-1B9 intrabody activity by Western blotting

The lysate fractions from section 2.13.1 were separated on a 12% SDS–PAGE gel under reducing conditions and then transferred onto a polyvinylidene-fluoride (PVDF) membrane. The membranes were blocked with 5% skimmed milk in PBS and traced by peroxidase-conjugated mAb anti-HA (Roche, Indianapolis, IN). The peroxidase reaction was visualized using an enhanced chemiluminescent substrate detection system.

To determine the binding activity of scFv-M6-1B9, biotin carboxyl carrier protein (BCCP) fusion proteins were separated on 12% SDS-PAGE, electroblotted onto PVDF membrane, probed with soluble lysate of 293A cells expressing scFv-M6-1B9 and traced by peroxidase-conjugated mAb anti-HA. The immunoreactive bands were visualized using an enhanced chemiluminescent substrate detection system.

2.13.3 Culture of the human cervical carcinoma cell line (HeLa)

The human cervical carcinoma cell line (HeLa) was kindly provided from Prof. Dr. Andre Lieber, University of Washington, Seattle, Washington, USA. Cells were cultured in Dulbecco’s modified Eagle’s medium (DMEM) supplemented with 10mM nonessential amino acids, 10% fetal bovine serum, penicillin (100 U/ml) and

streptomycin (100 μg/ml) and maintained in a humidified atmosphere of 5% CO_2 at 37 °C.

2.13.4 Flow cytometric analysis for CD147 surface expression

Five hundred microliters of 1.2×10^5 cells/ml 293A (or HeLa cells) were transduced with 10 MOI (~90% of the cells were infected) of adenovirus encoding scFv-M6-1B9 intrabody (Ad5-scFv-M6-1B9). After 36 h, 293A cells (or HeLa cells) were removed from 24-well tissue culture plates and washed 3 times with PBS. Cells were then blocked with human AB serum for 30 min on ice. Fifty microliters of 20 μg/ml purified mAb M6-1B9 in 1% BSA-PBS-NaN_3 were added to 50 μl of blocked cells and incubated on ice for 30 min. Cells were washed twice with 1% BSA-PBS-NaN_3 and resuspended with 20 μl 1% BSA-PBS-NaN_3. Subsequently, twenty-five microliters of PE-conjugated $F(ab')_2$ fragment of sheep anti-mouse immunoglobulins antibody were added and incubated on ice for 30 min. Finally, cells were washed 3 times with 1% BSA-PBS-NaN_3 and fixed with 1% paraformaldehyde-PBS. Fluorescence reactivity of the stained cells was investigated by flow cytometry. Adenovirus encoding scFv specific to survivin (scFv-SVV3) intrabody constructed by the same technique was used as transduction control.

2.13.5 Immunocytochemical analysis for CD147-intrabody colocalization

For analysis of CD147 and intrabodies on GFP-positive 293A, transfected cells were trypsinized and fixed for 10 min with 3.7% formaldehyde in PBS containing 50 mM $MgCl_2$. Fifty microliters of 1×10^6 fixed cells were placed on a silane-coated slide and air-dried. Following washing, cells were permeabilized with 0.2% Triton-X 100 for 12 min. Slides were then washed in PBS containing 50 mM

$MgCl_2$ and blocked with 1% BSA in SSC at RT for 5 min. Then, the fixed cells were incubated with a mixture of biotinylated anti-human extracellular matrix metalloproteinase inducer (EMMPRIN) mAb (0.1 μg/ml; R&D systems, Minneapolis, MN) and rabbit anti-HA mAb (Sigma) at 4 °C overnight. After washing, cells were blocked and then incubated with the mixture of Cy5-conjugated streptavidin (Amersham Life Sciences, Inc, Buckinghamshire, UK) and Cy3-conjugated anti-rabbit-IgG mAb (Sigma) at RT for 30 min. Nuclei were counterstained with DAPI. Imaging of stained cells was performed by using a Zeiss Apotome with an AxioCam HRM, AMCA, Cy3, Cy5 and FITC filters in combination with Planapo 63×/1.4 oil objective lens. Images were acquired by using AXIOVISION 4.4 (Carl Zeiss Canada Ltd., Toronto, ON, Canada) in multichanel mode.

12.13.6 Confocal analysis

The 1×10^4 HeLa cells were plated on eight-well Tissue-Tek chamber slides (Nalge Nunc International, Rochester, NY), and transduced with 10 MOI of Ad5-scFv-M6-1B9 for 48 h at 37 °C. Cells were washed, fixed in 4% formaldehyde in PBS containing 50 mM $MgCl_2$ and permeabilized with 0.1% Triton X-100. Slides were then washed in PBS containing 50 mM $MgCl_2$ and blocked with 2% skim milk in PBS containing 50 mM $MgCl_2$ at RT for 30 min. Then, the fixed cells were incubated with rabbit anti-HA antibody (Abcam, Cambridge, MA) at 37 °C for 1 h. After washing, cells were then incubated with Alexa Fluor 568-goat anti-rabbit IgG (Molecular Probes, Eugene, OR). The cellular nuclei were counterstained by DAPI.

Images were acquired using FLUOVIEW laser scanning confocal microscope (Olympus, FV1000; Olympus Optical, Japan).

RESULTS

3.1 Construction of a phagemid vector encoding scFv-M6-1B9

The heavy, Fd, and light chain domains of anti-CD147 mAb, M6-1B9 (Kasinrerk et al., 1999), were amplified, subcloned into the expression vector and then named as pCom3H-Fab-M6-1B9. Subsequently, the V_L and V_H were amplified from pCom3H-Fab-M6-1B9 and attached by a peptide linker to form the scFv. The amplified product was cloned into phagemid vector pComb3X, named pComb3X-scFv-M6-1B9, and then transformed into *E. coli* TG1. The nucleotide sequence of the inserted fragment, scFv, was obtained (**Figure 3.1**). The scFv construct was fused to the carboxy-terminal domain of the minor coat protein, gpIII, and displayed on the surface of phage particles. The deduced amino acid sequences of variable heavy (V_H) and light (V_L) chains are listed in **Figure 3.1.** The amino acid residues responsible for paratope in CDR regions were subsequently identified *via* the WAM (for Web antibody modelling) algorithm (Whitelegg and Rees, 2000). The sequence can be numbered following Kabat's rule (Kabat et al., 1976), in order to assure success in cloning the immunoglobulin variable domains.

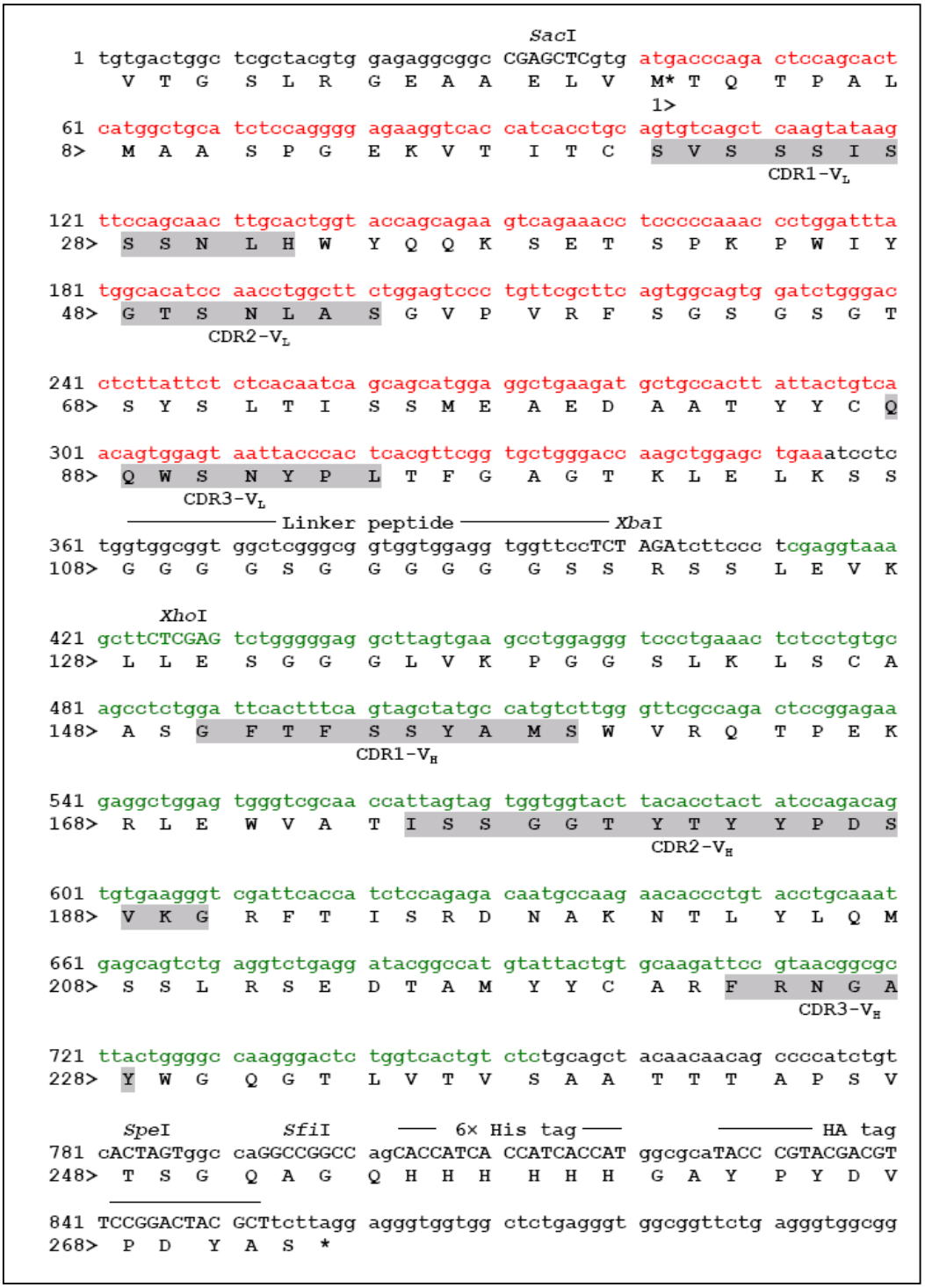
SacI
1 tgtgactggc tcgctacgtg gagaggcggc CGAGCTCgtg atgacccaga ctccagcact
V T G S L R G E A A E L V M* T Q T P A L
1>
61 catggctgca tctccagggg agaaggtcac catcacctgc agtgtcagct caagtataag
8> M A A S P G E K V T I T C S V S S S I S
CDR1-VL
121 ttccagcaac ttgcactggt accagcagaa gtcagaaacc tcccccaaac cctggattta
28> S S N L H W Y Q Q K S E T S P K P W I Y
181 tggcacatcc aacctggctt ctggagtccc tgttcgcttc agtggcagtg gatctgggac
48> G T S N L A S G V P V R F S G S G S G T
CDR2-VL
241 ctcttattct ctcacaatca gcagcatgga ggctgaagat gctgccactt attactgtca
68> S Y S L T I S S M E A E D A A T Y Y C Q
301 acagtggagt aattacccac tcacgttcgg tgctgggacc aagctggagc tgaaatcctc
88> Q W S N Y P L T F G A G T K L E L K S S
CDR3-VL
Linker peptide
XbaI
361 tggtggcggt ggctcgggcg gtggtggagg tggttccTCT AGAtcttccc tcgaggtaaa
108> G G G G S G G G G G G S S R S S L E V K
XhoI
421 gcttCTCGAG tctgggggag gcttagtgaa gcctggaggg tccctgaaac tctcctgtgc
128> L L E S G G G L V K P G G S L K L S C A
481 agcctctgga ttcactttca gtagctatgc catgtcttgg gttcgccaga ctccggagaa
148> A S G F T F S S Y A M S W V R Q T P E K
CDR1-VH
541 gaggctggag tgggtcgcaa ccattagtag tggtggtact tacacctact atccagacag
168> R L E W V A T I S S G G T Y T Y Y P D S
CDR2-VH
601 tgtgaagggt cgattcacca tctccagaga caatgccaag aacaccctgt acctgcaaat
188> V K G R F T I S R D N A K N T L Y L Q M
661 gagcagtctg aggtctgagg atacggccat gtattactgt gcaagattcc gtaacggcgc
208> S S L R S E D T A M Y Y C A R F R N G A
CDR3-VH
721 ttactggggc caagggactc tggtcactgt ctctgcagct acaacaacag ccccatctgt
228> Y W G Q G T L V T V S A A T T T A P S V
SpeI
SfiI
6× His tag
HA tag
781 cACTAGTggc caGGCCGGCC agCACCATCA CCATCACCAT ggcgcaTACC CGTACGACGT
248> T S G Q A G Q H H H H H H G A Y P Y D V
841 TCCGGACTAC GCTtcttagg agggtggtgg ctctgagggt ggcggttctg agggtggcgg
268> P D Y A S *

Figure 3.1 Nucleotide sequence of cDNA and deduced amino acid sequence of the scFv-M6-1B9. The cDNA sequence encoding scFv-M6-1B9 was shown. Restriction endonuclease sites, histidine tag, and HA tags are indicated. The deduced amino acid sequence of scFv-M6-1B9 corresponding to the complementary determining regions (CDRs) in the variable regions of the L (red letters) and H (green letters) chains, which were identified by the Kabat numbering scheme, are indicated by gray boxes. Amino acids were numbered from the initiator methionine (M*). The amber stop codon was shown by an asterisk (*). The details of the CDRs region of scFv-M6-1B9 are shown as CDR1-V_L C-(^{24}SV---LH^{35}) W, CDR2- V_L Y (^{51}GT---AS ^{57}) G, CDR3- V_L C (^{90}QQ---PL^{97}) T, CDR1- V_H S (^{153}GF---MS^{162})W, CDR2- V_H A(^{178}IS---KG^{193})R, and CDR3- V_H R (^{226}FR---GAY^{231})W.

3.2 Detection of phage-displayed scFv-M6-1B9

The expression of Fab- and scFv-M6-1B9 on phage particles was assessed by Western immunoblotting. Equal amounts of each recombinant phage were fractionated by SDS–PAGE, blotted, and investigated with anti-gpIII mAb. The immunoreactive bands of scFv-M6-1B9- and Fab-M6-1B9-gpIII fusion protein with the approximate molecular weight of 47 kDa were obtained (**Figure 3.2A**). The band corresponding to the scFv-gpIII fusion protein was more prominent than the band corresponding to the Fab-M6-1B9-gpIII fusion protein, reflecting the fact that scFv expression was superior to that of Fab obtained by the phage display technique. Antigen-specific binding of phage presenting the different antibody formats was verified by ELISA using recombinant CD147-BCCP as an antigen. scFv format demonstrated more favorable antigen-binding features than the Fab format (**Figure 3.2B**). In contrast, VCSM13 phage prepared from non-transformed TG-1 did not generate the signal against CD147-BCCP antigen. These results imply that phage presenting different antibody formats of M6-1B9 had been successfully produced and the scFv version was the better functional antibody fragment.

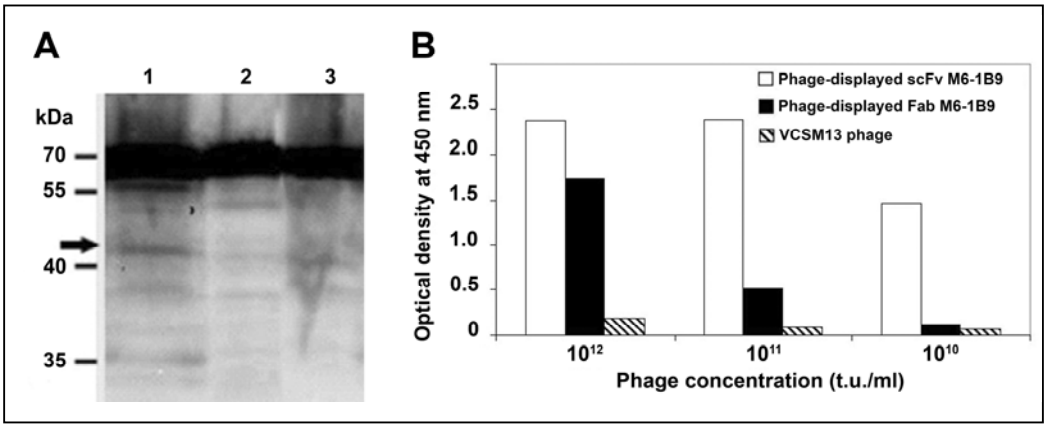

Figure 3.2 Verification of antibody phage presenting different formats. **(A)** Recombinant phages (10^{13} t.u./lane) were separated on a reducing 12% SDS–PAGE. The gpIII protein was probed using anti-gpIII mAb. The immunoreactive bands were visualized by chemiluminescence substrate detection system. Lane 1, phage-displayed scFv-M6-1B9; lane 2, phage-displayed Fab-M6-1B9 and lane 3, VCSM13 helper phage. Molecular weight markers in kDa are indicated. **(B)** CD147-BCCP was captured on wells coated with avidin. Three different concentrations, 10^{10}-10^{12} t.u./ml of phage-displayed scFv-M6-1B9 and phage-displayed Fab-M6-1B9 were added and traced by peroxidase-conjugated anti-M13 phage mAb. VCSM13 helper phage was used as wild-type phage control.

3.3 Detection and characterization of soluble scFv-M6-1B9 produced in *E. coli*

The pComb3X-scFv-M6-1B9 was transformed into *E. coli* HB2151 to produce the soluble scFv antibody. The presence of soluble scFv in the culture supernatant was detected by Western immunoblotting using antibodies specific to the HA and His tags. The reactive bands revealed by anti-HA or anti-His were located at the same molecular weight (~30 kDa) (**Figure 3.3A**). This result indicates that soluble scFv-M6-1B9 was successfully produced by *E. coli* HB2151. The specificity of soluble scFv-M6-1B9 was analyzed by ELISA using CD147-BCCP as antigen. At least 1:100 dilution of soluble scFv-M6-1B9 has been shown the strongly positive signal with CD147-BCCP (**Figure 3.3B**). No signal was detected in the control well of SVV-BCCP antigen. Subsequently, the specificity of the generated scFv-M6-1B9 against recombinant CD147 was confirmed by Western immunoblotting. A specific band of CD147-BCCP at ~35 kDa was detected by probing with soluble scFv-M6-1B9 (**Figure 3.3C**). In addition, the native epitope of CD147 on the U937 cell surface was recognized by soluble scFv-M6-1B9 using flow cytometric analysis. The mean fluorescence intensity (MFI) of CD147 cell surface expression on U937 cells stained with soluble scFv-M6-1B9 was 10.42 (**Figure 3.3D)**. This was similar to the value for the original antibody, M6-1B9, which MFI was 9.21 as shown in **Figure 3.3D**. These results strongly suggested that the generated soluble scFv-M6-1B9 carry a CD147-specific paratope which recognized both recombinant and native CD147.

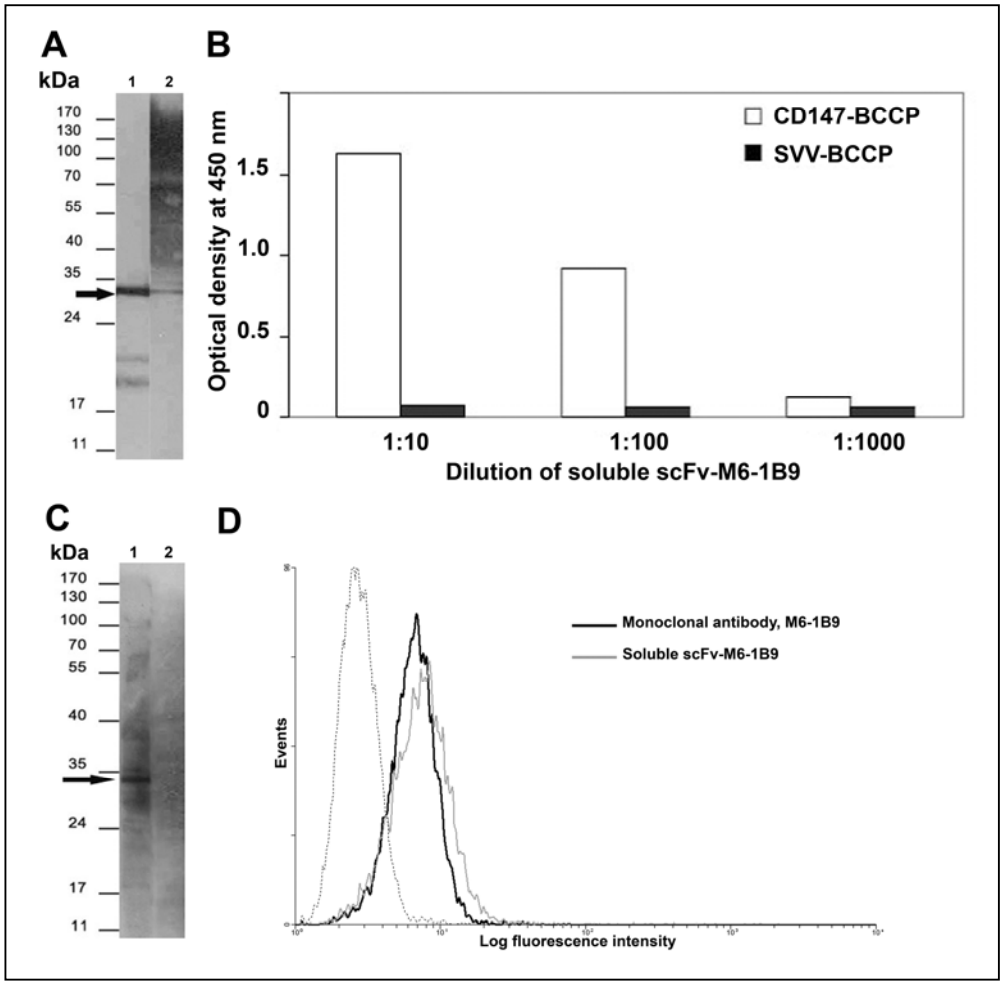

Figure 3.3 Detection of soluble scFv. (A) Soluble scFv-M6-1B9 was separated on 12% SDS-PAGE, electroblotted onto PVDF membrane, and probed with peroxidase-conjugated mAb anti-HA (lane 1) and anti-His mAb (lane 2). The immunoreactive bands were visualized by ECL substrate detection system. The molecular weight is indicated. (**B)** CD147-BCCP (open columns) or SVV-BCCP (black columns) was captured on the avidin-coated wells. Soluble scFv-M6-1B9 was subsequently added and the bound scFv was detected by peroxidase-conjugated mAb

anti-HA. **(C)** CD147-BCCP (lane 1) or SVV-BCCP (lane 2) proteins were separated on 12% SDS-PAGE, electroblotted onto a PVDF membrane, and then probed with soluble scFv-M6-1B9. The scFv was detected using peroxidase-conjugated mAb anti-HA. The positions of molecular mass markers are shown on the left. **(D)** CD147 on U937 cells was stained with soluble scFv-M6-1B9 and then probed by mouse anti-HA-biotin. Subsequently, FITC-conjugated sheep anti-mouse immunoglobulins antibody was added. Monoclonal antibody M6-1B9 was used as a control system for detecting CD147 on U937 cells. The immunofluorescence on cells stained with soluble scFv-M6-1B9 (bold line) or mAb M6-1B9 (thin line) is shown. The dashed line represents background fluorescence of negative control mAb. The *y* axis represents the number of events on a linear scale; the *x* axis shows the fluorescence intensity on a logarithmic scale.

To further characterize the specificity of the produced scFv, the inhibiting activity of soluble scFv-M6-1B9 with the original monoclonal antibody, M6-1B9, was tested. The optical density of mixture of soluble scFv-M6-1B9 and mAb M6-1B9 was lower than soluble scFv-M6-1B9 alone (**Figure 3.4**). In contrast, an irrelevant mAb (MT-SVV3) had no inhibitory effect on CD147 binding of soluble scFv-M6-1B9. This indicates that mAb M6-1B9 altered the binding of soluble scFv-M6-1B9 to recombinant CD147 and bound to the same epitope.

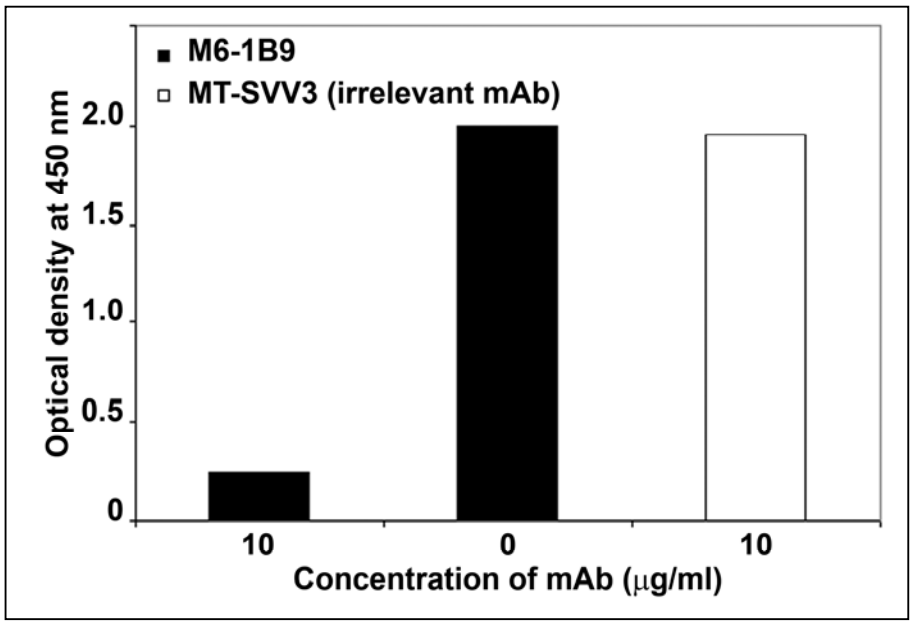

Figure 3.4 Competitive binding analysis of soluble scFv-M6-1B9 and mAb M61B9. CD147-BCCP was added onto avidin-coated wells. The mixture contained soluble scFv-M6-1B9 and mAb M6-1B9 at ratio 1:1 was added into the well. The bound scFv was detected by peroxidase-conjugated mAb anti-HA.

3.4 Soluble scFv-M6-1B9 inhibited CD3 mAb induced cell proliferation

To investigate the biological functions of soluble scFv-M6-1B9, the effect scFv-M6-1B9 on cell proliferation was assayed. PBMCs isolated from healthy donors were activated by immobilized CD3 mAb OKT3 in the presence or absence of CD147 mAb clone M6-1B9 or soluble scFv-M6-1B9. The results showed that soluble scFv-M6-1B9 inhibited colony formation (**Figure 3.5A**) and proliferation (**Figure 3.5B**) of PBMCs induced by CD3 mAb OKT3 as well as its original antibody (Chiampanichayakul et al., 2006). In contrast, mock bacterial protein lysate controls had no inhibitory effect on OKT3-mediated cell proliferation. These results demonstrate that the monomeric form of CD147 mAb could engage the CD147 molecule and induce negative regulation of OKT3-induced T cell proliferation. In addition, the results indicate that the produced soluble scFc-M6-1B9 is a biologically active protein.

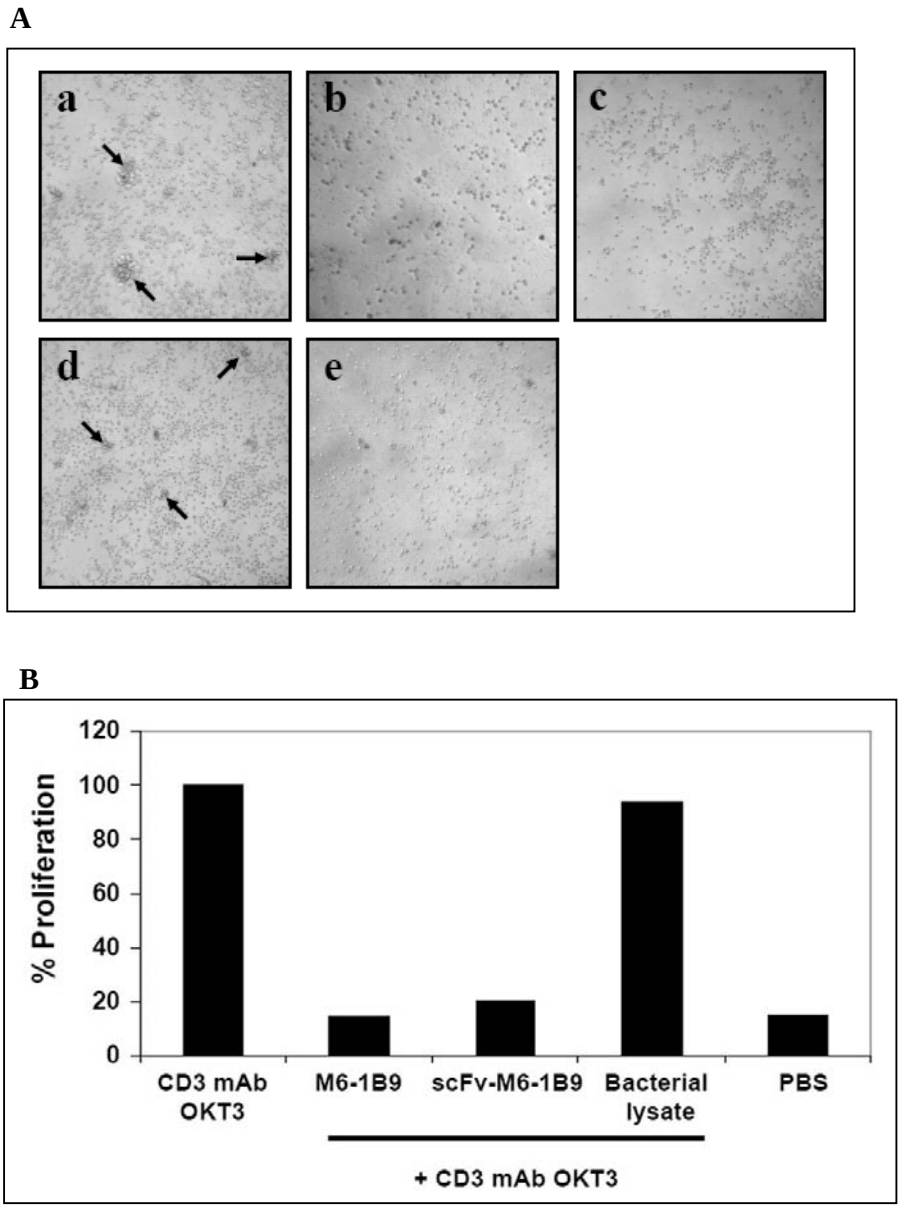

Figure 3.5 Soluble scFv-M6-1B9 inhibited CD3 mAb induced cell proliferation. (A) Photomicrography (100×) of colony formation of PBMC induced by CD3 mAb OKT3. Cells were stimulated with 20 ng/ml of immobilized CD3 mAb OKT3 in the presence or absence of CD147 mAb M6-1B9, scFv-M6-1B9 or bacterial protein lysate and observed under an inverted microscope. CD3 mAb OKT3 only (a),

CD3 mAb OKT3 plus M6-1B9 (20 μg/ml) (b), scFv-M6-1B9 (1:40) (c), bacterial protein lysate (1:40) (d), or PBS alone (e). Cell clustering is indicated by arrow. **(B)** Cell proliferation was determined by the measurement of CSFE incorporation using flow cytometry.

3.5 Generation of recombinant adenoviral vectors using the AdEasy method

To generate recombinant adenoviral vectors, *Pme*I linearized shuttle vector DNA (pAdT-scFv-M6-1B9) was co-transformed with supercoiled pAdEasy-1 plasmid into electrocompetent BJ5183 cells **(Figure 3.6A)**. Homologous recombinants were selected on LB plates containing 50 μg/ml kanamycin. Recombinant adenoviral vector was then extracted using Plasmid Mini Kit (QIAGEN). The corrected clone was analyzed by size and *Pac*I restriction mapping. Based on the migration rates, all clones were potential valid recombinants **(Figure 3.6B)**. Recombinants were generated by homologous recombination of the left and right arm sequences, but sometimes occurred between the plasmid *Ori* sequences shared between the shuttle and pAdEasy vector resulted in slightly different restriction patterns **(Figure 3.6C)**. Recombinant plasmids are propagated in a bacterial strain less prone to recombination than BJ5183, such as DH10B cells. Selected clones from DH10B cells were digested with *Pac*I restriction endonucleases to verify proper recombination. As shown in **Figure 3.6C**, a 3.0 kb (or 4.5 kb) fragment was produced when digested with *Pac*I.

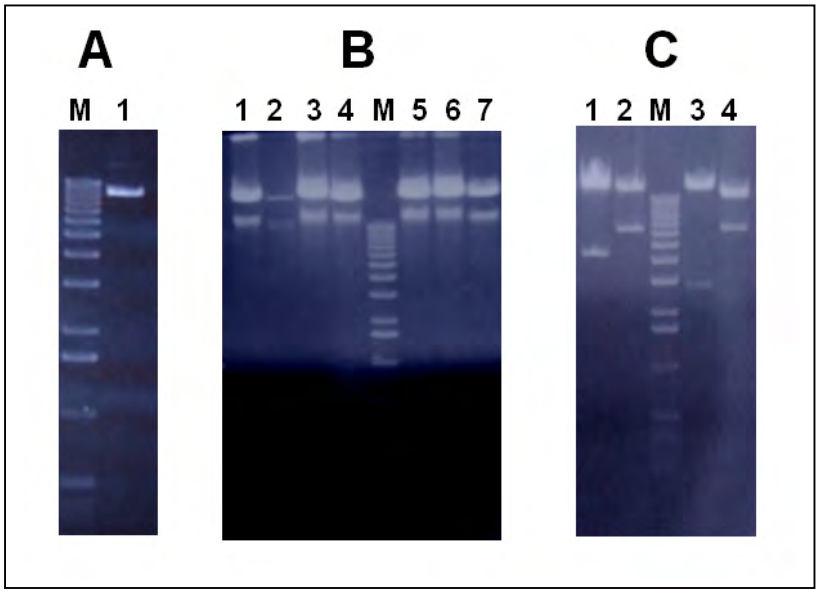

Figure 3.6 Generation of recombinant adenoviral vectors in bacterial cells. (A) pAdT-scFv-M6-1B9 was linearized with *Pme*I. **(B)** Recombinant pAdE-scFv-M6-1B9 (or pAdE/F35-scFv-M6-1B9) constructs derived from homologous recombination of pAdT-scFv-M6-1B9 and pAdEasy-1 (or pAdEasy-1/35) in BJ5183 cells were purified from minipreps. Lanes 1-4, four different pAdE-scFv-M6-1B9 clones, lanes 5-7, three different pAdE/F35-scFv-M6-1B9 clones and M, 1kb DNA marker. **(C)** Representative digestion with *Pac*I. Recombinant pAdE-scFv-M6-1B9 and pAdE/F35-scFv-M6-1B9 constructed from DH10B cells was purified from minipreps. Lanes 1 and 3, pAdE-scFv-M6-1B9 and pAdE/F35-scFv-M6-1B9 clones treated with *Pac*I, lanes 2 and 4, untreated *Pac*I and M, 1 kb DNA marker. The DNA was analyzed in supercoiled form by electrophoresis through an 0.8% agarose gel and ethidium bromide staining.

3.6 Generation of recombinant adenovirus expressing scFv-M61B9

The recombinant adenoviral plasmid vector (pAdE-scFv-M6-1B9 or pAdE/F35-scFv-M6-1B9) was linearized with *Pac*I to expose its inverted terminal repeats and transfected into a packaging cell line (293A) which constitutively expresses the E1 gene products required for the recombinant adenovirus propagation. The process of viral production can be followed in the packaging cells by visualization of the GFP reporter that is incorporated into the viral backbone (**Figure 3.7**). Comet-like adenovirus-producing foci became apparent at 5-7 days after transfection and plaques formation appeared at day 9-13. After 10–14 days, viruses were harvested, amplified by infecting packaging cells and purified by CsCl step gradients **(Figure 3.8)**. The band containing parental full-length virus was carefully collected from each tube **(Figure 3.8A)**, combined, and subjected to ultracentrifugation in an equilibrium gradient derived from 1.35 g/ml CsCl for 18 h at 14 °C and 35,000 rpm. The full-length band was collected again **(Figure 3.8B)** and dialyzed twice against 1 liter dialysis buffer at 4 °C in the dark for 6-8 h each. The virus is aliquoted and stored at –70 °C.

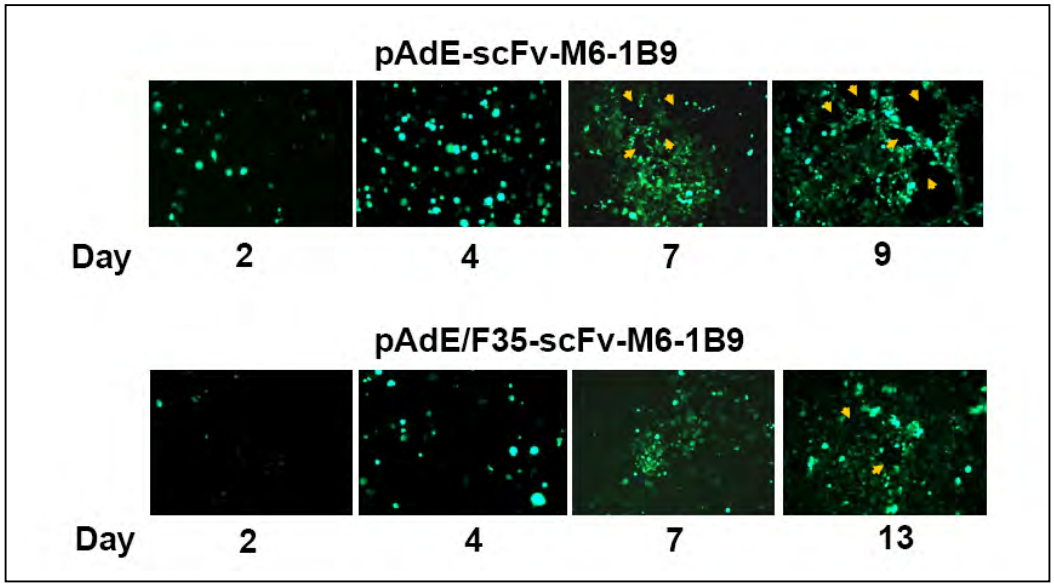

Figure 3.7 Adenovirus production after transfection of 293 cells. 293 cells were transfected with 5 μg of the *Pac*I digested pAdE-scFv-M6-1B9 (or pAd5/F35-scFv-M6-1B9) by transfection reagent. The transfected cells were monitored for GFP expression under fluorescence microscope at 100 × magnification. Yellow arrow head showed plaques formation.

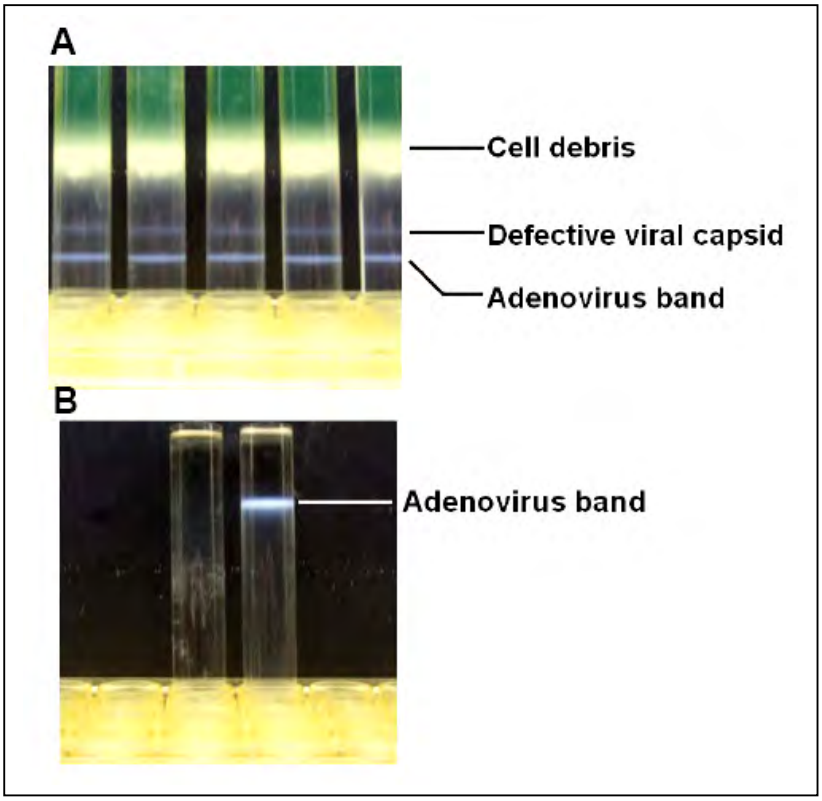

Figure 3.8 Adenovirus purification by CsCl step gradients. The band containing parental full-length virus was collected from ultracentrifuged tube. **(A)** first spinning and **(B)** second spinning.

3.7 Detection and characterization of scFv-M6-1B9 intrabody produced in 293A cells

To detect the presence of adenovirus knob, purified recombinant adenoviruses were employed for Ad5- and Ad35 knob amplification using specific primer sets. The result from polymerase chain reaction method showed a specific band at 220 bp. This result indicated that no cross contamination between recombinant Ad-scFv-M6-1B9 and Ad5/F35-scFv-M6-1B9 **(Figure 3.9)**.

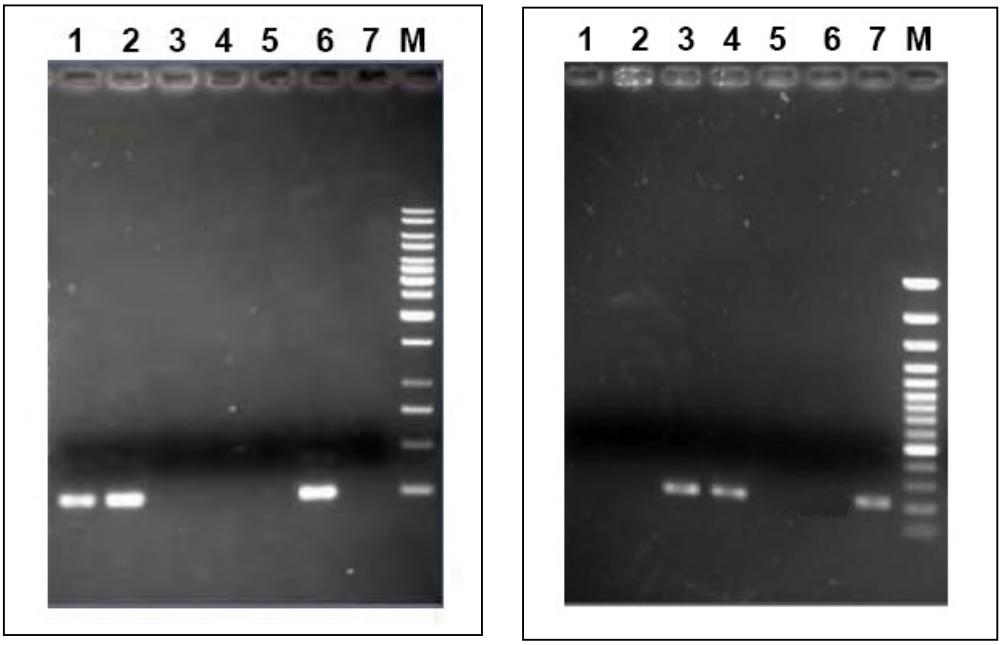

Figure 3.9 Adenovirus knob amplification. An equal amount of each adenovirus was amplified by PCR using Ad5 knob primers set **(A)** and Ad35 knob primer set **(B)**. Ad5-scFv-M6-1B9 (lane 1), Ad5-GFP (lane 2), Ad5/F35-scFv-M6-1B9 (lane 3), Ad5/F35-GFP (lane 4), negative control (lane 5), pAdE-scFv-M6-1B9 (lane 6) and pAdE/F35-scFv-M6-1B9 (lane 7) were used as a template. M indicated 1 kb DNA marker.

To confirm whether the recombinant adenovirus expressing scFv-M6-1B9, 293A cells were transduced with recombinant Ad-scFv-M6-1B9 (or Ad5/F35-scFv-M6-1B9) and harvested after 48 h. The lysate of transduced cells were separated on 12% SDS-PAGE and electroblotted onto a PVDF membrane. The presence of scFv-M6-1B9 intrabody in the cell lysate was detected by Western immunoblotting with an HA tag. The reactive band revealed by anti-HA was detected in the cell lysates from 293A transduced with both recombinant Ad-scFv-M6-1B9 and Ad5/F35-scFv-M6-1B9 (~35 kDa) and not found in the cell lysates from 293A transduced with recombinant Ad5-GFP, Ad5/F35-GFP and untransduced 293A cells (**Figure 3.10**). This result indicates that recombinant Ad-scFv-M6-1B9 and Ad5/F35-scFv-M6-1B9 was able to express a scFv-M6-1B9.

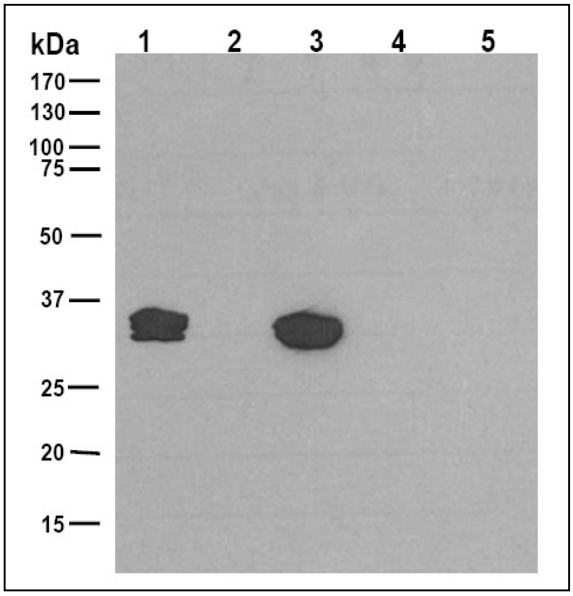

Figure 3.10 Detection of scFv-M6-1B9 intrabody expression by Western blotting. 293A cells were transduced with recombinant adenovirus harboring scFv-M6-1B9**.** Cells were lysated and separated on 12% SDS-PAGE, electroblotted onto a PVDF membrane. The produced scFv intrabody was detected using peroxidase-conjugated mAb anti-HA. The positions of molecular mass markers are shown on the left. The cell lysate obtained from Ad-scFv-M6-1B9 (lane 1), Ad5-GFP (lane2), Ad5/F35-scFv-M6-1B9 (lane 3), Ad5/F35-GFP (lane 4) transduced and untransduced 293A cells (lane 5) were indicated.

To further investigate the intracellular expression of scFv, the lysate fractions of transduced cells were separated on 12% SDS-PAGE and electroblotted onto a PVDF membrane. The presence of scFv-M6-1B9 intrabody in the fractionated cell lysate was detected in the endoplasmic reticulum fraction (~35 kDa) and not found in the nuclear and cytoplasmic fractions (**Figure 3.11A**). This result demonstrates that an intrabody with a carboxyl-terminal endoplasmic reticulum (ER) retention signal (KDEL) was retained in the ER compartment.

Subsequently, the specificity of scFv-M6-1B9 intrabody in cell lysate was analyzed by immunoblotting using CD147-BCCP as antigen (Tayapiwatana et al., 2006). A specific band of CD147-BCCP at ~35 kDa was detected by probing with soluble scFv-M6-1B9 intrabody (**Figure 3.11B**). As control, soluble scFv-M6-1B9 produced by non-suppressor *E. coli* strain HB2151 gave also a positive signal with CD147-BCCP. No signal was detected in the control panel of survivin-BCCP (SVV-BCCP) antigen and bacterial lysate proteins. This result indicates that a specific and active scFv-M6-1B9 intrabody was successfully produced inside the transduced 293A cells.

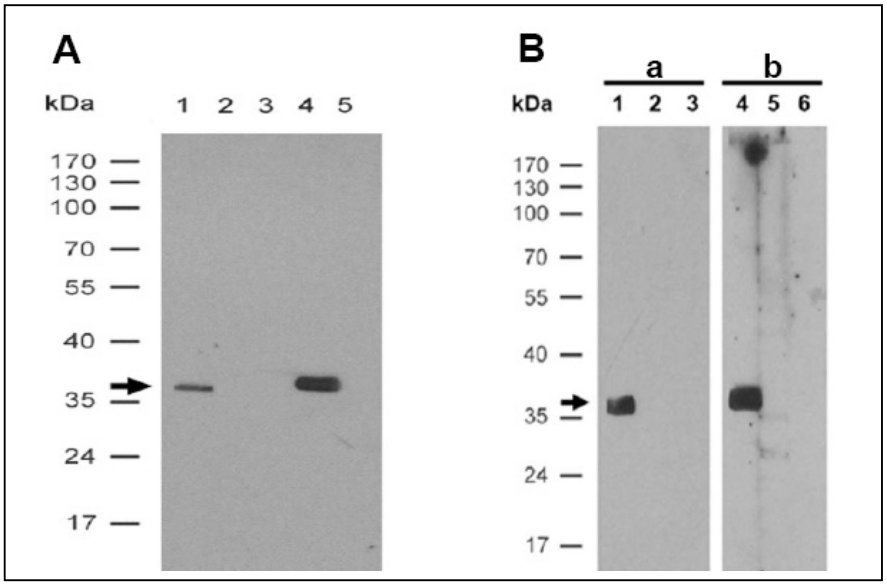

Figure 3.11 Detection of scFv-M6-1B9 intrabody activity by Western blotting. **(A)** 293A cells were transduced with recombinant adenovirus harboring scFv-M6-1B9**.** Cells were lysated and separated on 12% SDS-PAGE, electroblotted onto a PVDF membrane. The produced scFv intrabody was detected using peroxidase-conjugated mAb anti-HA. The positions of molecular mass markers are shown on the left. Soluble scFv-M6-1B9 produced by expressing pComb3X-scFv-M6-1B9 phagemid in the non-suppressor *E. coli* strain HB2151 was used as positive control (lane 1). Transduced 293A cell lysate obtained from nuclear fraction (lane 2), cytoplasmic fraction (lane 3), ER fraction (lane 4) and untransduced cells (lane 5) were indicated. **(B)** CD147-BCCP (lane 1, 4), SVV-BCCP (lane 2, 5) and bacterial lysate proteins (lane 3, 6) were separated on 12% SDS-PAGE, electroblotted onto a PVDF membrane, and then probed with M6-1B9 antibody (panel a) and soluble scFv-M6-1B9 intrabody (panel b). The M6-1B9 or scFv obtained from Ad-scFv-M6-1B9 transduced 293A cells was detected using peroxidase-conjugated goat-anti-mouse immunoglobulins or peroxidase-conjugated mAb anti-HA, respectively. Molecular mass markers are indicated on the left.

Next, the recognition of native CD147 on the HeLa cell surface by soluble lysate of scFv-M6-1B9 was determined using flow cytometric analysis (**Figure 3.12**). As predicted, the soluble scFv-M6-1B9 intrabody could react with CD147 expressed on HeLa cells. However, the signal (MFI) was lower than those obtained from the original antibody, M6-1B9. Contrarily, neither soluble lysate of scFv-SVV3 intrabody nor 293A cell lysate recognized the native CD147 on HeLa cell surface. This strongly suggests that the generated soluble lysate scFv-M6-1B9 from 293A cells carries a CD147-specific paratope which recognizes both recombinant and native CD147.

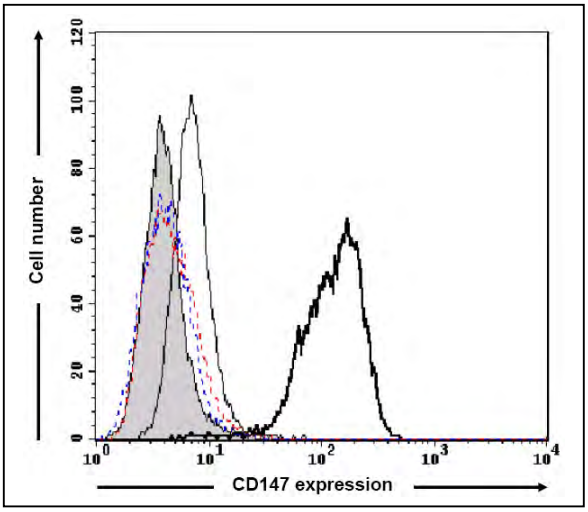

Figure 3.12 The scFv-M6-1B9 intrabody is specific to CD147 on HeLa cell surface. HeLa cell surface staining was performed using soluble lysate of scFv-M6-1B9 intrabody (thin line), scFv-SVV3 intrabody (red dash line), 293A lysate (blue dash line) and M6-1B9 antibody (solid line). Conjugate control was showed in solid shade.

To prove the efficiency of recombinant adenovirus transduction, HeLa (cervical cancer cell), Jurkat (T cell leukemia), U937 (monoblastic cell) and HepG2 (hepatoma cell) were selected as target cells to compare gene transfer efficiency between Ad-scFv-M6-1B9 and Ad5/F35-scFv-M6-1B9. Prior to perform the transduction experiment, all cells were determined the expression of CAR, αv-integrin and CD46. As shown in **Figure 3.13**, U937 and HepG2 cells do not express CAR and αv-integrin. Jurkat cells expressed CAR and αv-integrin at low level. Contrarily, high expression of CAR and αv-integrin was demonstrated in HeLa cells as in control, 293A cells. None of these cell lines express CD46 except HepG2 cells. The cells were subsequently transduced with 0, 100 or 1000 viral particles (VP) per cells. 293A cells were used as control for confirmation the infectivity of both recombinant adenovirus particles. Twenty-four hours after infection the cells were analyzed by flow cytometer for GFP expression. As shown in **Figure 3.14**, Ad5/F35-scFv-M6-1B9 has a significantly higher infectivity than Ad-scFv-M6-1B9 in U937 (60% maximum expression). Due to Ad5/F35-scFv-M6-1B9 used CD46 as a receptor for adenovirus entry, Ad-scFv-M6-1B9 and Ad5/F35-scFv-M6-1B9 had essentially identical and high infectivity for HeLa and Jurkat cells. However, neither Ad-scFv-M6-1B9 nor Ad5/F35-scFv-M6-1B9 could infect HepG2 cells, even at a very high MOI (data not shown).

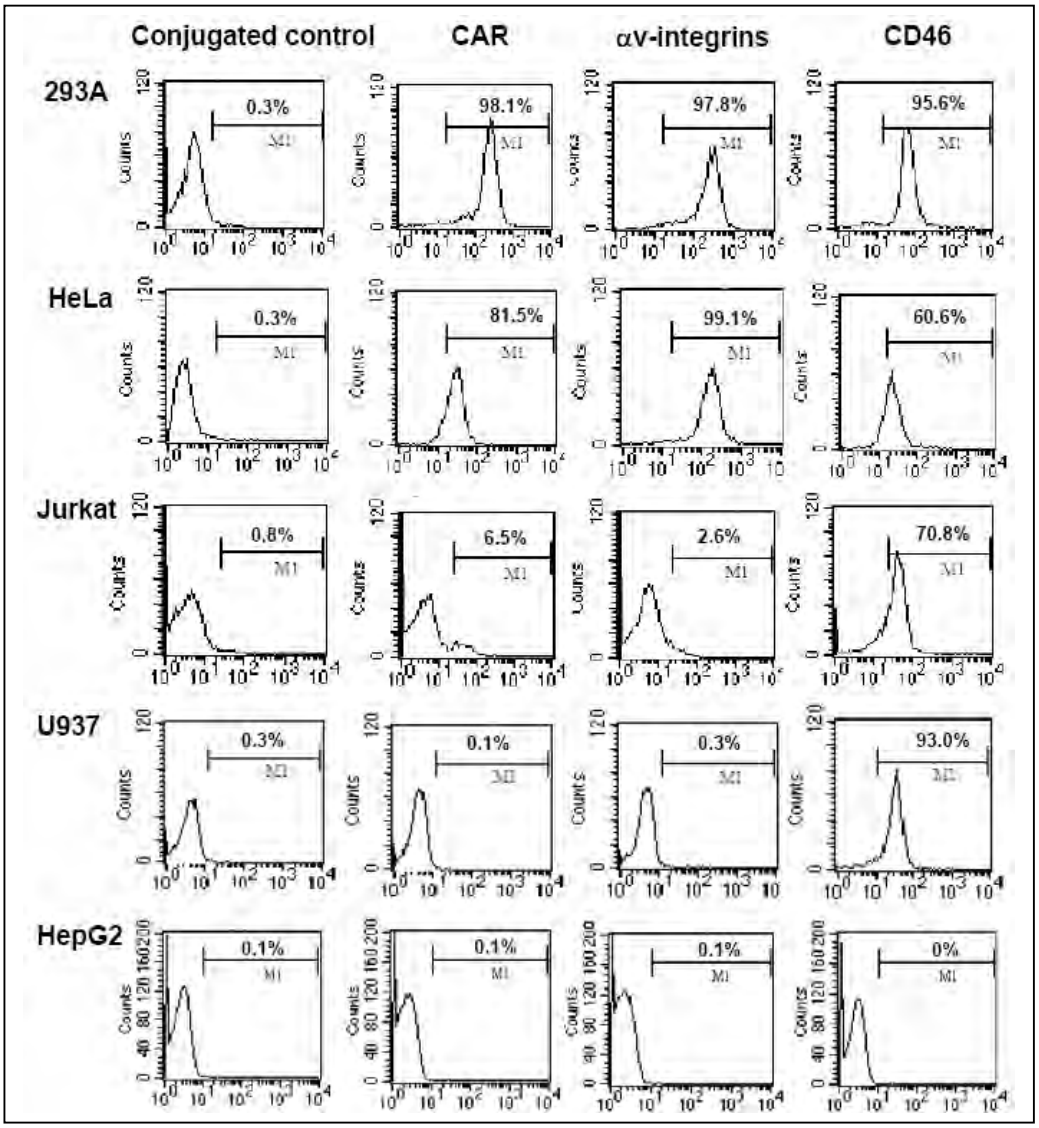

Figure 3.13 Expression of CAR and αv integrin on cell lines. For flow cytometric analysis, 293A, HeLa, Jurkat, U937 and HepG2 cells were incubated with an anti-CAR (RmcB; 1:100 dilution) or anti-αv integrin (L230; 1:100 dilution) mAb or PE-conjugated anti-CD46. The binding of primary antibodies (anti-CAR and anti-αv integrin) was detected by sheep anti-mouse immunoglobulins-PE conjugates (1:100 dilution).

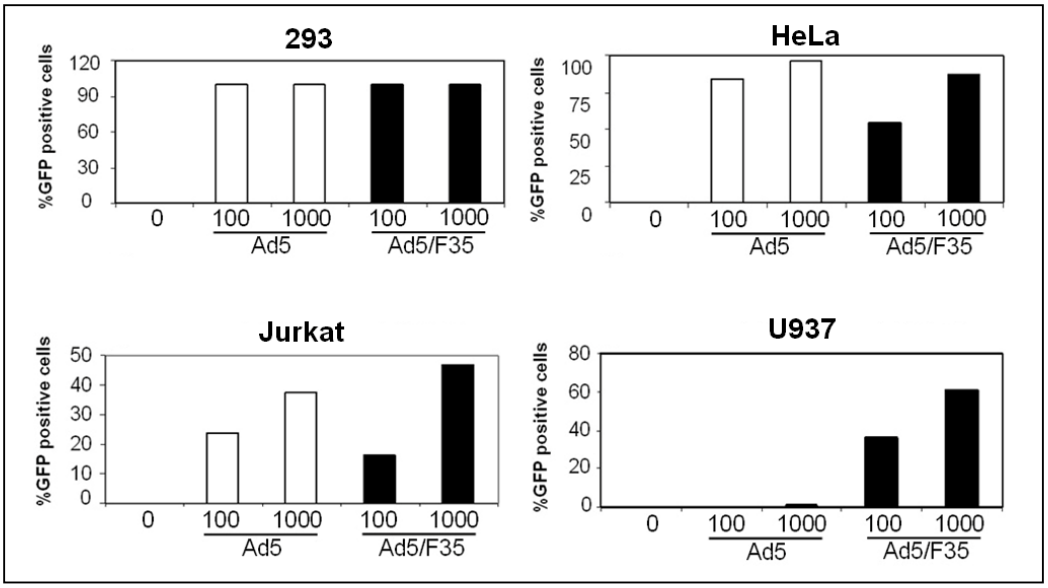

Figure 3.14 Efficient transduction of Ad5 and Ad5/F35 infectivity in four cell lines. Cells were transduced with 0, 100, 1000 viral particles (VP) per cell. After 24 h, the cells were analyzed for GFP expression by flow cytometer. Ad-scFv-M6-1B9 is notated as Ad5 and Ad5/F35-scFv-M6-1B9 as Ad5/F35.

3.8 Intracellular expression of scFv-M6-1B9 intrabody diminished cell surface expression of CD147

3.8.1 293A cells

The compatibility of scFv-M6-1B9 with a eukaryotic expression system was examined by transducing the recombinant adenovirus harboring scFv-M6-1B9 into 293A cells. Alteration of surface expression of CD147 in transduced 293A cells was examined at 36 h after transduction. CD147 cell surface expression was decreased in scFv-M6-1B9 adenovirus-transduced 293A cells compared to untransduced cells (**Figure 3.15**). In contrast, no alteration of CD147 expression was observed on scFv-SVV3 adenovirus transduced cells. This result revealed that intracellular expression of scFv-M6-1B9 as intrabody could diminish CD147 expression on cell surface of intrabody-expressing 293A cells.

Colocalization of scFv-M6-1B9 intrabody and CD147 within 293A cells was elucidated. As shown in **Figure 3.16** and in the three-dimensional movies **(Additional file 1)**, scFv-M6-1B9 intrabody was found intracellularly and colocalized with CD147. This result implied that scFv-M6-1B9 protein fused with ER-retention signal was successfully expressed and retained the CD147 molecule inside the cell.

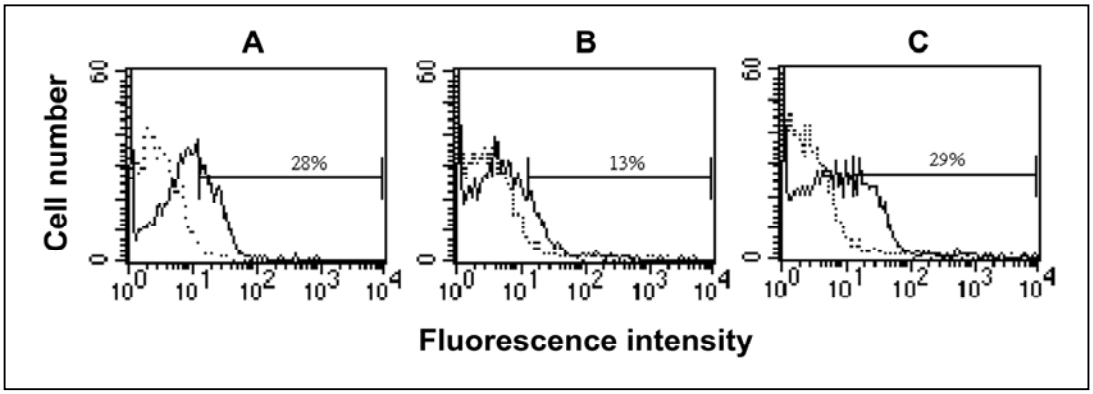

Figure 3.15 Inhibition of CD147 surface expression on 293A cells by M6-1B9 intrabody. 293A cells were transduced with recombinant adenovirus harboring scFv-M6-1B9 or scFv-SVV3. Cell surface staining of CD147 on untransduced **(A)** and scFv-M6-1B9 **(B)** or scFv-SVV3 transduced cells **(C)** was performed using CD147 mAb, M6-1B9 (bold lines) or irrelevant isotype matched mAb (dashed lines). PE-conjugated F(ab')2 fragment of sheep anti-mouse immunoglobulins antibody were used as a secondary antibody. The percentage (%) of CD147 positive cells was indicated.

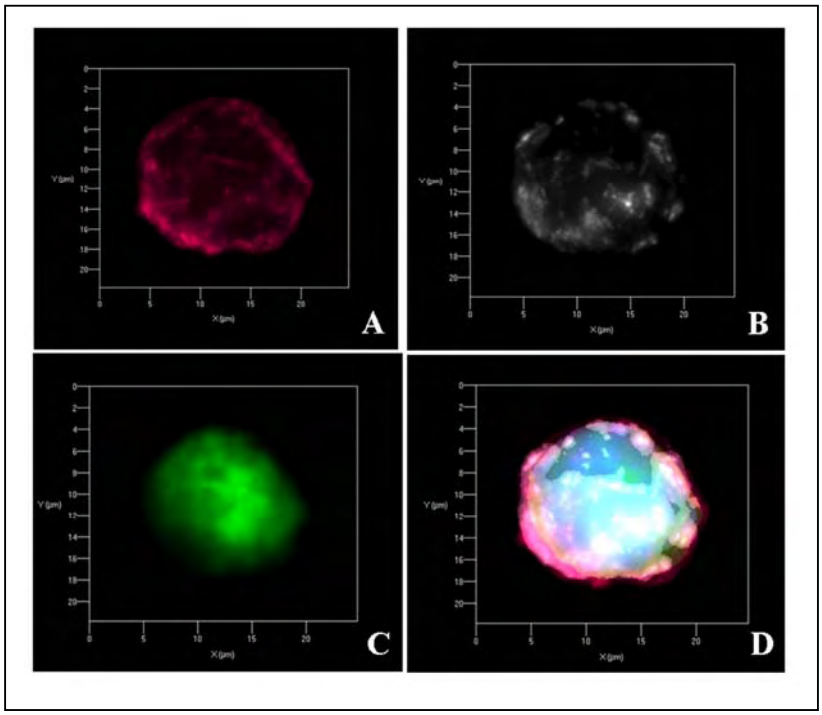

Figure 3.16 Immunocytochemical analysis for colocalization of CD147-intrabody. The transfected 293A cells were fixed and incubated with a mixture of biotinylated anti-human extracellular matrix metalloproteinase inducer (EMMPRIN) mAb and rabbit anti-HA mAb. Then, cells were stained with the mixture of Cy5-conjugated streptavidin and Cy3-conjugated anti-rabbit-IgG mAb. Nuclei were counterstained with DAPI (blue). Three-dimensional (3D) image of the transfected 293A cells was verified. **(A)** CD147 on 293A cell stained with biotinylated anti-human EMMPRIN mAb (red), **(B)** scFv-M6-1B9 intrabody in 293A cell stained with rabbit anti-HA mAb (white), **(C)** GFP positive in transfected cell and **(D)** overlay.

3.8.2 HeLa cells

HeLa cells were used as a representative cancer cell to elucidate the effect of scFv intrabody on the cell surface expression of CD147. HeLa cells were transduced with Ad-scFv-M6-1B9 and Ad-scFv-SVV3 at 200 pfu/cell and analyzed for the surface expression of CD147 at 36 h after transduction. The GFP expression in transduced HeLa cells was demonstrated in **Figure 3.17A.** Nearly 100% of HeLa cells were transduced with Ad-scFv-M6-1B9 and Ad-scFv-SVV3 at MOI of 200. This result indicates that both Ads had essentially identical and high infectivity for HeLa cells. Alteration of surface expression of CD147 in transduced HeLa cells was examined at 36 h after transduction. CD147 cell surface expression was decreased in scFv-M6-1B9 adenovirus-transduced HeLa cells compared to untransduced cells **(Figure 3.17B)**. Interestingly, no alteration of CD147 expression was observed on scFv-SVV3 adenovirus-transduced HeLa cells. The expression of scFv-M6-1B9 intrabody in HeLa cells was analyzed by immunofluorescent staining As shown in **Figure 3.18** and in the three-dimensional movies **(Additional file 2)**, scFv-M6-1B9 intrabody was found intracellularly **(Figure 3.18B)** and colocalized with CD147 **(Figure 3.18D and 3.18E)** . Colocalization between scFv-M6-1B9 intrabody and CD147 was analyzed by FV1000 software. Lambda scan and sequential features were used for separating the cross talk of fluorochromes, Alexa Fluor 488 and Alexa Fluor 568. GFP and Alexa Fluor 488 were separated by spectral unmixing function. The degree of colocalization was quantified using statistical analysis. Pearson's correlation coefficient was 0.51. This result reveals that intracellular expression of scFv-M6-1B9

as intrabody could abate CD147 expression on cell surface of intrabody-expressing HeLa cells.

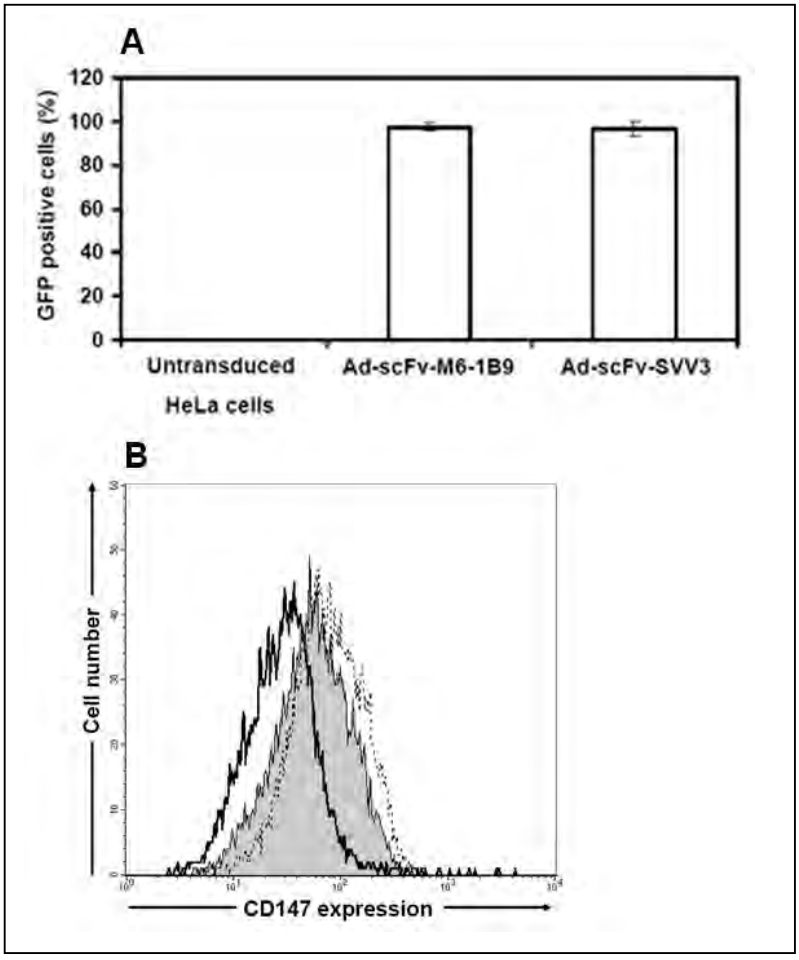

Figure 3.17 Inhibition of CD147 surface expression on HeLa cells by M6-1B9 intrabody. **(A)** HeLa cells were transduced with Ad-scFv-M6-1B9 or Ad-scFv-SVV3 at an MOI of 200 pfu/cell. After 36 h, the percentage of GFP-positive cells was determined by flow cytometry. Data represents the average percentage of GFP-expressing cells ± standard error mean (s.e.m.) of three experiments. **(B)** Transduced

HeLa cells with 200 pfu/cell of Ad-scFv-M6-1B9 or Ad-scFv-SVV3 were stained with mouse anti-CD147 mAb (M6-1B9). PE-conjugated F(ab')2 fragment of sheep anti-mouse immunoglobulins antibody were used as a secondary antibody. The fluorescence intensity of CD147 cell surface expression on untransduced HeLa cells (solid shade), transduced cells with Ad-scFv-M6-1B9 (bold line) or Ad-scFv-SVV3 (dash line) is shown. The *y* axis represents the number of events on a linear scale; the *x* axis shows the fluorescence intensity on a logarithmic scale.

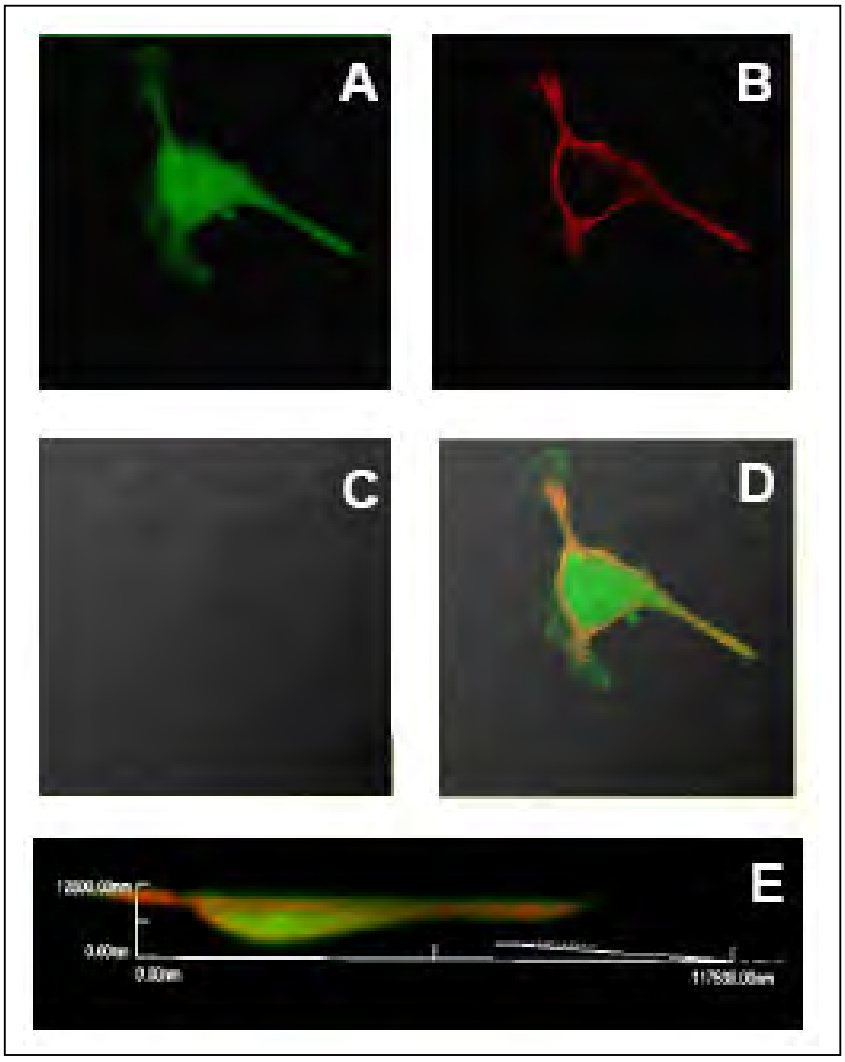

Figure 3.18 Intracellular localization of CD147 in HeLa cells harboring CD147 intrabody. Transduced HeLa cells were seeded on slide chamber, fixed in 4% paraformaldehyde, permeabilized with 0.1% Triton X-100 and stained with a mouse anti-CD147 antibody and a rabbit anti-HA antibody. Secondary detection was performed with Alexa Fluor 488 goat anti–mouse IgG antibody and Alexa Fluor 568 goat anti–rabbit IgG antibody. Images were acquired using an Olympus confocal microscope FV1000. **(A)** CD147 staining with mouse anti-CD147 mAb (green), **(B)**

intrabody scFv M6-1B9 staining with rabbit anti-HA mAb (red), **(C)** phase contrast, **(D)** overlay, colocalization of scFv-M6-1B9 and CD147 (yellowish-orange), and **(E)** three-dimensional (3D) image of the transduced HeLa cells was generated and shown the colocalization of scFv and CD147 (yellowish-orange).

3.8.3 Jurkat cells

In general, adenoviral vectors (Ad5) could poorly infect lymphoid leukemic cells. Thus, gene transfer ability of Ad5/F35-scFv-M6-1B9 was further assessed in Jurkat cells. Jurkat cells were transduced with Ad5/F35-scFv-M6-1B9 at various MOI and analyzed for the surface expression of CD147 at 36 h after transduction. The GFP expression in transduced Jurkat cells was demonstrated in **Figure 3.19A.** Fifty percentage of Jurkat cells were transduced with Ad5/F35-scFv-M6-1B9 at MOI of 1. Percentage of GFP-positive cells reached 75% for Jurkat cells transduced by Ad5/F35-scFv-M6-1B9 at an MOI of 100. This result indicates that Ad5/F35-scFv-M6-1B9 had high infectivity for Jurkat cells due to the high expression of CD46 on this cell line (**Figure 3.12**). Alteration of surface expression of CD147 in transduced Jurkat cells was also examined at 36 h after transduction. Interestingly, CD147 cell surface expression was reduced in Ad5/F35-scFv-M6-1B9-transduced Jurkat cells by dose-dependent manner **(Figure 3.19B).**

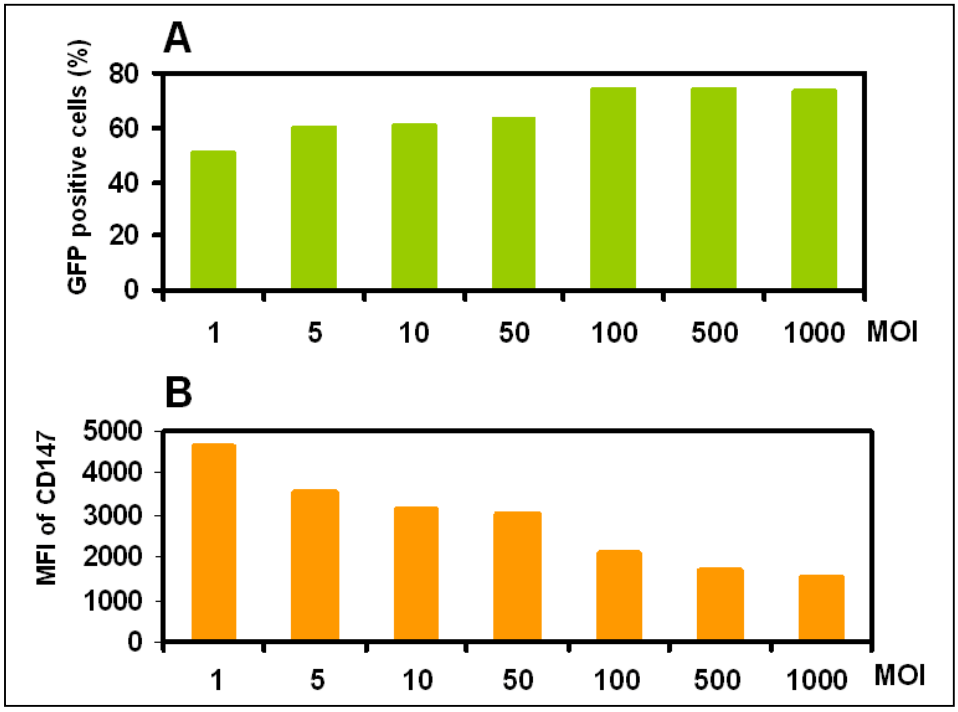

Figure 3.19 Inhibition of CD147 surface expression on Jurkat cells by M6-1B9 intrabody. **(A)** Jurkat cells were transduced with Ad5/F35-scFv-M6-1B9 at various MOI. After 36 h, the percentage of GFP-positive cells was determined by flow cytometry. **(B)** Transduced Jurkat cells with various MOI of Ad5/F35-scFv-M6-1B9 were stained with mouse anti-CD147 mAb (M6-1B9). PE-conjugated F(ab')2 fragment of sheep anti-mouse immunoglobulins antibody were used as a secondary antibody. The *y* axis represents the mean fluorescence intensity (MFI) of CD147 cell surface expression on transduced Jurkat cells; the *x* axis shows the MOI (pfu/cell) of Ad5/F35-scFv-M6-1B9.

DISCUSSION

CD147 is a member of the Ig superfamily that plays a crucial role in several tissues, but is particularly dense on the surface of activated T-lymphocytes (Kasinrerk et al., 1992; Koch et al., 1999) and several malignant tumor cells (Muraoka et al., 1993; Suzuki et al., 2004; Riethdorf et al., 2006). In T cells a negative regulatory signal arises from cross-linking of CD147 molecules and T cell regulation has been demonstrated (Igakura et al., 1996; Koch et al., 1999; Staffler et al., 2003; Chiampanichayakul et al., 2006). Recently, Chiampanichayakul *et. al.* demonstrated that two clones of anti-CD147 mAbs (M6-1E9 and M6-1B9), which react with the membrane-distal Ig domain, inhibited OKT3-induced T cell proliferation (Chiampanichayakul et al., 2006). These mAbs inhibited cell proliferation by delivery of a negative signal through CD147 to suppress CD25 and IL-2 expression (Chiampanichayakul et al., 2006). We thus decided to generate the monomeric scFv-M6-1B9 to investigate the extracellular effect of monomeric scFv-M6-1B9 on OKT3-induced T cell proliferation compared to its parental antibody (M6-1B9). We also generated an intrabody against CD147 to evaluate the intracellular function of scFv against CD147 on various cell types including 293A, HeLa and Jurkat cells. Diminishing the expression of CD147 on the cell surface could serve as a step towards exploring the significance of CD147 in cellular functions and tumor growth.

Prior to generating the scFv-M6-1B9, the critical residues implicated in antigen binding from a given antibody paratope are important for the construction of

different antibody formats. The deduced amino acid residues responsible for paratope in CDR regions of the scFv-M6-1B9 were identified *via* the WAM algorithm (Whitelegg and Rees, 2000) and can be numbered following Kabat's rule (Kabat et al., 1976b; Kabat et al., 1976a). These confirmed the precise cloning of the immunoglobulin variable domains of anti-CD147 mAb, M6-1B9, into the phagemid vector (**Figure 3.1**).

Two antibody formats, Fab and scFv, were exploited for antibody phage display. To assess whether Fab-M6-1B9 or scFv-M6-1B9 on gpIII of phage particles have exclusive activities, both antibody formats were generated and evaluated. The expression of phage-displayed scFv-M6-1B9 was significantly greater than phage-displayed Fab-M6-1B9, and both antibody fragments could recognize the CD147 protein (**Figure 3.2A**). Noticeably, the scFv format exhibited a greater binding activity compared to the Fab format (**Figure 3.2B**). The expression level of scFvs in *E. coli* is typically higher than Fabs and generates a more efficient antibody display on the phage particle. The interdomain disulfide bond at the C-terminal of the constant region, which plays an important role in Fab stabilization, is predisposed to provide lower production yield than scFvs (Rothlisberger et al., 2005).

Recognition of the amber stop codon between the scFv and gpIII genes that occurs during the expression of pComb3X-scFv-M6-1B9 in the non-suppressing HB2151 *E. coli* strain resulted in the production of soluble scFv-M6-1B9 (Barbas, 2001; Su et al., 2003). This antibody fragment was specifically targeted both recombinant CD147 (non-glycosylated form) (**Figure 3.3B**) and native CD147 (glycosylated form) expressed on the surface of U937 cell (**Figure 3.3D**). In addition,

the inhibition of soluble scFv-M6-1B9 by the original antibody, M6-1B9 was demonstrated (**Figure 3.4**). These data show that the soluble antibody fragment contained a properly folded, bioactive paratope which recognized both non-glycosylated and glycosylated forms of CD147. CD147 is a highly glycosylated membrane protein. The variation in its molecular weight, ranging between 30 and 66 kDa, arises from different glycosylation patterns (Biswas et al., 1995). Targeting of both glycosylated and non-glycosylated CD147 molecules *via* scFv-M6-1B9 will be useful as a tool to knockdown the molecules in various cell types.

Moreover, soluble scFv-M6-1B9, which contains only one binding site, had the same inhibitory effect as observed for the parental mAb (**Figure 3.5**). These results indicate that the monomeric scFv form of M6-1B9 is a biologically active protein that is able to activate CD147 and regulate T cell activation. These results also confirm the successful production of a recombinant scFv-M6-1B9 retaining a CD147-specific paratope that binds to its epitope. This result is in agreement with the anti-CD3 scFv-B7.1 fusion protein expressed on the surface of HeLa cells which bound to T lymphocytes and strongly induced T-cell activation (Yang et al., 2007b). Furthermore, many reports have described the same binding specificity and affinity of scFv as the monomeric form of their parental antibody (Bedzyk et al., 1990; Pantoliano et al., 1991; Kim et al., 2002). These studies indicate that in the absence of cross-linking and covalent dimerization of parental CD147 mAb, the monomeric form of anti-CD147 molecules can mediate signal transduction and exhibit the biological activity in T cells through their antigen-specific domain. Even though hybridoma cells can produce monoclonal antibodies for years, but

production involves a labor-intensive multistep process limited by the constant risk of contamination, often requires feeder cells, and may be genetically unstable (Harlow, 1998). Thus, our scFv format has a favorable circumstance to preserve the genetic source of the antibody fragment by cloning it into a phagemid vector and utilizing relatively simple production in bacteria. Furthermore, the small molecular size of scFv should provide high tissue penetration efficiency (Kioi et al., 2008; Liu et al., 2008; Stirnemann et al., 2008), and a lack of significant toxicity (Korn et al., 2004; Yang et al., 2007a; Nam et al., 2008) while giving rapid plasma clearance (Mao et al., 1999; Hamilton et al., 2002; Olafsen et al., 2004; Pavoni et al., 2006), which makes such an antibody a potentially suitable candidate for clinical application.

To assess whether scFv-M6-1B9 generated by mammalian cells possesses the same activity as scFv-M6-1B9 generated by bacterial cells, we evaluated the binding ability of scFv-M6-1B9 intrabody produced from 293A cells to CD147. This intrabody was specifically targeted to both recombinant CD147 (non-glycosylated form, **Figure 3.10B**) and native CD147 expressed on the surface of HeLa cells (**Figure 3.11**). Our results demonstrated that the soluble antibody fragment produced from bacteria and mammalian cells had correct folding and could recognize both the native and recombinant forms of CD147.

Generation of adenoviral recombinants carrying scFv-M6-1B9 intrabody in 293A cells was deemed successful, since the cell surface expression of CD147 on these transduced cells declined (**Figure 3.14**). This indicates that an intrabody with a carboxyl-terminal ER retention signal (KDEL) was retained in the membrane of the ER compartment. This sequestration resulted in the binding of

intrabody to the newly synthesized CD147 and retained this molecule inside the cells, as confirmed by three-dimensional imaging (**Figure 3.15**).

While non-viral strategies demonstrate low transduction efficiency and transient transgene expression, viral transfer methods seem to have a greater potential for a successful gene transfer (Yamaoka et al., 2005; Doebis et al., 2006; Boldicke, 2007). Intrabody expression in HeLa and Jurkat cells using the adenoviral system was achieved in this study and resulted in decreasing of CD147 cell surface expression on these transduced cells (**Figure 3.16B** and **3.18B**). Colocalization between scFv-M6-1B9 intrabody and CD147 was demonstrated *via* confocal microscopy (**Figure 3.17D** and **3.17E**). This supports the starting assumption that the specific interaction between CD147 and scFv-M6-1B9 specific intrabody leads to abate the surface CD147 expression. In other studies, targeting of intrabodies to the ER has been successfully applied to knockdown major histocompatibility complex I (MHC-I) expression (Mhashilkar et al., 2002; Beyer et al., 2004; Zdoroveac et al., 2008) and inactivate various neoplastic cell-surface receptors (Wheeler et al., 2003; Jendreyko et al., 2005; Peng et al., 2007). Additionally, the same strategy was used to block cell surface expression of the CCR5 receptor which is important for cell entry of HIV-1 (Steinberger et al., 2000). Thus the KDEL signal may be essential for the single-chain antibody protein to abate the expression of cell surface molecules. The remaining CD147 could be due to the incomplete knockdown effect resulting from transient expression of the scFv-M6-1B9 intrabody.

Overexpression of CD147 promotes invasion, metastasis, growth and survival of malignant cells (Yan et al., 2005). In previous studies CD147 has been

successfully downregulated by RNA interference (RNAi) technology in several cell lines, including prostate cancer (Wang et al., 2006), human malignant melanoma A375 (Chen et al., 2006), human ovarian cancer cell line HO-8910pm (Zou et al., 2007), and human Jurkat T-lymphoma (Chen et al., 2008). Knockdown of CD147 by siRNA resulted in decreased tumor cell proliferation and invasion activity *in vitro*. In addition, CD147 siRNA also downregulated the expression of VEGF at mRNA and protein levels in A375 cells (Chen et al., 2006). The urokinase-type plasminogen activator (uPA) system including uPA, its specific receptor uPAR and its primary inhibitor plasminogen activator inhibitor-1 (PAI-1) was also downregulated at the mRNA and protein levels in human breast epithelial cell line, NS2T2A. In human breast epithelial cell lines, MDA-MB 231 and Malme-3M, uPA was downregulated at the mRNA and protein levels (Quemener et al., 2007) and MCT4 was downregulated at the protein level (Gallagher et al., 2007). Intrabodies demonstrate an alternative strategy of gene inactivation that targets genomic DNA or mRNA. Unlike RNAi technology, intrabodies act at the posttranslational level and can be directed to relevant subcellular compartments (Lobato and Rabbitts, 2004; Heng et al., 2005; Boldicke, 2007). Because of their high affinity, high specificity and stability, intrabodies present an attractive alternative to modulate protein function and many protocols utilizing intracellular antibodies to neutralize the function of target proteins have been developed for cancer research (Cao and Heng, 2005; Heng et al., 2005). We feel that downregulating CD147 on cancer cells using intrabody technology is available strategy for studying the role of CD147 in tumor invasion and metastasis.

And furthermore, this methodology could prove to be a promising approach for cancer therapy.

In summary, we demonstrated the advantages of recombinant antibody technology and provided an alternative strategy to engineer low-cost antibodies with desirable affinity and specificity by enabling one to manipulate the basic domain structure of the immunoglobulin molecule. We have shown that soluble scFv-M6-1B9 binds to CD147 resulting in an inhibition of OKT3-mediated T cell proliferation. Furthermore, the scFv-M6-1B9 intrabody produced after adenoviral gene transfer was able to suppress the expression of CD147 on 293A, HeLa and Jurkat cells. These novel findings could prove to be a promising strategy for the study of the function of CD147 and provide ways to treat cancer in the near future.

CONCLUSION

This study aimed to generate and characterize a recombinant antibody fragment, scFv, which reacted specifically to CD147 and further investigated the biological properties, function and the effect of generated scFv on CD147 expression. Phage display technology was introduced to generate the functional antibody fragment to CD147. The recombinant antibody fragments, Fab and scFv, of the murine monoclonal antibody (clone M6-1B9) reacted specifically to CD147 as shown by indirect enzyme-linked immunosorbent assays (ELISA) using a recombinant CD147-BCCP as a target. This indicated that the Fab- and scFv-M6-1B9 displayed on phage surfaces were correctly folded and functionally active. In addition, the soluble scFv-M6-1B9 produced from *E. coli* HB2151 bound to CD147 surface molecule and restrained OKT3-induced T cell proliferation. We subsequently constructed a CD147-specific scFv that was expressed intracellularly and retained in the endoplasmic reticulum after adenoviral gene transfer. Likewise, soluble lysate of scFv-M6-1B9 from 293A cells, transduced with a scFv-M6-1B9 expressing adenovirus vector, recognized both recombinant and native CD147. These results indicate that scFv-M6-1B9 binds with high efficiency and specificity. Thereafter, the expression of CD147 on the surface of transduced cells was analyzed by flow cytometry. Importantly, scFv-M6-1B9 intrabody reduced the expression of CD147 on the cell surface of 293A, HeLa, and Jurkat cells suggesting that scFv-M6-1B9 is biologically active. Colocalization of scFv-M6-1B9 intrabody with CD147 in the ER network was

depicted using an immunofluorescence staining. In conclusion, we generated biologically active antibody fragments which bind specifically to both intracellular and extracellular CD147. The generated scFv-M6-1B9 may be an effective agent to study the cellular function of CD147 and may aid in efforts to develop a novel treatment for various human carcinomas.

REFERENCES

Abbasova, S.G., Shcheprova Zh, M., Laman, A.G., Shepelyakovskaya, A.O., Baidakova, L.K., Rodionov, I.L. and Kushlinskii, N.E. (2007) Epitope mapping of human Fas using peptide phage display. Bull Exp Biol Med 144, 515-9.

Afanasieva, T.A., Wittmer, M., Vitaliti, A., Ajmo, M., Neri, D. and Klemenz, R. (2003) Single-chain antibody and its derivatives directed against vascular endothelial growth factor: application for antiangiogenic gene therapy. Gene Ther 10, 1850-9.

Altruda, F., Cervella, P., Gaeta, M.L., Daniele, A., Giancotti, F., Tarone, G., Stefanuto, G. and Silengo, L. (1989) Cloning of cDNA for a novel mouse membrane glycoprotein (gp42): shared identity to histocompatibility antigens, immunoglobulins and neural-cell adhesion molecules. Gene 85, 445-51.

Alvarez, R.D., Barnes, M.N., Gomez-Navarro, J., Wang, M., Strong, T.V., Arafat, W., Arani, R.B., Johnson, M.R., Roberts, B.L., Siegal, G.P. and Curiel, D.T. (2000) A cancer gene therapy approach utilizing an anti-erbB-2 single-chain antibody-encoding adenovirus (AD21): a phase I trial. Clin Cancer Res 6, 3081-7.

Azzazy, H.M. and Highsmith, W.E., Jr. (2002) Phage display technology: clinical applications and recent innovations. Clin Biochem 35, 425-45.

Baneyx, F. and Mujacic, M. (2004) Recombinant protein folding and misfolding in *Escherichia coli.* Nat Biotechnol 22, 1399-408.

Barbas, C.F.3rd., Burton, D.R., Scott, J.K., Silverman, G.J. (2001) Phage display: a laboratory manual. Cold Spring Harbor Laboratory Press, NY.

Bardwell, J.C., McGovern, K. and Beckwith, J. (1991) Identification of a protein required for disulfide bond formation *in vivo*. Cell 67, 581-9.

Barouch, D.H. and Nabel, G.J. (2005) Adenovirus vector-based vaccines for human immunodeficiency virus type 1. Hum Gene Ther 16, 149-56.

Bass, S., Greene, R. and Wells, J.A. (1990) Hormone phage: an enrichment method for variant proteins with altered binding properties. Proteins 8, 309-14.

Baum, C., Dullmann, J., Li, Z., Fehse, B., Meyer, J., Williams, D.A. and von Kalle, C. (2003) Side effects of retroviral gene transfer into hematopoietic stem cells. Blood 101, 2099-114.

Bedzyk, W.D., Weidner, K.M., Denzin, L.K., Johnson, L.S., Hardman, K.D., Pantoliano, M.W., Asel, E.D. and Voss, E.W., Jr. (1990) Immunological and structural characterization of a high affinity anti-fluorescein single-chain antibody. J Biol Chem 265, 18615-20.

Beerli, R.R., Wels, W. and Hynes, N.E. (1994) Autocrine inhibition of the epidermal growth factor receptor by intracellular expression of a single-chain antibody. Biochem Biophys Res Commun 204, 666-72.

Berditchevski, F., Chang, S., Bodorova, J. and Hemler, M.E. (1997) Generation of monoclonal antibodies to integrin-associated proteins. Evidence that alpha3beta1 complexes with EMMPRIN/basigin/OX47/M6. J Biol Chem 272, 29174-80.

Bergelson, J.M., Cunningham, J.A., Droguett, G., Kurt-Jones, E.A., Krithivas, A., Hong, J.S., Horwitz, M.S., Crowell, R.L. and Finberg, R.W. (1997) Isolation of a common receptor for Coxsackie B viruses and adenoviruses 2 and 5. Science 275, 1320-3.

Berk, A.J. (2007) Adenoviridae: The viruses and their replication. In "Fields Virology" (D. M. Knipe, and P. M. Howley, 5th Eds.) Vol. II. Lippincott Williams & Wilkins, a Wolters Kluwer Business, Philadelphia.

Berntzen, G., Andersen, J.T., Ustgard, K., Michaelsen, T.E., Mousavi, S.A., Qian, J.D., Kristiansen, P.E., Lauvrak, V. and Sandlie, I. (2009) Identification of a high affinity FcgammaRIIA-binding peptide that distinguishes FcgammaRIIA from FcgammaRIIB and exploits FcgammaRIIA-mediated phagocytosis and degradation. J Biol Chem 284, 1126-35.

Beyer, F., Doebis, C., Busch, A., Ritter, T., Mhashilkar, A., Marasco, W.M., Laube, H., Volk, H.D. and Seifert, M. (2004) Decline of surface MHC I by adenoviral gene transfer of anti-MHC I intrabodies in human endothelial cells-new perspectives for the generation of universal donor cells for tissue transplantation. J Gene Med 6, 616-23.

Biswas, C., Zhang, Y., DeCastro, R., Guo, H., Nakamura, T., Kataoka, H. and Nabeshima, K. (1995) The human tumor cell-derived collagenase stimulatory factor (renamed EMMPRIN) is a member of the immunoglobulin superfamily. Cancer Res 55, 434-9.

Bitto, E. and McKay, D.B. (2002) Crystallographic structure of SurA, a molecular chaperone that facilitates folding of outer membrane porins. Structure 10, 1489-98.

Bitto, E. and McKay, D.B. (2003) The periplasmic molecular chaperone protein SurA binds a peptide motif that is characteristic of integral outer membrane proteins. J Biol Chem 278, 49316-22.

Bloomfield, V.A. (1996) DNA condensation. Curr Opin Struct Biol 6, 334-41.

Boldicke, T. (2007) Blocking translocation of cell surface molecules from the ER to the cell surface by intracellular antibodies targeted to the ER. J Cell Mol Med 11, 54-70.

Boldicke, T., Weber, H., Mueller, P.P., Barleon, B. and Bernal, M. (2005) Novel highly efficient intrabody mediates complete inhibition of cell surface expression of the human vascular endothelial growth factor receptor-2 (VEGFR-2/KDR). J Immunol Methods 300, 146-59.

Bukau, B. (1993) Regulation of the *Escherichia coli* heat-shock response. Mol Microbiol 9, 671-80.

Bukau, B. and Horwich, A.L. (1998) The Hsp70 and Hsp60 chaperone machines. Cell 92, 351-66.

Cao, T. and Heng, B.C. (2005) Intracellular antibodies (intrabodies) versus RNA interference for therapeutic applications. Ann Clin Lab Sci 35, 227-9.

Carlson, J.R. (1988) A new means of inducibly inactivating a cellular protein. Mol Cell Biol 8, 2638-46.

Cascales, E., Gavioli, M., Sturgis, J.N. and Lloubes, R. (2000) Proton motive force drives the interaction of the inner membrane TolA and outer membrane pal proteins in *Escherichia coli*. Mol Microbiol 38, 904-15.

Casey, J.L., Coley, A.M. and Foley, M. (2008) Phage display of peptides in ligand selection for use in affinity chromatography. Methods Mol Biol 421, 111-24.

Cattaneo, R. (2004) Four viruses, two bacteria, and one receptor: membrane cofactor protein (CD46) as pathogens' magnet. J Virol 78, 4385-8.

Cesareni, G. (1992) Peptide display on filamentous phage capsids: A new powerful tool to study protein-ligand interaction. FEBS Lett 307, 66-70.

Chen, X., Lin, J., Kanekura, T., Su, J., Lin, W., Xie, H., Wu, Y., Li, J., Chen, M. and Chang, J. (2006) A small interfering CD147-targeting RNA inhibited the proliferation, invasiveness, and metastatic activity of malignant melanoma. Cancer Res 66, 11323-30.

Chen, X., Su, J., Chang, J., Kanekura, T., Li, J., Kuang, Y.H., Peng, S., Yang, F., Lu, H. and Zhang, J.L. (2008) Inhibition of CD147 Gene Expression via RNA Interference Reduces Tumor Cell Proliferation, Activation, Adhesion, and Migration Activity in the Human Jurkat T-Lymphoma Cell Line. Cancer Invest, 1.

Chiampanichayakul, S., Peng-In, P., Khunkaewla, P., Stockinger, H. and Kasinrerk, W. (2006) CD147 contains different bioactive epitopes involving the regulation of cell adhesion and lymphocyte activation. Immunobiology 211, 167-78.

Choi, J.H. and Lee, S.Y. (2004) Secretory and extracellular production of recombinant proteins using *Escherichia coli*. Appl Microbiol Biotechnol 64, 625-35.

Cohen, C.J., Shieh, J.T., Pickles, R.J., Okegawa, T., Hsieh, J.T. and Bergelson, J.M. (2001) The coxsackievirus and adenovirus receptor is a transmembrane component of the tight junction. Proc Natl Acad Sci U S A 98, 15191-6.

Curtin, K.D., Meinertzhagen, I.A. and Wyman, R.J. (2005) Basigin (EMMPRIN/CD147) interacts with integrin to affect cellular architecture. J Cell Sci 118, 2649-60.

Danese, P.N. and Silhavy, T.J. (1997) The sigma(E) and the Cpx signal transduction systems control the synthesis of periplasmic protein-folding enzymes in *Escherichia coli*. Genes Dev 11, 1183-93.

Danese, P.N., Snyder, W.B., Cosma, C.L., Davis, L.J. and Silhavy, T.J. (1995) The Cpx two-component signal transduction pathway of *Escherichia coli* regulates transcription of the gene specifying the stress-inducible periplasmic protease, DegP. Genes Dev 9, 387-98.

Darby, N.J. and Creighton, T.E. (1995) Catalytic mechanism of DsbA and its comparison with that of protein disulfide isomerase. Biochemistry 34, 3576-87.

de Gier, J.W. and Luirink, J. (2001) Biogenesis of inner membrane proteins in *Escherichia coli*. Mol Microbiol 40, 314-22.

de Keyzer, J., van der Does, C. and Driessen, A.J. (2003) The bacterial translocase: a dynamic protein channel complex. Cell Mol Life Sci 60, 2034-52.

De Las Penas, A., Connolly, L. and Gross, C.A. (1997) The sigmaE-mediated response to extracytoplasmic stress in *Escherichia coli* is transduced by RseA and RseB, two negative regulators of sigmaE. Mol Microbiol 24, 373-85.

Dechecchi, M.C., Melotti, P., Bonizzato, A., Santacatterina, M., Chilosi, M. and Cabrini, G. (2001) Heparan sulfate glycosaminoglycans are receptors sufficient to mediate the initial binding of adenovirus types 2 and 5. J Virol 75, 8772-80.

Deng, L.W., Malik, P. and Perham, R.N. (1999) Interaction of the globular domains of pIII protein of filamentous bacteriophage fd with the F-pilus of *Escherichia coli*. Virology 253, 271-7.

Deshane, J., Cabrera, G., Grim, J.E., Siegal, G.P., Pike, J., Alvarez, R.D. and Curiel, D.T. (1995a) Targeted eradication of ovarian cancer mediated by intracellular expression of anti-erbB-2 single-chain antibody. Gynecol Oncol 59, 8-14.

Deshane, J., Siegal, G.P., Alvarez, R.D., Wang, M.H., Feng, M., Cabrera, G., Liu, T., Kay, M. and Curiel, D.T. (1995b) Targeted tumor killing via an intracellular antibody against erbB-2. J Clin Invest 96, 2980-9.

Dobson, C.M. (2003) Protein folding and misfolding. Nature 426, 884-90.

Doebis, C., Schu, S., Ladhoff, J., Busch, A., Beyer, F., Reiser, J., Nicosia, R.F., Broesel, S., Volk, H.D. and Seifert, M. (2006) An anti-major histocompatibility complex class I intrabody protects endothelial cells from an attack by immune mediators. Cardiovasc Res 72, 331-8.

Doerfler, W., Schubbert, R., Heller, H., Kammer, C., Hilger-Eversheim, K., Knoblauch, M. and Remus, R. (1997) Integration of foreign DNA and its consequences in mammalian systems. Trends Biotechnol 15, 297-301.

Driessen, A.J., Fekkes, P. and van der Wolk, J.P. (1998) The Sec system. Curr Opin Microbiol 1, 216-22.

Driskell, R.A. and Engelhardt, J.F. (2003) Current status of gene therapy for inherited lung diseases. Annu Rev Physiol 65, 585-612.

Emadi, S., Barkhordarian, H., Wang, M.S., Schulz, P. and Sierks, M.R. (2007) Isolation of a human single chain antibody fragment against oligomeric alpha-synuclein that inhibits aggregation and prevents alpha-synuclein-induced toxicity. J Mol Biol 368, 1132-44.

Erickson, J.W. and Gross, C.A. (1989) Identification of the sigma E subunit of *Escherichia coli* RNA polymerase: a second alternate sigma factor involved in high-temperature gene expression. Genes Dev 3, 1462-71.

Fadool, J.M. and Linser, P.J. (1993) 5A11 antigen is a cell recognition molecule which is involved in neuronal-glial interactions in avian neural retina. Dev Dyn 196, 252-62.

Fekkes, P., de Wit, J.G., van der Wolk, J.P., Kimsey, H.H., Kumamoto, C.A. and Driessen, A.J. (1998) Preprotein transfer to the *Escherichia coli* translocase requires the co-operative binding of SecB and the signal sequence to SecA. Mol Microbiol 29, 1179-90.

Fekkes, P. and Driessen, A.J. (1999) Protein targeting to the bacterial cytoplasmic membrane. Microbiol Mol Biol Rev 63, 161-73.

Fessler, S.P. and Young, C.S. (1998) Control of adenovirus early gene expression during the late phase of infection. J Virol 72, 4049-56.

Fleischli, C., Verhaagh, S., Havenga, M., Sirena, D., Schaffner, W., Cattaneo, R., Greber, U.F. and Hemmi, S. (2005) The distal short consensus repeats 1 and 2 of the membrane cofactor protein CD46 and their distance from the cell membrane determine productive entry of species B adenovirus serotype 35. J Virol 79, 10013-22.

Fossum, S., Mallett, S. and Barclay, A.N. (1991) The MRC OX-47 antigen is a member of the immunoglobulin superfamily with an unusual transmembrane sequence. Eur J Immunol 21, 671-9.

Frech, C., Wunderlich, M., Glockshuber, R. and Schmid, F.X. (1996) Preferential binding of an unfolded protein to DsbA. EMBO J 15, 392-98.

Fulford, W. and Model, P. (1984) Gene X of bacteriophage f1 is required for phage DNA synthesis. Mutagenesis of in-frame overlapping genes. J Mol Biol 178, 137-53.

Gabison, E.E., Mourah, S., Steinfels, E., Yan, L., Hoang-Xuan, T., Watsky, M.A., De Wever, B., Calvo, F., Mauviel, A. and Menashi, S. (2005) Differential expression of extracellular matrix metalloproteinase inducer (CD147) in normal and ulcerated corneas: role in epithelio-stromal interactions and matrix metalloproteinase induction. Am J Pathol 166, 209-19.

Gaggar, A., Shayakhmetov, D.M. and Lieber, A. (2003) CD46 is a cellular receptor for group B adenoviruses. Nat Med 9, 1408-12.

Gaggar, A., Shayakhmetov, D.M., Liszewski, M.K., Atkinson, J.P. and Lieber, A. (2005) Localization of regions in CD46 that interact with adenovirus. J Virol 79, 7503-13.

Gailus, V., Ramsperger, U., Johner, C., Kramer, H. and Rasched, I. (1994) The role of the adsorption complex in the termination of filamentous phage assembly. Res Microbiol 145, 699-709.

Gallagher, S.M., Castorino, J.J., Wang, D. and Philp, N.J. (2007) Monocarboxylate transporter 4 regulates maturation and trafficking of CD147 to the plasma membrane in the metastatic breast cancer cell line MDA-MB-231. Cancer Res 67, 4182-9.

Gamer, J., Multhaup, G., Tomoyasu, T., McCarty, J.S., Rudiger, S., Schonfeld, H.J., Schirra, C., Bujard, H. and Bukau, B. (1996) A cycle of binding and release of the DnaK, DnaJ and GrpE chaperones regulates activity of the Escherichia coli heat shock transcription factor sigma32. EMBO J 15, 607-17.

Glasgow, J.N., Bauerschmitz, G.J., Curiel, D.T. and Hemminki, A. (2004) Transductional and transcriptional targeting of adenovirus for clinical applications. Curr Gene Ther 4, 1-14.

Goenaga, A.L., Zhou, Y., Legay, C., Bougherara, H., Huang, L., Liu, B., Drummond, D.C., Kirpotin, D.B., Auclair, C., Marks, J.D. and Poul, M.A. (2007) Identification and characterization of tumor antigens by using antibody phage display and intrabody strategies. Mol Immunol 44, 3777-88.

Goncalves, M.A. (2005) Adeno-associated virus: from defective virus to effective vector. Virol J 2, 43.

Goodrum, F.D. and Ornelles, D.A. (1999) Roles for the E4 orf6, orf3, and E1B 55-kilodalton proteins in cell cycle-independent adenovirus replication. J Virol 73, 7474-88.

Greber, U.F. (2002) Signalling in viral entry. Cell Mol Life Sci 59, 608-26.

Griesenbach, U., Geddes, D.M. and Alton, E.W. (2006) Gene therapy progress and prospects: cystic fibrosis. Gene Ther 13, 1061-7.

Griffin, H., Elston, R., Jackson, D., Ansell, K., Coleman, M., Winter, G. and Doorbar, J. (2006) Inhibition of papillomavirus protein function in cervical cancer cells by intrabody targeting. J Mol Biol 355, 360-78.

Guo, H., Zucker, S., Gordon, M.K., Toole, B.P. and Biswas, C. (1997) Stimulation of matrix metalloproteinase production by recombinant extracellular matrix metalloproteinase inducer from transfected Chinese hamster ovary cells. J Biol Chem 272, 24-7.

Hacein-Bey-Abina, S., von Kalle, C., Schmidt, M., Le Deist, F., Wulffraat, N., McIntyre, E., Radford, I., Villeval, J.L., Fraser, C.C., Cavazzana-Calvo, M. and Fischer, A. (2003) A serious adverse event after successful gene therapy for X-linked severe combined immunodeficiency. N Engl J Med 348, 255-6.

Halbert, D.N., Cutt, J.R. and Shenk, T. (1985) Adenovirus early region 4 encodes functions required for efficient DNA replication, late gene expression, and host cell shutoff. J Virol 56, 250-7.

Hamilton, S., Odili, J., Wilson, G.D. and Kupsch, J.M. (2002) Reducing renal accumulation of single-chain Fv against melanoma-associated proteoglycan by coadministration of L-lysine. Melanoma Res 12, 373-9.

Hammond, C. and Helenius, A. (1995) Quality control in the secretory pathway. Curr Opin Cell Biol 7, 523-9.

Han, J., Sabbatini, P., Perez, D., Rao, L., Modha, D. and White, E. (1996) The E1B 19K protein blocks apoptosis by interacting with and inhibiting the p53-inducible and death-promoting Bax protein. Genes Dev 10, 461-77.

Hao, J., Serohijos, A.W., Newton, G., Tassone, G., Wang, Z., Sgroi, D.C., Dokholyan, N.V. and Basilion, J.P. (2008) Identification and rational redesign of peptide ligands to CRIP1, a novel biomarker for cancers. PLoS Comput Biol 4, e1000138.

Harlow, E., Lane, D. (1998) Antibodies: A Laboratory Manual. Cold Spring Harbor Laboratory Press, NY.

Harms, N., Koningstein, G., Dontje, W., Muller, M., Oudega, B., Luirink, J. and de Cock, H. (2001) The early interaction of the outer membrane protein phoe with the periplasmic chaperone Skp occurs at the cytoplasmic membrane. J Biol Chem 276, 18804-11.

Hartl, F.U. and Hayer-Hartl, M. (2002) Molecular chaperones in the cytosol: from nascent chain to folded protein. Science 295, 1852-8.

Hay, R.T., Freeman, A., Leith, I., Monaghan, A. and Webster, A. (1995) Molecular interactions during adenovirus DNA replication. Curr Top Microbiol Immunol 199 (Pt 2), 31-48.

He, T.C., Zhou, S., da Costa, L.T., Yu, J., Kinzler, K.W. and Vogelstein, B. (1998) A simplified system for generating recombinant adenoviruses. Proc Natl Acad Sci U S A 95, 2509-14.

Hearing, P., Samulski, R.J., Wishart, W.L. and Shenk, T. (1987) Identification of a repeated sequence element required for efficient encapsidation of the adenovirus type 5 chromosome. J Virol 61, 2555-8.

Hell, R.C., Amim, P., de Andrade, H.M., de Avila, R.A., Felicori, L., Oliveira, A.G., Oliveira, C.A., Nascimento, E., Tavares, C.A., Granier, C. and Chavez-Olortegui, C. (2009) Immunodiagnosis of human neurocysticercosis using a synthetic peptide selected by phage-display. Clin Immunol.

Heller, M., von der Ohe, M., Kleene, R., Mohajeri, M.H. and Schachner, M. (2003) The immunoglobulin-superfamily molecule basigin is a binding protein for oligomannosidic carbohydrates: an anti-idiotypic approach. J Neurochem 84, 557-65.

Heng, B.C., Kemeny, D.M., Liu, H. and Cao, T. (2005) Potential applications of intracellular antibodies (intrabodies) in stem cell therapeutics. J Cell Mol Med 9, 191-5.

Heppner, K.J., Matrisian, L.M., Jensen, R.A. and Rodgers, W.H. (1996) Expression of most matrix metalloproteinase family members in breast cancer represents a tumor-induced host response. Am J Pathol 149, 273-82.

Hertveldt, K., Belien, T. and Volckaert, G. (2009) General M13 phage display: M13 phage display in identification and characterization of protein-protein interactions. Methods Mol Biol 502, 321-39.

Hiniker, A. and Bardwell, J.C. (2003) Disulfide bond isomerization in prokaryotes. Biochemistry 42, 1179-85.

Holliger, P. and Hudson, P.J. (2005) Engineered antibody fragments and the rise of single domains. Nat Biotechnol 23, 1126-36.

Holliger, P. and Riechmann, L. (1997) A conserved infection pathway for filamentous bacteriophages is suggested by the structure of the membrane penetration domain of the minor coat protein g3p from phage fd. Structure 5, 265-75.

Holmgren, A. (1989) Thioredoxin and glutaredoxin systems. J Biol Chem 264, 13963-6.

Hong, S.S., Karayan, L., Tournier, J., Curiel, D.T. and Boulanger, P.A. (1997) Adenovirus type 5 fiber knob binds to MHC class I alpha2 domain at the surface of human epithelial and B lymphoblastoid cells. EMBO J 16, 2294-306.

Hoogenboom, H.R., de Bruine, A.P., Hufton, S.E., Hoet, R.M., Arends, J.W. and Roovers, R.C. (1998) Antibody phage display technology and its applications. Immunotechnology 4, 1-20.

Hoyer, W., Gronwall, C., Jonsson, A., Stahl, S. and Hard, T. (2008) Stabilization of a beta-hairpin in monomeric Alzheimer's amyloid-beta peptide inhibits amyloid formation. Proc Natl Acad Sci U S A 105, 5099-104.

http://www.alt.med-rz.uni-sb.de/med_fak/biochemie/MartinJ/Eninformation.html

http://www.athenaes.com/tech_brief_ACESyebf.php

Huang, S., Kamata, T., Takada, Y., Ruggeri, Z.M. and Nemerow, G.R. (1996) Adenovirus interaction with distinct integrins mediates separate events in cell entry and gene delivery to hematopoietic cells. J Virol 70, 4502-8.

Hudson, P.J. (1998) Recombinant antibody fragments. Curr Opin Biotechnol 9, 395-402.

Igakura, T., Kadomatsu, K., Taguchi, O., Muramatsu, H., Kaname, T., Miyauchi, T., Yamamura, K., Arimura, K. and Muramatsu, T. (1996) Roles of basigin, a member of the immunoglobulin superfamily, in behavior as to an irritating odor, lymphocyte response, and blood-brain barrier. Biochem Biophys Res Commun 224, 33-6.

Intasai, N., Arooncharus, P., Kasinrerk, W. and Tayapiwatana, C. (2003) Construction of high-density display of CD147 ectodomain on VCSM13 phage via gpVIII: effects of temperature, IPTG, and helper phage infection-period. Protein Expr Purif 32, 323-31.

Intasai, N., Mai, S., Kasinrerk, W. and Tayapiwatana, C. (2006) Binding of multivalent CD147 phage induces apoptosis of U937 cells. Int Immunol 18, 1159-69.

Jager, S., Jahnke, A., Wilmes, T., Adebahr, S., Vogtle, F.N., Delima-Hahn, E., Pfeifer, D., Berg, T., Lubbert, M. and Trepel, M. (2007) Leukemia-targeting ligands isolated from phage-display peptide libraries. Leukemia 21, 411-20.

Jannot, C.B., Beerli, R.R., Mason, S., Gullick, W.J. and Hynes, N.E. (1996) Intracellular expression of a single-chain antibody directed to the EGFR leads to growth inhibition of tumor cells. Oncogene 13, 275-82.

Jendreyko, N., Popkov, M., Beerli, R.R., Chung, J., McGavern, D.B., Rader, C. and Barbas, C.F., 3rd. (2003) Intradiabodies, bispecific, tetravalent antibodies for

the simultaneous functional knockout of two cell surface receptors. J Biol Chem 278, 47812-9.

Jendreyko, N., Popkov, M., Rader, C. and Barbas, C.F., 3rd. (2005) Phenotypic knockout of VEGF-R2 and Tie-2 with an intradiabody reduces tumor growth and angiogenesis in vivo. Proc Natl Acad Sci U S A 102, 8293-8.

Jia, L., Xu, H., Zhao, Y., Jiang, L., Yu, J. and Zhang, J. (2008) Expression of CD147 mediates tumor cells invasion and multidrug resistance in hepatocellular carcinoma. Cancer Invest 26, 977-83.

Jones, C.H., Danese, P.N., Pinkner, J.S., Silhavy, T.J. and Hultgren, S.J. (1997) The chaperone-assisted membrane release and folding pathway is sensed by two signal transduction systems. EMBO J 16, 6394-406.

Jung, D., Neron, S., Drouin, M. and Jacques, A. (2005) Efficient gene transfer into normal human B lymphocytes with the chimeric adenoviral vector Ad5/F35. J Immunol Methods 304, 78-87.

Kabat, E.A., Wu, T.T. and Bilofsky, H. (1976a) Attempts to locate residues in complementarity-determining regions of antibody combining sites that make contact with antigen. Proc Natl Acad Sci U S A 73, 617-9.

Kabat, E.A., Wu, T.T. and Bilofsky, H. (1976b) Some correlations between specificity and sequence of the first complementarity-determining segments of human kappa light chains. Proc Natl Acad Sci U S A 73, 4471-3.

Kabat, E.A., Wu, T.T., Bilofsky, H. and National Institutes of Health (U.S.). Division of Research Resources. (1976c) Variable regions of immunoglobulin chains :

tabulations and analyses of amino acid sequences. Medical Computer Systems, Cambridge, Mass.

Kannabiran, C., Morris, G.F. and Mathews, M.B. (1999) Dual action of the adenovirus E1A 243R oncoprotein on the human proliferating cell nuclear antigen promoter: repression of transcriptional activation by p53. Oncogene 18, 7825-33.

Kaplan, J.M., Armentano, D., Scaria, A., Woodworth, L.A., Pennington, S.E., Wadsworth, S.C., Smith, A.E. and Gregory, R.J. (1999) Novel role for E4 region genes in protection of adenovirus vectors from lysis by cytotoxic T lymphocytes. J Virol 73, 4489-92.

Karlsson, F., Borrebaeck, C.A., Nilsson, N. and Malmborg-Hager, A.C. (2003) The mechanism of bacterial infection by filamentous phages involves molecular interactions between TolA and phage protein 3 domains. J Bacteriol 185, 2628-34.

Kasinrerk, W., Fiebiger, E., Stefanova, I., Baumruker, T., Knapp, W. and Stockinger, H. (1992) Human leukocyte activation antigen M6, a member of the Ig superfamily, is the species homologue of rat OX-47, mouse basigin, and chicken HT7 molecule. J Immunol 149, 847-54.

Kasinrerk, W., Tokrasinwit, N. and Phunpae, P. (1999) CD147 monoclonal antibodies induce homotypic cell aggregation of monocytic cell line U937 via LFA-1/ICAM-1 pathway. Immunology 96, 184-92.

Kato-Takagaki, K., Mizukoshi, Y., Yoshizawa, Y., Akazawa, D., Torii, Y., Ono, K., Tanimura, R., Shimada, I. and Takahashi, H. (2009) Structural and interaction

analysis of glycoprotein VI-binding peptide selected from phage display library. J Biol Chem.

Kaufman, R.J. (2002) Orchestrating the unfolded protein response in health and disease. J Clin Invest 110, 1389-98.

Kay, M.A., Glorioso, J.C. and Naldini, L. (2001) Viral vectors for gene therapy: the art of turning infectious agents into vehicles of therapeutics. Nat Med 7, 33-40.

Keiler, K.C., Silber, K.R., Downard, K.M., Papayannopoulos, I.A., Biemann, K. and Sauer, R.T. (1995) C-terminal specific protein degradation: activity and substrate specificity of the Tsp protease. Protein Sci 4, 1507-15.

Khokhlova, O.V. and Nesmeianova, M.A. (2003) [Interaction of SecB and SecA with the N-terminal region of mature alkaline phosphatase on its secretion in *Escherichia coli*]. Mol Biol (Mosk) 37, 712-8.

Khunkeawla, P., Moonsom, S., Staffler, G., Kongtawelert, P. and Kasinrerk, W. (2001) Engagement of CD147 molecule-induced cell aggregation through the activation of protein kinases and reorganization of the cytoskeleton. Immunobiology 203, 659-69.

Kiefhaber, T., Rudolph, R., Kohler, H.H. and Buchner, J. (1991) Protein aggregation *in vitro* and *in vivo*: a quantitative model of the kinetic competition between folding and aggregation. Biotechnology (N Y) 9, 825-9.

Kim, D.J., Chung, J.H., Ryu, Y.S., Rhim, J.H., Kim, C.W., Suh, Y. and Chung, H.K. (2002) Production and characterisation of a recombinant scFv reactive with human gastrointestinal carcinomas. Br J Cancer 87, 405-13.

Kim, J., Chen, C.P. and Rice, K.G. (2005) The proteasome metabolizes peptide-mediated nonviral gene delivery systems. Gene Ther 12, 1581-90.

Kioi, M., Seetharam, S. and Puri, R.K. (2008) Targeting IL-13Ralpha2-positive cancer with a novel recombinant immunotoxin composed of a single-chain antibody and mutated Pseudomonas exotoxin. Mol Cancer Ther 7, 1579-87.

Kirsch, A.H., Diaz, L.A., Jr., Bonish, B., Antony, P.A. and Fox, D.A. (1997) The pattern of expression of CD147/neurothelin during human T-cell ontogeny as defined by the monoclonal antibody 8D6. Tissue Antigens 50, 147-52.

Kleerebezem, M., Crielaard, W. and Tommassen, J. (1996) Involvement of stress protein PspA (phage shock protein A) of *Escherichia coli* in maintenance of the protonmotive force under stress conditions. EMBO J 15, 162-71.

Kobayashi, T., Kishigami, S., Sone, M., Inokuchi, H., Mogi, T. and Ito, K. (1997) Respiratory chain is required to maintain oxidized states of the DsbA-DsbB disulfide bond formation system in aerobically growing *Escherichia coli* cells. Proc Natl Acad Sci U S A 94, 11857-62.

Koch, C., Staffler, G., Huttinger, R., Hilgert, I., Prager, E., Cerny, J., Steinlein, P., Majdic, O., Horejsi, V. and Stockinger, H. (1999) T cell activation-associated epitopes of CD147 in regulation of the T cell response, and their definition by antibody affinity and antigen density. Int Immunol 11, 777-86.

Kontermann, R., Dübel, S. (2001) Antibody engineering. Springer.

Kontermann, R.E. (2004) Intrabodies as therapeutic agents. Methods 34, 163-70.

Korn, T., Nettelbeck, D.M., Volkel, T., Muller, R. and Kontermann, R.E. (2004) Recombinant bispecific antibodies for the targeting of adenoviruses to CEA-

expressing tumour cells: a comparative analysis of bacterially expressed single-chain diabody and tandem scFv. J Gene Med 6, 642-51.

Kwong, K.Y., Baskar, S., Zhang, H., Mackall, C.L. and Rader, C. (2008) Generation, affinity maturation, and characterization of a human anti-human NKG2D monoclonal antibody with dual antagonistic and agonistic activity. J Mol Biol 384, 1143-56.

Lai, C.M., Lai, Y.K. and Rakoczy, P.E. (2002) Adenovirus and adeno-associated virus vectors. DNA Cell Biol 21, 895-913.

Lazdunski, C.J., Bouveret, E., Rigal, A., Journet, L., Lloubes, R. and Benedetti, H. (1998) Colicin import into *Escherichia coli* cells. J Bacteriol 180, 4993-5002.

Lazzaroni, J.C., Germon, P., Ray, M.C. and Vianney, A. (1999) The Tol proteins of *Escherichia coli* and their involvement in the uptake of biomolecules and outer membrane stability. FEMS Microbiol Lett 177, 191-7.

Lewin, B., Cassimeris, L., Lingappa, V.F. and Plopper, G. (2007) Cells. Jones and Bartlett Publisners Ontario.

Li, E., Brown, S.L., Stupack, D.G., Puente, X.S., Cheresh, D.A. and Nemerow, G.R. (2001) Integrin alpha(v)beta1 is an adenovirus coreceptor. J Virol 75, 5405-9.

Li, H., Cybulsky, M.I., Gimbrone, M.A., Jr. and Libby, P. (1993) An atherogenic diet rapidly induces VCAM-1, a cytokine-regulatable mononuclear leukocyte adhesion molecule, in rabbit aortic endothelium. Arterioscler Thromb 13, 197-204.

Li, Q.Q., Wang, W.J., Xu, J.D., Cao, X.X., Chen, Q., Yang, J.M. and Xu, Z.D. (2007) Up-regulation of CD147 and matrix metalloproteinase-2, -9 induced by P-

glycoprotein substrates in multidrug resistant breast cancer cells. Cancer Sci 98, 1767-74.

Liberek, K., Galitski, T.P., Zylicz, M. and Georgopoulos, C. (1992) The DnaK chaperone modulates the heat shock response of *Escherichia coli* by binding to the sigma 32 transcription factor. Proc Natl Acad Sci U S A 89, 3516-20.

Lim, M., Martinez, T., Jablons, D., Cameron, R., Guo, H., Toole, B., Li, J.D. and Basbaum, C. (1998) Tumor-derived EMMPRIN (extracellular matrix metalloproteinase inducer) stimulates collagenase transcription through MAPK p38. FEBS Lett 441, 88-92.

Liu, D. and Knapp, J.E. (2001) Hydrodynamics-based gene delivery. Curr Opin Mol Ther 3, 192-7.

Liu, F., Lu, Q., Ye, X., Fang, C., Zhao, Y., Liang, M., Hu, F., Lieber, A. and Chen, H.Z. (2008) Cancer gene therapy of adenovirus-mediated anti-4-1BB scFv in immunocompetent mice. Cancer Biol Ther 7, 448-53.

Liu, M.Y., Han, W., Ding, Y.L., Zhou, T.H., Tian, R.Y., Yang, S.L., Liu, H. and Gong, Y. (2005) Generation and characterization of C305, a murine neutralizing scFv antibody that can inhibit BLyS binding to its receptor BCMA. Acta Biochim Biophys Sin (Shanghai) 37, 415-20.

Lobato, M.N. and Rabbitts, T.H. (2004) Intracellular antibodies as specific reagents for functional ablation: future therapeutic molecules. Curr Mol Med 4, 519-28.

Lowman, H.B. (1997) Bacteriophage display and discovery of peptide leads for drug development. Annu Rev Biophys Biomol Struct 26, 401-24.

Lowman, H.B., Bass, S.H., Simpson, N. and Wells, J.A. (1991) Selecting high-affinity binding proteins by monovalent phage display. Biochemistry 30, 10832-8.

Lowman, H.B. and Wells, J.A. (1993) Affinity maturation of human growth hormone by monovalent phage display. J Mol Biol 234, 564-78.

Luo, J., Deng, Z.L., Luo, X., Tang, N., Song, W.X., Chen, J., Sharff, K.A., Luu, H.H., Haydon, R.C., Kinzler, K.W., Vogelstein, B. and He, T.C. (2007) A protocol for rapid generation of recombinant adenoviruses using the AdEasy system. Nat Protoc 2, 1236-47.

Lutz, P., Rosa-Calatrava, M. and Kedinger, C. (1997) The product of the adenovirus intermediate gene IX is a transcriptional activator. J Virol 71, 5102-9.

Lynch, S.M., Zhou, C. and Messer, A. (2008) An scFv intrabody against the nonamyloid component of alpha-synuclein reduces intracellular aggregation and toxicity. J Mol Biol 377, 136-47.

Majhen, D. and Ambriovic-Ristov, A. (2006) Adenoviral vectors--how to use them in cancer gene therapy? Virus Res 119, 121-33.

Majmudar, G., Nelson, B.R., Jensen, T.C. and Johnson, T.M. (1994) Increased expression of matrix metalloproteinase-3 (stromelysin-1) in cultured fibroblasts and basal cell carcinomas of nevoid basal cell carcinoma syndrome. Mol Carcinog 11, 29-33.

Makrides, S.C. (1996) Strategies for achieving high-level expression of genes in *Escherichia coli*. Microbiol Rev 60, 512-38.

Mao, S., Gao, C., Lo, C.H., Wirsching, P., Wong, C.H. and Janda, K.D. (1999) Phage-display library selection of high-affinity human single-chain antibodies to tumor-associated carbohydrate antigens sialyl Lewisx and Lewisx. Proc Natl Acad Sci U S A 96, 6953-8.

Marasco, W.A., Chen, S., Richardson, J.H., Ramstedt, U. and Jones, S.D. (1998) Intracellular antibodies against HIV-1 envelope protein for AIDS gene therapy. Hum Gene Ther 9, 1627-42.

Marasco, W.A., Haseltine, W.A. and Chen, S.Y. (1993) Design, intracellular expression, and activity of a human anti-human immunodeficiency virus type 1 gp120 single-chain antibody. Proc Natl Acad Sci U S A 90, 7889-93.

Martin, J.L., Bardwell, J.C. and Kuriyan, J. (1993) Crystal structure of the DsbA protein required for disulphide bond formation *in vivo*. Nature 365, 464-8.

McCafferty, J., Griffiths, A.D., Winter, G. and Chiswell, D.J. (1990) Phage antibodies: filamentous phage displaying antibody variable domains. Nature 348, 552-4.

Menashi, S., Serova, M., Ma, L., Vignot, S., Mourah, S. and Calvo, F. (2003) Regulation of extracellular matrix metalloproteinase inducer and matrix metalloproteinase expression by amphiregulin in transformed human breast epithelial cells. Cancer Res 63, 7575-80.

Mergulhao, F.J., Summers, D.K. and Monteiro, G.A. (2005) Recombinant protein secretion in *Escherichia coli*. Biotechnol Adv 23, 177-202.

Messer, A. and McLear, J. (2006) The therapeutic potential of intrabodies in neurologic disorders: focus on Huntington and Parkinson diseases. BioDrugs 20, 327-33.

Mhashilkar, A.M., Bagley, J., Chen, S.Y., Szilvay, A.M., Helland, D.G. and Marasco, W.A. (1995) Inhibition of HIV-1 Tat-mediated LTR transactivation and HIV-1 infection by anti-Tat single chain intrabodies. EMBO J 14, 1542-51.

Mhashilkar, A.M., Doebis, C., Seifert, M., Busch, A., Zani, C., Soo Hoo, J., Nagy, M., Ritter, T., Volk, H.D. and Marasco, W.A. (2002) Intrabody-mediated phenotypic knockout of major histocompatibility complex class I expression in human and monkey cell lines and in primary human keratinocytes. Gene Ther 9, 307-19.

Millimaggi, D., Mari, M., D'Ascenzo, S., Carosa, E., Jannini, E.A., Zucker, S., Carta, G., Pavan, A. and Dolo, V. (2007) Tumor vesicle-associated CD147 modulates the angiogenic capability of endothelial cells. Neoplasia 9, 349-57.

Missiakas, D., Georgopoulos, C. and Raina, S. (1993) Identification and characterization of the *Escherichia coli* gene dsbB, whose product is involved in the formation of disulfide bonds *in vivo*. Proc Natl Acad Sci U S A 90, 7084-8.

Missiakas, D. and Raina, S. (1997) Protein misfolding in the cell envelope of *Escherichia coli*: new signaling pathways. Trends Biochem Sci 22, 59-63.

Missiakas, D., Schwager, F., Betton, J.M., Georgopoulos, C. and Raina, S. (1996) Identification and characterization of HsIV HsIU (ClpQ ClpY) proteins

involved in overall proteolysis of misfolded proteins in *Escherichia coli*. EMBO J 15, 6899-909.

Miyauchi, T., Kanekura, T., Yamaoka, A., Ozawa, M., Miyazawa, S. and Muramatsu, T. (1990) Basigin, a new, broadly distributed member of the immunoglobulin superfamily, has strong homology with both the immunoglobulin V domain and the beta-chain of major histocompatibility complex class II antigen. J Biochem 107, 316-23.

Miyauchi, T., Masuzawa, Y. and Muramatsu, T. (1991) The basigin group of the immunoglobulin superfamily: complete conservation of a segment in and around transmembrane domains of human and mouse basigin and chicken HT7 antigen. J Biochem 110, 770-4.

Mizuguchi, H. and Hayakawa, T. (2002) Adenovirus vectors containing chimeric type 5 and type 35 fiber proteins exhibit altered and expanded tropism and increase the size limit of foreign genes. Gene 285, 69-77.

Mizuguchi, H. and Hayakawa, T. (2004) Targeted adenovirus vectors. Hum Gene Ther 15, 1034-44.

Mizuguchi, H., Kay, M.A. and Hayakawa, T. (2001) Approaches for generating recombinant adenovirus vectors. Adv Drug Deliv Rev 52, 165-76.

Mohrluder, J., Stangler, T., Hoffmann, Y., Wiesehan, K., Mataruga, A. and Willbold, D. (2007) Identification of calreticulin as a ligand of GABARAP by phage display screening of a peptide library. FEBS J 274, 5543-55.

Mori, H. and Ito, K. (2001) The Sec protein-translocation pathway. Trends Microbiol 9, 494-500.

Mori, H. and Ito, K. (2003) Biochemical characterization of a mutationally altered protein translocase: proton motive force stimulation of the initiation phase of translocation. J Bacteriol 185, 405-12.

Mullen, L.M., Nair, S.P., Ward, J.M., Rycroft, A.N. and Henderson, B. (2006) Phage display in the study of infectious diseases. Trends Microbiol 14, 141-7.

Munro, S. and Pelham, H.R. (1987) A C-terminal signal prevents secretion of luminal ER proteins. Cell 48, 899-907.

Muramatsu, T. and Miyauchi, T. (2003) Basigin (CD147): a multifunctional transmembrane protein involved in reproduction, neural function, inflammation and tumor invasion. Histol Histopathol 18, 981-7.

Muraoka, K., Nabeshima, K., Murayama, T., Biswas, C. and Koono, M. (1993) Enhanced expression of a tumor-cell-derived collagenase-stimulatory factor in urothelial carcinoma: its usefulness as a tumor marker for bladder cancers. Int J Cancer 55, 19-26.

Nabeshima, K., Iwasaki, H., Koga, K., Hojo, H., Suzumiya, J. and Kikuchi, M. (2006a) Emmprin (basigin/CD147): matrix metalloproteinase modulator and multifunctional cell recognition molecule that plays a critical role in cancer progression. Pathol Int 56, 359-67.

Nabeshima, K., Iwasaki, H., Nishio, J., Koga, K., Shishime, M. and Kikuchi, M. (2006b) Expression of emmprin and matrix metalloproteinases (MMPs) in peripheral nerve sheath tumors: emmprin and membrane-type (MT)1-MMP expressions are associated with malignant potential. Anticancer Res 26, 1359-67.

Nam, C.H., Lobato, M.N., Appert, A., Drynan, L.F., Tanaka, T. and Rabbitts, T.H. (2008) An antibody inhibitor of the LMO2-protein complex blocks its normal and tumorigenic functions. Oncogene.

Neering, S.J., Hardy, S.F., Minamoto, D., Spratt, S.K. and Jordan, C.T. (1996) Transduction of primitive human hematopoietic cells with recombinant adenovirus vectors. Blood 88, 1147-55.

Nehme, C.L., Cesario, M.M., Myles, D.G., Koppel, D.E. and Bartles, J.R. (1993) Breaching the diffusion barrier that compartmentalizes the transmembrane glycoprotein CE9 to the posterior-tail plasma membrane domain of the rat spermatozoon. J Cell Biol 120, 687-94.

Neri, D., Petrul, H. and Roncucci, G. (1995) Engineering recombinant antibodies for immunotherapy. Cell Biophys 27, 47-61.

Nevins, J.R., DeGregori, J., Jakoi, L. and Leone, G. (1997) Functional analysis of E2F transcription factor. Methods Enzymol 283, 205-19.

Nilsson, M., Ljungberg, J., Richter, J., Kiefer, T., Magnusson, M., Lieber, A., Widegren, B., Karlsson, S. and Fan, X. (2004) Development of an adenoviral vector system with adenovirus serotype 35 tropism; efficient transient gene transfer into primary malignant hematopoietic cells. J Gene Med 6, 631-41.

Nishiyama, K., Fukuda, A., Morita, K. and Tokuda, H. (1999) Membrane deinsertion of SecA underlying proton motive force-dependent stimulation of protein translocation. EMBO J 18, 1049-58.

Nissim, A., Hoogenboom, H.R., Tomlinson, I.M., Flynn, G., Midgley, C., Lane, D. and Winter, G. (1994) Antibody fragments from a 'single pot' phage display library as immunochemical reagents. EMBO J 13, 692-8.

Olafsen, T., Tan, G.J., Cheung, C.W., Yazaki, P.J., Park, J.M., Shively, J.E., Williams, L.E., Raubitschek, A.A., Press, M.F. and Wu, A.M. (2004) Characterization of engineered anti-p185HER-2 (scFv-CH3)2 antibody fragments (minibodies) for tumor targeting. Protein Eng Des Sel 17, 315-23.

Paetzel, M., Karla, A., Strynadka, N.C. and Dalbey, R.E. (2002) Signal peptidases. Chem Rev 102, 4549-80.

Pantoliano, M.W., Bird, R.E., Johnson, S., Asel, E.D., Dodd, S.W., Wood, J.F. and Hardman, K.D. (1991) Conformational stability, folding, and ligand-binding affinity of single-chain Fv immunoglobulin fragments expressed in *Escherichia coli*. Biochemistry 30, 10117-25.

Pavoni, E., Flego, M., Dupuis, M.L., Barca, S., Petronzelli, F., Anastasi, A.M., D'Alessio, V., Pelliccia, A., Vaccaro, P., Monteriu, G., Ascione, A., De Santis, R., Felici, F., Cianfriglia, M. and Minenkova, O. (2006) Selection, affinity maturation, and characterization of a human scFv antibody against CEA protein. BMC Cancer 6, 41.

Peng, J.L., Wu, S., Zhao, X.P., Wang, M., Li, W.H., Shen, X., Liu, J., Lei, P., Zhu, H.F. and Shen, G.X. (2007) Downregulation of transferrin receptor surface expression by intracellular antibody. Biochem Biophys Res Commun 354, 864-71.

Pingmuang, P. (2008) Construction of adenovirus expression systems for comparison of single chain Fv production in cytoplasmic compartment and endoplasmic reticulum and as a secreting molecule. Department of Medical Technology, Faculty of Associated Medical Sciences, Master of Science. Chiang Mai University.

Pogliano, J., Lynch, A.S., Belin, D., Lin, E.C. and Beckwith, J. (1997) Regulation of *Escherichia coli* cell envelope proteins involved in protein folding and degradation by the Cpx two-component system. Genes Dev 11, 1169-82.

Poller, W., Schneider-Rasp, S., Liebert, U., Merklein, F., Thalheimer, P., Haack, A., Schwaab, R., Schmitt, C. and Brackmann, H.H. (1996) Stabilization of transgene expression by incorporation of E3 region genes into an adenoviral factor IX vector and by transient anti-CD4 treatment of the host. Gene Ther 3, 521-30.

Popkov, M., Jendreyko, N., McGavern, D.B., Rader, C. and Barbas, C.F., 3rd. (2005) Targeting tumor angiogenesis with adenovirus-delivered anti-Tie-2 intrabody. Cancer Res 65, 972-81.

Pushkarsky, T., Yurchenko, V., Vanpouille, C., Brichacek, B., Vaisman, I., Hatakeyama, S., Nakayama, K.I., Sherry, B. and Bukrinsky, M.I. (2005) Cell surface expression of CD147/EMMPRIN is regulated by cyclophilin 60. J Biol Chem 280, 27866-71.

Quemener, C., Gabison, E.E., Naimi, B., Lescaille, G., Bougatef, F., Podgorniak, M.P., Labarchede, G., Lebbe, C., Calvo, F., Menashi, S. and Mourah, S. (2007) Extracellular matrix metalloproteinase inducer up-regulates the

urokinase-type plasminogen activator system promoting tumor cell invasion. Cancer Res 67, 9-15.

Raina, S., Missiakas, D. and Georgopoulos, C. (1995) The rpoE gene encoding the sigma E (sigma 24) heat shock sigma factor of *Escherichia coli*. EMBO J 14, 1043-55.

Rainov, N.G. and Ren, H. (2003) Clinical trials with retrovirus mediated gene therapy--what have we learned? J Neurooncol 65, 227-36.

Rao, L., Perez, D. and White, E. (1996) Lamin proteolysis facilitates nuclear events during apoptosis. J Cell Biol 135, 1441-55.

Rea, D., Havenga, M.J., van Den Assem, M., Sutmuller, R.P., Lemckert, A., Hoeben, R.C., Bout, A., Melief, C.J. and Offringa, R. (2001) Highly efficient transduction of human monocyte-derived dendritic cells with subgroup B fiber-modified adenovirus vectors enhances transgene-encoded antigen presentation to cytotoxic T cells. J Immunol 166, 5236-44.

Rebel, V.I., Hartnett, S., Denham, J., Chan, M., Finberg, R. and Sieff, C.A. (2000) Maturation and lineage-specific expression of the coxsackie and adenovirus receptor in hematopoietic cells. Stem Cells 18, 176-82.

Reimers, N., Zafrakas, K., Assmann, V., Egen, C., Riethdorf, L., Riethdorf, S., Berger, J., Ebel, S., Janicke, F., Sauter, G. and Pantel, K. (2004) Expression of extracellular matrix metalloproteases inducer on micrometastatic and primary mammary carcinoma cells. Clin Cancer Res 10, 3422-8.

Reinman, M., Jantti, J., Alfthan, K., Keranen, S., Soderlund, H. and Takkinen, K. (2003) Functional inactivation of the conserved Sem1p in yeast by intrabodies. Yeast 20, 1071-84.

Ren, Z. and Black, L.W. (1998) Phage T4 SOC and HOC display of biologically active, full-length proteins on the viral capsid. Gene 215, 439-44.

Richardson, J.H. and Marasco, W.A. (1995) Intracellular antibodies: development and therapeutic potential. Trends Biotechnol 13, 306-10.

Riethdorf, S., Reimers, N., Assmann, V., Kornfeld, J.W., Terracciano, L., Sauter, G. and Pantel, K. (2006) High incidence of EMMPRIN expression in human tumors. Int J Cancer 119, 1800-10.

Rietsch, A., Belin, D., Martin, N. and Beckwith, J. (1996) An *in vivo* pathway for disulfide bond isomerization in *Escherichia coli*. Proc Natl Acad Sci U S A 93, 13048-53.

Robbins, P.D., Tahara, H. and Ghivizzani, S.C. (1998) Viral vectors for gene therapy. Trends Biotechnol 16, 35-40.

Roberts, B.L., Markland, W., Ley, A.C., Kent, R.B., White, D.W., Guterman, S.K. and Ladner, R.C. (1992) Directed evolution of a protein: selection of potent neutrophil elastase inhibitors displayed on M13 fusion phage. Proc Natl Acad Sci U S A 89, 2429-33.

Robles, Y., Gonzalez, E., Govezensky, T., Mungia, M.E., Acero, G., Bobes, R.J., Gevorkian, G. and Manoutcharian, K. (2005) Isolation of the Taenia crassiceps antigens from a phage display cDNA library and evaluation of their use for diagnosis of neurocysticercosis. Clin Immunol 116, 265-70.

Rothlisberger, D., Honegger, A. and Pluckthun, A. (2005) Domain interactions in the Fab fragment: a comparative evaluation of the single-chain Fv and Fab format engineered with variable domains of different stability. J Mol Biol 347, 773-89.

Russel, M., Linderoth, N.A. and Sali, A. (1997) Filamentous phage assembly: variation on a protein export theme. Gene 192, 23-32.

Russel, M., Whirlow, H., Sun, T.P. and Webster, R.E. (1988) Low-frequency infection of F- bacteria by transducing particles of filamentous bacteriophages. J Bacteriol 170, 5312-6.

Russell, W.C. (2000) Update on adenovirus and its vectors. J Gen Virol 81, 2573-604.

Sakurai, F., Mizuguchi, H., Yamaguchi, T. and Hayakawa, T. (2003) Characterization of *in vitro* and *in vivo* gene transfer properties of adenovirus serotype 35 vector. Mol Ther 8, 813-21.

Sakurai, F., Murakami, S., Kawabata, K., Okada, N., Yamamoto, A., Seya, T., Hayakawa, T. and Mizuguchi, H. (2006) The short consensus repeats 1 and 2, not the cytoplasmic domain, of human CD46 are crucial for infection of subgroup B adenovirus serotype 35. J Control Release 113, 271-8.

Santini, C., Brennan, D., Mennuni, C., Hoess, R.H., Nicosia, A., Cortese, R. and Luzzago, A. (1998) Efficient display of an HCV cDNA expression library as C-terminal fusion to the capsid protein D of bacteriophage lambda. J Mol Biol 282, 125-35.

Saul, F.A., Arie, J.P., Vulliez-le Normand, B., Kahn, R., Betton, J.M. and Bentley, G.A. (2004) Structural and functional studies of FkpA from *Escherichia coli*, a

cis/trans peptidyl-prolyl isomerase with chaperone activity. J Mol Biol 335, 595-608.

Schlosshauer, B. and Herzog, K.H. (1990) Neurothelin: an inducible cell surface glycoprotein of blood-brain barrier-specific endothelial cells and distinct neurons. J Cell Biol 110, 1261-74.

Schrama, D., Reisfeld, R.A. and Becker, J.C. (2006) Antibody targeted drugs as cancer therapeutics. Nat Rev Drug Discov 5, 147-59.

Schroers, R., Hildebrandt, Y., Hasenkamp, J., Glass, B., Lieber, A., Wulf, G. and Piesche, M. (2004) Gene transfer into human T lymphocytes and natural killer cells by Ad5/F35 chimeric adenoviral vectors. Exp Hematol 32, 536-46.

Schubert, U., Anton, L.C., Gibbs, J., Norbury, C.C., Yewdell, J.W. and Bennink, J.R. (2000) Rapid degradation of a large fraction of newly synthesized proteins by proteasomes. Nature 404, 770-4.

Schuster, V.L., Lu, R., Kanai, N., Bao, Y., Rosenberg, S., Prie, D., Ronco, P. and Jennings, M.L. (1996) Cloning of the rabbit homologue of mouse 'basigin' and rat 'OX-47': kidney cell type-specific expression, and regulation in collecting duct cells. Biochim Biophys Acta 1311, 13-9.

Segerman, A., Atkinson, J.P., Marttila, M., Dennerquist, V., Wadell, G. and Arnberg, N. (2003) Adenovirus type 11 uses CD46 as a cellular receptor. J Virol 77, 9183-91.

Seulberger, H., Lottspeich, F. and Risau, W. (1990) The inducible blood--brain barrier specific molecule HT7 is a novel immunoglobulin-like cell surface glycoprotein. EMBO J 9, 2151-8.

Shayakhmetov, D.M., Papayannopoulou, T., Stamatoyannopoulos, G. and Lieber, A. (2000) Efficient gene transfer into human CD34(+) cells by a retargeted adenovirus vector. J Virol 74, 2567-83.

Shokri, A., Sanden, A.M. and Larsson, G. (2003) Cell and process design for targeting of recombinant protein into the culture medium of *Escherichia coli*. Appl Microbiol Biotechnol 60, 654-64.

Sidhu, S.S. (2000) Phage display in pharmaceutical biotechnology. Curr Opin Biotechnol 11, 610-6.

Sidhu, S.S. (2001) Engineering M13 for phage display. Biomol Eng 18, 57-63.

Sidhu, S.S., Mengistab, A.T., Tauscher, A.N., LaVail, J. and Basbaum, C. (2004) The microvesicle as a vehicle for EMMPRIN in tumor-stromal interactions. Oncogene 23, 956-63.

Smith, G.P. (1985) Filamentous fusion phage: novel expression vectors that display cloned antigens on the virion surface. Science 228, 1315-7.

Smith, G.P. and Petrenko, V.A. (1997) Phage Display. Chem Rev 97, 391-410.

Snyder, W.B., Davis, L.J., Danese, P.N., Cosma, C.L. and Silhavy, T.J. (1995) Overproduction of NlpE, a new outer membrane lipoprotein, suppresses the toxicity of periplasmic LacZ by activation of the Cpx signal transduction pathway. J Bacteriol 177, 4216-23.

Staffler, G. and Stockinger, H. (2000) Cd147. J Biol Regul Homeost Agents 14, 327-30.

Staffler, G., Szekeres, A., Schutz, G.J., Saemann, M.D., Prager, E., Zeyda, M., Drbal, K., Zlabinger, G.J., Stulnig, T.M. and Stockinger, H. (2003) Selective

inhibition of T cell activation via CD147 through novel modulation of lipid rafts. J Immunol 171, 1707-14.

Steinberger, P., Andris-Widhopf, J., Buhler, B., Torbett, B.E. and Barbas, C.F., 3rd. (2000a) Functional deletion of the CCR5 receptor by intracellular immunization produces cells that are refractory to CCR5-dependent HIV-1 infection and cell fusion. Proc Natl Acad Sci U S A 97, 805-10.

Steinberger, P., Sutton, J.K., Rader, C., Elia, M. and Barbas, C.F., 3rd. (2000b) Generation and characterization of a recombinant human CCR5-specific antibody. A phage display approach for rabbit antibody humanization. J Biol Chem 275, 36073-8.

Stirnemann, K., Romero, J.F., Baldi, L., Robert, B., Cesson, V., Besra, G.S., Zauderer, M., Wurm, F., Corradin, G., Mach, J.P., Macdonald, H.R. and Donda, A. (2008) Sustained activation and tumor targeting of NKT cells using a CD1d-anti-HER2-scFv fusion protein induce antitumor effects in mice. J Clin Invest 118, 994-1005.

Stockinger, H. (1997) Interaction of GPI-anchored cell surface proteins and complement receptor type 3. Exp Clin Immunogenet 14, 5-10.

Stockinger H, Ebel T, Hansmann C, Koch C., Majdic O., Prager E., Patel D.D., Fox D.A., Horejsi V., Sagawa K., and Shen D.C. CD147 (neurothelin/basigin) workshop panel report. In Kishimoto T., Kikutani H., von dem Borne A.E.G.K., Goyert S>M., Mason D.Y., Miyasaka M., Moretta L., Okumura K., Shaw S.,cSpringer T.A., Sugamura K., and Zola H.,. eds, Leukocyte Typing VI, p. 760. Garland Publishing, New York. 1997:760.

Stocks, M.R. (2004) Intrabodies: production and promise. Drug Discov Today 9, 960-6.

Su, Y.C., Lim, K.P. and Nathan, S. (2003) Bacterial expression of the scFv fragment of a recombinant antibody specific for Burkholderia pseudomallei exotoxin. J Biochem Mol Biol 36, 493-8.

Sun, J. and Hemler, M.E. (2001) Regulation of MMP-1 and MMP-2 production through CD147/extracellular matrix metalloproteinase inducer interactions. Cancer Res 61, 2276-81.

Suzuki, S., Sato, M., Senoo, H. and Ishikawa, K. (2004) Direct cell-cell interaction enhances pro-MMP-2 production and activation in co-culture of laryngeal cancer cells and fibroblasts: involvement of EMMPRIN and MT1-MMP. Exp Cell Res 293, 259-66.

Tamm, L.K., Hong, H. and Liang, B. (2004) Folding and assembly of beta-barrel membrane proteins. Biochim Biophys Acta 1666, 250-63.

Tanaka, T., Williams, R.L. and Rabbitts, T.H. (2007) Tumour prevention by a single antibody domain targeting the interaction of signal transduction proteins with RAS. Embo J 26, 3250-9.

Tang, J., Wu, Y.M., Zhao, P., Yang, X.M., Jiang, J.L. and Chen, Z.N. (2008) Overexpression of HAb18G/CD147 promotes invasion and metastasis via alpha3beta1 integrin mediated FAK-paxillin and FAK-PI3K-Ca2+ pathways. Cell Mol Life Sci 65, 2933-42.

Tang, W., Chang, S.B. and Hemler, M.E. (2004a) Links between CD147 function, glycosylation, and caveolin-1. Mol Biol Cell 15, 4043-50.

Tang, Y., Kesavan, P., Nakada, M.T. and Yan, L. (2004b) Tumor-stroma interaction: positive feedback regulation of extracellular matrix metalloproteinase inducer (EMMPRIN) expression and matrix metalloproteinase-dependent generation of soluble EMMPRIN. Mol Cancer Res 2, 73-80.

Tang, Y., Nakada, M.T., Kesavan, P., McCabe, F., Millar, H., Rafferty, P., Bugelski, P. and Yan, L. (2005) Extracellular matrix metalloproteinase inducer stimulates tumor angiogenesis by elevating vascular endothelial cell growth factor and matrix metalloproteinases. Cancer Res 65, 3193-9.

Taraboletti, G., D'Ascenzo, S., Borsotti, P., Giavazzi, R., Pavan, A. and Dolo, V. (2002) Shedding of the matrix metalloproteinases MMP-2, MMP-9, and MT1-MMP as membrane vesicle-associated components by endothelial cells. Am J Pathol 160, 673-80.

Tavladoraki, P., Benvenuto, E., Trinca, S., De Martinis, D., Cattaneo, A. and Galeffi, P. (1993) Transgenic plants expressing a functional single-chain Fv antibody are specifically protected from virus attack. Nature 366, 469-72.

Tavladoraki, P., Girotti, A., Donini, M., Arias, F.J., Mancini, C., Morea, V., Chiaraluce, R., Consalvi, V. and Benvenuto, E. (1999) A single-chain antibody fragment is functionally expressed in the cytoplasm of both *Escherichia coli* and transgenic plants. Eur J Biochem 262, 617-24.

Tayapiwatana, C., Arooncharus, P. and Kasinrerk, W. (2003) Displaying and epitope mapping of CD147 on VCSM13 phages: influence of *Escherichia coli* strains. J Immunol Methods 281, 177-85.

Tayapiwatana, C., Chotpadiwetkul, R. and Kasinrerk, W. (2006) A novel approach using streptavidin magnetic bead-sorted *in vivo* biotinylated survivin for monoclonal antibody production. J Immunol Methods 317, 1-11.

Tollefson, A.E., Ryerse, J.S., Scaria, A., Hermiston, T.W. and Wold, W.S. (1996) The E3-11.6-kDa adenovirus death protein (ADP) is required for efficient cell death: characterization of cells infected with adp mutants. Virology 220, 152-62.

Toole, B.P. (2003) Emmprin (CD147), a cell surface regulator of matrix metalloproteinase production and function. Curr Top Dev Biol 54, 371-89.

Tuve, S., Chen, B.M., Liu, Y., Cheng, T.L., Toure, P., Sow, P.S., Feng, Q., Kiviat, N., Strauss, R., Ni, S., Li, Z.Y., Roffler, S.R. and Lieber, A. (2007) Combination of tumor site-located CTL-associated antigen-4 blockade and systemic regulatory T-cell depletion induces tumor-destructive immune responses. Cancer Res 67, 5929-39.

Ura, T., Yoshida, A., Xin, K.Q., Yoshizaki, S., Yashima, S., Abe, S., Mizuguchi, H. and Okuda, K. (2008) Designed recombinant adenovirus type 5 vector induced envelope-specific CD8(+) cytotoxic T lymphocytes and cross-reactive neutralizing antibodies against human immunodeficiency virus type 1. J Gene Med.

Uren, A.G., Kool, J., Berns, A. and van Lohuizen, M. (2005) Retroviral insertional mutagenesis: past, present and future. Oncogene 24, 7656-72.

Walton, T.A. and Sousa, M.C. (2004) Crystal structure of Skp, a prefoldin-like chaperone that protects soluble and membrane proteins from aggregation. Mol Cell 15, 367-74.

Wang, L., Ku, X.M., Li, Y., Bian, H.J., Zhang, S.H., Ye, H., Yao, X.Y., Li, B.H., Yang, X.M., Liao, C.G. and Chen, Z.N. (2006) Regulation of matrix metalloproteinase production and tumor cell invasion by four monoclonal antibodies against different epitopes of HAb18G/CD147 extracellular domain. Hybridoma (Larchmt) 25, 60-7.

Wang, L., Miller, A. and Kendall, D.A. (2000) Signal peptide determinants of SecA binding and stimulation of ATPase activity. J Biol Chem 275, 10154-9.

Wang, W.J., Li, Q.Q., Xu, J.D., Cao, X.X., Li, H.X., Tang, F., Chen, Q., Yang, J.M., Xu, Z.D. and Liu, X.P. (2008) Interaction between CD147 and P-glycoprotein and their regulation by ubiquitination in breast cancer cells. Chemotherapy 54, 291-301.

Weiner, L. and Model, P. (1994) Role of an *Escherichia coli* stress-response operon in stationary-phase survival. Proc Natl Acad Sci U S A 91, 2191-5.

Wheeler, Y.Y., Chen, S.Y. and Sane, D.C. (2003a) Intrabody and intrakine strategies for molecular therapy. Mol Ther 8, 355-66.

Wheeler, Y.Y., Kute, T.E., Willingham, M.C., Chen, S.Y. and Sane, D.C. (2003b) Intrabody-based strategies for inhibition of vascular endothelial growth factor receptor-2: effects on apoptosis, cell growth, and angiogenesis. FASEB J 17, 1733-5.

Whitelegg, N.R. and Rees, A.R. (2000) WAM: an improved algorithm for modelling antibodies on the WEB. Protein Eng 13, 819-24.

Wickham, T.J. (2000) Targeting adenovirus. Gene Ther 7, 110-4.

Wickham, T.J., Mathias, P., Cheresh, D.A. and Nemerow, G.R. (1993) Integrins alpha v beta 3 and alpha v beta 5 promote adenovirus internalization but not virus attachment. Cell 73, 309-19.

Wiethoff, C.M. and Middaugh, C.R. (2003) Barriers to nonviral gene delivery. J Pharm Sci 92, 203-17.

Williams, B.R. and Zhu, Z. (2006) Intrabody-based approaches to cancer therapy: status and prospects. Curr Med Chem 13, 1473-80.

Wilson, M.C., Meredith, D. and Halestrap, A.P. (2002) Fluorescence resonance energy transfer studies on the interaction between the lactate transporter MCT1 and CD147 provide information on the topology and stoichiometry of the complex in situ. J Biol Chem 277, 3666-72.

Wilson, M.R. and Easterbrook-Smith, S.B. (2000) Clusterin is a secreted mammalian chaperone. Trends Biochem Sci 25, 95-8.

Winter, G., Griffiths, A.D., Hawkins, R.E. and Hoogenboom, H.R. (1994) Making antibodies by phage display technology. Annu Rev Immunol 12, 433-55.

Witty, M., Sanz, C., Shah, A., Grossmann, J.G., Mizuguchi, K., Perham, R.N. and Luisi, B. (2002) Structure of the periplasmic domain of Pseudomonas aeruginosa TolA: evidence for an evolutionary relationship with the TonB transporter protein. EMBO J 21, 4207-18.

Woodbury, R.L., Topping, T.B., Diamond, D.L., Suciu, D., Kumamoto, C.A., Hardy, S.J. and Randall, L.L. (2000) Complexes between protein export chaperone SecB and SecA. Evidence for separate sites on SecA providing binding energy and regulatory interactions. J Biol Chem 275, 24191-8.

Worn, A. and Pluckthun, A. (2001) Stability engineering of antibody single-chain Fv fragments. J Mol Biol 305, 989-1010.

Wright, M., Grim, J., Deshane, J., Kim, M., Strong, T.V., Siegal, G.P. and Curiel, D.T. (1997) An intracellular anti-erbB-2 single-chain antibody is specifically cytotoxic to human breast carcinoma cells overexpressing erbB-2. Gene Ther 4, 317-22.

Wu, E. and Nemerow, G.R. (2004) Virus yoga: the role of flexibility in virus host cell recognition. Trends Microbiol 12, 162-9.

Yamaoka, T., Yonemitsu, Y., Komori, K., Baba, H., Matsumoto, T., Onohara, T. and Maehara, Y. (2005) Ex vivo electroporation as a potent new strategy for nonviral gene transfer into autologous vein grafts. Am J Physiol Heart Circ Physiol 289, H1865-72.

Yan, L., Zucker, S. and Toole, B.P. (2005) Roles of the multifunctional glycoprotein, emmprin (basigin; CD147), in tumour progression. Thromb Haemost 93, 199-204.

Yang, H., Zou, W., Li, Y., Chen, B. and Xin, X. (2007a) Bridge linkage role played by CD98hc of anti-tumor drug resistance and cancer metastasis on cisplatin-resistant ovarian cancer cells. Cancer Biol Ther 6, 942-7.

Yang, J.M., Xu, Z., Wu, H., Zhu, H., Wu, X. and Hait, W.N. (2003) Overexpression of extracellular matrix metalloproteinase inducer in multidrug resistant cancer cells. Mol Cancer Res 1, 420-7.

Yang, W., Meng, L., Wang, H., Chen, R., Wang, R., Ma, X., Xu, G., Zhou, J., Wang, S., Lu, Y. and Ma, D. (2006) Inhibition of proliferative and invasive capacities of breast cancer cells by arginine-glycine-aspartic acid peptide *in vitro*. Oncol Rep 15, 113-7.

Yang, Y., Yang, S., Ye, Z., Jaffar, J., Zhou, Y., Cutter, E., Lieber, A., Hellstrom, I. and Hellstrom, K.E. (2007b) Tumor cells expressing anti-CD137 scFv induce a tumor-destructive environment. Cancer Res 67, 2339-44.

Yang, Z.M., Li, E.M., Lai, B.C., Wang, Y.L. and Si, L.S. (2007c) Anti-CD3 scFv-B7.1 fusion protein expressed on the surface of HeLa cells provokes potent T-lymphocyte activation and cytotoxicity. Biochem Cell Biol 85, 196-202.

Yotnda, P., Onishi, H., Heslop, H.E., Shayakhmetov, D., Lieber, A., Brenner, M. and Davis, A. (2001) Efficient infection of primitive hematopoietic stem cells by modified adenovirus. Gene Ther 8, 930-7.

Yurchenko, V., Pushkarsky, T., Li, J.H., Dai, W.W., Sherry, B. and Bukrinsky, M. (2005) Regulation of CD147 cell surface expression: involvement of the proline residue in the CD147 transmembrane domain. J Biol Chem 280, 17013-9.

Zdoroveac, A., Doebis, C., Laube, H., Brosel, S., Schmitt-Knosalla, I., Volk, H.D. and Seifert, M. (2008) Modulation of graft arteriosclerosis in a rat carotid transplantation model. J Surg Res 145, 161-9.

Zhang, Y. and Bergelson, J.M. (2005) Adenovirus receptors. J Virol 79, 12125-31.

Zou, W., Yang, H., Hou, X., Zhang, W., Chen, B. and Xin, X. (2007) Inhibition of CD147 gene expression via RNA interference reduces tumor cell invasion, tumorigenicity and increases chemosensitivity to paclitaxel in HO-8910pm cells. Cancer Lett 248, 211-8.

BMC Biotechnology

Research article

Generation of functional scFv intrabody to abate the expression of CD147 surface molecule of 293A cells

Khajornsak Tragoolpua[†1], Nutjeera Intasai[†2], Watchara Kasinrerk[1,3], Sabine Mai[4], Yuan Yuan[5,6] and Chatchai Tayapiwatana[*1,7]

Address: [1]Division of Clinical Immunology, Department of Medical Technology, Faculty of Associated Medical Sciences, Chiang Mai University, Chiang Mai, 50200, Thailand, [2]Division of Clinical Microscopy, Department of Medical Technology, Faculty of Associated Medical Sciences, Chiang Mai University, Chiang Mai, 50200, Thailand, [3]Biomedical Technology Research Unit, National Center for Genetic Engineering and Biotechnology, National Science and Technology Development Agency at the Faculty of Associated Medical Sciences, Chiang Mai University, Chiang Mai, 50200, Thailand, [4]Department of Physiology, Manitoba Institute of Cell Biology, CancerCare Manitoba, University of Manitoba, Winnipeg R3E 0V9, Canada, [5]Department of Molecular Biology and the Skaggs Institute for Chemical Biology, The Scripps Research Institute, La Jolla, California 92037, USA, [6]Millipore Bioscience Division, 28820 Single Oak Drive, Temecula, CA 92590, USA and [7]BioMedical Engineering Center, Chiang Mai University, Chiang Mai, 50200, Thailand

Email: Khajornsak Tragoolpua - kjornsak@chiangmai.ac.th; Nutjeera Intasai - nutjeera@chiangmai.ac.th; Watchara Kasinrerk - watchara@chiangmai.ac.th; Sabine Mai - smai@cc.umanitoba.ca; Yuan Yuan - maomaoxiong0875@hotmail.com; Chatchai Tayapiwatana* - asimi002@chiangmai.ac.th

* Corresponding author †Equal contributors

Published: 29 January 2008

BMC Biotechnology 2008, **8**:5 doi:10.1186/1472-6750-8-5

Received: 22 June 2007
Accepted: 29 January 2008

This article is available from: http://www.biomedcentral.com/1472-6750/8/5

Abstract

Background: Expression of intracellular antibodies (intrabodies) has become a broadly applicable technology for generation of phenotypic knockouts *in vivo*. The method uses surface depletion of cellular membrane proteins to examine their biological function. In this study, we used this strategy to block the transport of cell surface molecule CD147 to the cell membrane. Phage display technology was introduced to generate the functional antibody fragment to CD147, and we subsequently constructed a CD147-specific scFv that was expressed intracellularly and retained in the endoplasmic reticulum by adenoviral gene transfer.

Results: The recombinant antibody fragments, Fab and scFv, of the murine monoclonal antibody (clone M6-1B9) reacted specifically to CD147 by indirect enzyme-linked immunosorbent assays (ELISA) using a recombinant CD147-BCCP as a target. This indicated that the Fab- and scFv-M6-1B9 displaying on phage surfaces were correctly folded and functionally active. We subsequently constructed a CD147-specific scFv, scFv-M6-1B9-intrabody, in 293A cells. The expression of CD147 on 293A cell surface was monitored at 36 h after transduction by flow cytometry and demonstrated remarkable reduction. Colocalization of scFv-M6-1B9 intrabody with CD147 in the ER network was depicted using a 3D deconvolution microscopy system.

Conclusion: The results suggest that our approach can generate antibody fragments suitable for decreasing the expression of CD147 on 293A cells. This study represents a step toward understanding the role of the cell surface protein, CD147.

Background

CD147 is a 50–60 kDa transmembrane glycoprotein. The molecule has an external domain consisting of two regions exhibiting the features of the immunoglobulin superfamily [1-3]. CD147 is widely expressed in both hematopoietic and non-hematopoietic cells and tissues [4-7]. However, the molecule is strongly expressed on various cancer cells, thymocytes and activated T lymphocytes [3,6,8-12]. CD147 is involved in cellular adhesion [8,13,14], lymphocyte activation [14-16], membrane transport [17-19] and signal transduction [20-23]. In addition, CD147 plays a crucial role in the invasive and metastatic activity of tumor cells [9,24,25]. Inhibition of CD147 cell surface expression may help to elucidate these physiological functions of CD147.

A negative regulatory function for CD147 in T cell regulation has been demonstrated [14-16,26]. Recently, two anti-CD147 mAbs, M6-1E9 and M6-1B9, which react with the membrane-distal Ig domain, have been shown to inhibit OKT3-induced T cell proliferation [14]. Presumably, prevention of cell division is caused by delivery of a negative signal *via* CD147. Another possibility is prevention of CD147 becoming associated with its cell surface partners, which may cooperate in CD3 signaling to generate the complete activation signal. The latter hypothesis may be investigated by blocking the expression of surface CD147.

Intracellularly expressed antibodies (intrabodies) can inhibit protein function in specific cellular compartments [27]. They have the capacity to inhibit the translocation of cell surface molecules from the endoplasmic reticulum (ER) to the cell surface as ER-intrabodies [27-29]. Intrabodies offer an effective alternative to gene-based knockout technology [30]. This technique has several advantages compared to RNA interference (RNAi) technology, since intrabodies possess a much longer active half-life than RNA, are much more specific to their target molecules [31,32] and generally do not disrupt target gene transcription. Moreover, gene knockout and silencing techniques cannot be used to analyze domain functions and post-translationally modified protein functions.

The aim of the present study was to generate an intrabody against CD147 in order to down-regulate the cell surface expression of CD147 and retain this surface molecule inside the cell. Sequences encoding both variable regions of heavy chain (V_H) and light chain (V_L) domains against CD147 were cloned from hybridomas producing monoclonal antibody clone M6-1B9. These sequences were joined by a flexible peptide linker sequence, allowing the expression of scFv as a single polypeptide chain. The functional activities of this intrabody, *i.e.* target tracing and capturing, were verified in a human embryonic kidney cell line, 293A, which naturally expresses CD147. This manipulation of cell surface CD147 expression could serve as a basis for the generation of CD147-down regulated cells, and represents a step toward characterizing the role of CD147 in regulation of lymphocyte activation and induction of matrix metalloproteinase production by tumor cells.

Results

Construction of a phagemid vector encoding scFv-M6-1B9

The heavy, Fd, and light chain domains of anti-CD147 mAb, M6-1B9 [8], were amplified, subcloned into the expression vector and then named as pCom3H-Fab-M6-1B9. Subsequently, the V_L and V_H were amplified from pCom3H-Fab-M6-1B9 and attached by a peptide linker to form the scFv. The amplified product was cloned into phagemid vector pComb3X, named pComb3X-scFv-M6-1B9, and then transformed into *E. coli* TG1. The nucleotide sequence of the inserted fragment, scFv, was obtained (Figure 1). The scFv construct was fused to the carboxy-terminal domain of the minor coat protein, gpIII, and displayed on the surface of phage particles. The deduced amino acid sequences of variable heavy (V_H) and light (V_L) chains are listed in Figure 1. The amino acid residues responsible for paratope in CDR regions were subsequently identified *via* the WAM (for Web Antibody Modelling) algorithm [33]. The sequence can be numbered following Kabat's rule [34], in order to assure success in cloning the immunoglobulin variable domains.

Detection of phage-displayed scFv-M6-1B9

The expression of Fab- and scFv-M6-1B9 on phage particles was assessed by Western immunoblotting. Equal amounts of each recombinant phage were fractionated by SDS-PAGE, blotted, and probed with anti-gpIII mAb. Wild-type gpIII has a calculated molecular mass of approximately 44 kDa. However, a 62 kDa protein detected in Western blots using anti-gpIII specific antibodies has been previously demonstrated [35-37]. The truncated form of gpIII is used in pComb3 vector which has a molecular mass of 18.7 kDa. In case of Fab antibody fusion format in the present study, Fd fragment was fused to truncated gpIII. This resulted in migration of Fd-gpIII fusion at 47 kDa as indicated by arrow (28.7 kDa of Fd fused with 18.7 kDa of truncated gpIII). Likewise, the molecular mass of scFv is also approximately 28.7 kDa which resulted in a molecular weight of 47 kDa of scFv-gpIII fusion protein. Thus, the immunoreactive bands of scFv-M6-1B9- and Fab-M6-1B9-gpIII fusion protein with the approximate molecular weight of 47 kDa were obtained (Figure 2A). Noticeably, the band corresponding to the scFv-gpIII fusion protein was more prominent than the band corresponding to the Fab-M6-1B9-gpIII fusion protein, reflecting the fact that expression of scFv was superior to that of Fab obtained by the phage display tech-

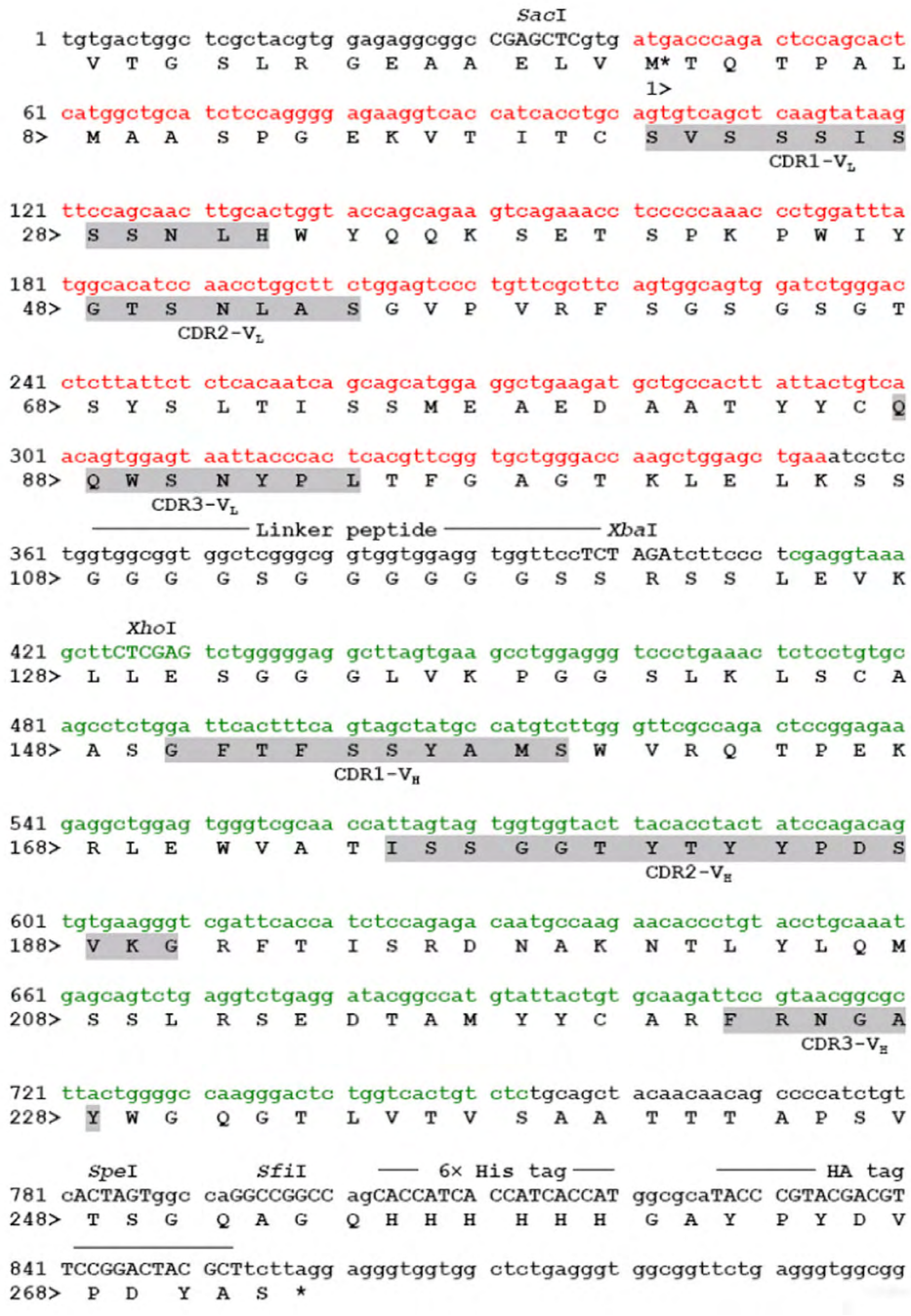

Figure 1

Nucleotide sequence of cDNA and deduced amino acid sequence of the scFv-M6-1B9. The cDNA sequence encoding scFv-M6-1B9 was shown. Restriction endonuclease sites, His tags, and HA tag are indicated. The deduced amino acid sequence of scFv-M6-1B9 corresponding to the complementary determining regions (CDRs) in the variable regions of the L (red letters) and H (green letters) chains, which were identified by the Kabat numbering scheme, are indicated by gray boxes. Amino acids were numbered from the initiator methionine (M*). The amber stop codon was shown by an asterisk (*). The details of the CDRs region of scFv-M6-1B9 are shown as CDR1-V_L C (^{24}SV---LH^{35}) W, CDR2-V_L Y (^{51}GT---AS ^{57}) G, CDR3-V_L C (^{90}QQ---PL^{97}) T, CDR1-V_H S (^{153}GF---MS^{162}) W, CDR2-V_H A (^{178}IS---KG^{193}) R, and CDR3-V_H R (^{226}FR---GAY^{231}) W.

nique. Antigen-specific binding of phage presenting the different antibody formats was verified by ELISA using recombinant CD147-biotin carboxyl carrier protein (BCCP) fusion protein as an antigen. The scFv format demonstrated more favorable antigen-binding features than the Fab format (Figure 2B). In contrast, VCSM13 phage prepared from non-transformed TG-1 did not generate the signal against CD147-BCCP antigen. These

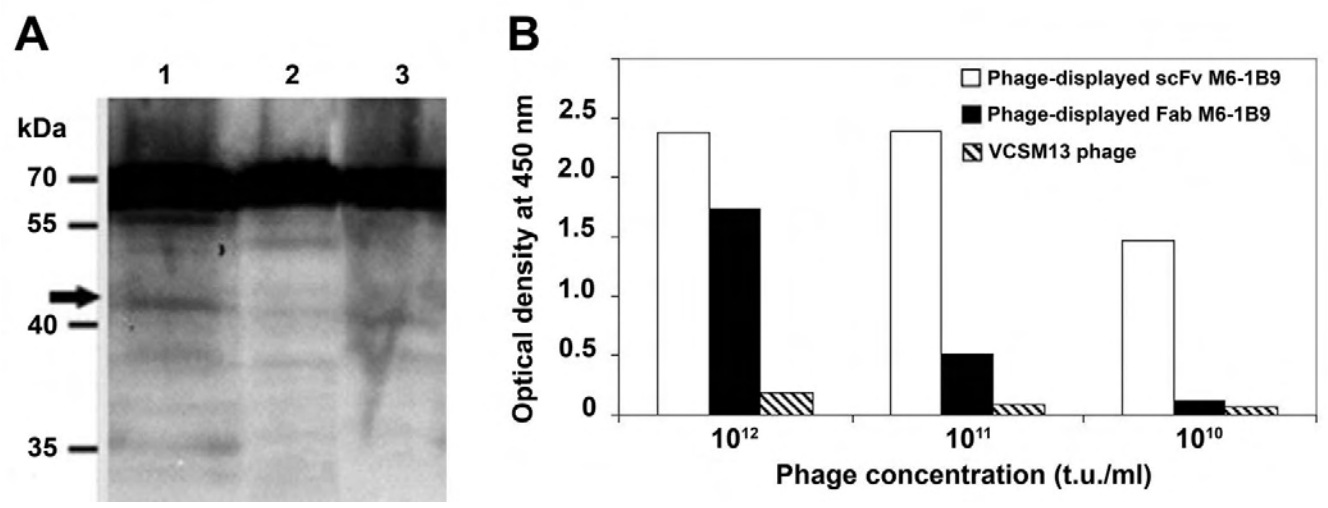

Figure 2

Verification of antibody phage presenting different formats. **A** Recombinant phages (10^{13} t.u./lane) were separated on a reducing 12% SDS-PAGE. The gpIII protein was probed using anti-gpIII mAb. The immunoreactive bands were visualized by chemiluminescence substrate detection system. Lane 1, phage-displayed scFv-M6-1B9; lane 2, phage-displayed Fab-M6-1B9 and lane 3, VCSM13 helper phage. Molecular weight markers in kDa are indicated. Arrow indicates recombinant antibody fragment-gpIII fusion proteins (~47 kDa). **B** CD147-BCCP was captured on wells coated with avidin. Three different concentrations, 10^{10} – 10^{12} t.u./ml of phage-displayed scFv-M6-1B9 and phage-displayed Fab-M6-1B9 were added and traced by peroxidase-conjugated anti-M13 phage mAb. VCSM13 helper phage and mAb M6-1B9 specific for CD147 [8] were used as wild-type phage control and antibody control, respectively.

results suggest that phage presenting different antibody formats of M6-1B9 had been successfully produced and that the scFv version was the better functional antibody fragment.

Detection and characterization of soluble scFv-M6-1B9 produced in E. coli

The pComb3X-scFv-M6-1B9 was subsequently transformed into *E. coli* HB2151 to produce the soluble scFv antibody. The presence of soluble scFv in the culture supernatant was detected by Western immunoblotting regarding HA and His tags. The reactive bands revealed by anti-HA or anti-His were located at the same molecular weight (~30 kDa) (Figure 3A). This result indicates that soluble scFv-M6-1B9 was successfully produced by *E. coli* HB2151.

The specificity of soluble scFv-M6-1B9 was analyzed by ELISA using CD147-BCCP as antigen (Figure 3B). Various dilutions of soluble scFv-M6-1B9 were represented the positive signal with CD147-BCCP. No signal was detected in the control well of survivin-BCCP (SVV-BCCP) antigen. Subsequently, Western immunoblotting was used to confirm the specificity of the generated scFv-M6-1B9 against recombinant CD147. A specific band of CD147-BCCP at ~35 kDa was detected by probing with soluble scFv-M6-1B9 (Figure 3C). In addition, the native epitope of CD147 on the U937 cell surface was recognized by soluble scFv-M6-1B9 using flow cytometric analysis. The mean fluorescence intensity (MFI) of CD147 cell surface expression on U937 cells stained with soluble scFv-M6-1B9 was 10.42 (Figure 3D). This was similar to the value for the original antibody, M6-1B9, which MFI was 9.21 as shown in Figure 3D. These results strongly suggested that the generated soluble scFv-M6-1B9 carry a CD147-specific paratope which recognized both recombinant and native CD147.

To further characterize the specificity of the produced scFv, the inhibiting activity of soluble scFv-M6-1B9 with the original monoclonal antibody, M6-1B9, was tested. The optical density of mixture of soluble scFv-M6-1B9 and mAb M6-1B9 was lower than soluble scFv-M6-1B9 alone (Figure 4). In contrast, the irrelevant mAb MT-SVV3 did not show the inhibition effect. This indicates that the scFv-M6-1B9 recognized the same antigenic determinant as its original mAb M6-1B9.

Intracellular expression of scFv-M6-1B9 intrabody abated cell surface expression of CD147 on 293A cells

The compatibility of scFv-M6-1B9 with a eukaryotic expression system was examined by transducing the recombinant adenovirus harboring scFv-M6-1B9 into 293A cells. Alteration of surface expression of CD147 in transduced 293A cells was examined at 36 h after transduction. CD147 cell surface expression was decreased in scFv-M6-1B9 adenovirus-transduced 293A cells compared to untransduced cells (Figure 5). In contrast, no alteration of CD147 expression was observed on scFv-SVV3 adenovirus-transduced cells (Figure 5). This result revealed that intracellular expression of scFv-M6-1B9 as intrabody

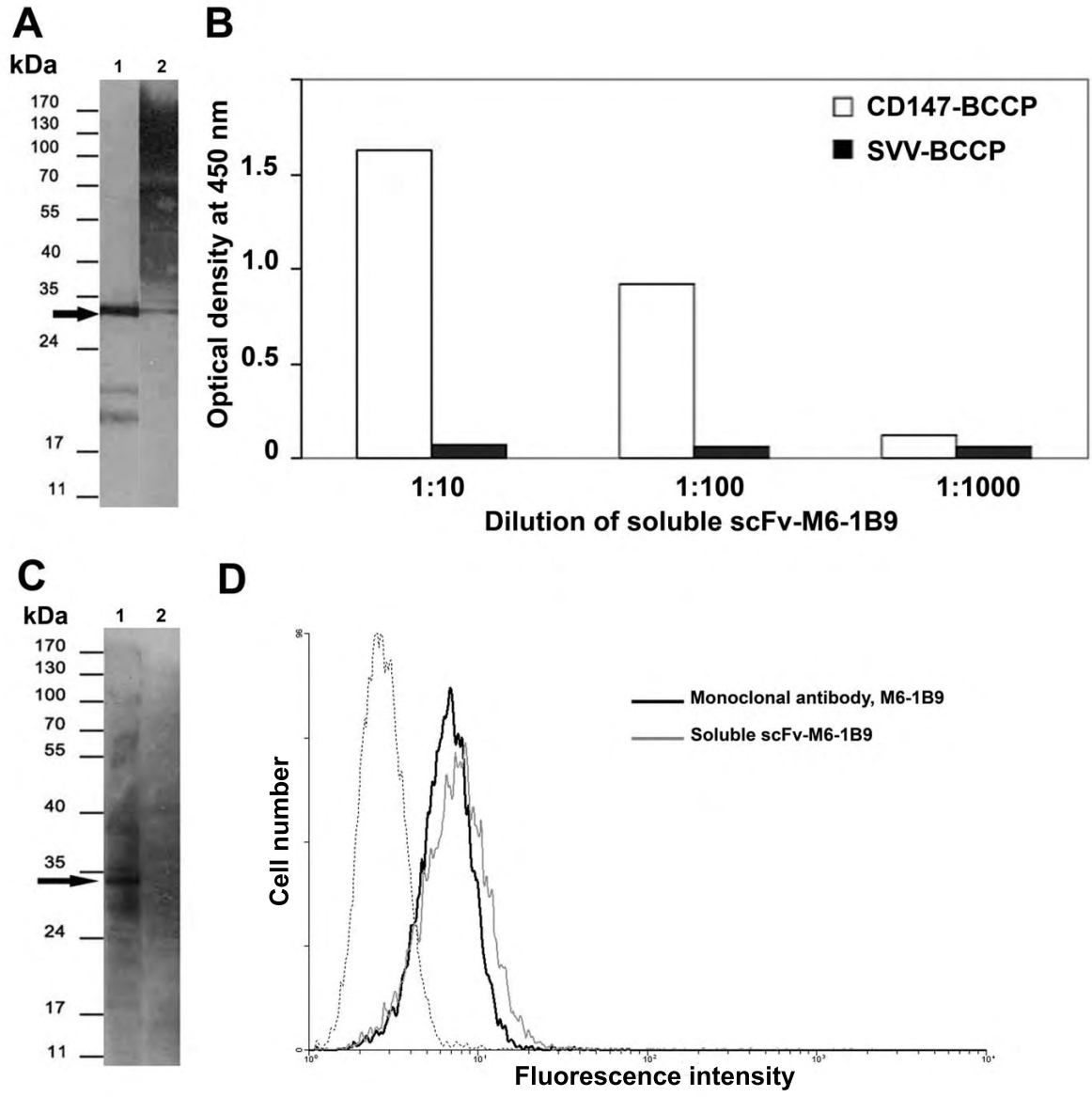

Figure 3

Detection of soluble scFv. **A** Soluble scFv-M6-1B9 was separated on 12% SDS-PAGE, electroblotted onto PVDF membrane, and probed with peroxidase-conjugated mAb anti-HA (lane 1) and anti-His mAb (lane 2). The immunoreactive bands were visualized by ECL substrate detection system. The molecular weight is indicated. **B** CD147-BCCP (open columns) or SVV-BCCP (black columns) was captured on the avidin-coated wells. Soluble scFv-M6-1B9 was subsequently added and the bound scFv was detected by peroxidase-conjugated mAb anti-HA. **C** CD147-BCCP (lane 1) or SVV-BCCP (lane 2) proteins were separated on 12% SDS-PAGE, electroblotted onto a PVDF membrane, and then probed with soluble scFv-M6-1B9. The scFv was detected using peroxidase-conjugated mAb anti-HA. The positions of molecular mass markers are shown on the left. **D** CD147 on U937 cells was stained with soluble scFv-M6-1B9 and then probed by mouse anti-HA-biotin. Subsequently, FITC-conjugated sheep anti-mouse immunoglobulins antibody was added. Monoclonal antibody M6-1B9 was used as a control system for detecting CD147 on U937 cells. The immunofluorescence on cells stained with soluble scFv-M6-1B9 (bold line) or mAb M6-1B9 (thin line) is shown. The dashed line represents background fluorescence of negative control mAb. The *y* axis represents the number of events on a linear scale; the *x* axis shows the fluorescence intensity on a logarithmic scale.

could diminish CD147 expression on cell surface of intrabody-expressing 293A cells.

Colocalization of scFv-M6-1B9 intrabody and CD147 in 293A cells

Colocalization of scFv-M6-1B9 intrabody and CD147 within transfected 293A cells was elucidated. As shown in Figure 6 and in the three-dimensional movies (Additional file 1), scFv-M6-1B9 intrabody was found intracellularly and colocalized with CD147. This result implied that scFv-M6-1B9 protein fused with ER-retention signal was successfully expressed and retained the CD147 molecule inside the cell.

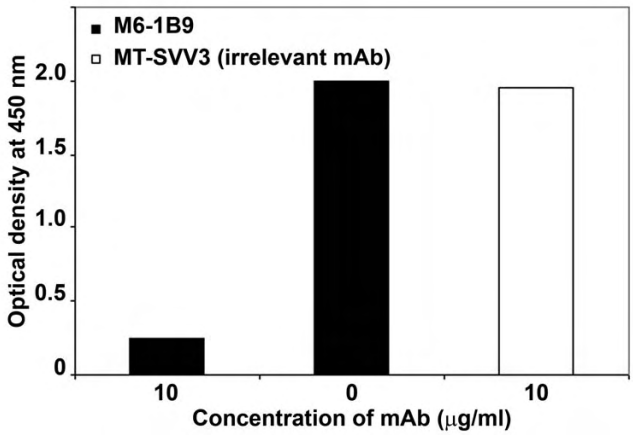

Figure 4

Competitive binding analysis of soluble scFv-M6-1B9 and mAb M6-1B9. CD147-BCCP was added onto avidin-coated wells. The mixture contained soluble scFv-M6-1B9 and mAb M6-1B9 or mAb MT-SVV3 at ratio 1:1 was added into the well. The bound scFv was detected by peroxidase-conjugated mAb anti-HA.

Discussion

CD147 plays a crucial role in several tissues, but is particularly dense on the surface of activated T-lymphocytes [1,16] and malignant tumor cells [38-40]. Diminishing the expression of CD147 on the cell surface could serve as a step towards exploring the significance of CD147 in cellular functions. In the present study, we successfully employed an intrabody-based approach to reduce the expression of CD147 on the 293A cell surface. This opens new prospects for uncovering the functional role of CD147.

Critical residues implicated in antigen binding from a given antibody paratope are important for the construction of different antibody formats. The deduced amino acid residues responsible for paratope in CDR regions of the scFv-M6-1B9 were identified *via* the WAM algorithm [33] and can be numbered following Kabat's rule [34]. These confirmed the precise cloning of the immunoglobulin variable domains of anti-CD147 mAb, M6-1B9, into the phagemid vector.

Two antibody formats, Fab and scFv, were exploited for antibody phage display. To assess whether Fab-M6-1B9 or scFv-M6-1B9 on gpIII of phage particles have exclusive activities, both antibody formats were generated and evaluated. The expression of phage-displayed scFv-M6-1B9 was significantly greater than phage-displayed Fab-M6-1B9, and both antibody fragments could recognize the CD147 protein. Noticeably, the scFv format exhibited a greater binding activity compared to the Fab format. The expression level of scFvs in *E. coli* is typically higher than Fabs and generates a more efficient antibody display on the phage particle. The interdomain disulfide bond at the C-terminal of the constant region, which plays an important role in Fab stabilization, is predisposed to provide lower production yield than scFvs [41].

Recognition of the amber stop codon between the scFv and gpIII genes that occurs during the expression of pComb3X-scFv-M6-1B9 in the non-suppressing HB2151 *E. coli* strain resulted in the production of soluble scFv-M6-1B9 [42,43]. This antibody fragment was specifically targeted both recombinant CD147 (non-glycosylated form) and native CD147 (glycosylated form) expressed on U937 cell surface. In addition, we demonstrated the

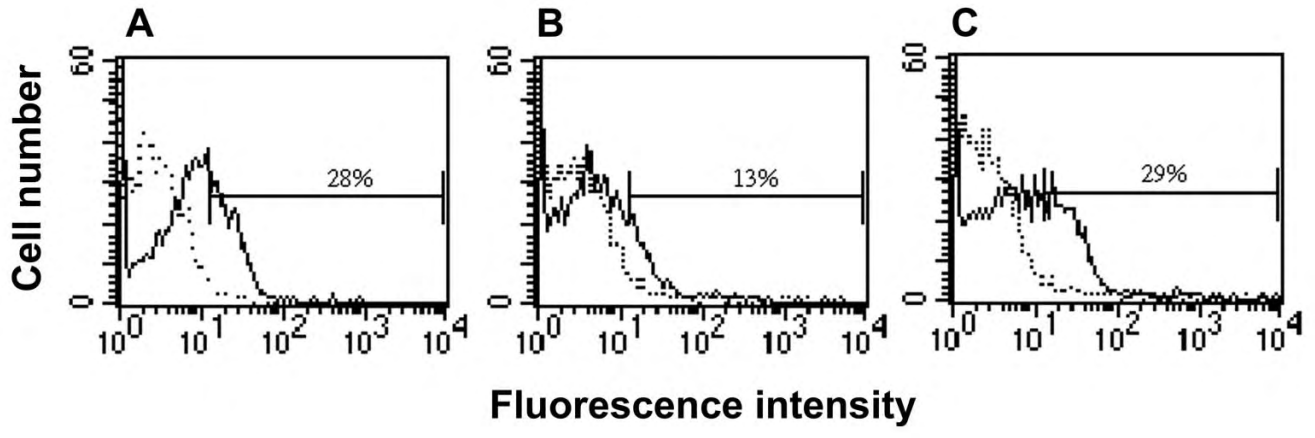

Figure 5

Inhibition of CD147 surface expression on 293A cells by M6-1B9 intrabody. 293A cells were transduced with recombinant adenovirus harboring scFv-M6-1B9 or scFv-SVV3. Cell surface staining of CD147 on **A** untransduced and **B** scFv-M6-1B9 or **C** scFv-SVV3 transduced cells was performed using CD147 mAb, M6-1B9 (bold lines) or irrelevant isotype matched mAb (dashed lines). PE-conjugated F(ab')2 fragment of sheep anti-mouse immunoglobulins antibody were used as a secondary antibody. The percentage (%) of CD147 positive cells was indicated.

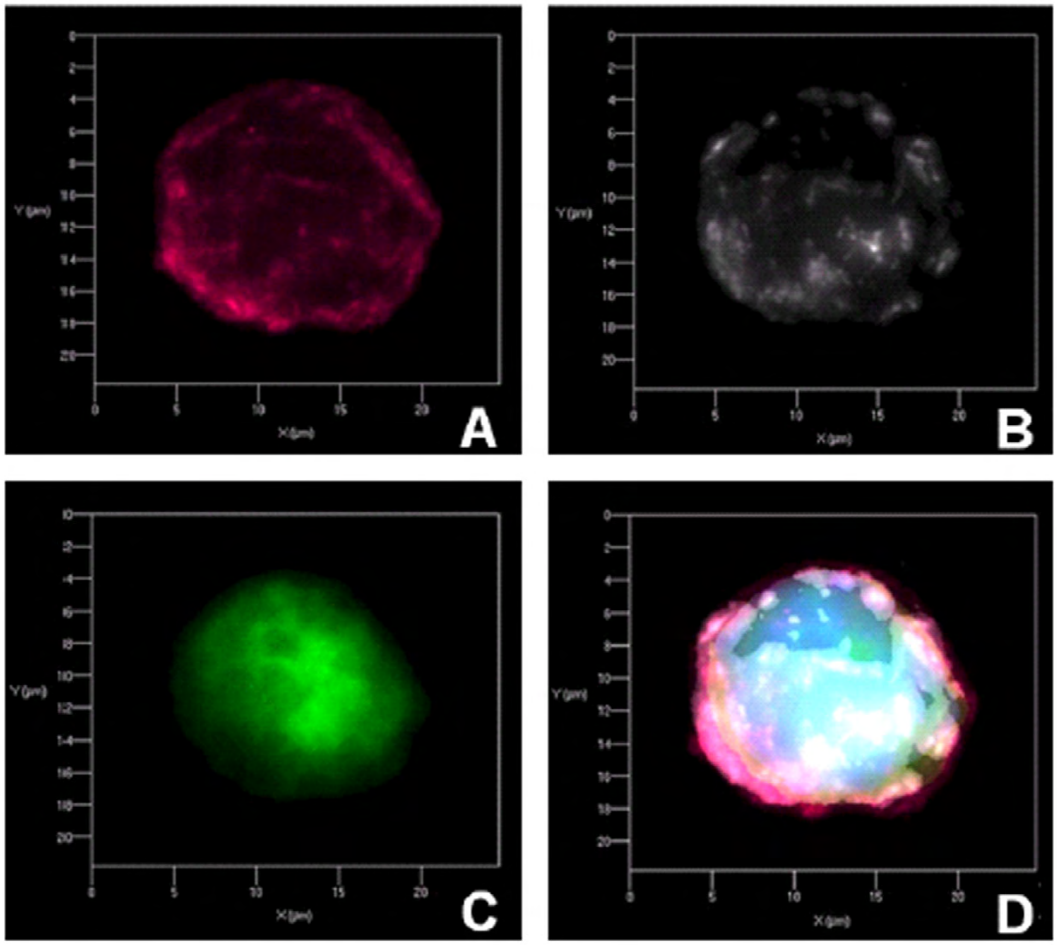

Figure 6

Immunocytochemical analysis for colocalization of CD147-intrabody. The transfected 293A cells were fixed and incubated with a mixture of biotinylated anti-human extracellular matrix metalloproteinase inducer (EMMPRIN) mAb and rabbit anti-HA mAb. Then, cells were stained with the mixture of Cy5-conjugated streptavidin and Cy3-conjugated anti-rabbit-IgG mAb. Nuclei were counterstained with DAPI (blue). Three-dimensional (3D) image of the transfected 293A cells was verified. **A** CD147 on transfected 293A cell stained with biotinylated anti-human EMMPRIN mAb (red), **B** scFv-M6-1B9 intrabody in transfected 293A cell stained with rabbit anti-HA mAb (white), **C** GFP positive in transfected 293A cell and **D** overlay. For 3D image of colocalization of CD147-intrabody see additional file.

inhibition of soluble scFv-M6-1B9 by the original antibody, M6-1B9. These data show that the soluble antibody fragment contained a properly folded, bioactive paratope which recognized both non-glycosylated and glycosylated forms of CD147. CD147 is a highly glycosylated membrane protein. The variation in its molecular weight, ranging between 30 and 66 kDa, arises from different glycosylation patterns [2]. Targeting of both glycosylated and non-glycosylated CD147 molecules *via* scFv-M6-1B9 will be useful as a tool to knockdown the molecules in various cell types.

Generation of adenoviral recombinants carrying scFv-M6-1B9 intrabody in 293A cells was deemed successful, since the cell surface expression of CD147 on these transduced cells declined (Figure 5). It is an open question as to whether this is due to the disruption of CD147 production or the retention of CD147 within the cells. Possibly the ER retention signal, KDEL, sequestered scFv-M6-1B9 intrabody in the ER. This sequestration resulted in the binding of intrabody to the newly synthesized CD147 and retains this molecule inside the cells, as demonstrated by three-dimensional imaging. This result coincided with the functional knockdown of major histocompatibility complex I (MHC-I). Anti-MHC-I intrabody containing this ER retention signal could reduce the surface expression of MHC-I on human umbilical vein endothelial cells (HUVEC) [44]. Thus the KDEL may be necessary for the single-chain antibody protein to diminish the expression of cell surface molecules. The remaining CD147 could be due to the incomplete knockdown effect resulting from transient expression of the scFv-M6-1B9 intrabody.

Intrabodies demonstrate an alternative strategy of gene inactivation that targets genomic DNA or mRNA. Unlike RNAi technology, intrabodies act at the posttranslational level and can be directed to relevant subcellular compartments [27,31,32]. This technique has been employed to diminish expression of a variety cell surface molecules [44-46]. Downregulation of the CD147 surface molecule on 293A cells by means of scFv intrabody expression was achieved in the present study. Nevertheless, RNAi technology has been successfully employed to restrain the expression of CD147 and study the function and mechanism of CD147 in the development of tumor cell lines [25,47]. We therefore aim to introduce the intrabody approach as an alternative method for studying the function and mechanism of CD147 in a variety of metastatic tumors in the near future.

Conclusion

We provide evidence that intrabody technology can be used to diminish the expression of CD147 on 293A cells. Assessment of the fundamental function of CD147 could be achieved in the near future.

Methods

1. Cell culture

Hybridoma cells producing anti-CD147 mAb, M6-1B9 (isotype IgG3) [8,14] were cultured in Iscove's Modified Dulbecco's medium (Gibco, Grand Island, NY) supplemented with 10% fetal bovine serum (FBS) (Gibco), 40 μg/ml gentamicin and 2.5 μg/ml amphotericin B. An embryonic human kidney cell line (293A) (Invitrogen, Carlsbad, CA) was cultured in Dulbecco's Modified Eagle's medium (DMEM) (Gibco) supplemented with 10 mM non-essential amino acids, 10% FBS, penicillin (100 Units/ml), and streptomycin (100 μg/ml). The human monocytic cell line (U937) was cultured in RPMI 1640 medium (Gibco), penicillin (100 Units/ml), and streptomycin (100 μg/ml). All cells were maintained in a humidified atmosphere of 5% CO_2 at 37°C.

2. E. coli *strains and vectors*

E. coli strains, TG-1 and HB2151 were kindly provided by Dr. A.D. Griffiths, MRC, Cambridge, UK. *E. coli* strains, Origami B and XL-1 Blue were purchased from Novagen (Madison, WI) and Stratagene (La Jolla, CA), respectively. The pComb3HSS, pComb3X, modified pAdTrack and pAdEasy vectors were generous gifts from Dr. C.F. Barbas [28,29], The Scripps Research Institute, La Jolla, CA. The pAK400cb vector was a kind gift from Dr. V. Santala (University of Turku, Finland).

3. Generation of Fab-M6-1B9 cDNA fragments

Total RNA was extracted from 5 × 10^6 M6-1B9-producing hybridoma cells using TRIzol® (Invitrogen) according to the manufacturer's instructions. Complementary DNA (cDNA) was synthesized from 1μg total RNA using specific primers, *i.e.* heavy-chain Fd 3' primer (5'-GGG GGT act agt CTT GGG TAT TCT AGG CTC-3'; the *Spe*I restriction site at 5' overhang designated in small letters) and murineκ light-chain 5' primers (5'-GCG CCG tct aga ATT AAC ACT CAT TCC TGT TGA A-3'; the *Xba*I restriction site at 5' overhang designated in small letters). Resulting first-strand cDNA was used as a template for the amplification of Fab fragments. Specific oligonucleotide primers [42] were used to amplify heavy chain and light chain gene segments *i.e.* heavy-chain variable forward primer (5'-AGG TCC AGC TGc tcg agT CTG G-3'; the *Xho*I restriction site at 5' overhang designated in small letters) and heavy-chain Fd 3' primer; murine light-chain variable forward primer (5'-CCA GTT CCg agc tcg TGA TGA CAC AGT CTC CA-3'; the *Sac*I restriction site at 5' overhang designated in small letters) and murineκ light-chain 3' primers. PCR amplification was performed as formerly described [28].

4. Construction of phagemid expressing Fab-M6-1B9

The phagemid expressing Fab-M6-1B9 was constructed. The DNA fragments were digested with *Spe*I/*Xho*I and *Sac*I/*Xba*I, respectively, and then cloned into *Spe*I/*Xho*I and *Sac*I/*Xba*I sites of the phagemid expression vector pComb3HSS. The ligation product was transformed into the competent *E. coli* XL-1 Blue cells. The clones with both inserts were selected on Luria-Bertani (LB) agar containing 100 μg/ml of ampicillin. The plasmid from transformed *E. coli* XL-1 blue was prepared by QIAGEN Miniprep Kit (Qiagen, Hilden, Germany) and digested with *Spe*I/*Xho*I and *Sac*I/*Xba*I. The corrected plasmid was subsequently transformed into *E. coli* TG-1. The transformant bacteria were selected on LB agar containing ampicillin (100 μg/ml). Restriction fragment analysis of the purified plasmid was performed using *Spe*I/*Xho*I and *Sac*I/*Xba*I. The amplified product was checked for an inserted gene in the purified plasmid as described above. The ligated product was named pCom3H-Fab-M6-1B9.

5. Conversion of a M6-1B9 specific Fab into a single chain antibody fragment (scFv)

IgG-specific variable heavy (V_H) and light (V_L) chain gene fragments from purified pCom3H-Fab-M6-1B9 were amplified using PCR system (Eppendorf, Germany) for 30 cycles in the first round (at 94°C for 15 sec, at 56°C for 30 sec, at 72°C for 90 sec and 10 min at 72°C for final extension), with each forward and backward oligonucleotide primers set, *i.e.*, V_H fragments used MSCVH14 (5'-GGT GGT TCC TCT AGA TCT TCC CTC GAG GTR AAG CTT CTC GAG TC-3') and MSCG3_B (5'-CCT GGC CGG CCT GGC CAC TAG TGA CAG ATG GGG CTG TTG TTG T-3') primers, V_L fragments used OmpSeq (5'-AAG ACA GCT ATC GCG ATT GCA G-3') and MSCJK5-BL (5'-GGA AGA TCT AGA GGA ACC ACC CCC ACC ACC GCC CGA GCC ACC GCC ACC AGA GGA TTT CAG CTC CAG CTT GGT

CCC-3') primers as described previously [42]. Then, the purified fragments from QIAGEN PCR purification kit (Qiagen) were used as templates for the second round of PCR amplification to extend a linker. The amplified V_H-linker and V_L-linker PCR products were combined in a PCR reaction mixture. Twenty cycles (at 94°C for 15 sec, at 56°C for 30 sec, at 72°C for 2 min and final extension for 10 min at the same temperature) were performed. These products were gel-purified, digested with *Sfi*I, cloned into phagemid vector pComb3X and transformed into electrocompetent *E. coli* TG1. The transformed cells were then grown and plated onto LB agar containing ampicillin. Colonies bearing the pComb3X-scFv-M6-1B9 construct were confirmed by *Sfi*I restriction enzyme digestion and PCR. Finally, the inserted gene fragment was sequenced using an ABI 3100 automatic sequencer.

6. Preparation of phage-displayed scFv-M6-1B9

A single colony of *E. coli* TG1 harboring pComb3X-scFv-M6-1B9 was chosen from an LB agar plate containing ampicillin for phage-displayed scFv-M6-1B9 preparation as previously described [48]. In brief, transformed bacteria were grown in 2× TY broth containing ampicillin (100 μg/ml) at 37°C with shaking at 200 rpm. The precultured bacteria were subsequently transferred to the same medium containing 1% (w/v) glucose, 1 mM Isopropyl-β-D-thiogalactopyranoside (IPTG) and cultivated at 25°C until the optical density at 600 nm (OD_{600}) reach 0.5. After induction, the bacterial culture was further infected with 10^{12} t.u./ml of VCSM13 helper phages and left at 37°C for 30 min without shaking. The subsequent steps were performed as described previously [48].

7. Preparation of plasmid vector encoding CD147Ex-BCCP

A pair of specific primers, CD147*Nde*I (5'-GAG GAG GAG GTc ata tgG CTG CCG GCA CAG TCT TC-3' ; the *Nde*I restriction site at 5' overhang designated in small letters) and CD147*EcoR*I (5'-GAG GAG GAG CTg aat tcG TGG CTG CGC ACG CGG AG-3' ; the *EcoR*I restriction site at 5' overhang designated in small letters), were synthesized in order to amplify CD147 extracellular domain coding sequence from the phagemid pComb8-CD147Ex vector [48] using ProofStart DNA polymerase (Qiagen). The subsequent steps for protein expression using pAK400cb backbone in *E. coli* Origami B strain were performed as described previously [49,50]. The biotinylated CD147Ex-BCCP fusion protein was detected by indirect ELISA using mouse anti-CD147 mAbs including M6-1D4, M6-1B9, M6-1E9, M6-1F3, M6-2B1 and M6-2F9 [8] and peroxidase-conjugated goat-anti-mouse immunoglobulins (KPL, Gaithersburg, MD).

8. Immunoassay for phage-displayed scFv-M6-1B9 by ELISA

Microtiter plates (NUNC, Roskilde, Denmark) were coated with 50 μl of 10 μg/ml avidin in carbonate/bicarbonate buffer pH 8.6 overnight at 4°C. The plate was then blocked with 200 μl of 2% skimmed milk in PBS for 1 h at room temperature (RT). The wells were washed five times with 0.05% Tween-20 in PBS. After washing, 50 μl of 100 μg/ml BCCP fusion proteins, *i.e.* CD147-BCCP or SVV-BCCP [50] in 2% skimmed milk, was added and the mixture was incubated for 1 h at RT. Unbound antigen was washed out and 50 μl of phage-displayed scFv-M6-1B9 were added and incubated in a moist chamber for 1 h at RT. The plate was washed thoroughly with 0.05% Tween 20 in PBS 5 times, and peroxidase-conjugated anti-M13 phage mAb (Amersham Pharmacia Biotech, Buckinghamshire, UK) was added to each well. Wells were then washed again prior to adding 100 μl 3,3',5,5'-tetramethyl-benzidine (TMB) substrate. The OD at 450 nm was measured by an ELISA plate reader (TECAN, Austria) after adding 1 N HCl to stop the reaction. mAb M6-1B9 specific for CD147 [8] was used as an antibody control in the ELISA system.

9. Preparation of soluble scFv-M6-1B9

Soluble scFv-M6-1B9 was produced by expressing pComb3X-scFv-M6-1B9 phagemid in the non-suppressor *E. coli* strain HB2151. Transformed bacteria were grown in 10 ml of SB broth containing ampicillin (100 μg/ml) at 37°C for 18 h. Ten microlitres of precultured bacteria were subsequently transferred to 10 ml of the same medium containing 1% (w/v) glucose and ampicillin (100 μg/ml), then cultivated at 37°C until the absorption at 600 nm reached 0.5. The precultured bacteria were then transferred to 90 ml of the same medium and cultivated at the same temperature until the OD_{600} reached 1.5. Then, IPTG was added to the culture at a final concentration of 1 mM. After induction, the bacteria were grown at 25°C for 20 h. Cells were centrifuged at 15,000 g for 30 min at 4°C to collect the supernatant (containing extracellular soluble scFv). Protein was precipitated with saturated $(NH_4)_2SO_4$ in an ice bath and concentrated with Amicon Ultra centrifugal filter units (Millipore, Cork, Ireland). Finally, the concentrated protein was reconstituted with 500 μl of 0.15 M PBS, pH 7.2. ELISA, Western immunoblotting and flow cytometric analysis were performed to detect the antigen-binding affinity of soluble scFv-M6-1B9.

10. Binding assay of soluble scFv-M6-1B9 by ELISA

Microtiter plates were coated with 50 μl of 10 μg/ml avidin in carbonate/bicarbonate buffer pH 8.6 overnight at 4°C. The plates were then blocked with 200 μl of 2% bovine serum albumin (BSA) in PBS for 1 h at RT. The wells were washed five times with 0.05% Tween-20 in PBS

and 50 μl of 100 μg/ml BCCP fusion proteins [50] in 2% BSA were added and incubated for 1 h at RT. The unbound antigen was washed out. Fifty microlitres of scFv-M6-1B9 at various dilutions were added and incubated in a moist chamber for 1 h at RT. The plates were washed thoroughly with 0.05% Tween 20 in PBS for 5 times and peroxidase-conjugated mAb anti-HA (Roche, Indianapolis, IN) was added to each well. The wells were then washed again prior to adding 100 μl TMB substrate and the OD at 450 nm measured after adding 1 N HCl to stop the reaction. mAb M6-1B9 was used as an antibody control in the ELISA system.

11. Competitive binding analysis of soluble scFv-M6-1B9 and mAb M6-1B9

Microtiter plates were coated with 50 μl of 10 μg/ml avidin in carbonate/bicarbonate buffer (pH 8.6) and left overnight at 4°C. The plate was then blocked with 200 μl of 2% BSA in PBS for 1 h at RT. The wells were washed 5 times with 0.05% Tween-20 in PBS and 50 μl of 100 μg/ml BCCP fusion proteins [50] in 2% BSA were added and incubated for 1 h at RT. The unbound antigen was washed out. Fifty microlitres of the mixture containing soluble scFv-M6-1B9 at dilution 1:250 and 20 μg/ml mAb M6-1B9 or mAb against survivin (MT-SVV3) at ratio 1:1 were added. After incubation in a moist chamber for 1 h at RT, the plate was washed thoroughly with 0.05% Tween 20 in PBS for 5 times. Peroxidase-conjugated mAb anti-HA was added to each well. The wells were then washed again prior to adding 100 μl TMB substrate. The OD at 450 nm was measured after adding 1 N HCl to stop the reaction.

12. Immunofluorescence analysis of the reactivity of soluble scFv-M6-1B9

U937 cells were adjusted to 1×10^7 cells/ml with 1% BSA-PBS-NaN_3 and blocked on ice with human AB serum at the ratio of 1:10 for 30 min. Fifty microlitres of 1:10 dilution in 1% BSA-PBS-NaN_3 of soluble scFv-M6-1B9 were added to 50 μl of blocked cells and incubated on ice for 30 min. Cells were washed twice with 1% BSA-PBS-NaN_3. Subsequently, fifty microlitres of 20 μg/ml mouse anti-HA-biotin (Sigma, St Louis, MO) were added and the cells were incubated on ice for 30 min. After washing, cells were resuspended with 20 μl 1% BSA-PBS-NaN_3. FITC-conjugated sheep anti-mouse immunoglobulins antibody (Chemicon International, Melbourne, Australia) was then added. Cells were incubated on ice for another 30 min. Finally, cells were washed 3 times with 1% BSA-PBS-NaN_3 and fixed with 1% paraformaldehyde-PBS. Fluorescence reactivity of soluble scFv-M6-1B9 with CD147 on U937 cells was analyzed by flow cytometry.

13. Immunoblot analysis

Recombinant phage antibodies were separated on a 12% SDS-PAGE gel under reducing conditions, then transferred onto a polyvinyllidene fluoride (PVDF) membrane. The membranes were blocked with 5% skimmed milk in PBS, and then incubated with mouse anti-gpIII mAb (Exalpha Biologicals, Inc., Watertown, MA). After washing, peroxidase-conjugated goat anti-mouse immunoglobulins antibody were added to the membranes. The peroxidase reaction was visualized using an enhanced chemiluminescent (ECL) substrate detection system (GE Healthcare, Buckinghamshire, UK).

To determine the binding activity of soluble scFv-M6-1B9, BCCP fusion proteins were separated on 12% SDS-PAGE, electroblotted onto PVDF membrane, and then were probed with soluble scFv-M6-1B9 and traced by peroxidase-conjugated mAb anti-HA. The immunoreactive bands were visualized as described previously.

14. Assembly of intrabody construct in pAdTrackCMV

The scFv coding regions were flanked by a human κ light chain leader sequence at the 5'-end, and a sequence encoding the HA tag (YPYDVPDYA) and the ER retention signal (KDEL) at the 3'-end. The intrabody coding regions from pComb3X-scFv-M6-1B9 were then excised by digestion with *Sfi*I and cloned into modified pAdTrackCMV [28]. This adapter fragment contains compatible *Sfi*I sites, which were used for cloning the scFv-M6-1B9 intrabody against CD147 into the adenovirus vector. The generation of recombinant adenoviruses was done essentially as previously described [51]. Briefly, 6×10^4 293A cells in 500 μl DMEM containing 10% FBS and antibiotics were plated on a polystyrene 24-well plate for 24 h before transfection. Transfection mixture was prepared by adding 1 μg pAdE-scFv-M6-1B9 in 50 μl DMEM to 0.25 μl transfectin (Bio-Rad, Hercules, CA) in 50 μl DMEM and followed by incubation at RT for 20 min. The mixture was then added to the cells and incubated at 37°C in 5% CO_2 for 4 h. Four hundred microlitres of DMEM containing 10% FBS and antibiotics were added into the wells and plates were further incubated at 37°C in 5% CO_2 for 7 days. High titer viral stocks were produced and purified using a ViraBind™ Adenovirus purification kit (Cell Biolabs, San Diego, CA).

15. Flow cytometry analysis for CD147 surface expression

Five hundred microlitres of 1.2×10^5 cells/ml 293A were transduced with 10 MOI (~80% of the cells were infected) of adenovirus encoding scFv-M6-1B9 intrabody. After 36 h, 293A cells were removed from 24-well tissue culture plates and washed 3 times with PBS. Cells were then blocked with human AB serum for 30 min on ice. Fifty microlitres of 20 μg/ml purified mAb M6-1B9 in 1% BSA-PBS-NaN_3 were added to 50 μl of blocked cells and incubated on ice for 30 min. Cells were washed twice with 1% BSA-PBS-NaN_3 and resuspended with 20 μl 1% BSA-PBS-NaN_3. Subsequently, twenty-five microlitres of PE-conjugated $F(ab')_2$ fragment of sheep anti-mouse immunoglob-

ulins antibody were added and incubated on ice for 30 min. Finally, cells were washed 3 times with 1% BSA-PBS-NaN_3 and fixed with 1% paraformaldehyde-PBS. Fluorescence reactivity of the stained cells was investigated by flow cytometry. Adenovirus encoding scFv specific to survivin (scFv-SVV3) intrabody constructed by the same technique was used as transduction control.

16. Immunocytochemical analysis for CD147-intrabody colocalization

For analysis of CD147 and intrabodies on GFP-positive 293A, transfected cells were trypsinized and fixed for 10 min with 3.7% formaldehyde in PBS containing 50 mM $MgCl_2$. Fifty microlitres of 1×10^6 fixed cells were placed on a silane-coated slide and air-dried. Following washing, cells were permeabilized with 0.2% Triton-X 100 for 12 min. Slides were then washed in PBS containing 50 mM $MgCl_2$ and blocked with 1% BSA in SSC at RT for 5 min. Then, the fixed cells were incubated with a mixture of biotinylated anti-human extracellular matrix metalloproteinase inducer (EMMPRIN) mAb (0.1 μg/ml; R&D systems, Minneapolis, MN) and rabbit anti-HA mAb (Sigma) at 4°C overnight. After washing, cells were blocked and then incubated with the mixture of Cy5-conjugated streptavidin (Amersham Life Sciences, Inc, Buckinghamshire, UK) and Cy3-conjugated anti-rabbit-IgG mAb (Sigma) at RT for 30 min. Nuclei were counterstained with DAPI. Imaging of stained cells was performed by using a Zeiss Apotome with an AxioCam HRM, AMCA, Cy3, Cy5 and FITC filters in combination with Planapo 63×/1.4 oil objective lens. Images were acquired by using AXIOVISION 4.4 (Carl Zeiss Canada Ltd., Toronto, ON, Canada) in multichanel mode.

17. 3D image acquisitions

AXIOVISION 4.4 with deconvolution module and rendering module were used. For every fluorochrome, the 3D image consists of a stack of 80 images with a sampling distance of 200 nm along the *z* and 107 nm in the *xy* direction. The constrained iterative algorithm option was used [52].

Authors' contributions

KT and NI contributed equally to this work. YY participated in adenoviral vector gene transfer. SM participated in the 3D image analysis. WK participated in the generation of hybridomas, experimental design, co-ordination, and drafted the manuscript. CT established the experimental design, and helped to draft the manuscript. KT, NI, WK and CT wrote the paper. All authors read and approved the final manuscript.

Additional material

Additional file 1

Colocalization of CD147 and intrabody. *Colocalization of CD147 (red) and intrabody (white) in the transfected 293A cell was demonstrated in pink. Image acquisition and analysis is as described in Materials and Methods.*

Click here for file

[http://www.biomedcentral.com/content/supplementary/1472-6750-8-5-S1.WMV]

Acknowledgements

This work was supported by a scholarship from the Commission on Higher Education, the Thailand Research Fund and the National Center for Genetic Engineering and Biotechnology (BIOTEC), Thailand and Canadian Institutes of Health Research Strategic Training Program 'Innovative Technologies in Multidisciplinary Health Research Training', Canada. The authors are grateful to Dr. Andrew D. Griffiths for the generous gift of *E. coli* strains, TG-1 and HB2151, and Dr. Ville Santala for pAK400cb vector. We also gratefully acknowledge Dr. Carlos F. Barbas III for providing pComb3HSS, pComb3X, modified pAdTrack and pAdEasy vectors. We are thankful to Somphot Saoin, Wutigri Nimlamool, Watinee Yatfoong and Supansa Pata for their technical assistances. The authors would like to thank Dr. Dale E. Taneyhill for proofreading the manuscript and advice.

References

1. Kasinrerk W, Fiebiger E, Stefanova I, Baumruker T, Knapp W, Stockinger H: **Human leukocyte activation antigen M6, a member of the Ig superfamily, is the species homologue of rat OX-47, mouse basigin, and chicken HT7 molecule.** *J Immunol* 1992, **149(3):**847-854.
2. Biswas C, Zhang Y, DeCastro R, Guo H, Nakamura T, Kataoka H, Nabeshima K: **The human tumor cell-derived collagenase stimulatory factor (renamed EMMPRIN) is a member of the immunoglobulin superfamily.** *Cancer Res* 1995, **55(2):**434-439.
3. Zola H Swart B, Nicholson I, Voss E.: **Leukocyte ans Stromal Cell Molecules: The CD Markers.** New Jersey , John Wiley & Sons, Inc.; 2007.
4. Fossum S, Mallett S, Barclay AN: **The MRC OX-47 antigen is a member of the immunoglobulin superfamily with an unusual transmembrane sequence.** *Eur J Immunol* 1991, **21(3):**671-679.
5. Noguchi Y, Sato T, Hirata M, Hara T, Ohama K, Ito A: **Identification and characterization of extracellular matrix metalloproteinase inducer in human endometrium during the menstrual cycle in vivo and in vitro.** *J Clin Endocrinol Metab* 2003, **88(12):**6063-6072.
6. Gabison EE, Mourah S, Steinfels E, Yan L, Hoang-Xuan T, Watsky MA, De Wever B, Calvo F, Mauviel A, Menashi S: **Differential expression of extracellular matrix metalloproteinase inducer (CD147) in normal and ulcerated corneas: role in epithelio-stromal interactions and matrix metalloproteinase induction.** *Am J Pathol* 2005, **166(1):**209-219.
7. Smedts AM, Lele SM, Modesitt SC, Curry TE: **Expression of an extracellular matrix metalloproteinase inducer (basigin) in the human ovary and ovarian endometriosis.** *Fertil Steril* 2006, **86(3):**535-542.
8. Kasinrerk W, Tokrasinwit N, Phunpae P: **CD147 monoclonal antibodies induce homotypic cell aggregation of monocytic cell line U937 via LFA-1/ICAM-1 pathway.** *Immunology* 1999, **96(2):**184-192.
9. Zhang W, Erkan M, Abiatari I, Giese NA, Felix K, Kayed H, Buchler MW, Friess H, Kleeff J: **Expression of Extracellular Matrix Metalloproteinase Inducer (EMMPRIN/CD147) in Pancreatic Neoplasm and Pancreatic Stellate Cells.** *Cancer Biol Ther* 2007, **6(2):**218-227.

10. Vigneswaran N, Beckers S, Waigel S, Mensah J, Wu J, Mo J, Fleisher KE, Bouquot J, Sacks PG, Zacharias W: **Increased EMMPRIN (CD 147) expression during oral carcinogenesis.** *Exp Mol Pathol* 2006, **80(2):**147-159.
11. Renno T, Wilson A, Dunkel C, Coste I, Maisnier-Patin K, Benoit de Coignac A, Aubry JP, Lees RK, Bonnefoy JY, MacDonald HR, Gauchat JF: **A role for CD147 in thymic development.** *J Immunol* 2002, **168(10):**4946-4950.
12. Kirsch AH, Diaz LA Jr., Bonish B, Antony PA, Fox DA: **The pattern of expression of CD147/neurothelin during human T-cell ontogeny as defined by the monoclonal antibody 8D6.** *Tissue Antigens* 1997, **50(2):**147-152.
13. Jia L, Zhou H, Wang S, Cao J, Wei W, Zhang J: **Deglycosylation of CD147 down-regulates Matrix Metalloproteinase-11 expression and the adhesive capability of murine hepatocarcinoma cell HcaF in vitro.** *IUBMB Life* 2006, **58(4):**209-216.
14. Chiampanichayakul S, Peng-In P, Khunkaewla P, Stockinger H, Kasinrerk W: **CD147 contains different bioactive epitopes involving the regulation of cell adhesion and lymphocyte activation.** *Immunobiology* 2006, **211(3):**167-178.
15. Staffler G, Szekeres A, Schutz GJ, Saemann MD, Prager E, Zeyda M, Drbal K, Zlabinger GJ, Stulnig TM, Stockinger H: **Selective inhibition of T cell activation via CD147 through novel modulation of lipid rafts.** *J Immunol* 2003, **171(4):**1707-1714.
16. Koch C, Staffler G, Huttinger R, Hilgert I, Prager E, Cerny J, Steinlein P, Majdic O, Horejsi V, Stockinger H: **T cell activation-associated epitopes of CD147 in regulation of the T cell response, and their definition by antibody affinity and antigen density.** *Int Immunol* 1999, **11(5):**777-786.
17. Philp NJ, Ochrietor JD, Rudoy C, Muramatsu T, Linser PJ: **Loss of MCT1, MCT3, and MCT4 expression in the retinal pigment epithelium and neural retina of the 5A11/basigin-null mouse.** *Invest Ophthalmol Vis Sci* 2003, **44(3):**1305-1311.
18. Clamp MF, Ochrietor JD, Moroz TP, Linser PJ: **Developmental analyses of 5A11/Basigin, 5A11/Basigin-2 and their putative binding partner MCT1 in the mouse eye.** *Exp Eye Res* 2004, **78(4):**777-789.
19. Deora AA, Philp N, Hu J, Bok D, Rodriguez-Boulan E: **Mechanisms regulating tissue-specific polarity of monocarboxylate transporters and their chaperone CD147 in kidney and retinal epithelia.** *Proc Natl Acad Sci U S A* 2005, **102(45):**16245-16250.
20. Khunkeawla P, Moonsom S, Staffler G, Kongtawelert P, Kasinrerk W: **Engagement of CD147 molecule-induced cell aggregation through the activation of protein kinases and reorganization of the cytoskeleton.** *Immunobiology* 2001, **203(4):**659-669.
21. Boulos S, Meloni BP, Arthur PG, Majda B, Bojarski C, Knuckey NW: **Evidence that intracellular cyclophilin A and cyclophilin A/CD147 receptor-mediated ERK1/2 signalling can protect neurons against in vitro oxidative and ischemic injury.** *Neurobiol Dis* 2007, **25(1):**54-64.
22. Tang Y, Nakada MT, Rafferty P, Laraio J, McCabe FL, Millar H, Cunningham M, Snyder LA, Bugelski P, Yan L: **Regulation of vascular endothelial growth factor expression by EMMPRIN via the PI3K-Akt signaling pathway.** *Mol Cancer Res* 2006, **4(6):**371-377.
23. Yang JM, O'Neill P, Jin W, Foty R, Medina DJ, Xu Z, Lomas M, Arndt GM, Tang Y, Nakada M, Yan L, Hait WN: **Extracellular matrix metalloproteinase inducer (CD147) confers resistance of breast cancer cells to Anoikis through inhibition of Bim.** *J Biol Chem* 2006, **281(14):**9719-9727.
24. Nabeshima K, Iwasaki H, Koga K, Hojo H, Suzumiya J, Kikuchi M: **Emmprin (basigin/CD147): matrix metalloproteinase modulator and multifunctional cell recognition molecule that plays a critical role in cancer progression.** *Pathol Int* 2006, **56(7):**359-367.
25. Chen X, Lin J, Kanekura T, Su J, Lin W, Xie H, Wu Y, Li J, Chen M, Chang J: **A small interfering CD147-targeting RNA inhibited the proliferation, invasiveness, and metastatic activity of malignant melanoma.** *Cancer Res* 2006, **66(23):**11323-11330.
26. Igakura T, Kadomatsu K, Taguchi O, Muramatsu H, Kaname T, Miyauchi T, Yamamura K, Arimura K, Muramatsu T: **Roles of basigin, a member of the immunoglobulin superfamily, in behavior as to an irritating odor, lymphocyte response, and blood-brain barrier.** *Biochem Biophys Res Commun* 1996, **224(1):**33-36.
27. Lobato MN, Rabbitts TH: **Intracellular antibodies as specific reagents for functional ablation: future therapeutic molecules.** *Curr Mol Med* 2004, **4(5):**519-528.
28. Steinberger P, Andris-Widhopf J, Buhler B, Torbett BE, Barbas CF 3rd: **Functional deletion of the CCR5 receptor by intracellular immunization produces cells that are refractory to CCR5-dependent HIV-1 infection and cell fusion.** *Proc Natl Acad Sci U S A* 2000, **97(2):**805-810.
29. Jendreyko N, Popkov M, Beerli RR, Chung J, McGavern DB, Rader C, Barbas CF 3rd: **Intradiabodies, bispecific, tetravalent antibodies for the simultaneous functional knockout of two cell surface receptors.** *J Biol Chem* 2003, **278(48):**47812-47819.
30. Stocks MR: **Intrabodies: production and promise.** *Drug Discov Today* 2004, **9(22):**960-966.
31. Heng BC, Cao T: **Making cell-permeable antibodies (Transbody) through fusion of protein transduction domains (PTD) with single chain variable fragment (scFv) antibodies: potential advantages over antibodies expressed within the intracellular environment (Intrabody).** *Med Hypotheses* 2005, **64(6):**1105-1108.
32. Heng BC, Hong YH, Cao T: **Modulating gene expression in stem cells without recombinant DNA and permanent genetic modification.** *Cell Tissue Res* 2005, **321(2):**147-150.
33. Whitelegg NR, Rees AR: **WAM: an improved algorithm for modelling antibodies on the WEB.** *Protein Eng* 2000, **13(12):**819-824.
34. Kabat EA, Wu TT, Bilofsky H, National Institutes of Health (U.S.). Division of Research Resources.: **Variable regions of immunoglobulin chains : tabulations and analyses of amino acid sequences.** Cambridge, Mass. , Medical Computer Systems; 1976:v, 130 p..
35. Verhaert RM, Van Duin J, Quax WJ: **Processing and functional display of the 86 kDa heterodimeric penicillin G acylase on the surface of phage fd.** *Biochem J* 1999, **342 (Pt 2):**415-422.
36. Kramer RA, Cox F, van der Horst M, van der Oudenrijn S, Res PC, Bia J, Logtenberg T, de Kruif J: **A novel helper phage that improves phage display selection efficiency by preventing the amplification of phages without recombinant protein.** *Nucleic Acids Res* 2003, **31(11):**e59.
37. Rasched I, Oberer E: **Ff coliphages: structural and functional relationships.** *Microbiol Rev* 1986, **50(4):**401-427.
38. Muraoka K, Nabeshima K, Murayama T, Biswas C, Koono M: **Enhanced expression of a tumor-cell-derived collagenase-stimulatory factor in urothelial carcinoma: its usefulness as a tumor marker for bladder cancers.** *Int J Cancer* 1993, **55(1):**19-26.
39. Suzuki S, Sato M, Senoo H, Ishikawa K: **Direct cell-cell interaction enhances pro-MMP-2 production and activation in co-culture of laryngeal cancer cells and fibroblasts: involvement of EMMPRIN and MT1-MMP.** *Exp Cell Res* 2004, **293(2):**259-266.
40. Polette M, Gilles C, Marchand V, Lorenzato M, Toole B, Tournier JM, Zucker S, Birembaut P: **Tumor collagenase stimulatory factor (TCSF) expression and localization in human lung and breast cancers.** *J Histochem Cytochem* 1997, **45(5):**703-709.
41. Rothlisberger D, Honegger A, Pluckthun A: **Domain interactions in the Fab fragment: a comparative evaluation of the single-chain Fv and Fab format engineered with variable domains of different stability.** *J Mol Biol* 2005, **347(4):**773-789.
42. Barbas CF 3rd: **Phage display : a laboratory manual.** Cold Spring Harbor, NY , Cold Spring Harbor Laboratory Press; 2001:1 v. in various pagings.
43. Su YC, Lim KP, Nathan S: **Bacterial expression of the scFv fragment of a recombinant antibody specific for Burkholderia pseudomallei exotoxin.** *J Biochem Mol Biol* 2003, **36(5):**493-498.
44. Beyer F, Doebis C, Busch A, Ritter T, Mhashilkar A, Marasco WM, Laube H, Volk HD, Seifert M: **Decline of surface MHC I by adenoviral gene transfer of anti-MHC I intrabodies in human endothelial cells-new perspectives for the generation of universal donor cells for tissue transplantation.** *J Gene Med* 2004, **6(6):**616-623.
45. Peng JL, Wu S, Zhao XP, Wang M, Li WH, Shen X, Liu J, Lei P, Zhu HF, Shen GX: **Downregulation of transferrin receptor surface expression by intracellular antibody.** *Biochem Biophys Res Commun* 2007, **354(4):**864-871.
46. Jendreyko N, Popkov M, Rader C, Barbas CF 3rd: **Phenotypic knockout of VEGF-R2 and Tie-2 with an intradiabody reduces tumor growth and angiogenesis in vivo.** *Proc Natl Acad Sci U S A* 2005, **102(23):**8293-8298.

47. Zou W, Yang H, Hou X, Zhang W, Chen B, Xin X: **Inhibition of CD147 gene expression via RNA interference reduces tumor cell invasion, tumorigenicity and increases chemosensitivity to paclitaxel in HO-8910pm cells.** *Cancer Lett* 2007, **248(2):**211-218.
48. Intasai N, Mai S, Kasinrerk W, Tayapiwatana C: **Binding of multivalent CD147 phage induces apoptosis of U937 cells.** *Int Immunol* 2006, **18(7):**1159-1169.
49. Santala V, Lamminmaki U: **Production of a biotinylated single-chain antibody fragment in the cytoplasm of Escherichia coli.** *J Immunol Methods* 2004, **284(1-2):**165-175.
50. Tayapiwatana C, Chotpadiwetkul R, Kasinrerk W: **A novel approach using streptavidin magnetic bead-sorted in vivo biotinylated survivin for monoclonal antibody production.** *J Immunol Methods* 2006, **317(1-2):**1-11.
51. He TC, Zhou S, da Costa LT, Yu J, Kinzler KW, Vogelstein B: **A simplified system for generating recombinant adenoviruses.** *Proc Natl Acad Sci U S A* 1998, **95(5):**2509-2514.
52. Schaefer LH, Schuster D, Herz H: **Generalized approach for accelerated maximum likelihood based image restoration applied to three-dimensional fluorescence microscopy.** *J Microsc* 2001, **204(Pt 2):**99-107.

Available online at www.sciencedirect.com
ScienceDirect
Immunobiology 214 (2009) 410–421
Immunobiology
www.elsevier.de/imbio

Potent inhibition of OKT3-induced T cell proliferation and suppression of CD147 cell surface expression in HeLa cells by scFv-M6-1B9

Nutjeera Intasai[a,1], Khajornsak Tragoolpua[b,1], Prakitnavin Pingmuang[b], Panida Khunkaewla[c,d], Seangdeun Moonsom[c], Watchara Kasinrerk[b,c], André Lieber[e], Chatchai Tayapiwatana[b,c,f,*]

[a]*Division of Clinical Microscopy, Department of Medical Technology, Faculty of Associated Medical Sciences, Chiang Mai University, Chiang Mai 50200, Thailand*
[b]*Division of Clinical Immunology, Department of Medical Technology, Faculty of Associated Medical Sciences, Chiang Mai University, Chiang Mai 50200, Thailand*
[c]*Biomedical Technology Research Unit, National Center for Genetic Engineering and Biotechnology, National Science and Technology Development Agency at the Faculty of Associated Medical Sciences, Chiang Mai University, Chiang Mai 50200, Thailand*
[d]*School of Biochemistry, Institute of Science, Suranaree University of Technology, NakhonRatchasima 30000, Thailand*
[e]*Division of Medical Genetics, University of Washington, Seattle, WA 98195, USA*
[f]*BioMedical Engineering Center, Chiang Mai University, Chiang Mai 50200, Thailand*

Received 9 September 2008; received in revised form 11 December 2008; accepted 12 December 2008

Abstract

CD147, a multifunctional type I transmembrane glycoprotein, has been implicated in various physiological and pathological processes. It is involved in signal transduction pathways and also plays a crucial role in the invasive and metastatic activity of malignant tumor cells. Diminished expression of this molecule has been shown to be beneficial in suppression of tumor progression. In a previous study, we generated and characterized a recombinant antibody fragment, scFv, which reacted specifically to CD147. In the present study, we further investigated the biological properties, function and the effect of generated scFv on CD147 expression. The *in vitro* study showed that soluble scFv-M6-1B9 produced from *E. coli* HB2151 bound to CD147 surface molecule and inhibited OKT3-induced T cell proliferation. Furthermore, soluble lysate of scFv-M6-1B9 from 293A cells, transduced with a scFv-M6-1B9 expressing adenovirus vector, recognized both recombinant and native CD147. These results indicate that scFv-M6-1B9 binds with high efficiency and specificity. Importantly, scFv-M6-1B9 intrabody reduced the expression of CD147 on the cell surface of HeLa cells suggesting that scFv-M6-1B9 is biologically active. In conclusion, our present study demonstrated that scFv-M6-1B9 has a great potential to target both the intracellular and the extracellular CD147. The

Abbreviations: scFv, single-chain variable fragment; PBMCs, peripheral blood mononuclear cells; FBS, fetal bovine serum; MOI, multiplicity of infection; PBS, phosphate-buffered saline; BSA, bovine serum albumin; $CaCl_2$, calcium chloride; NaCl, sodium chloride; NaN_3, sodium azide; HA, the influenza hemagglutinin epitope YPYDVPDYA; Ad, adenovirus; SVV-BCCP, survivin-biotin carboxyl carrier protein.

*Corresponding author at: Division of Clinical Immunology, Department of Medical Technology, Faculty of Associated Medical Sciences, Chiang Mai University, Chiang Mai 50200, Thailand. Tel.: +66 53 945070; fax: +66 53 946042.
E-mail address: asimi002@chiangmai.ac.th (C. Tayapiwatana).
[1]These authors contributed equally.

doi:10.1016/j.imbio.2008.12.006

generated scFv-M6-1B9 may be an effective agent to clarify the cellular function of CD147 and may aid in efforts to develop a novel treatment in various human carcinomas.

Keywords: scFv antibody; Intrabody; CD147; T cell proliferation; HeLa cells

Introduction

CD147 is a cell surface glycoprotein that belongs to the immunoglobulin superfamily. It plays an important role in mediating signal transduction induced by the binding of specific ligands and regulating central cellular processes such as cell proliferation (Wang et al., 2006), apoptosis (Intasai et al., 2006) or cell adhesion (Kasinrerk et al., 1999; Khunkeawla et al., 2001). In addition, CD147 also is involved in the invasion and metastasis processes of tumor cells in many types of cancers (Reimers et al., 2004; Tang et al., 2005; Nabeshima et al., 2006). An increase in expression of CD147 in cancer cells has not only been linked to deregulation of epidermal growth factor receptor (EGFR) signaling but may also be a response to transforming growth factor-β stimulation (Gabison et al., 2005). CD147, also named extracellular matrix metalloproteinase inducer (EMMPRIN), has been identified as a cell surface inducer of matrix metalloproteinases (MMPs) both in tumor and stromal cells (Sun and Hemler, 2001; Gabison et al., 2005; Yan et al., 2005). Furthermore, CD147 is also defined as a lymphocyte activation-associated molecule (Kasinrerk et al., 1992; Stockinger, 1997; Koch et al., 1999). In T cells a negative regulatory signal arises from cross-linking of CD147 molecules and T cell regulation has been demonstrated (Igakura et al., 1996; Koch et al., 1999; Staffler et al., 2003; Chiampanichayakul et al., 2006). Recently, we demonstrated that two anti-CD147 mAbs, M6-1E9 and M6-1B9, which react with the membrane-distal Ig domain, inhibited OKT3-induced T cell proliferation (Chiampanichayakul et al., 2006). These mAbs inhibited cell proliferation by delivery of a negative signal through CD147 to suppress CD25 and IL-2 expression (Chiampanichayakul et al., 2006).

Recent advances in recombinant technology have facilitated the manipulation, cloning and expression of antibody in various formats. One of the most popular antibody formats is single-chain antibody fragment (scFv) (Boehm et al., 2000) which binds as specifically to antigen as its parental monoclonal antibody. The development of scFv facilitated the engineering and expression of the intrabody. Recent studies have demonstrated that an intrabody strategy can successfully produce both phenotypic and functional knockouts of target molecules (Alvarez et al., 2000; Steinberger et al., 2000; Wheeler et al., 2003; Liu et al., 2005; Peng et al., 2007). This approach depends on a receptor-mediated system for retention of certain proteins within the endoplasmic reticulum (ER). Intrabodies could be a useful tool not only for clinical applications such as neurologic disorders (Messer and McLear, 2006; Emadi et al., 2007; Lynch et al., 2008) and cancer therapy (Popkov et al., 2005; Griffin et al., 2006; Tanaka et al., 2007) but also for functional analysis of proteins inside the cells (Wheeler et al., 2003; Boldicke et al., 2005; Doebis et al., 2006; Goenaga et al., 2007). Recently, we successfully produced soluble scFv against CD147 (scFv-M6-1B9) from its parental mAb, M6-1B9, using bacteria *Escherichia coli.* We have been able to generate this antibody fragment inside 293A cells to knockdown CD147 cell surface expression (Tragoolpua et al., 2008). However, the biological properties and function of scFv-M6-1B9 have not been fully investigated.

In this study, we employed the soluble scFv against CD147 to further investigate the extracellular effect of monomeric scFv-M6-1B9 on OKT3-induced T cell proliferation compared to its parental antibody (M6-1B9). We also introduced an intrabody against CD147 to evaluate the intracellular function of scFv against CD147 on HeLa cells. Here we show that the soluble scFv-M6-1B9 was as able to inhibit a co-stimulatory signal for OKT3-mediated T cell proliferation as its original mAb. Moreover, intrabody against CD147 reduced levels of CD147 surface expression on of HeLa cells.

Materials and methods

Cell culture

An embryonic human kidney cell line (293A) (Invitrogen, Carlsbad, CA) was cultured in Dulbecco's Modified Eagle's medium (DMEM) (Gibco, Carlsbad, CA) supplemented with 10 mM non-essential amino acids, 10% FBS, penicillin (100 Units/ml), and streptomycin (100 μg/ml). HeLa cervical carcinoma cells were kindly obtained from Dr. A. Lieber, University of Washington, Seattle, WA. HeLa cells were maintained in the same medium. PBMCs were prepared by density centrifugation over IsoPrep (Robbins Scientific Corporation, Sunnyvale, CA) and cultured in RPMI 1640 medium (Gibco), 10% FBS, penicillin (100 Units/ml),

and streptomycin (100 μg/ml). All cells were maintained in a humidified atmosphere of 5% CO_2 at 37 °C.

E. coli strains and vectors

E. coli strains, Origami B and XL-1 Blue were purchased from Novagen (Madison, WI) and Stratagene (La Jolla, CA), respectively. *E. coli* strains, TG-1 and HB2151 were kindly provided by Dr. A.D. Griffiths, MRC, Cambridge, UK. The pComb3HSS, pComb3X, modified pAdTrack and pAdEasy vectors were generous gifts from Dr. C.F. Barbas, The Scripps Research Institute, La Jolla, CA. The pAK400cb vector was a kind gift from Dr. V. Santala (University of Turku, Finland).

Preparation of soluble scFv-M6-1B9

Soluble scFv-M6-1B9 was produced by expressing pComb3X-scFv-M6-1B9 phagemid in the non-suppressor *E. coli* strain HB2151 as previously reported (Tragoolpua et al., 2008). Briefly, transformed bacteria were grown in SB broth containing ampicillin at 37 °C for 18 h. The precultured bacteria were then transferred and cultivated at the same temperature and medium until the OD_{600} reached 1.5. Then, the transformed *E. coli* were grown at 25 °C for 20 h with isopropyl-β-D-thiogalactopyranoside (IPTG) stimulation. After induction, cells were pelleted and the supernatant containing extracellular soluble scFv was collected. Proteins in the supernatant were precipitated with saturated $(NH_4)_2SO_4$ in an ice bath and concentrated with Amicon Ultra centrifugal filter units (Millipore, Cork, Ireland). Finally, the antigen-binding affinity of soluble scFv-M6-1B9 was evaluated by ELISA, Western immunoblotting and flow cytometric analysis as described previously (Tragoolpua et al., 2008).

Cell proliferation assay

Cell proliferation was assessed using 5-carboxyfluorescein diacetate succinimidyl ester (CFSE) labeling. PBMCs were washed with PBS for 3 times and adjusted into 1×10^7 PBMCs/ml with PBS. CSFE (Molecular Probes, Eugene, OR) in the form of 5 mM stock solution in DMSO was added at final concentration of 0.5 μM for 10 min at 37 °C. To determine the effect of soluble scFv M6-1B9 on T-cell proliferation, triplicate aliquots of 1×10^5 PBMCs were cultured with immobilized CD3 mAb OKT3 (20 ng/ml) in the presence or absence of CD147 mAb clone M6-1B9 or soluble scFv M6-1B9. The culture was incubated for 5 days in a 5% CO_2 incubator at 37 °C. Cells from each treatment group were then washed twice with PBS, fixed with 1% formaldehyde in PBS and analyzed by a FACSCalibur flow cytometer (Becton Dickinson, Sunnyvale, CA).

The generation of adenovirus expressing scFv-M6-1B9 (Ad-scFv-M6-1B9)

Adenovirus expression of scFv-M6-1B9 carrying GFP gene was generated, propagated and purified as described elsewhere (Carlson et al., 2002; Tragoolpua et al., 2008). Titers were determined by plaque titration in 293 cells (Carlson et al., 2002) and the contamination level of wild-type (wt) virus was examined by real-time PCR (Bernt et al., 2002).

Immunoblot analysis

The 293A cells were transduced at an MOI of 10 pfu/cell of Ad-scFv-M6-1B9 and harvested after 48 h. Transduced cells were fractionated using Fraction-PREP™ Cell Fractionation System (BioVision, Mountain View, CA) according to the manufacturer's instructions. The lysate fractions were separated on a 12% SDS-PAGE gel under reducing conditions and then transferred onto a polyvinylidene-fluoride (PVDF) membrane. The membranes were blocked with 5% skimmed milk in PBS and traced by peroxidase-conjugated mAb anti-HA (Roche, Indianapolis, IN). The peroxidase reaction was visualized using an enhanced chemiluminescent substrate detection system (GE Healthcare, Buckinghamshire, UK).

To determine the binding activity of scFv-M6-1B9, biotin carboxyl carrier protein (BCCP) fusion proteins were separated on 12% SDS-PAGE, electroblotted onto PVDF membrane, probed with soluble lysate of 293A cells expressing scFv-M6-1B9 and traced by peroxidase-conjugated mAb anti-HA. The immunoreactive bands were visualized using an enhanced chemiluminescent substrate detection system.

Immunofluorescence analysis of the reactivity of scFv-M6-1B9

HeLa cells were detached from culture plate by treatment with 1 mM EDTA and washed 3 times with PBS. Cells were adjusted to 1×10^7 cells/ml with 1% BSA-PBS-NaN_3 and blocked with human AB serum at the ratio of 1:10 for 30 min on ice. Fifty microlitres of cell lysate from 293A cells expressing scFv-M6-1B9 was added into 50 μl of blocked cells and incubated on ice for 30 min. Cells were washed twice with 1% BSA-PBS-NaN_3. Subsequently, 50 μl of 20 μg/ml rat anti-HA-biotin (Sigma, St. Louis, MO) was added and incubated on ice for 30 min. After washing, FITC-conjugated rabbit anti-rat immunoglobulins antibody (Chemicon International, Melbourne, Australia) was added and

incubated on ice for another 30 min. Finally, cells were washed 3 times and fixed with 1% paraformaldehyde-PBS. Fluorescence reactivity of soluble scFv-M6-1B9 with CD147 on HeLa cell surface was analyzed by flow cytometry.

Confocal analysis

The 1×10^4 HeLa cells were plated on eight-well Tissue-Tek chamber slides (Nalge Nunc International, Rochester, NY), and transduced with Ad-scFv-M6-1B9 for 48 h at 37 °C. Cells were washed, fixed in 4% formaldehyde in PBS containing 50 mM $MgCl_2$ and permeabilized with 0.1% Triton X-100. Slides were then washed in PBS containing 50 mM $MgCl_2$ and blocked with 2% skim milk in PBS containing 50 mM $MgCl_2$ at RT for 30 min. Then, the fixed cells were incubated with rabbit anti-HA antibody (Abcam, Cambridge, MA) at 37 °C for 1 h. After washing, cells were then incubated with Alexa Fluor 568-goat anti-rabbit IgG (Molecular Probes, Eugene, OR). The cellular nuclei were counter-stained by DAPI. Images were acquired using FLUO-VIEW laser scanning confocal microscope (Olympus, FV1000; Olympus Optical, Japan).

Flow cytometric analysis for CD147 cell surface expression on transduced HeLa cells

Five hundred microlitres of 1.2×10^5 cells/ml HeLa were transduced with adenovirus encoding scFv-M6-1B9 intrabody. After 36 h, HeLa cells were removed from 24-well tissue culture plates and washed 3 times with PBS. Cells were then blocked with human AB serum for 30 min on ice. Fifty microlitres of 20 μg/ml purified mAb M6-1B9 were added to 50 μl of blocked cells and incubated on ice for 30 min. After washing, PE-conjugated $F(ab')_2$ fragment of sheep anti-mouse immunoglobulins antibody (BD Pharmingen, San Jose, CA) were added and incubated on ice for 30 min. Finally, cells were washed 3 times and fluorescence reactivity of the stained cells was assayed by flow cytometry.

Gelatin zymography

To analyze gelatinase activity in the culture supernatant from CD147-knockdown HeLa cells, gelatin zymography was performed. The 4×10^5 HeLa cells were cultured in medium supplemented with 10% FBS. After 48 h incubation, cells were washed twice with medium containing no FBS and transduced with Ad-scFv-M6-1B9 for 24 h at 37 °C. Adenovirus carrying green fluorescent protein (Ad-GFP) was used as a negative control. Cells were then washed twice with medium containing no FBS and followed by cell cultivation in serum-free medium (Gibco). After 48 h, the supernatant was collected and centrifuged at 11,600 g for 10 min at 4 °C. The serum free conditioned medium was mixed with the loading buffer which did not contain reducing agents (0.0625 M Tris-HCl, 2% SDS, 10% glycerol, 0.01% Bromophenol blue, pH 6.8) and then separated by SDS-PAGE containing 1 mg/ml gelatin type B (Sigma) in the resolving gel. After protein electrophoresis, gel was analyzed for MMP activity using the modified method (Gogly et al., 1998). Briefly, gel was rocked twice in washing solution (50 mM Tris-HCl, 5 mM $CaCl_2$, 2.5% Triton X-100, pH 7.4) for 30 min at 37 °C. Gel was then incubated in a digestion buffer (50 mM Tris, 10 mM $CaCl_2$, 150 mM NaCl, 0.02% NaN_3, pH 7.4) with gentle rocking at 37 °C for 16 h. For analysis, the gel was visualized with 0.2% Coomassie Brilliant Blue. The zones of gelatinase activity were shown by negative staining (clear zone).

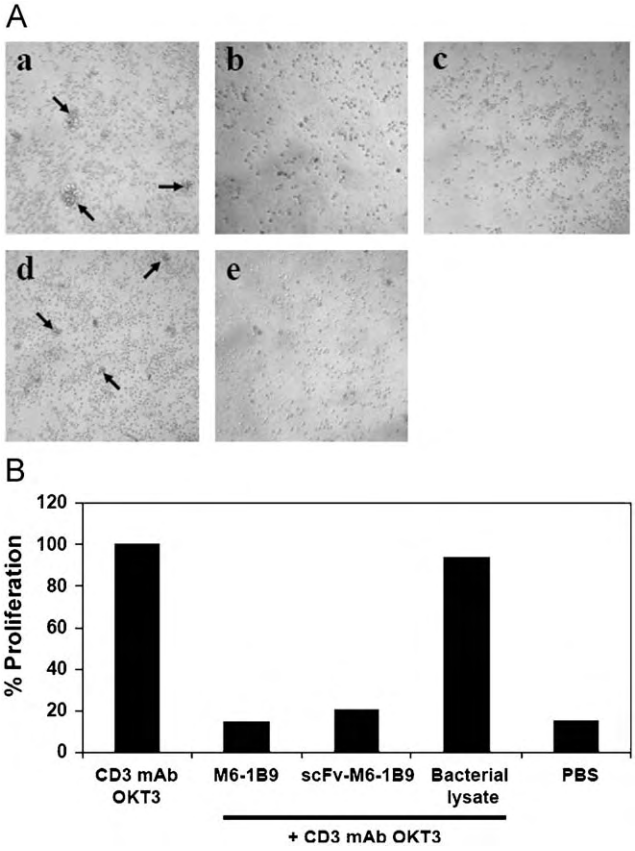

Fig. 1. Soluble scFv-M6-1B9 inhibited CD3 mAb induced cell proliferation. (A) Photomicrography (100 ×) of colony formation of PBMC induced by CD3 mAb OKT3. Cells were stimulated with 20 ng/ml of immobilized CD3 mAb OKT3 in the presence or absence of CD147 mAb M6-1B9, scFv-M6-1B9 or bacterial protein lysate and observed under an inverted microscope. CD3 mAb OKT3 only (a), CD3 mAb OKT3 plus M6-1B9 (20 μg/ml) (b), scFv-M6-1B9 (1:40) (c), bacterial protein lysate (1:40) (d) or PBS alone (e). Cell clustering is indicated by arrow. (B) Cell proliferation was determined by the measurement of CSFE incorporation using flow cytometry.

Results

Soluble scFv-M6-1B9 inhibited CD3 mAb induced cell proliferation

The production of soluble scFv-M6-1B9 from *E. coli* HB2151 was accomplished previously (Tragoolpua et al., 2008). However, the biological functions of soluble scFv-M6-1B9 have yet to be investigated. In the present study, we assayed the effect scFv-M6-1B9 on cell proliferation. PBMCs isolated from healthy donors were activated by immobilized CD3 mAb OKT3 in the presence or absence of CD147 mAb clone M6-1B9 or soluble scFv-M6-1B9. The results showed that soluble scFv-M6-1B9 inhibited colony formation (Fig. 1A) and proliferation (Fig. 1B) of PBMCs induced by CD3 mAb OKT3 as well as its original antibody (Chiampanichayakul et al., 2006). In contrast, mock bacterial protein lysate controls had no inhibitory effect on OKT3-mediated cell proliferation. These results indicate that the monomeric form of CD147 mAb could engage the CD147 molecule and induce negative regulation of OKT3-induced T cell proliferation. In addition, the results indicate that the produced soluble scFc-M6-1B9 is a biologically active protein.

Detection and characterization of scFv-M6-1B9 intrabody produced in 293A cells

To further investigate the intracellular expression of scFv, 293A cells were transduced with recombinant Ad-scFv-M6-1B9 and harvested after 48 h. The lysate fractions of transduced cells were separated on 12% SDS-PAGE and electroblotted onto a PVDF membrane. The presence of scFv-M6-1B9 intrabody in the fractionated cell lysate was detected by Western immunoblotting with an HA tag. The reactive band revealed by anti-HA was located in the ER fraction (~35 kDa) and not found in the nuclear and cytoplasmic fractions (Fig. 2A). This result indicates that an intrabody with a carboxyl-terminal ER retention signal (KDEL) was retained in the ER compartment.

Subsequently, the specificity of scFv-M6-1B9 intrabody in cell lysate was analyzed by immunoblotting using CD147-BCCP as antigen (Tayapiwatana et al., 2006). A specific band of CD147-BCCP at ~35 kDa was

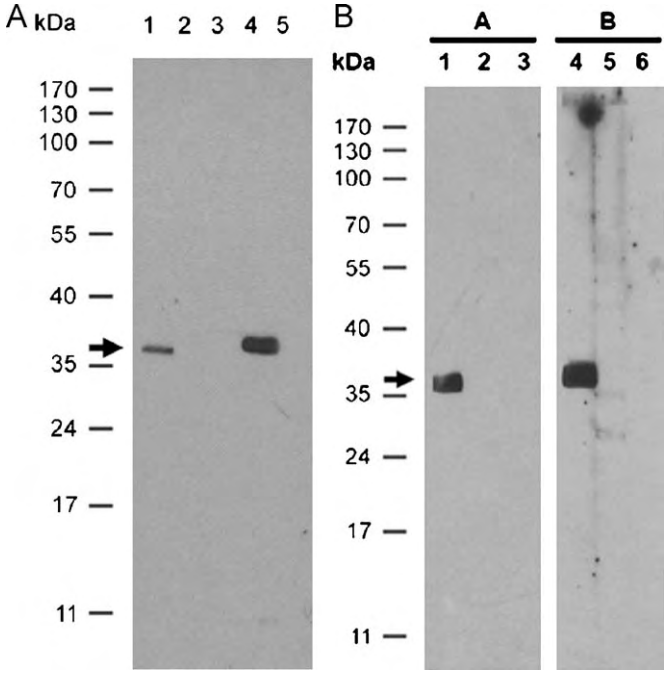

Fig. 2. Detection of scFv-M6-1B9 intrabody activity by Western blotting. (A) 293A cells were transduced with recombinant adenovirus harboring scFv-M6-1B9. Cells were lysated and separated on 12% SDS-PAGE, electroblotted onto a PVDF membrane. The produced scFv intrabody was detected using peroxidase-conjugated mAb anti-HA. The positions of molecular mass markers are shown on the left. Soluble scFv-M6-1B9 produced by expressing pComb3X-scFv-M6-1B9 phagemid in the non-suppressor *E. coli* strain HB2151 was used as positive control (lane 1) (Tragoolpua et al., 2008). Transduced 293A cell lysate obtained from nuclear fraction (lane 2), cytoplasmic fraction (lane 3), ER fraction (lane 4) and untransduced cells (lane 5) were indicated. (B) CD147-BCCP (lane 1, 4), SVV-BCCP (lane 2, 5) and bacterial lysate proteins (lane 3, 6) were separated on 12% SDS-PAGE, electroblotted onto a PVDF membrane, and then probed with M6-1B9 antibody (panel A) and soluble scFv-M6-1B9 intrabody (panel B). The M6-1B9 or scFv obtained from Ad-scFv-M6-1B9 transduced 293A cells was detected using peroxidase-conjugated goat-anti-mouse immunoglobulins or peroxidase-conjugated mAb anti-HA, respectively. Molecular mass markers are indicated on the left.

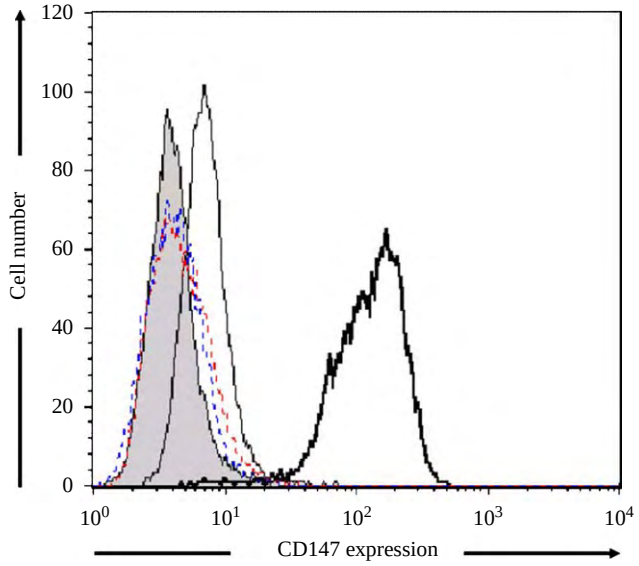

Fig. 3. The scFv-M6-1B9 intrabody is specific to CD147 on HeLa cell surface. HeLa cell surface staining was performed using soluble lysate of scFv-M6-1B9 intrabody (thin line), scFv-SVV3 intrabody (red dash line), 293A lysate (blue dash line) and M6-1B9 antibody (solid line). Conjugate control was showed in solid shade. (For interpretation of the references to colour in this figure legend, the reader is referred to the web version of this article.)

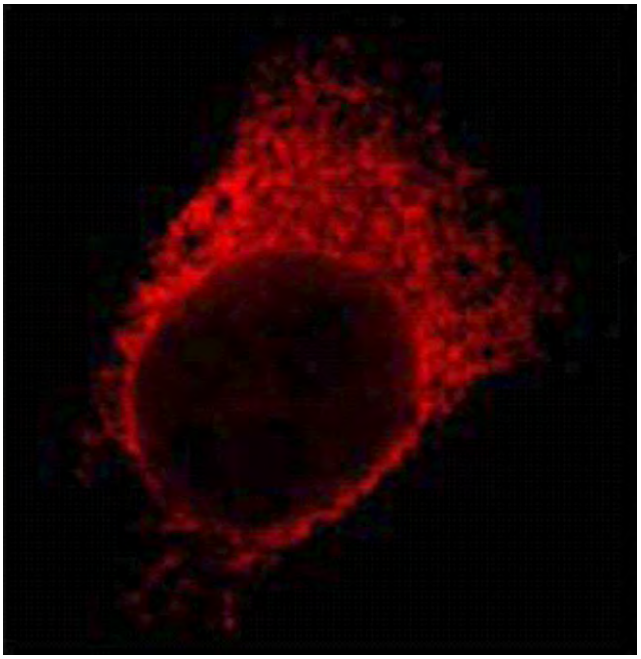

Fig. 4. Intrabody scFv-M6-1B9 staining. Transduced HeLa cells were seeded on slide chamber, fixed in 4% paraformaldehyde, permeabilized with 0.1% Triton X-100 and stained with a rabbit anti-HA antibody. Secondary detection was performed with Alexa Fluor 568 goat anti-rabbit IgG. Images were acquired using an Olympus confocal microscope.

detected by probing with soluble scFv-M6-1B9 intrabody (Fig. 2B). As control, soluble scFv-M6-1B9 produced by non-suppressor *E. coli* strain HB2151 gave also a positive signal with CD147-BCCP (Tragoolpua et al., 2008). No signal was detected in the control panel of survivin-BCCP (SVV-BCCP) antigen and bacterial lysate proteins. This result indicates that a specific and active scFv-M6-1B9 intrabody was successfully produced inside the transduced 293A cells.

Next, we determined the recognition of native CD147 on the HeLa cell surface by soluble lysate of scFv-M6-1B9 using flow cytometric analysis (Fig. 3). As predicted, the soluble scFv-M6-1B9 intrabody could react with CD147 expressed on HeLa cells, however, the signal (MFI) was lower than those obtained from the original antibody, M6-1B9. Contrarily, neither soluble lysate of scFv-SVV3 intrabody nor 293A cell lysate recognized the native CD147 on HeLa cell surface. This strongly suggests that the generated soluble lysate scFv-M6-1B9 from 293A cells carries a CD147-specific paratope which recognizes both recombinant and native CD147.

Intracellular expression of scFv-M6-1B9 intrabody diminished cell surface expression of CD147 on HeLa cells

To generate the CD147 knockdown HeLa cells, recombinant Ad-scFv-M6-1B9 were transduced into HeLa cells. The expression of scFv-M6-1B9 intrabody in HeLa cells was analyzed by immunofluorescent staining. ScFv-M6-1B9 intrabody was found inside HeLa cells (Fig. 4).

To elucidate the effect of scFv intrabody on the cell surface expression of CD147, HeLa cells were transduced with Ad-scFv-M6-1B9 and Ad-scFv-SVV3 at 200 pfu/cell and analyzed for the surface expression of CD147 at 36 h after transduction. The expression of GFP in transduced HeLa cells was demonstrated in Fig. 5A. Nearly 100% of HeLa cells were transduced with Ad-scFv-M6-1B9 and Ad-scFv-SVV3 at MOI of 200. This result indicates that both Ads had essentially identical and high infectivity for HeLa cells. Alteration of surface expression of CD147 in transduced HeLa cells was examined at 36 h after transduction. CD147 cell surface expression was decreased in scFv-M6-1B9 adenovirus-transduced HeLa cells compared to untransduced cells (Fig. 5B). Interestingly, no alteration of CD147 expression was observed on scFv-SVV3 adenovirus-transduced HeLa cells. This result reveals that intracellular expression of scFv-M6-1B9 as intrabody could abate CD147 expression on cell surface of intrabody-expressing HeLa cells.

Gelatinase activities in HeLa cells transduced with Ad-scFv-M6-1B9 and Ad-GFP

To demonstrate the scFv-M6-1B9 intrabody against CD147 involved in the regulation of MMPs activity in

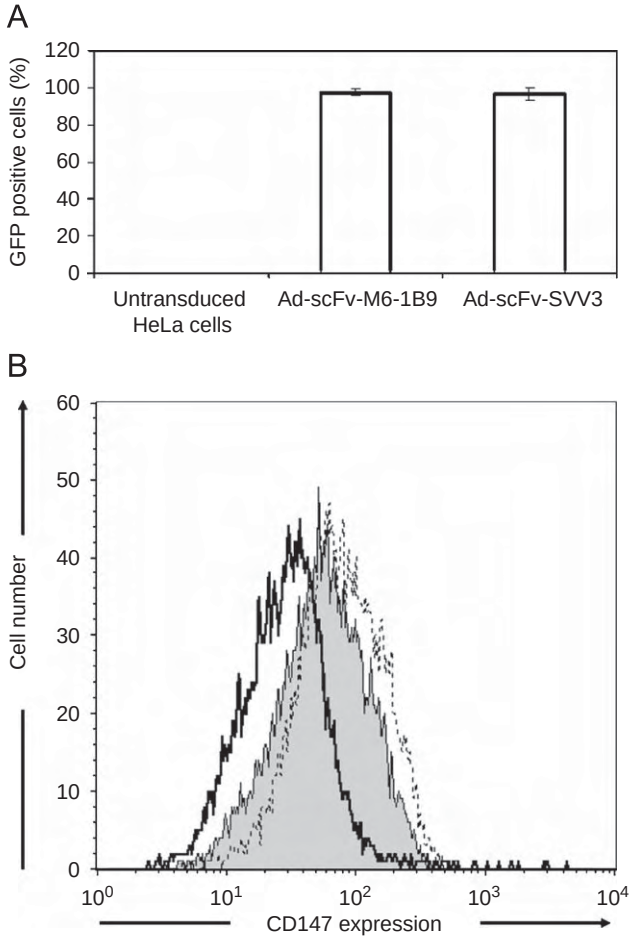

Fig. 5. Inhibition of CD147 surface expression on HeLa cells by M6-1B9 intrabody. (A) HeLa cells were transduced with Ad-scFv-M6-1B9 or Ad-scFv-SVV3 at an MOI of 200 pfu/cell. After 36 h, the percentage of GFP-positive cells was determined by flow cytometry. Data represents the average percentage of GFP-expressing cells ± standard error mean (s.e.m.) of three experiments. (B) Transduced HeLa cells with 200 pfu/cell of Ad-scFv-M6-1B9 or Ad-scFv-SVV3 were stained with mouse anti-CD147 mAb (M6-1B9). PE-conjugated F(ab′)2 fragment of sheep anti-mouse immunoglobulins antibody were used as a secondary antibody. The fluorescence intensity of CD147 cell surface expression on untransduced HeLa cells (solid shade), transduced cells with Ad-scFv-M6-1B9 (bold line) or Ad-scFv-SVV3 (dash line) is shown. The *y* axis represents the number of events on a linear scale; the *x* axis shows the fluorescence intensity on a logarithmic scale.

HeLa cells. HeLa cells were transduced with Ad-scFv-M6-1B9 and Ad-GFP at 50 and 100 pfu/cell and the supernatants were analyzed by gelatin zymography. The results reveal no differences in gelatinase activity between the supernatants from HeLa cells harboring CD147 intrabody and transduction control (Fig. 6).

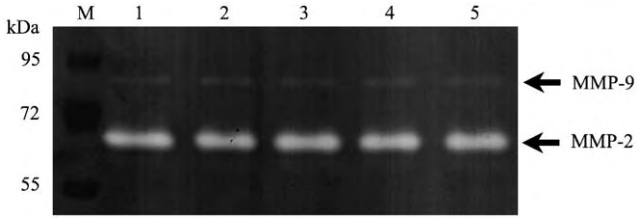

Fig. 6. MMP activities in HeLa cells harboring CD147 intrabody. Culture supernatants were collected from HeLa cells grown in serum free medium (lane 1), transduced with 50 MOI (lane 2) and 100 MOI (lane 3) of Ad-scFv-M6-1B9 or treated with same MOI of Ad-GFP (lanes 4 and 5, respectively). An equal volume of supernatants were analyzed by gelatin zymography. Upper and lower-clear bands correspond to gelatinolytic activity of MMP-2 and MMP-9, respectively.

Discussion

CD147 is a member of the Ig superfamily that plays an essential role in normal tissues and several malignant tumor cells (Suzuki et al., 2004; Riethdorf et al., 2006). Moreover, it is particularly enriched on the surface of activated T-lymphocytes (Kasinrerk et al., 1992; Koch et al., 1999). In our previous study using intact antibody molecule, anti-CD147 mAbs (M6-1B9 and M6-1E9) inhibited OKT3-induced T cell proliferation (Chiampanichayakul et al., 2006). It was suggested that these mAbs inhibited cell proliferation by delivery of a negative signal through CD147 to suppress CD25 and IL-2 expression (Chiampanichayakul et al., 2006). Interestingly, soluble scFv-M6-1B9, which contains only one binding site, had the inhibitory effect as observed in the parental mAb (Fig. 1B). These results indicate that the monomeric scFv form of M6-1B9 is a biologically active protein that is able to activate CD147 and regulate T cell activation. The results in our present study also confirm the successful production of a recombinant scFv-M6-1B9 retaining a CD147-specific paratope that binds to its epitope. We feel that this result corresponds with the anti-CD3 scFv-B7.1 fusion protein expressed on the surface of HeLa cells binding to T lymphocytes and strongly inducing T-cell activation (Yang et al., 2007b). Furthermore, many reports have described the same binding specificity and affinity of scFv as the monomeric form of their parental antibody (Bedzyk et al., 1990; Pantoliano et al., 1991; Kim et al., 2002). Our results indicate that in the absence of cross-linking and covalent dimerization of parental CD147 mAb, the monomeric form of anti-CD147 molecules can mediate signal transduction and exhibit biological activity in T cells through their antigen-specific domain. The reasoning behind our scFv format was to preserve the genetic source of the antibody fragment by cloning it into a phagemid vector and utilizing relatively simple production in bacteria. Furthermore, the small molecular size of scFv should provide high tissue penetration efficiency (Kioi et al., 2008; Liu et al., 2008; Stirnemann et al., 2008), and a

lack of significant toxicity (Korn et al., 2004; Yang et al., 2007a; Nam et al., 2008) while giving rapid plasma clearance (Mao et al., 1999; Hamilton et al., 2002; Olafsen et al., 2004; Pavoni et al., 2006), which makes such an antibody a potentially suitable candidate for clinical application.

To assess whether scFv-M6-1B9 generated by mammalian cells possesses the same activity as scFv-M6-1B9 generated by bacterial cells, we evaluated the binding ability of scFv-M6-1B9 intrabody produced from 293A cells to CD147. This intrabody was specifically targeted to both recombinant CD147 (non-glycosylated form, Fig. 2B) and native CD147 expressed on the surface of HeLa cells (Fig. 3). The soluble scFv-M6-1B9 has been produced from the *E. coli* HB2151 strain in our laboratory (Tragoolpua et al., 2008). In the present study, we demonstrated that soluble antibody fragment produced from bacteria and mammalian cells has correct folding and can recognize both native and recombinant of CD147 molecule. In addition, the expression of scFv-M6-1B9 intrabody was found in the ER fractionated cell lysate (Fig. 2A). This indicates that an intrabody with a carboxyl-terminal ER retention signal (KDEL) was retained in the membrane of the ER compartment.

Because non-viral strategies demonstrate low transduction efficiency and transient transgene expression, viral transfer methods seem to have a greater potential for a successful gene transfer (Yamaoka et al., 2005; Doebis et al., 2006; Boldicke, 2007). Intrabody expression in HeLa cells using the adenoviral system was achieved in this study and resulted in decreasing of CD147 cell surface expression on these transduced cells (Fig. 5B). Since intrabody was successfully captured in the lumen of the ER by KDEL ER-retention signal sequence, it is possible that the intrabody binds to CD147 and retains these molecules in the membrane of the ER compartment and subsequently diminishes CD147 expression on the cell surface. In other studies, targeting of intrabodies to the ER has been successfully applied to knockdown major histocompatibility complex I (MHC-I) expression (Mhashilkar et al., 2002; Beyer et al., 2004; Zdoroveac et al., 2008) and inactivate various neoplastic cell-surface receptors (Wheeler et al., 2003; Jendreyko et al., 2005; Peng et al., 2007). Additionally, the same strategy was used to block cell surface expression of the CCR5 receptor which is important for cell entry of HIV-1 (Steinberger et al., 2000). Thus the KDEL may be essential for the single-chain antibody protein to abate the expression of cell surface molecules.

Overexpression of CD147 promotes invasion, metastasis, growth and survival of malignant cells (Yan et al., 2005). In previous studies CD147 has been successfully downregulated by RNA interference (RNAi) technology in several cell lines, including; prostate cancer (Wang et al., 2006), human malignant melanoma A375 (Chen et al., 2006), human ovarian cancer cell line HO-8910pm (Zou et al., 2007) and human Jurkat T-lymphoma (Chen et al., 2008). Knockdown of CD147 by siRNA resulted in decreased tumor cell proliferation and invasion activity *in vitro*. In addition, CD147 siRNA also downregulated the expression of VEGF at mRNA and protein levels in A375 cells (Chen et al., 2006). The urokinase-type plasminogen activator (uPA) system including uPA, its specific receptor uPAR and its primary inhibitor plasminogen activator inhibitor-1 (PAI-1) was also downregulated at the mRNA and protein levels in human breast epithelial cell line, NS2T2A. In human breast epithelial cell lines, MDA-MB 231 and Malme-3 M, uPA was downregulated at the mRNA and protein levels (Quemener et al., 2007) and MCT4 was downregulated at the protein level only in MDA-MB-231 human breast cancer cells (Gallagher et al., 2007). Because of their high affinity, high specificity and stability, intrabodies present an attractive alternative to modulate protein function and many protocols utilizing intracellular antibodies to neutralize the function of target proteins have been developed for cancer research. We feel that downregulating CD147 on cancer cells using intrabody technology is available strategy for studying the role of CD147 in tumor invasion and metastasis. And furthermore, this methodology could prove to be a promising approach for cancer therapy.

The biological effect of scFv-M6-1B9 on the MMP expression in HeLa cells was analyzed by gelatin zymography. There was no difference in MMPs expression between HeLa cells carrying scFv-M6-1B9 intrabody and HeLa cells transduced with Ad-GFP (Fig. 6). This result is concordant with the finding of Schreiner, 2007 (Schreiner et al., 2007). MMP activities in the supernatant of HeLa expressing CD147 siRNA revealed no difference between CD147-knockdown and control cells. Nevertheless, the interaction between CD147 and MMPs has been reported in other cell types (Biswas et al., 1995; Bordador et al., 2000; Kanekura et al., 2002). The expression of CD147 was enhanced in various human carcinomas and was relevant in tumor progression and invasion by inducing the production of MMPs (Biswas et al., 1995; Tang et al., 2005). Furthermore, some tumor antigens such as CML66 also involved in proliferation, migration and invasion activities of HeLa cells *in vitro* (Wang et al., 2008). In addition, tissue inhibitors of metalloproteinase 3 (TIMP-3) could inhibit all MMP activities, especially MMP-2 and MMP-9 (Yu and Woessner, 2000; Hidalgo and Eckhardt, 2001). Thus, our data implied that CD147 is not sufficient to influence the MMP activities in HeLa cells.

Our present study demonstrated the advantages of recombinant antibody technology and provided an

alternative strategy to engineer low-cost antibodies with desirable affinity and specificity by enabling one to manipulate the basic domain structure of the immunoglobulin molecule. We have shown that soluble scFv-M6-1B9 binds to CD147 resulting in an inhibition of OKT3-mediated T cell proliferation. Furthermore, the scFv-M6-1B9 intrabody produced in this study was able to suppress the expression of CD147 on HeLa cells. This novel finding could prove to be a promising strategy for the functional study of CD147 and provide ways to treat cancer in the future.

Acknowledgments

The authors are grateful to Dr. Andrew D. Griffiths for the generous gift of *E. coli* strains, TG-1 and HB2151, and Dr. Ville Santala for pAK400cb vector. We also gratefully acknowledge Dr. Carlos F. Barbas III for providing pComb3HSS, pComb3X, modified pAdTrack, pAdEasy vectors. We thank Dr. Wattana Weerachatyanukul, Department of Anatomy, Faculty of Science, Mahidol University, for manipulating confocal scanning microscope and imaging analysis. We are thankful to Somphot Saoin, Wutigri Nimlamool, Supansa Pata and Narin Konkum for their technical assistances. The authors would like to thank Brian W. Biegler for proofreading the manuscript. This work was supported by the BioMedical Engineering Center research grant, Chiang Mai University, the scholarship from the Commission on Higher Education, the Thailand Research Fund and the National Center for Genetic Engineering and Biotechnology (BIOTEC), Thailand.

References

Alvarez, R.D., Barnes, M.N., Gomez-Navarro, J., Wang, M., Strong, T.V., Arafat, W., Arani, R.B., Johnson, M.R., Roberts, B.L., Siegal, G.P., Curiel, D.T., 2000. A cancer gene therapy approach utilizing an anti-erbB-2 single-chain antibody-encoding adenovirus (AD21): a phase I trial. Clin. Cancer Res. 6, 3081–3087.

Bedzyk, W.D., Weidner, K.M., Denzin, L.K., Johnson, L.S., Hardman, K.D., Pantoliano, M.W., Asel, E.D., Voss Jr., E.W., 1990. Immunological and structural characterization of a high affinity anti-fluorescein single-chain antibody. J. Biol. Chem. 265, 18615–18620.

Bernt, K., Liang, M., Ye, X., Ni, S., Li, Z.Y., Ye, S.L., Hu, F., Lieber, A., 2002. A new type of adenovirus vector that utilizes homologous recombination to achieve tumor-specific replication. J. Virol. 76, 10994–11002.

Beyer, F., Doebis, C., Busch, A., Ritter, T., Mhashilkar, A., Marasco, W.M., Laube, H., Volk, H.D., Seifert, M., 2004. Decline of surface MHC I by adenoviral gene transfer of anti-MHC I intrabodies in human endothelial cells – new perspectives for the generation of universal donor cells for tissue transplantation. J. Gene Med. 6, 616–623.

Biswas, C., Zhang, Y., DeCastro, R., Guo, H., Nakamura, T., Kataoka, H., Nabeshima, K., 1995. The human tumor cell-derived collagenase stimulatory factor (renamed EMMPRIN) is a member of the immunoglobulin superfamily. Cancer Res. 55, 434–439.

Boehm, M.K., Corper, A.L., Wan, T., Sohi, M.K., Sutton, B.J., Thornton, J.D., Keep, P.A., Chester, K.A., Begent, R.H., Perkins, S.J., 2000. Crystal structure of the anti-(carcinoembryonic antigen) single-chain Fv antibody MFE-23 and a model for antigen binding based on intermolecular contacts. Biochem. J. 346 (Pt 2), 519–528.

Boldicke, T., 2007. Blocking translocation of cell surface molecules from the ER to the cell surface by intracellular antibodies targeted to the ER. J. Cell. Mol. Med. 11, 54–70.

Boldicke, T., Weber, H., Mueller, P.P., Barleon, B., Bernal, M., 2005. Novel highly efficient intrabody mediates complete inhibition of cell surface expression of the human vascular endothelial growth factor receptor-2 (VEGFR-2/KDR). J. Immunol. Methods 300, 146–159.

Bordador, L.C., Li, X., Toole, B., Chen, B., Regezi, J., Zardi, L., Hu, Y., Ramos, D.M., 2000. Expression of emmprin by oral squamous cell carcinoma. Int. J. Cancer 85, 347–352.

Carlson, C.A., Steinwaerder, D.S., Stecher, H., Shayakhmetov, D.M., Lieber, A., 2002. Rearrangements in adenoviral genomes mediated by inverted repeats. Methods Enzymol. 346, 277–292.

Chen, X., Lin, J., Kanekura, T., Su, J., Lin, W., Xie, H., Wu, Y., Li, J., Chen, M., Chang, J., 2006. A small interfering CD147-targeting RNA inhibited the proliferation, invasiveness, and metastatic activity of malignant melanoma. Cancer Res. 66, 11323–11330.

Chen, X., Su, J., Chang, J., Kanekura, T., Li, J., Kuang, Y.H., Peng, S., Yang, F., Lu, H., Zhang, J.L., 2008. Inhibition of CD147 gene expression via RNA interference reduces tumor cell proliferation, activation, adhesion, and migration activity in the human Jurkat T-lymphoma cell line. Cancer Invest. 1.

Chiampanichayakul, S., Peng-In, P., Khunkaewla, P., Stockinger, H., Kasinrerk, W., 2006. CD147 contains different bioactive epitopes involving the regulation of cell adhesion and lymphocyte activation. Immunobiology 211, 167–178.

Doebis, C., Schu, S., Ladhoff, J., Busch, A., Beyer, F., Reiser, J., Nicosia, R.F., Broesel, S., Volk, H.D., Seifert, M., 2006. An anti-major histocompatibility complex class I intrabody protects endothelial cells from an attack by immune mediators. Cardiovasc. Res. 72, 331–338.

Emadi, S., Barkhordarian, H., Wang, M.S., Schulz, P., Sierks, M.R., 2007. Isolation of a human single chain antibody fragment against oligomeric alpha-synuclein that inhibits aggregation and prevents alpha-synuclein-induced toxicity. J. Mol. Biol. 368, 1132–1144.

Gabison, E.E., Mourah, S., Steinfels, E., Yan, L., Hoang-Xuan, T., Watsky, M.A., De Wever, B., Calvo, F., Mauviel, A., Menashi, S., 2005. Differential expression of extracellular matrix metalloproteinase inducer (CD147) in normal and ulcerated corneas: role in epithelio-stromal interactions and matrix metalloproteinase induction. Am. J. Pathol. 166, 209–219.

Gallagher, S.M., Castorino, J.J., Wang, D., Philp, N.J., 2007. Monocarboxylate transporter 4 regulates maturation and trafficking of CD147 to the plasma membrane in the metastatic breast cancer cell line MDA-MB-231. Cancer Res. 67, 4182–4189.

Goenaga, A.L., Zhou, Y., Legay, C., Bougherara, H., Huang, L., Liu, B., Drummond, D.C., Kirpotin, D.B., Auclair, C., Marks, J.D., Poul, M.A., 2007. Identification and characterization of tumor antigens by using antibody phage display and intrabody strategies. Mol. Immunol. 44, 3777–3788.

Gogly, B., Groult, N., Hornebeck, W., Godeau, G., Pellat, B., 1998. Collagen zymography as a sensitive and specific technique for the determination of subpicogram levels of interstitial collagenase. Anal. Biochem. 255, 211–216.

Griffin, H., Elston, R., Jackson, D., Ansell, K., Coleman, M., Winter, G., Doorbar, J., 2006. Inhibition of papillomavirus protein function in cervical cancer cells by intrabody targeting. J. Mol. Biol. 355, 360–378.

Hamilton, S., Odili, J., Wilson, G.D., Kupsch, J.M., 2002. Reducing renal accumulation of single-chain Fv against melanoma-associated proteoglycan by coadministration of L-lysine. Melanoma Res. 12, 373–379.

Hidalgo, M., Eckhardt, S.G., 2001. Development of matrix metalloproteinase inhibitors in cancer therapy. J. Natl. Cancer Inst. 93, 178–193.

Igakura, T., Kadomatsu, K., Taguchi, O., Muramatsu, H., Kaname, T., Miyauchi, T., Yamamura, K., Arimura, K., Muramatsu, T., 1996. Roles of basigin, a member of the immunoglobulin superfamily, in behavior as to an irritating odor, lymphocyte response, and blood-brain barrier. Biochem. Biophys. Res. Commun. 224, 33–36.

Intasai, N., Mai, S., Kasinrerk, W., Tayapiwatana, C., 2006. Binding of multivalent CD147 phage induces apoptosis of U937 cells. Int. Immunol. 18, 1159–1169.

Jendreyko, N., Popkov, M., Rader, C., Barbas III, C.F., 2005. Phenotypic knockout of VEGF-R2 and Tie-2 with an intradiabody reduces tumor growth and angiogenesis in vivo. Proc. Natl. Acad. Sci. USA 102, 8293–8298.

Kanekura, T., Chen, X., Kanzaki, T., 2002. Basigin (CD147) is expressed on melanoma cells and induces tumor cell invasion by stimulating production of matrix metalloproteinases by fibroblasts. Int. J. Cancer 99, 520–528.

Kasinrerk, W., Fiebiger, E., Stefanova, I., Baumruker, T., Knapp, W., Stockinger, H., 1992. Human leukocyte activation antigen M6, a member of the Ig superfamily, is the species homologue of rat OX-47, mouse basigin, and chicken HT7 molecule. J. Immunol. 149, 847–854.

Kasinrerk, W., Tokrasinwit, N., Phunpae, P., 1999. CD147 monoclonal antibodies induce homotypic cell aggregation of monocytic cell line U937 via LFA-1/ICAM-1 pathway. Immunology 96, 184–192.

Khunkeawla, P., Moonsom, S., Staffler, G., Kongtawelert, P., Kasinrerk, W., 2001. Engagement of CD147 molecule-induced cell aggregation through the activation of protein kinases and reorganization of the cytoskeleton. Immunobiology 203, 659–669.

Kim, D.J., Chung, J.H., Ryu, Y.S., Rhim, J.H., Kim, C.W., Suh, Y., Chung, H.K., 2002. Production and characterisation of a recombinant scFv reactive with human gastrointestinal carcinomas. Br. J. Cancer 87, 405–413.

Kioi, M., Seetharam, S., Puri, R.K., 2008. Targeting IL-13Ralpha2-positive cancer with a novel recombinant immunotoxin composed of a single-chain antibody and mutated Pseudomonas exotoxin. Mol. Cancer Ther. 7, 1579–1587.

Koch, C., Staffler, G., Huttinger, R., Hilgert, I., Prager, E., Cerny, J., Steinlein, P., Majdic, O., Horejsi, V., Stockinger, H., 1999. T cell activation-associated epitopes of CD147 in regulation of the T cell response, and their definition by antibody affinity and antigen density. Int. Immunol. 11, 777–786.

Korn, T., Nettelbeck, D.M., Volkel, T., Muller, R., Kontermann, R.E., 2004. Recombinant bispecific antibodies for the targeting of adenoviruses to CEA-expressing tumour cells: a comparative analysis of bacterially expressed single-chain diabody and tandem scFv. J. Gene Med. 6, 642–651.

Liu, F., Lu, Q., Ye, X., Fang, C., Zhao, Y., Liang, M., Hu, F., Lieber, A., Chen, H.Z., 2008. Cancer gene therapy of adenovirus-mediated anti-4-1BB scFv in immunocompetent mice. Cancer Biol. Ther. 7, 448–453.

Liu, M.Y., Han, W., Ding, Y.L., Zhou, T.H., Tian, R.Y., Yang, S.L., Liu, H., Gong, Y., 2005. Generation and characterization of C305, a murine neutralizing scFv antibody that can inhibit BLyS binding to its receptor BCMA. Acta Biochim. Biophys. Sin (Shanghai) 37, 415–420.

Lynch, S.M., Zhou, C., Messer, A., 2008. An scFv intrabody against the nonamyloid component of alpha-synuclein reduces intracellular aggregation and toxicity. J. Mol. Biol. 377, 136–147.

Mao, S., Gao, C., Lo, C.H., Wirsching, P., Wong, C.H., Janda, K.D., 1999. Phage-display library selection of high-affinity human single-chain antibodies to tumor-associated carbohydrate antigens sialyl Lewisx and Lewisx. Proc. Natl. Acad. Sci. USA 96, 6953–6958.

Messer, A., McLear, J., 2006. The therapeutic potential of intrabodies in neurologic disorders: focus on Huntington and Parkinson diseases. BioDrugs 20, 327–333.

Mhashilkar, A.M., Doebis, C., Seifert, M., Busch, A., Zani, C., Soo Hoo, J., Nagy, M., Ritter, T., Volk, H.D., Marasco, W.A., 2002. Intrabody-mediated phenotypic knockout of major histocompatibility complex class I expression in human and monkey cell lines and in primary human keratinocytes. Gene Ther. 9, 307–319.

Nabeshima, K., Iwasaki, H., Koga, K., Hojo, H., Suzumiya, J., Kikuchi, M., 2006. Emmprin (basigin/CD147): matrix metalloproteinase modulator and multifunctional cell recognition molecule that plays a critical role in cancer progression. Pathol. Int. 56, 359–367.

Nam, C.H., Lobato, M.N., Appert, A., Drynan, L.F., Tanaka, T., Rabbitts, T.H., 2008. An antibody inhibitor of the LMO2-protein complex blocks its normal and tumorigenic functions. Oncogene 27, 4962–4968.

Olafsen, T., Tan, G.J., Cheung, C.W., Yazaki, P.J., Park, J.M., Shively, J.E., Williams, L.E., Raubitschek, A.A., Press, M.F., Wu, A.M., 2004. Characterization of engineered anti-p185HER-2 (scFv-CH3)2 antibody fragments

(minibodies) for tumor targeting. Protein Eng. Des. Sel. 17, 315–323.

Pantoliano, M.W., Bird, R.E., Johnson, S., Asel, E.D., Dodd, S.W., Wood, J.F., Hardman, K.D., 1991. Conformational stability, folding, and ligand-binding affinity of single-chain Fv immunoglobulin fragments expressed in *Escherichia coli*. Biochemistry 30, 10117–10125.

Pavoni, E., Flego, M., Dupuis, M.L., Barca, S., Petronzelli, F., Anastasi, A.M., D'Alessio, V., Pelliccia, A., Vaccaro, P., Monteriu, G., Ascione, A., De Santis, R., Felici, F., Cianfriglia, M., Minenkova, O., 2006. Selection, affinity maturation, and characterization of a human scFv antibody against CEA protein. BMC Cancer 6, 41.

Peng, J.L., Wu, S., Zhao, X.P., Wang, M., Li, W.H., Shen, X., Liu, J., Lei, P., Zhu, H.F., Shen, G.X., 2007. Down-regulation of transferrin receptor surface expression by intracellular antibody. Biochem. Biophys. Res. Commun. 354, 864–871.

Popkov, M., Jendreyko, N., McGavern, D.B., Rader, C., Barbas III, C.F., 2005. Targeting tumor angiogenesis with adenovirus-delivered anti-Tie-2 intrabody. Cancer Res. 65, 972–981.

Quemener, C., Gabison, E.E., Naimi, B., Lescaille, G., Bougatef, F., Podgorniak, M.P., Labarchede, G., Lebbe, C., Calvo, F., Menashi, S., Mourah, S., 2007. Extracellular matrix metalloproteinase inducer up-regulates the urokinase-type plasminogen activator system promoting tumor cell invasion. Cancer Res. 67, 9–15.

Reimers, N., Zafrakas, K., Assmann, V., Egen, C., Riethdorf, L., Riethdorf, S., Berger, J., Ebel, S., Janicke, F., Sauter, G., Pantel, K., 2004. Expression of extracellular matrix metalloproteases inducer on micrometastatic and primary mammary carcinoma cells. Clin. Cancer Res. 10, 3422–3428.

Riethdorf, S., Reimers, N., Assmann, V., Kornfeld, J.W., Terracciano, L., Sauter, G., Pantel, K., 2006. High incidence of EMMPRIN expression in human tumors. Int. J. Cancer 119, 1800–1810.

Schreiner, A., Ruonala, M., Jakob, V., Suthaus, J., Boles, E., Wouters, F., Starzinski-Powitz, A., 2007. Junction protein shrew-1 influences cell invasion and interacts with invasion-promoting protein CD147. Mol. Biol. Cell 18, 1272–1281.

Staffler, G., Szekeres, A., Schutz, G.J., Saemann, M.D., Prager, E., Zeyda, M., Drbal, K., Zlabinger, G.J., Stulnig, T.M., Stockinger, H., 2003. Selective inhibition of T cell activation via CD147 through novel modulation of lipid rafts. J. Immunol. 171, 1707–1714.

Steinberger, P., Andris-Widhopf, J., Buhler, B., Torbett, B.E., Barbas III, C.F., 2000. Functional deletion of the CCR5 receptor by intracellular immunization produces cells that are refractory to CCR5-dependent HIV-1 infection and cell fusion. Proc. Natl. Acad. Sci. USA 97, 805–810.

Stirnemann, K., Romero, J.F., Baldi, L., Robert, B., Cesson, V., Besra, G.S., Zauderer, M., Wurm, F., Corradin, G., Mach, J.P., Macdonald, H.R., Donda, A., 2008. Sustained activation and tumor targeting of NKT cells using a CD1d-anti-HER2-scFv fusion protein induce antitumor effects in mice. J. Clin. Invest. 118, 994–1005.

Stockinger, H., 1997. Interaction of GPI-anchored cell surface proteins and complement receptor type 3. Exp. Clin. Immunogenet. 14, 5–10.

Sun, J., Hemler, M.E., 2001. Regulation of MMP-1 and MMP-2 production through CD147/extracellular matrix metalloproteinase inducer interactions. Cancer Res. 61, 2276–2281.

Suzuki, S., Sato, M., Senoo, H., Ishikawa, K., 2004. Direct cell-cell interaction enhances pro-MMP-2 production and activation in co-culture of laryngeal cancer cells and fibroblasts: involvement of EMMPRIN and MT1-MMP. Exp. Cell Res. 293, 259–266.

Tanaka, T., Williams, R.L., Rabbitts, T.H., 2007. Tumour prevention by a single antibody domain targeting the interaction of signal transduction proteins with RAS. Embo J. 26, 3250–3259.

Tang, Y., Nakada, M.T., Kesavan, P., McCabe, F., Millar, H., Rafferty, P., Bugelski, P., Yan, L., 2005. Extracellular matrix metalloproteinase inducer stimulates tumor angiogenesis by elevating vascular endothelial cell growth factor and matrix metalloproteinases. Cancer Res. 65, 3193–3199.

Tayapiwatana, C., Chotpadiwetkul, R., Kasinrerk, W., 2006. A novel approach using streptavidin magnetic bead-sorted in vivo biotinylated survivin for monoclonal antibody production. J. Immunol. Methods 317, 1–11.

Tragoolpua, K., Intasai, N., Kasinrerk, W., Mai, S., Yuan, Y., Tayapiwatana, C., 2008. Generation of functional scFv intrabody to abate the expression of CD147 surface molecule of 293A cells. BMC Biotechnol. 8, 5.

Wang, L., Ku, X.M., Li, Y., Bian, H.J., Zhang, S.H., Ye, H., Yao, X.Y., Li, B.H., Yang, X.M., Liao, C.G., Chen, Z.N., 2006. Regulation of matrix metalloproteinase production and tumor cell invasion by four monoclonal antibodies against different epitopes of HAb18G/CD147 extracellular domain. Hybridoma (Larchmt) 25, 60–67.

Wang, Q., Li, M., Wang, Y., Zhang, Y., Jin, S., Xie, G., Liu, Z., Wang, S., Zhang, H., Shen, L., Ge, H., 2008. RNA interference targeting CML66, a novel tumor antigen, inhibits proliferation, invasion and metastasis of HeLa cells. Cancer Lett. 269, 127–138.

Wheeler, Y.Y., Kute, T.E., Willingham, M.C., Chen, S.Y., Sane, D.C., 2003. Intrabody-based strategies for inhibition of vascular endothelial growth factor receptor-2: effects on apoptosis, cell growth, and angiogenesis. Faseb J. 17, 1733–1735.

Yamaoka, T., Yonemitsu, Y., Komori, K., Baba, H., Matsumoto, T., Onohara, T., Maehara, Y., 2005. Ex vivo electroporation as a potent new strategy for nonviral gene transfer into autologous vein grafts. Am. J. Physiol. Heart Circ. Physiol. 289, H1865–H1872.

Yan, L., Zucker, S., Toole, B.P., 2005. Roles of the multifunctional glycoprotein, emmprin (basigin; CD147), in tumour progression. Thromb. Haemost. 93, 199–204.

Yang, Y., Yang, S., Ye, Z., Jaffar, J., Zhou, Y., Cutter, E., Lieber, A., Hellstrom, I., Hellstrom, K.E., 2007a. Tumor cells expressing anti-CD137 scFv induce a tumor-destructive environment. Cancer Res. 67, 2339–2344.

Yang, Z.M., Li, E.M., Lai, B.C., Wang, Y.L., Si, L.S., 2007b. Anti-CD3 scFv-B7.1 fusion protein expressed on the surface of HeLa cells provokes potent T-lymphocyte

activation and cytotoxicity. Biochem. Cell Biol. 85, 196–202.

Yu, W.H., Woessner Jr., J.F., 2000. Heparan sulfate proteoglycans as extracellular docking molecules for matrilysin (matrix metalloproteinase 7). J. Biol. Chem. 275, 4183–4191.

Zdoroveac, A., Doebis, C., Laube, H., Brosel, S., Schmitt-Knosalla, I., Volk, H.D., Seifert, M., 2008. Modulation of graft arteriosclerosis in a rat carotid transplantation model. J. Surg. Res. 145, 161–169.

Zou, W., Yang, H., Hou, X., Zhang, W., Chen, B., Xin, X., 2007. Inhibition of CD147 gene expression via RNA interference reduces tumor cell invasion, tumorigenicity and increases chemosensitivity to paclitaxel in HO-8910pm cells. Cancer Lett. 248, 211–218.

HYBRIDOMA
Volume 29, Number 1, 2010

DOI: 10.1089/hyb.2009.0096

A Competitive ELISA for Quantifying Serum CD147: Reduction of Soluble CD147 Levels in Cancer Patient Sera

Seangdeun Moonsom,[1] Chatchai Tayapiwatana,[1,2] Sopit Wongkham,[3] Prachya Kongtawelert,[4] and Watchara Kasinrerk[1,2]

CD147/EMMPRIN (extracellular matrix metalloproteinase inducer) is a cell surface glycoprotein that displays increased expression in many cancers. It has been previously demonstrated to participate in cancer metastasis and progression. In this study we used an anti-CD147 monoclonal antibody and a recombinant CD147 protein generated in our laboratory to establish a competitive ELISA for quantifying serum CD147 levels. Unexpectedly, the CD147 level was highest in sera of normal subjects and significantly reduced in sera of cancer patients. There was no significant difference in serum CD147 level between benign, non-metastatic, and metastatic stages of cancers. In regard to liver diseases, the maximal CD147 level was observed in sera of patients with hepatitis and hepatocellular carcinoma, and significantly decreased in patients with liver cirrhosis and cholangiocarcinoma. Our results imply that there may be homeostasis of CD147 levels in sera under normal physiological conditions, while such a level is altered in cancer patients.

Introduction

The molecule CD147 is a cell surface glycoprotein of the immunoglobulin superfamily. This molecule is expressed in various cell types. However, its expression is remarkably up-regulated in many cancers.[1–2] Multi-functions of the CD147 protein have been demonstrated. In the immune system, CD147 is highly expressed in immature thymocytes and is requisite for T cell maturation.[3] Induction of CD147 expression is observed in activated lymphocytes and differentiated macrophages.[4–6] Negative regulatory signaling and T cell regulation arising from cross-linking of CD147 molecules have been demonstrated as well.[7–10] Mediation of leukocyte cell adhesion by CD147 has also been demonstrated.[6,11] In many cancers, CD147 has been demonstrated to participate in tumor invasion and metastasis.[12–14] CD147 is also known as extracellular matrix metalloproteinase inducer (EMMPRIN), and has been identified as an inducer of matrix metalloproteinases (MMPs) in both tumor and stromal cells.[15–17] The induced MMPs then mediate the degradation of the extracellular matrix, thus alleviating the physical constraint to tumor cell movement *in vivo*. In addition, increase in the expression of CD147 in cancer cells is associated with epidermal growth factor receptor (EGFR) signaling and the response to transforming growth factor-β stimulation.[16]

Several studies have demonstrated that CD147 induces the production of several MMPs, including MMP1, MMP2, MMP3, MMP9, and MMP11.[18,19] Both CD147- expressing tumor cells and conditioned medium obtained from tumor cell cultures are capable of inducing MMP production.[20,21] These observations indicated that CD147 could be secreted from tumor cells in a soluble form and that it plays a significant role in tumor metastasis.[2,22] Such evidence leads to the speculation that cancer patients' serum may contain soluble CD147, and participate in tumor progression.[23,24] In this study, an ELISA procedure was established for determination of CD147 levels in sera from various cancer patients. Unexpectedly, our study demonstrated a reduction in serum CD147 levels in cancer patients, contradictory to our expectations and to previous reports of the increased cell surface expression and concentration of serum CD147 in cancer patient sera.

[1]Biomedical Technology Research Center, National Center for Genetic Engineering and Biotechnology, National Science and Technology Development Agency at the Faculty of Associated Medical Sciences, Chiang Mai University, Chiang Mai, Thailand.
[2]Division of Clinical Immunology, Department of Medical Technology, Faculty of Associated Medical Sciences, Chiang Mai University, Chiang Mai, Thailand.
[3]Department of Biochemistry, Faculty of Medicine, Khon Kaen University, Khon Kaen, Thailand.
[4]Thailand Excellence Center for Tissue Engineering, Department of Biochemistry, Faculty of Medicine, Chiang Mai University, Chiang Mai, Thailand.

Materials and Methods

Recombinant CD147 production and purification

Chinese Hamster Ovarian (CHO) cells carrying the gene encoding CD147 extracellular domain-human Fc fusion protein (CD147-Rg)[8] were kindly provided by Prof. Hannes Stockinger (Medical University of Vienna, Austria). Cells were maintained in Iscove's Modified Dulbecco's Medium (IMDM; Gibco, Grand Island, NY) supplemented with 10% fetal calf serum (FCS; Gibco), 40 mg/mL gentamycin, 5 μg/mL amphotericin B, and 10 mM methotrexate at 37°C in a 5% CO_2 incubator. To produce the recombinant CD147-Rg protein, the culture media were changed to serum-free media SM II (Gibco) containing 5 mM methotrexate without addition of FCS. Cell culture supernatant was harvested by centrifugation at 10,000 *g* at 4°C for 15 min and filtered through a 0.2 μm membrane unit (Millipore, Bedford, MA). The CD147-Rg fusion protein was then purified from cultured supernatants using a protein G column (GE Healthcare, Uppsala, Sweden). The bound protein was eluted with 0.1 M glycine-HCl (pH 2.7) and dialyzed against 50 mM PBS (pH 7.2). The purified protein was concentrated using an ultracentrifugal filter device (Amicon, Millipore). Protein concentration was determined by Bradford's method and the purity of the obtained protein was verified by SDS-polyacrylamide gel electrophoresis (SDS-PAGE).

The pAK400cb vector[25] harboring the gene encoding CD147 was constructed in our laboratory and transformed into *Escherichia coli* Origami B as described previously.[26] Bacterial lysate containing biotinylated CD147-BCCP fusion protein was prepared as described previously.[26] The transformed *E. coli* were cultured in broth containing 12.5 μg/mL tetracycline, 25 μg/mL chloramphenicol, 15 μg/mL kanamycin, and 4 mM of biotin (Sigma-Aldrich, St. Louis, MO) at 37°C until the OD_{600} reached 1.0. Protein expression was induced by 0.1 mM isopropyl-β-D-thiogalactopyranoside (IPTG) at 30°C for 18 h. Cells were harvested, cell extracts were prepared by freeze-thaw, and proteins were extracted using a B-PER II kit (Pierce, Rockford, IL). The concentration of obtained cell lysate was determined using a bicinchoninic acid protein assay (BCA) kit (Pierce).

Enzyme-linked immunosorbent assay

Indirect ELISA was employed for determination of the optimal dilution of anti-CD147 MAb. Avidin (10 μg/mL; Sigma-Aldrich) was immobilized onto a 96-well plate (Corning Inc., Corning, NY) using 0.1 M carbonate-bicarbonate (pH 9.6) at 4°C overnight. After washing four times with PBS containing 0.05% Tween-20, wells were blocked with 2% skimmed milk in PBS (pH 7.2) at 37°C for 1 h. Bacterial extracts (200 μg/mL) containing CD147-BCCP were added into the avidin-coated wells and incubated for 1 h. The plate was washed four times, and the immobilized CD147-BCCP was exposed to various concentrations of anti-CD147 MAb clone M6-1E9.[6] Afterward, horseradish peroxidase (HRP)-conjugated anti-mouse immunoglobulins (Dako, Glostrup, Sweden) was added and the plate incubated for 1 h at 37°C. TMB substrate (Zymed, Carlsbad, CA) was added, and the reaction was stopped by 1 N HCl. Optical density (OD) was measured at 450 nm using an ELISA reader (Sunrise, Männedorf, Switzerland).

To determine serum CD147 levels, a competitive ELISA was performed. CD147-BCCP was immobilized onto the avidin-coated plate as described above. Tested sera were mixed with anti-CD147 MAb M6-1E9 prior to application onto the CD147-BCCP immobilized plate. The plate was incubated at 37°C for 1 h and washed four times. HRP-conjugated anti-mouse immunoglobulin (Dako) was added and incubated for 1 h at 37°C. TMB substrate (Zymed) was added and the OD of the reaction was measured at 450 nm. The level of CD147 in tested sera was represented as percent competition using the equation $(A - B)/A \times 100\%$, where A is OD of the reaction between M6-1E9 MAb and CD147-BCCP in the absence of serum, and B is OD of the reaction between serum pre-incubated M6-1E9 MAb and CD147-BCCP.

Study subjects

All subjects recruited in this study had given their informed consent before participating and being admitted to Lampang Cancer Research Center Hospital (Lampang Province, Thailand). Blood samples were collected and sera were separated and kept at −20°C. Cancer diagnosis was based on characteristic features of histopathology. The Research Ethics Committee (Faculty of Medicine, Chiang Mai University) approved all procedures.

Statistical analysis

Differences in CD147 levels between tested sera groups were analyzed using Student's *t* test. A p value <0.05 was taken as significant.

Results

In order to establish an ELISA for determination of serum CD147 level, two types of recombinant CD147 proteins were produced and employed. The first recombinant protein was a CD147-BCCP fusion protein. Plasmid vector carrying the CD147 encoding sequence and a BCCP fusion tag was constructed and expressed *E. coli* Origami B. The biotinylated CD147 recombinant protein (CD147-BCCP) was then obtained.[26] The second recombinant protein was CD147-human IgG Fc fusion protein (CD147-Rg). CHO cells stably expressing CD147-Rg[8] were cultured with serum-free medium to produce a soluble CD147-Rg, which was then further purified using a protein G column. The produced recombinant proteins, CD147-BCCP and CD147-Rg, were then used in the development of a competitive ELISA for determination of CD147 levels in human sera.

An optimal concentration of anti-CD147 MAb was required for the competitive ELISA development. To determine the optimal concentration of anti-CD147 MAb, the CD147-BCCP was captured on an avidin-coated well by the biotin-avidin interaction. The bound CD147 was reacted with various concentrations of anti-CD147 MAb clone M6-1E9.[6] Anti-CD147 MAb M6-1E9, but not control anti-survivin MAb MT-SVV-1,[26] reacted specifically with the CD147-BCCP (Fig. 1). In controls using immobilized survivin-BCCP (SVV-BCCP), the SVV-BCCP reacted with the MT-SVV-1 MAb but not with the M6-1E9 MAb (Fig. 1). Various concentrations of M6-1E9 were then examined for the optimal concentration. We selected 2.5 ng/mL of the M6-1E9 MAb, which gave the optical density around 1, for use in the competitive ELISA (Fig. 1).

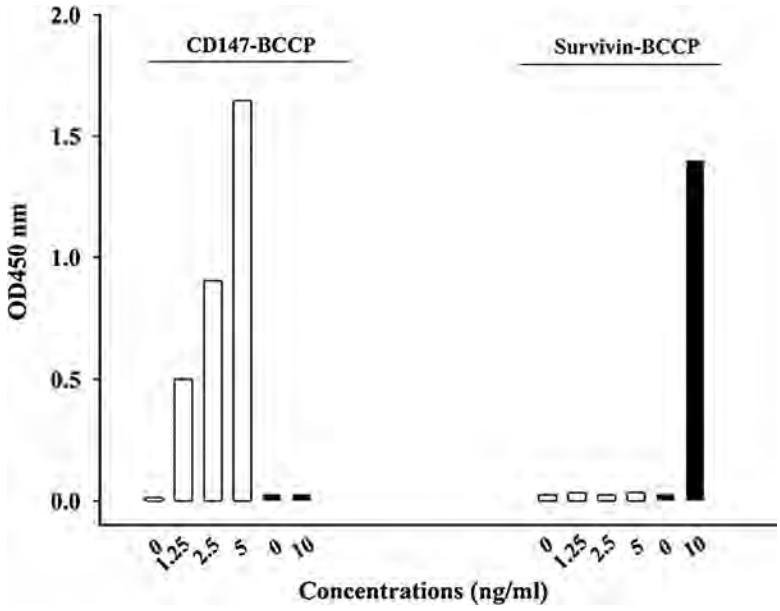

FIG. 1. Specific binding of M6-1E9 monoclonal antibody and BCCP-CD147. CD147-BCCP and survivin-BCCP recombinant proteins were immobilized in a plate by reaction with avidin. The bound proteins were reacted with various concentrations (as indicated) of anti-CD147 MAb M6-1E9 (blank) or anti-survivin MAb MT-SSV-1 (filled), followed by HRP-conjugated anti-mouse immunoglobulin antibodies.

To set up the competitive ELISA, various concentrations of CD147-Rg were preincubated with 2.5 ng/mL of M6-1E9 prior to reaction with the immobilized CD147-BCCP. As shown in Figure 2, the recombinant CD147-Rg, but not CD31-Rg, was able to inhibit M6-1E9 binding in a dose-dependent manner. According to the inhibitory curve, 78 ng/mL of the recombinant CD147-Rg inhibited 50% binding of M6-1E9 MAb to CD147-BCCP.

The established competitive ELISA was then applied for detection of CD147 in sera of normal subjects, and from various types of cancer patients and subjects with liver disorders. The observed distribution of CD147 level in tested sera, in terms of percent inhibition, is shown in Figure 3. The CD147 levels, ranging from the highest to the lowest, were observed in normal subjects ($n = 125$; mean $\pm$ SD, 34.23 ± 21.40), cancer of cervical uteri ($n = 12$; 29.58 ± 9.70), cancers of gastrointestinal

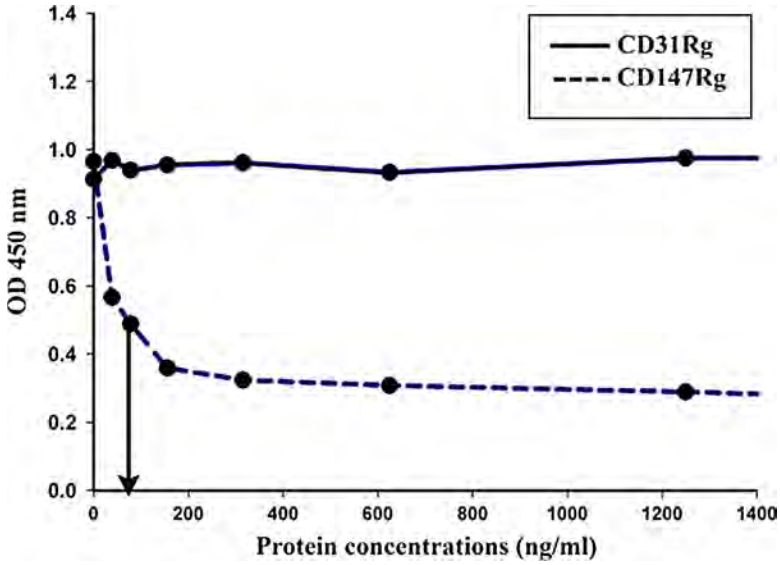

FIG. 2. Specific inhibition of the CD147-Rg protein to the reaction of M6-1E9 and CD147-BCCP. CD147-BCCP was immobilized onto a plate by reaction with avidin. M6-1E9 MAb was preincubated with various concentrations of the recombinant CD147-Rg or CD31-Rg prior to reaction with the immobilized CD147-BCCP. A bound antibody was detected by HRP-conjugated anti-mouse immunoglobulin antibodies. The OD of each reaction was transformed into percent inhibition as described in the section on Materials and Methods. The solid line represents the reaction of M6-1E9 preincubated with CD31-Rg, and the dashed line represents the reactions of M6-1E9 pre-reacted with CD147-Rg. Arrows indicate IC_{50} or the concentration of CD147-Rg that decreased binding between M6-1E9 and BCCP-CD147 to 50%.

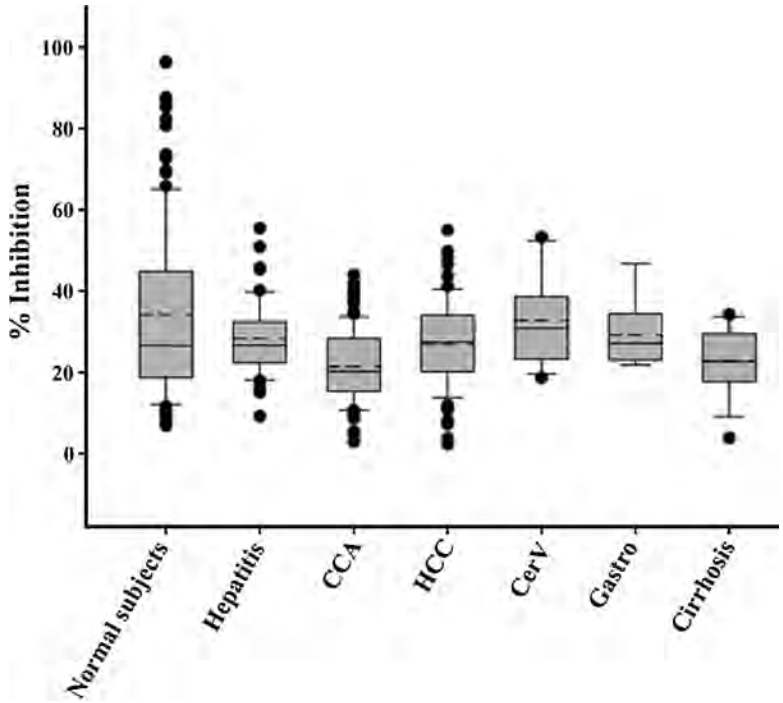

FIG. 3. Distribution of CD147 level in sera of normal, hepatitis, cirrhosis, and cancer patients. M6-1E9 MAb was preincubated with serum of normal subjects (n = 125), hepatitis (n = 51), cholangiocarcinoma (CCA; n = 128), hepatocellular carcinoma (HCC; n = 99), cancers of cervical uteri (CerV, n = 12), cancers of gastrointestinal tract (Gastro; n = 9), and cirrhosis (n = 14) prior to reaction with BCCP-CD147. Bound M6-1E9 MAb was detected by HRP-conjugated anti-mouse immunoglobulin antibodies. OD of reactions was transformed into percent inhibition. Distribution of CD147 in serum is represented by a box plot. The range of a box is the interquartile range (IQR), while upper and lower limits of the box are the 25th and 75th percentiles, respectively. T-shape lines that extend from the ends of the box represent adjacent values that are $\leq$1.5 times IQR plus the 75th percentile (the lower-adjacent value) or the 25th percentile (the upper-adjacent value). Dots represent samples that are outside the upper and lower adjacent values. A solid line is drawn in through the middle of the box at the median, while the dashed line is at the mean.

tract (n = 9; 29.10 ± 8.15), hepatitis (n = 51; 28.23 ± 8.97), hepatocellular carcinoma (HCC) (n = 99; 26.88 ± 10.62), cirrhosis (n = 14; 22.85 ± 8.27), and cholangiocarcinoma (CCA) (n = 128; 21.46 ± 8.67), respectively (Fig. 3). The CD147 level in sera of normal subjects was significantly higher than in those with non-metastatic tumors ($p < 0.01$; n = 228) comprising CCA (n = 128), HCC (n = 79), cancers of cervical uteri (n = 12), cancers of gastrointestinal tract (n = 9), and metastatic carcinoma ($p < 0.001$, n = 20) (Fig. 4A). However, the CD147 level of normal subjects was not significantly different to those of patients with benign tumors (n = 33) of bile duct (n = 18), hepatocytes (n = 3), cervical uteri (n = 8), and gastrointestinal tract (n = 4). Moreover, there was no significance in the CD147 level among sera obtained from patients with benign tumors, non-metastatic tumors, and metastatic carcinoma (n = 20) (Fig. 4A).

Within liver diseases, the level of CD147 in sera of normal subjects was not significantly different from those of hepatitis patients; however, the observed level was higher than that of patients with liver cirrhosis, HCC ($p < 0.01$), and CCA ($p < 0.001$) (Fig. 4B). The level of CD147 in sera of hepatitic patients was also higher than that of patients with cirrhosis ($p < 0.05$). Between two major types of liver cancers, the CD147 level in HCC patients was clearly increased when compared to those with CCA ($p < 0.001$) (Fig. 4B).

Discussion

Cancer metastasis requires several processes, including alterations in the cytoskeletal architecture, expression of surface adhesion molecules, and penetration of the basement membrane. All of these processes have been allied with CD147/EMMPRIN functions.[1,13,27] CD147 is found to be overexpressed in many cancers, which, together with its ability to induce MMP production, suggests that it serves as a key regulator for oncogenesis. In addition to the expression as a membrane-bound form, a soluble form of CD147 has been detected in cultured supernatants of tumor cells.[22,28] CD147 may possibly be released from tumor cells by two different pathways, shedding through the release of microvesicles or by proteolytic cleavage.[29,30] The released CD147 was demonstrated to function in stimulation of MMP activity, thus allowing tumor progression.[31,32] Several proteins such as α-fetoprotein, prostate-specific antigen, carcinoembryonic antigen, and E-selectin have been demonstrated to be released by tumor cells and detected in cancer patient sera.[33,34] Thus, several researchers speculated that tumor cells would release CD147 into serum and that it would play a significant role in the regulation of tumor invasion.[23,24,35]

In order to detect soluble CD147 in serum, as a small amount of the CD147 may be present, high specificity and

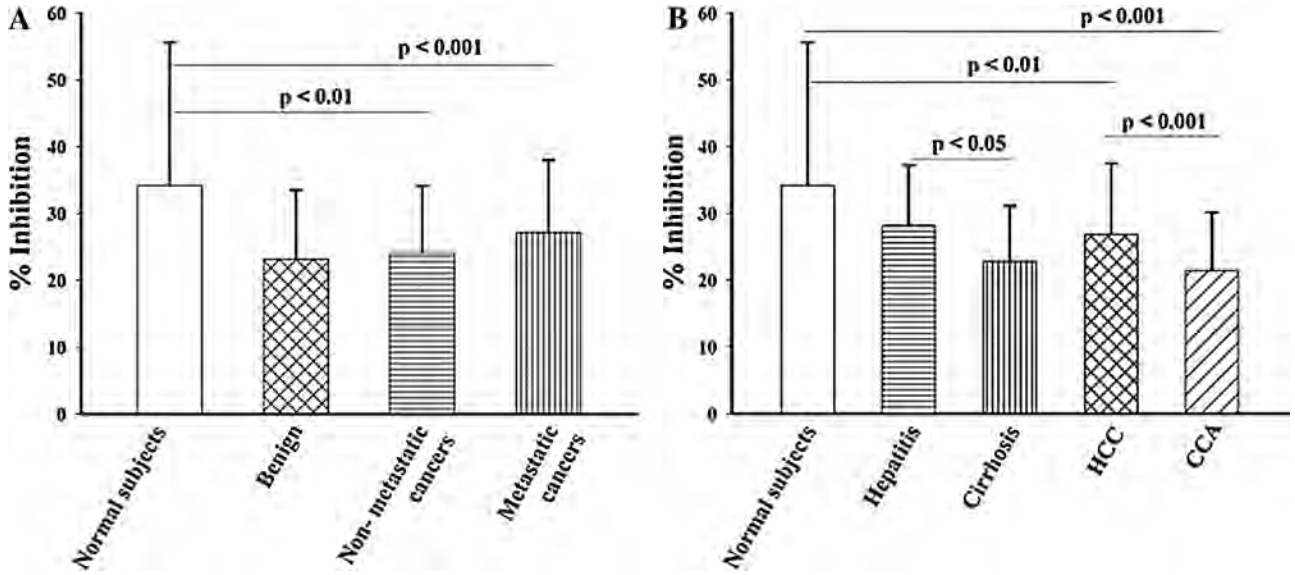

FIG. 4. Levels of CD147 in sera of normal subjects, benign, non-metastatic, and metastatic cancers, and liver disorders. (**A**) Normal subjects (n = 125), patients with benign tumors (n = 33) of bile duct (n = 18), hepatocytes (n = 3), cervical uteri (n = 8), and gastrointestinal tract (n = 4), and malignant tumors (n = 248) comprising non-metastatic CCA (n = 128), HCC (n = 79), CerV (n = 12) and Gastro (n = 9), and metastatic carcinoma (n = 20) were included in the determination. The CD147 levels in sera are represented as mean ± SD. (**B**) The CD147 level in sera of patients with cirrhosis, CCA, and HCC in comparison with that of normal subjects.

sensitivity of the detection method are desirable. In the present study, a competitive ELISA was established for determination of the CD147 level in serum. Several anti-CD147 MAbs, previously generated in our laboratory,[10] as well as two recombinant CD147 proteins, helped us to develop the competitive ELISA. A prokaryotic expression system was used to produce the first recombinant CD147-BCCP fusion protein.[26] Using this approach, the biotin carboxyl carrier protein (BCCP), a small biotinylated subunit of *E. coli* acetyl-CoA carboxylase,[36] was used as a fusion partner of CD147 extracellular domain.[37,38] The BCCP fusion tag was cloned in frame and downstream to the CD147 encoding sequence. The CD147-BCCP fusion protein was expressed in *E. coli* Origami B upon IPTG induction. Within bacterial cells, the heterologous hybrid molecules were synthesized and biotinylated at the BCCP motif.[39] The biotinylated CD147-BCCP molecules were verified by indirect ELISA using an anti-CD147 MAb M6-1E9 reacting with the membrane-distal domain of the CD147 extracellular part.[10] M6-1E9 MAb specifically reacted to the fusion protein captured on an avidin-coated plate. The reaction bridge confirmed the presence of biotinylated CD147 recombinant protein in the transformed bacterial lysate and that it was recognized by the anti-CD147 MAb M6-1E9. As the recombinant CD147 was produced as a biotinylated form, it was simple to immobilize onto the ELISA plate, via biotin-avidin interaction, by using a precoated avidin plate. Thus, the bacterial lysate containing CD147 recombinant protein could be directly applied into the competitive ELISA without any purification process. The second recombinant protein involved in this study was CD147-human IgG Fc fusion protein (CD147-Rg).[8,10] CHO cells stably secreting the CD147-Rg protein[8] were cultured in serum-free medium to allow the production of CD147 fusion protein in the culture supernatant. As the recombinant CD147 was produced in mammalian cells, its conformation is compatible to that produced by human cells. This recombinant protein, therefore, was appropriate for setting up a competitive ELISA for measurement of human CD147 protein. According to its IgG Fc part, the CD147-Rg was purified using a protein G-Sepharose column. Since CHO cells were cultured in serum-free conditions, no contamination of calf immunoglobulins in the purified materials could have arisen. The purified CD147-Rg was then included in the development of the competitive ELISA.

To develop a competitive ELISA for determination of serum CD147, the biotin carried on the CD147-BCCP facilitated specific capture of the recombinant CD147-BCCP onto the ELISA plate via the precoated avidin. Various concentrations of CD147-Rg were mixed with anti-CD147 MAb and competitive reactions of anti-CD147 MAb to the captured CD147-BCCP were determined. The established competitive ELISA displayed a high specificity and sensitivity for detection of mammalian CD147 molecules (Fig. 2). The developed competitive ELISA was then applied to determine the CD147 level of normal subjects and those with various types of cancers. In our experiments, we were aware that the normal subjects recruited may have had unidentified symptomless cancers. All normal sera were, therefore, tested for HA. HA is a ubiquitous glycoaminoglycan found in the extracellular matrix. Concentration of HA is elevated in several cancers.[40] HA has been used as a marker for diagnosis of several types of cancer.[41,42] All normal sera used in this study were negative for HA, indicating that they were appropriate for employment as normal controls. Unexpectedly, the CD147 level was significantly lower in cancer patient sera compared to that of normal subjects. So far we have no simple explanation of our results, which are contradictory to those in previous reports.[23,24] It is possible that the discrepancy might be due to the difference in the types of cancers examined. As CD147 is present in normal cells and plays a role in several normal physiological processes,[2,43] a high level of CD147 in the blood of normal

subjects may reflect homeostasis of this protein under normal physiological conditions. However, biochemical characterization and function of serum CD147 is hitherto unknown. The homeostatic balance of the CD147 level may be altered in tumors. In cancers, while several studies have demonstrated that membrane CD147 enhances tumor growth and metastasis, the negative correlation between membranous form and soluble CD147 in cancer patient sera observed in our experiments may suggest a mechanism of CD147 regulation via inhibitor presence in serum or by negative feedback of serum CD147. Recently, CD147 has been proposed as a receptor for cyclophilins,[44] the ubiquitously expressed intracellular proteins.[45] Overexpression of cyclophilins in many cancer cells has been reported.[46–51] In some circumstances, such as oxidative stress, hypoxia, sepsis, inflammation as well as tumors, plasma cyclophilin levels have been shown to be greatly increased.[52–54] Plasma cyclophilins may bind to CD147 molecules. If so, this binding may interfere with the release of soluble CD147 molecules, or it may shorten the CD147 serum half-life. Therefore, the level of serum CD147 is lower in cancers compared to that of normal subjects.

Levels of serum CD147 were also compared among patients with several liver abnormalities. Sera of hepatitis patients showed the highest CD147 levels, but this was not significantly different from that of normal subjects. The level of CD147 was decreased in patients with cirrhosis, HCC, and CCA. Decreased CD147 levels in patients with cirrhosis compared to hepatitis may suggest a degree of liver tissue impairment. Hence, the current results suggest that a decrease in serum CD147 level may indicate not only malignancy but also a degree of liver tissue damage. HCC originates from hepatocytes, whereas CCA arise from bile duct.[55] In the context of carcinogenesis of liver cancers, chronic viral infections and alcoholism are major causes of liver cirrhosis. Liver cirrhosis is considered to be the main risk factor for an onset of HCC.[56,57] In contrast, an incidence of CCA, which is most prevalent in the northeast of Thailand, is strongly correlated with infection of bile duct by *Opisthorchis viverrini* or liver fluke.[58] Therefore, difference in CD147 levels between HCC and CCA patients may be contributed by discrepancy in distinct mechanisms in their tumorigenesis.

Although the functional role of serum CD147 is still unknown, we have described a difference in the level of serum CD147 in normal, liver disease, and cancerous serum samples. Accordingly, this phenomenon may be of interest for further identification of the role of serum CD147 in liver pathogenesis and oncogenesis.

Acknowledgments

This study was supported by the NSTDA Research Chair Grant, National Sciences and Technology Development Agency (Thailand) and The Thailand Research Fund. A postdoctoral scholarship to SM was provided by THE National Center for Genetic Engineering and Biotechnology, National Sciences and Technology Development Agency (Thailand). We thank Dr. Dale E. Taneyhill for proofreading the manuscript.

References

1. Tang J, Wu YM, Zhao P, Yang XM, Jiang JL, and Chen ZN: Overexpression of HAb18G/CD147 promotes invasion and metastasis via alpha3beta1 integrin mediated FAK-paxillin and FAK-PI3K-Ca2+ pathways. Cell Mol Life Sci 2008; 65:2933–2942.
2. Gabison EE, Hoang-Xuan T, Mauviel A, and Menashi S: EMMPRIN/CD147, an MMP modulator in cancer, development and tissue repair. Biochimie 2005;87:361–368.
3. Renno T, Wilson A, Dunkel C, Coste I, Maisnier-Patin K, Benoit de Coignac A, Aubry JP, Lees RK, Bonnefoy JY, MacDonald HR, and Gauchat JF: A role for CD147 in thymic development. J Immunol 2002;168:4946–4950.
4. Major TC, Liang L, Lu X, Rosebury W, and Bocan TM: Extracellular matrix metalloproteinase inducer (EMMPRIN) is induced upon monocyte differentiation and is expressed in human atheroma. Arterioscler Thromb Vasc Biol 2002;22: 1200–1207.
5. Kasinrerk W, Fiebiger E, Stefanova I, Baumruker T, Knapp W, and Stockinger H: Human leukocyte activation antigen M6, a member of the Ig superfamily, is the species homologue of rat OX-47, mouse basigin, and chicken HT7 molecule. J Immunol 1992;149:847–854.
6. Kasinrerk W, Tokrasinwit N, and Phunpae P: CD147 monoclonal antibodies induce homotypic cell aggregation of monocytic cell line U937 via LFA-1/ICAM-1 pathway. Immunology 1999;96:184–192.
7. Igakura T, Kadomatsu K, Taguchi O, Muramatsu H, Kaname T, Miyauchi T, Yamamura K, Arimura K, and Muramatsu T: Roles of basigin, a member of the immunoglobulin superfamily, in behavior as to an irritating odor, lymphocyte response, and blood-brain barrier. Biochem Biophys Res Commun 1996;224:33–36.
8. Koch C, Staffler G, Huttinger R, Hilgert I, Prager E, Cerny J, Steinlein P, Majdic O, Horejsi V, and Stockinger H: T cell activation-associated epitopes of CD147 in regulation of the T cell response, and their definition by antibody affinity and antigen density. Int Immunol 1999;11:777–786.
9. Staffler G, Szekeres A, Schutz GJ, Saemann MD, Prager E, Zeyda M, Drbal K, Zlabinger GJ, Stulnig TM, and Stockinger H: Selective inhibition of T cell activation via CD147 through novel modulation of lipid rafts. J Immunol 2003;171:1707–1714.
10. Chiampanichayakul S, Peng-in P, Khunkaewla P, Stockinger H, and Kasinrerk W: CD147 contains different bioactive epitopes involving the regulation of cell adhesion and lymphocyte activation. Immunobiology 2006;211:167–178.
11. Khunkaewla P, Schiller HB, Paster W, Leksa V, Cermak L, Andera L, Horejsi V, and Stockinger H: LFA-1-mediated leukocyte adhesion regulated by interaction of CD43 with LFA-1 and CD147. Mol Immunol 2008;45:1703–1711.
12. Reimers N, Zafrakas K, Assmann V, Egen C, Riethdorf L, Riethdorf S, Berger J, Ebel S, Janicke F, Sauter G, and Pantel K: Expression of extracellular matrix metalloproteases inducer on micrometastatic and primary mammary carcinoma cells. Clin Cancer Res 2004;10:3422–3428.
13. Tang Y, Nakada MT, Kesavan P, McCabe F, Millar H, Rafferty P, Bugelski P, and Yan L: Extracellular matrix metalloproteinase inducer stimulates tumor angiogenesis by elevating vascular endothelial cell growth factor and matrix metalloproteinases. Cancer Res 2005;65:3193–3199.
14. Nabeshima K, Iwasaki H, Koga K, Hojo H, Suzumiya J, and Kikuchi M: Emmprin (basigin/CD147): matrix metalloproteinase modulator and multifunctional cell recognition molecule that plays a critical role in cancer progression. Pathol Int 2006;56:359–367.
15. Sun J, and Hemler ME: Regulation of MMP-1 and MMP-2 production through CD147/extracellular matrix metallo-

proteinase inducer interactions. Cancer Res 2001;61:2276–2281.
16. Gabison EE, Mourah S, Steinfels E, Yan L, Hoang-Xuan T, Watsky MA, De Wever B, Calvo F, Mauviel A, and Menashi S: Differential expression of extracellular matrix metalloproteinase inducer (CD147) in normal and ulcerated corneas: role in epithelio-stromal interactions and matrix metalloproteinase induction. Am J Pathol 2005;166:209–219.
17. Yan L, Zucker S, and Toole BP: Roles of the multifunctional glycoprotein, emmprin (basigin; CD147), in tumour progression. Thromb Haemost 2005;93:199–204.
18. Zhong WD, Han ZD, He HC, Bi XC, Dai QS, Zhu G, Ye YK, Liang YX, Qin WJ, Zhang Z, Zeng GH, and Chen ZN: CD147, MMP-1, MMP-2 and MMP-9 protein expression as significant prognostic factors in human prostate cancer. Oncology 2008;75:230–236.
19. Jia L, Zhou H, Wang S, Cao J, Wei W, and Zhang J: Deglycosylation of CD147 down-regulates matrix metalloproteinase-11 expression and the adhesive capability of murine hepatocarcinoma cell HcaF in vitro. IUBMB Life 2006; 58:209–216.
20. Biswas C: Collagenase stimulation in cocultures of human fibroblasts and human tumor cells. Cancer Lett 1984;24:201–207.
21. Hanata K, Yamaguchi N, Yoshikawa K, Mezaki Y, Miura M, Suzuki S, Senoo H, and Ishikawa K: Soluble EMMPRIN (extra-cellular matrix metalloproteinase inducer) stimulates the migration of HEp-2 human laryngeal carcinoma cells, accompanied by increased MMP-2 production in fibroblasts. Arch Histol Cytol 2007;70:267–277.
22. Millimaggi D, Mari M, D'Ascenzo S, Carosa E, Jannini EA, Zucker S, Carta G, Pavan A, and Dolo V: Tumor vesicle-associated CD147 modulates the angiogenic capability of endothelial cells. Neoplasia 2007;9:349–357.
23. Zhang W, Erkan M, Abiatari I, Giese NA, Felix K, Kayed H, Buchler MW, Friess H, and Kleeff J: Expression of extracellular matrix metalloproteinase inducer (EMMPRIN/CD147) in pancreatic neoplasm and pancreatic stellate cells. Cancer Biol Ther 2007;6:218–227.
24. Zhifan X, Jie L, Shioqiong C, Zhihui Z, Li L, Zhengying L, Yanru K, and Lina X: Significance of the expression and serum levels of CD147 and MMP-2 in patients with colorectal cancer. Chin J Clin Oncol 2008;35:1064–1067.
25. Krebber A, Bornhauser S, Burmester J, Honegger A, Willuda J, Bosshard HR, and Pluckthun A: Reliable cloning of functional antibody variable domains from hybridomas and spleen cell repertoires employing a reengineered phage display system. J Immunol Methods 1997;201:35–55.
26. Tayapiwatana C, Chotpadiwetkul R, and Kasinrerk W: A novel approach using streptavidin magnetic bead-sorted in vivo biotinylated survivin for monoclonal antibody production. J Immunol Methods 2006;317:1–11.
27. Qian AR, Zhang W, Cao JP, Yang PF, Gao X, Wang Z, Xu HY, Weng YY, and Shang P: Downregulation of CD147 expression alters cytoskeleton architecture and inhibits gelatinase production and SAPK pathway in human hepatocellular carcinoma cells. J Exp Clin Cancer Res 2008;27:50.
28. Caudroy S, Polette M, Tournier JM, Burlet H, Toole B, Zucker S, and Birembaut P: Expression of the extracellular matrix metalloproteinase inducer (EMMPRIN) and the matrix metalloproteinase-2 in bronchopulmonary and breast lesions. J Histochem Cytochem 1999;47:1575–1580.
29. Sidhu SS, Mengistab AT, Tauscher AN, LaVail J, and Basbaum C: The microvesicle as a vehicle for EMMPRIN in tumor-stromal interactions. Oncogene 2004;23:956–963.
30. Egawa N, Koshikawa N, Tomari T, Nabeshima K, Isobe T, and Seiki M: Membrane type 1 matrix metalloproteinase (MT1-MMP/MMP-14) cleaves and releases a 22-kDa extracellular matrix metalloproteinase inducer (EMMPRIN) fragment from tumor cells. J Biol Chem 2006;281:37576–37585.
31. Taylor PM, Woodfield RJ, Hodgkin MN, Pettitt TR, Martin A, Kerr DJ, and Wakelam MJ: Breast cancer cell-derived EMMPRIN stimulates fibroblast MMP2 release through a phospholipase A(2) and 5-lipoxygenase catalyzed pathway. Oncogene 2002;21:5765–5772.
32. Tang Y, Kesavan P, Nakada MT, and Yan L: Tumor-stroma interaction: positive feedback regulation of extracellular matrix metalloproteinase inducer (EMMPRIN) expression and matrix metalloproteinase-dependent generation of soluble EMMPRIN. Mol Cancer Res 2004;2:73–80.
33. Bidart JM, Thuillier F, Augereau C, Chalas J, Daver A, Jacob N, Labrousse F, and Voitot H: Kinetics of serum tumor marker concentrations and usefulness in clinical monitoring. Clin Chem 1999;45:1695–1707.
34. Hoshino M, Kawashima H, Ogose A, Kudo N, Ariizumi T, Hotta T, Umezu H, Hatano H, Morita T, Nishio J, Iwasaki H, and Endo N: Serum CA 125 expression as a tumor marker for diagnosis and monitoring the clinical course of epithelioid sarcoma. J Cancer Res Clin Oncol 2010;136:457–464.
35. Taylor DD, Lyons KS, and Gercel-Taylor C: Shed membrane fragment-associated markers for endometrial and ovarian cancers. Gynecol Oncol 2002;84:443–448.
36. Chapman-Smith A, and Cronan JE Jr: In vivo enzymatic protein biotinylation. Biomol Eng 1999;16:119–125.
37. Tragoolpua K, Intasai N, Kasinrerk W, Mai S, Yuan Y, and Tayapiwatana C: Generation of functional scFv intrabody to abate the expression of CD147 surface molecule of 293A cells. BMC Biotechnol 2008;8:5.
38. Santala V, and Lamminmaki U: Production of a biotinylated single-chain antibody fragment in the cytoplasm of Escherichia coli. J Immunol Methods 2004;284:165–175.
39. Prinz WA, Aslund F, Holmgren A, and Beckwith J: The role of the thioredoxin and glutaredoxin pathways in reducing protein disulfide bonds in the Escherichia coli cytoplasm. J Biol Chem 1997;272:15661–15667.
40. Laurent TC, and Fraser JR: Hyaluronan. FASEB J 1992;6: 2397–2404.
41. Posey JT, Soloway MS, Ekici S, Sofer M, Civantos F, Duncan RC, and Lokeshwar VB: Evaluation of the prognostic potential of hyaluronic acid and hyaluronidase (HYAL1) for prostate cancer. Cancer Res 2003;63:2638–2644.
42. Passerotti CC, Bonfim A, Martins JR, Dall'Oglio MF, Sampaio LO, Mendes A, Ortiz V, Srougi M, Dietrich CP, and Nader HB: Urinary hyaluronan as a marker for the presence of residual transitional cell carcinoma of the urinary bladder. Eur Urol 2006;49:71–75.
43. Iacono KT, Brown AL, Greene MI, and Saouaf SJ: CD147 immunoglobulin superfamily receptor function and role in pathology. Exp Mol Pathol 2007;83:283–295.
44. Jiang JL, and Tang J: CD147 and its interacting proteins in cellular functions. Sheng Li Xue Bao 2007;59:517–523.
45. Yao Q, Li M, Yang H, Chai H, Fisher W, and Chen C: Roles of cyclophilins in cancers and other organ systems. World J Surg 2005;29:276–280.
46. Fillies T, Werkmeister R, van Diest PJ, Brandt B, Joos U, and Buerger H: HIF1-alpha overexpression indicates a good prognosis in early stage squamous cell carcinomas of the oral floor. BMC Cancer 2005;5:84.

47. Choi KJ, Piao YJ, Lim MJ, Kim JH, Ha J, Choe W, and Kim SS: Overexpressed cyclophilin A in cancer cells renders resistance to hypoxia- and cisplatin-induced cell death. Cancer Res 2007;67:3654–3662.
48. Shen J, Person MD, Zhu J, Abbruzzese JL, and Li D: Protein expression profiles in pancreatic adenocarcinoma compared with normal pancreatic tissue and tissue affected by pancreatitis as detected by two-dimensional gel electrophoresis and mass spectrometry. Cancer Res 2004;64: 9018–9026.
49. Rey O, Baluda MA, and Park NH: Differential gene expression in neoplastic and human papillomavirus-immortalized oral keratinocytes. Oncogene 1999;18:827–831.
50. Howard BA, Zheng Z, Campa MJ, Wang MZ, Sharma A, Haura E, Herndon JE 2nd, Fitzgerald MC, Bepler G, and Patz EF Jr: Translating biomarkers into clinical practice: prognostic implications of cyclophilin A and macrophage migratory inhibitory factor identified from protein expression profiles in non-small cell lung cancer. Lung Cancer 2004;46:313–323.
51. Howard BA, Furumai R, Campa MJ, Rabbani ZN, Vujaskovic Z, Wang XF, and Patz EF Jr: Stable RNA interference-mediated suppression of cyclophilin A diminishes non-small-cell lung tumor growth in vivo. Cancer Res 2005; 65:8853–8860.
52. Tegeder I, Schumacher A, John S, Geiger H, Geisslinger G, Bang H, and Brune K: Elevated serum cyclophilin levels in patients with severe sepsis. J Clin Immunol 1997;17:380–386.
53. Billich A, Winkler G, Aschauer H, Rot A, and Peichl P: Presence of cyclophilin A in synovial fluids of patients with rheumatoid arthritis. J Exp Med 1997;185:975–980.
54. Jin ZG, Lungu AO, Xie L, Wang M, Wong C, and Berk BC: Cyclophilin A is a proinflammatory cytokine that activates endothelial cells. Arterioscler Thromb Vasc Biol 2004;24:1186–1191.
55. Tischoff I, and Tannapfel A: [Hepatocellular carcinoma and cholangiocarcinoma—different prognosis, pathogenesis and therapy]. Zentralbl Chir 2007;132:300–305.
56. Songsivilai S, Dharakul T, and Kanistanon D: Hepatitis C virus genotypes in patients with hepatocellular carcinoma and cholangiocarcinoma in Thailand. Trans R Soc Trop Med Hyg 1996;90:505–507.
57. Franca AV, Elias Junior J, Lima BL, Martinelli AL, and Carrilho FJ: Diagnosis, staging and treatment of hepatocellular carcinoma. Braz J Med Biol Res 2004;37:1689–1705.
58. Sripa B, and Kaewkes S: Localisation of parasite antigens and inflammatory responses in experimental opisthorchiasis. Int J Parasitol 2000;30:735–740.

Address correspondence to:
Watchara Kasinrerk, Ph.D.
Division of Clinical Immunology
Department of Medical Technology
Faculty of Associated Medical Sciences
Chiang Mai University
Chiang Mai 50200
Thailand

E-mail: watchara@chiangmai.ac.th

Received: November 16, 2009
Accepted: January 7, 2010